A COMPREHENSIVE UNDERSTANDING OF BONE HOMEOSTASIS IN BROILERS WITH OXIDATIVE STRESS AND *EIMERIA* INFECTION

by

YUGUO HOU TOMPKINS

(Under the Direction of Woo Kyun Kim)

ABSTRACT

The genetic selection for heavy muscle gain and fast growth in broilers has been linked to the increased prevalence of leg problems. Meanwhile, coccidiosis which is caused by *Eimeria* spp., has become one of the most economically impactful diseases in poultry production. Current study reported that *Eimeria*-infected birds had high levels of oxidative stress and lower antioxidant capacity in the bone marrow, and a lower bone mineral content, density, and slower bone formation. The second experiment showed that other than malnutrition, inflammation-mediated osteoclast activity attributed to bone mineral loss and oxidative stress negatively correlated with bone formation rate during *Eimeria* infection. In order to further understand the interaction between oxidative stress and bone metabolism, chicken primary mesenchymal stem cells (MSCs) were exposed to hydrogen peroxide (H_2O_2) to induce oxidative stress in *vitro* study. Moreover, microinjection of H_2O_2 into chicken embryo was used to induce systemic oxidative stress at the early embryonic development. Both *in vitro* and *in ovo* studies showed that oxidative stress negatively regulated the expression of the osteogenic differentiation gene

markers in the chicken MSCs, and inhibited bone formation in embryos. In the last part of the study, fish oil was used as a dietary supplement to reduce performance loss due to coccidiosis in broilers. Fish oil supplementation enhanced intestinal barrier integrity and positively impacted bone mineral content and growth performance in broilers during coccidiosis.

Taken together, current studies demonstrate that oxidative stress and inflammation are key factors that mediate bone loss by suppressing bone formation and increasing bone resorption during *Eimeria* infection in broilers. The results provide more accurate understanding of bone homeostasis that aim to uncover the pathology of the chicken bone disorder.

INDEX WORDS: Broiler bone, osteoblast, osteogenesis, oxidative stress, osteoimmunology, chicken bone health

A COMPREHENSIVE UNDERSTANDING OF BONE HOMEOSTASIS IN BROILERS WITH OXIDATIVE STRESS AND *EIMERIA* INFECTION

by

YUGUO HOU TOMPKINS

B.S., Sichuan Agricultural University, 2012

M.S., Sichuan Agricultural University, 2015

M.S., Virginia Polytechnic Institute and State University, 2017

A Dissertation Submitted to the Graduate Faculty of The University of Georgia in Partial Fulfillment of the Requirements for the Degree

DOCTOR OF PHILOSOPHY

ATHENS, GEORGIA

2022

A COMPREHENSIVE UNDERSTANDING OF BONE HOMEOSTASIS IN BROILERS WITH OXIDATIVE STRESS AND *EIMERIA* INFECTION

by

YUGUO HOU TOMPKINS

Major Professor:	Woo Kyun Kim
Committee:	Rami Dalloul
	Hea Jin Park
	Luke Mortensen

Electronic Version Approved:

Ron Walcott
Vice Provost for Graduate Education and Dean of the Graduate School
The University of Georgia
December 2022

DEDICATION

A dissertation is not the outcome of the efforts of entirely one individual.

I owe much gratitude to my family and my friends for their unwavering support. Thanks to my mom, Professor Rong Yu, who teaches me everything with love and patience. You are the inspiration and role model in my life.

For my dad, Ke Hou, who teaches me strength and resilience. Thank you for always being there for me and supporting me no matter the situation.

For my husband, Philip Tompkins, my best “teammate”, thank you for supporting and helping me to accomplish this journey.

For my daughter, Rose Tompkins, thank you for giving me the strength to keep going. Being your mom is the best thing in my life.

Many people have contributed to and supported its development. At this time, I take the opportunity to thank all my family, my friends and all the people along with me on my doctoral journey and accomplishment.

ACKNOWLEDGEMENTS

Thank you to my dissertation advisor and mentor, Dr. Woo Kyun Kim, who recognized our potential and led the completion of my dissertation with his encouragement, guidance and instruction, not only during the course of this study, but throughout my graduate experience and career development here at the University of Georgia.

I further would like to express my gratitude to Dr. Rami Dalloul, Dr. Hea Jin Park and Dr. Luke Mortensen for their advice and support.

I would like to acknowledge all our previous or current labmates, Dr. Chongxiao Chen, Dr. Po-Yun Teng, Dr. Fernanda Castro, Dr. Jinquan Wang, Brett Marshall, Dr. Sudhir Yadav, Dr. Amit Singh, Dr. Oscar Tejeda, Dima white, Hanyi Shi, Guanchen Liu, Milan Kumar Sharma, Janghan Choi, Hanseo Ko, Doyun Goo, Deependra Paneru, Venkata Sesha Reddy Choppa, Hamid Reza, Fatemeh Mahdavi, Dr. Jinhwan Lee. Thank you for all the help and support to accomplish my experiments.

Finally, I am indebted to the faculty, staff, and students at the Department of Poultry Science, University of Georgia, who have aided me in every aspect of completing this work.

TABLE OF CONTENTS

Page

LIST OF TABLES

Page

LIST OF FIGURES

Page

CHAPTER 1

INTRODUCTION AND REVIEW OF RELEVANT LITERATURE

Bone biology, formation and development

Bone is often stereotyped only as a framework for the body. In fact, bone is more than just a supportive structure. It is a storage unit that stores crucial nutrients, minerals, and lipids to nourish the body; An endocrine organ that produces hormones and proteins which play roles in the regulation of many metabolisms (Zhou, et al., 2021); It's also an organ that generates different types of cells that play a vital role in protecting the body against infection (Thakker, et al., 2017). Moreover, bone has a dynamic structure that constantly remodels and changes shape to adapt to the mechanical pressure and physical requirement (Miller, et al., 2021). The bone formation and development varied at different stages of growth. Intramembranous ossification mainly occurs at the flat bone, where bone develops from fibrous membranes and deposits the minerals on the out layer of the membrane (Rath and Durairaj, 2022). On the other hand, endochondral ossification is essential in long bone growth that bone develops by replacing hyaline cartilage with a mineralized structure (Mackie, et al., 2008). Both intramembranous and endochondral developments request the differentiation of mesenchymal stem cells (MSCs) into osteoblasts (Tortelli, et al., 2010).

The physiological structure of long bone can be divided into three major regions includes epiphysis, metaphysis and diaphysis. Those regions are physiologically distinct, and each has its own unique developmental characteristics (Itoh and Hatano, 1964; Dilworth and Day, 1965; Applegate and Lilburn, 2002). The diaphysis is the midsection of a long bone that is majorly composed of dense cortical bone (compact bone), where the outer periosteal surface continuously has mineral deposition, and inner endosteal surface mineral resorption leads to the diameter increased with larger marrow space expanding, and the hollow space formed the medullary cavity that eventually filled with bone marrow (Clarke, 2008). Radical growth rate can be reflects at cortical bone at the diaphysis, where cortical bone is essential for structural strength (Isojima and Sims, 2021). In general, higher mineral density and less water content can be detected in cortical bone compared with trabecular bone (Gong, et al., 1964). Bone breaking strength has been shown to be correlated with cortical bone thickness; therefore, the cortical bone quality is a crucial indicator of bone development and quality (Peretz, et al., 1998). The epiphysis is the end section of the long bones which is covered with articular cartilage at the joint. The metaphysis is between epiphysis and diaphysis, and this section contains an epiphyseal plate (growth plate) which is essential in longitudinal growth (Clarke, 2008; Grabowski, 2009). The growth plate cartilage proliferates and differentiates, and is subsequently mineralized and replaced by solid bone tissue (Kronenberg, 2003).

During growth, there are two main stages in bone homeostasis, bone modeling and bone remodeling. In general, modeling is attributed to skeletal growth, where the bones gradually change shape and size to adapt to physiologic impact or mechanical

forces (Frost, 1994; Allen and Burr, 2014). Remodeling is a dynamic and lifetime-continuous process by renewing bone units to maintain bone quality with limited change in structure and shape (Bolamperti, et al., 2022). The remodeling process involves sequential bone resorption and formation works to replace the older or damaged bone structure with newer bone formatted at the exact location (Frost, 1994; Allen and Burr, 2014). It preserved the mechanical strength and ensured bone quality by remodeling process (Parfitt, 1994; Langdahl, et al., 2016). The mineral resorption and deposition are necessary to be well-coordinated to maintain the remodeling balance. Aging, inflammation and certain stress can break the balance (Gibon, et al., 2017; Bolamperti, et al., 2022). However, due to market needs, broilers (meat chicken) will be on the market at 42 days of age, bone modelling is still dominant process over remodeling. The remodeling process is more frequently observed in the layers, or the broilers under pathogen infection or special physical stress (Aguado, et al., 2015; Akbari Moghaddam Kakhki, et al., 2019; Tompkins, et al., 2022b). The trabecular bone not only contributes bone strength but also functions as the calcium resource for metabolic homeostasis (Whitehead and Fleming, 2000; Passi and Gefen, 2005). Trabecular has a biomechanics function by transferring mechanical force from the articular surface to the cortical bone (Ott, 2018). Moreover, the trabecular bone accounts for nearly ten times of the surface than cortical bone, the large surface provides a broader surface for osteoclast metabolism and metabolic activity (Eriksen, 1986; Oftadeh, et al., 2015). Trabecular bone homeostasis is more sensitive to mineral depletion and more active in remodeling than cortical bones (Kent, et al., 1990; Bjornerem, 2016). For example, in the study of calcium

deficiency in mice, the calcium-restricted diet did not change body weight, growth rate or feed conversion ratio. However, the low calcium diet decreased trabecular bone density (Kim and Park, 2013). Trabecular bone mineral loss under a disease condition is closely associated with the health status of broilers, or increased bone turnover can be observed in layers during the laying stage (Passi and Gefen, 2005). Differences in mineralization rates, microstructure, growth characteristics, and metabolic dynamics suggest that the functionality and integrity of the bone should not be assumed solely from region-specific measurements. Therefore, more than just the bone-breaking strength and mineral content, the bone dynamics in the specific structural regions is very important to understand bone modeling and remodeling in chickens.

Bone modeling and remodeling result from the activity balance between bone-related cells. Three types of bone cells are mainly involved in bone hemostasis: chondrocytes, osteoblasts and osteoclast. Osteoblasts and chondrocytes share a common precursor, mesenchymal stem cells, whereas osteoclasts are of hematopoietic origin (Zomorodian and Baghaban Eslaminejad, 2012). Bone formation is accomplished by osteoblasts, and bone reabsorption is accomplished by osteoclasts (Hambli, 2014). The balance between osteoclasts and osteoblasts mediates skeletal homeostasis in healthy and disease statuses (Feng and McDonald, 2011). Osteoblasts can synthesize collagenous matrix, and meanwhile osteoblasts are endocrine cells that can secrete hormones and proteins to regulate bone mineralization (Lee, et al., 2007). Type I collagen is the most abundant protein product from osteoblasts, which is usually considered a biomarker of bone formation. Bone mineralization is a well-regulated process, and bone metabolic

markers are bone-derived molecules that could describe bone formation (Franz-Odendaal, et al., 2006). Osteocalcin is a protein that is solely secreted by osteoblasts, it is commonly used as a serum marker of osteoblastic bone formation, and it also acts as a hormone that is participated in glucose homeostasis (Brennan-Speranza and Conigrave, 2015; Rubert and De la Piedra, 2020). Glucose is the primary energy nutrient for osteoblasts and its progenitors, and glucose uptake favors osteoblast differentiation and promotes bone formation (Ducy, et al., 1997; Wei, et al., 2015; Lee, et al., 2017b). Besides, alkaline phosphatase (ALP), which is secreted by osteoblasts, growth factor bone morphogenetic protein 2 (BMP2), and transcription factor runt-related transcription factor 2 (RUNX2; or CBFA1), all play pivotal roles in the osteogenic differentiation, mineralization, and bone formation (Ducy, et al., 1997; Huang, et al., 2007; Khosla, et al., 2008; Chatakun, et al., 2014). RUNX2 is an essential transcriptional that regulate osteoblastogenesis and cell cycle (Galindo, et al., 2005). RUNX2 that located at the intersection of many signaling pathways, it is not only expressed at the early stages of osteoblastic differentiation, but also expressed in osteochondral progenitors (Lee, et al., 2000; Javed, et al., 2008). The WNT pathway is one of the most important signaling pathway to promotes osteoblast differentiation and regulating osteogenesis, the activation of this pathway showed an anti-adipogenesis and anti-chondrogenesis (but promotes chondrocyte hypertrophy) function during bone formation (Olivares-Navarrete, et al., 2011; Lee, et al., 2017b; Riddle and Clemens, 2017). The non-canonical signaling pathway, which is the pathways included β-catenin participation, is a cross-talk path between osteogenesis and adipogenesis of bone marrow mesenchymal progenitors (Bilkovski, et al., 2010). The activation of WNT

pathway can block PPAR-gamma-induced adipogenesis and induce RUNX2 expression, which commit mesenchymal stem cells differentiated into the osteoblast phenotype (Takada, et al., 2007; Santos, et al., 2010). Besides, In *vitro*, BMP2 treatment increases RUNX2 gene expression and ALP protein levels in a human stem cell line (Javed, et al., 2008). Multifunctional cytokines BMPs, members of the transforming growth factor-β (TGF-β) superfamily, are also played an essential role in regulating osteoblastogenesis (Wu, et al., 2016). Receptor-regulated Smads can be phosphorylated by BMP receptors, and the activated protein complex can be translocated to the nucleus to further activate transcription factors such as RUNX2 (Kokabu, et al., 2012). Therefore, plays a critical role in the regulation of bone remodeling by affecting both osteoblast and osteoclast functions (Zou, et al., 2021). At the completion of bone formation, the majority of the osteoblasts undergo apoptosis (Xing and Boyce, 2005), and a small portion of the remaining cells will gradually shape into lining cells (Dobnig and Turner, 1995).

Proper bone growth and maintenance required continuous bone resorption by osteoclasts (Lemma, et al., 2016). Osteoclasts, which originate from hematopoietic stem cells (HSC) in bone marrow, are characterized by a unique multinucleated form located on the endosteum surface of the bone (Teitelbaum, 2007). Osteoclasts can secret hydrogen ions and enzymes to dissolve and digest the mineral component and collagen matrix of bone as the starting process of bone resorption (Boyle, et al., 2003; Boyce, et al., 2009). Osteoclasts highly expressed tartrate-resistant acid phosphatase (TRAP, TRAPase), which allows TRAP enzyme and its coding gene (TRACP5b, ACP5) to be considered as a biomarker of osteoclasts formation (Leibbrandt and Penninger, 2008).

Receptor activator of nuclear factor-kB ligand (RANKL) belongs to the TNF superfamily and is critical for osteoclastogenesis (Teitelbaum and Ross, 2003; Indo, et al., 2013). RANKL is a critical cytokine that regulates osteoclastogenesis and activity. RANKL is majorly expressed on osteoblasts to bind with its receptor RANK, which is mainly expressed on osteoclasts and dendritic cells (Taichman, 2005; Lorenzo, et al., 2008; Takahashi, et al., 2014). The binding of RANKL to its receptor RANK triggers osteoclast precursors to differentiate into osteoclasts, which increases the number of osteoclasts on their bone surfaces (Teitelbaum and Ross, 2003; Park, et al., 2017). Mice that were injected with the inhibitor of RANKL resulted in a larger bone mass (Furuya, et al., 2011). In mammals, the binding between RANKL and RANK receptor can be inhibited by the soluble decoy receptor osteoprotegerin (OPG). OPG is secreted by osteoblast lineage cells and acts as a natural decoy receptor for RANKL, therefore negatively regulating RANK-RANKL binding and signaling. By modulating the expression of OPG/RANKL which can affect the activity of osteoblasts, when the ratio of RANKL to OPG is upregulated, more binding between RANKL and RANK leads to increased osteoclast-mediated bone resorption, and vice versa (Boyce and Xing, 2008). Many factors that mediate osteoclastogenesis, including hormones that significantly regulate the calcium homeostasis (Han, et al., 2018). For example, calcitonin, which is mainly expressed in ultimobranchial and pituitary glands in chicken (Dent, et al., 1969; Maddineni, et al., 2007), can inhibit the activity of osteoclasts and decrease calcium released from the bone to the bloodstream (Monier-Faugere, et al., 1996; Heino, et al., 2002; Swarthout, et al., 2002). Glucocorticoids, an “stress hormone”, has been used as an

animal welfare marker in animal production (Möstl and Palme, 2002; Scanes, 2016). Glucocorticoids can stimulate osteoclast differentiation and accelerate bone resorption by suppressing OPG synthesis but stimulating RANKL synthesis in preosteoblast cells (Hardy, et al., 2018). Apoptosis of osteoclasts is the ending point of the cells, the apoptosis rate of osteoclasts directly mediated bone resorption activity and bone remolding rate (Soysa and Alles, 2019). Decreasing of osteoclast apoptosis leads to increased bone loss, and vice versa (Hughes, et al., 1996; Wu, et al., 2003; Zhang, et al., 2005).

General Introduction of Broiler Skeletal Disorder

Bone is a multifunctional endocrine organ that provides not only structural support for the movement and protection of the internal organs but also the skeleton system; especially the long bone also functions as a dynamic organ that plays a vital role in immunology and animal nutrition (Zhou, et al., 2021; Rath and Durairaj, 2022). Chicken muscle yield has been considered one of the most important traits in genetic breed selection (Bailey, et al., 2020). However, the continuous selection for rapid growth and high muscle yield has shifted the broilers' center of gravity and altered the biomechanical structure (Huang, et al., 2019).

The unbalanced development between muscle and skeleton has been unexpectedly associated with the incidence of metabolic and skeletal disorders in modern broiler breeds. For broilers, most of skeleton disorders occur on the long bone (tibia and femur)(Cook, 2000; Çapar Akyüz and Onbaşılar, 2020). Thus, leg disorders are a significant cause of poor welfare in broilers. Several studies showed that as high as 50%

of broilers suffered from lameness which was reflected by high gait scores (Granquist, et al., 2019), and at least 30% of birds showed poor locomotion (Knowles, et al., 2008; Kittelsen, et al., 2017), which interfered with chicken' accessibility to feed and water, predominantly reducing the growth and caused an economic loss in production. Besides, poor bone quality or low bone strength increases the risk of fractures during rearing, catching, or transportation, decreasing production quality (Wideman, 2016; Zhang, et al., 2020). In recent years, pain and discomfort in leg problems that impaired walking ability has significantly compromised the well-being of the birds, and chicken bone disorder has grown into a major welfare issue that aroused society' s concern (Phibbs, et al., 2021). The bone-related disorder could be majorly concluded into two categories, infectious disorder and non-infectious disorder. Researches have successfully identified several pathologic factors in bone problems, but the exact etiology of these diseases is still debatable. Studies concluded that the non-infectious bone disorder was majorly caused by genetic factors and management (Kestin, et al., 1992; Talaty, et al., 2009). However, several studies also indicated that the direct correlations between genetic selection and leg problems are weak (Bihan-Duval, et al., 1997; Rekaya, et al., 2013; González-Cerón, et al., 2015). Currently, the diagnosed of the early-stage leg problems relied on manually histological examination and macroscopic evaluation (Almeida Paz, et al., 2005; Wideman, 2016). And there is no suitable clinical biomarker or behavior indicators to predict the later-stage-leg problems. Accordingly, the leg problem in poultry production is almost certainly underestimated (Leach and Monsonego-Ornan, 2007; Wideman, 2016). With the complexity of the bone disorder, factors such as genetics, nutrition, and

management systems and the interactions between these factors are involved in the etiology of bone disorders. Continued efforts are needed to improve genetic, nutritional, and management techniques to minimize these problems (de Jong, et al., 2012).

Bone deformity such as tibial dyschondroplasia (TD) is one of the most common development disorders in broiler. Tibial metaphysis has been extensively studied because it is where TD most often occurs (Leach and Monsonego-Ornan, 2007). TD is also heavily influenced by nutrition deficiencies or diet quality (Leach and Monsonego-Ornan, 2007), such as an imbalance ratio of calcium to phosphorus, high chloride content, excess cysteine content, and diet contamination with mycotoxins or toxins. Those dietary challenges could result in similar pathologic lesions (Orth and Cook, 1994). However, an optimized diet and balanced nutrition do not absolutely prevent TD in broilers, indicating that it is more than just a nutritional issue. So far, the exact etiology of tibial dyschondroplasia remains largely unknown. Several studies indicated that TD results from interfered growth plate cartilage degradation (Cook, et al., 1994; Orth, et al., 1999). In TD, the complete differentiation of the chondrocytes is important for cartilage vascularization and mineralization. Chondrocytes fail to undergo differentiation and hypertrophy will result in decreased vascular penetration and reduced metabolic exchange, which inhibited endochondral ossification (Farquharson and Jefferies, 2000). With a thicker plateau developed with non-vascularized or noncalcified characters, the abnormality growth plate structure increased the chance of growth plate fracture and cause the bone/join lesion over that region (Praul, et al., 2000). Gene expression studies indicated that the expression of BMP2 and RUNX2 were down-regulated in artificially

induced TD chicken (Yao, et al., 2018), where both genes are essential in bone formation. Moreover, abnormal chondrocyte protein secretion was detected in TD chicken, which include type II collagen, bone adhesion protein (osteonectin, SPARC), and osteopontin (OPN, SPP1) (Yao, et al., 2018). The altered expression pattern of those proteins is closely associated with the depressed proliferation and differentiation of chondrocytes and osteoblasts, which can result in the retardation of bone growth. Interestingly, the number of osteoclasts was found to be markedly reduced in the severe lesion bones under the dietary introduced TD model (Walser, et al., 1982). The reduced bone resorption can be a factor attributed to the growth plate abnormality.

Bacterial chondronecrosis with osteomyelitis (BCO) is another important cause of lameness in poultry production. It is the most common bone necrosis disease and is characterized by severe degeneration with a bacterial infection on cartilage and bone tissue (Wideman, 2016). Intestinal or respiratory epithelial barrier damage increases the chance of pathogenic bacteria entering the bloodstream, then translocating to joints and colonialized over the microfracture on the bone (Wideman, 2016). Both long bone and spinal can be infected, and the lesion is more common to present in growth plate or trabecular bone structure where the morphology of bone is rarely changed, thus BCO can be underdiagnosed (Wideman, 2016). BCO necrosis is associated with many factors including management, inflammation, and nutritional factors. Optimized management, and nutritional strategies tend to reduce the incidence in chicken production (Wideman, 2016). Moreover, immune response and genetics have been implicated in the etiology of spontaneous BCO, where the fastest-growing broiler showed a higher occurrence

(Wideman, et al., 2013; Gilley, et al., 2014; Wideman, et al., 2015). For example, birds infected with the immunosuppressive virus had a higher incidence of BCO (McNamee and Smyth, 2000). Recent studies showed downregulated expression of bone and cartilage formation genes in BCO-affected broilers, indicating the osteochondrosis caused by lacking of ossification can be the primary cause of broiler BCO in broilers, and the bacterial infection may can be a subsequent condition after bone growth retardation (de Oliveira, et al., 2020). The BCO pathogenesis can be initiated by poorly mineralized cartilage damage, followed by colonization of opportunistic bacteria (de Oliveira, et al., 2020). Hence, poor bone quality of broilers can increase the risk of bone fracture and may further accelerate the problem.

Complicate joint lesions can also be associated with certain pathogens infection primary by reovirus or mycoplasma (Kleven and Ferguson-Noel, 2008; Rath and Durairaj, 2022). Mycoplasma *synoviae* is one of the most significant pathogens that infect birds' joints and bones (Kleven and Ferguson-Noel, 2008). Joint lesion and poor bone quality has been observed following infection with mycoplasma *synoviae*, low morbidity and high mortality were typically observed in affected avian species flocks (Olson and Kerr, 1970; Jordan, 1981). Egg production can be reduced in affected layers (Kleven, 2008; Roberts, et al., 2011).

Inflammation and Bone Health

Bone marrow serves as the cradle of hematopoiesis and cytokines (Taichman, 2005). Bone marrow provides a place where the bone homeostasis and immune response have a chance to communicate with each other. Many immune factors and inflammatory

cytokines have osteoclastogenic effects by mediating osteoclast formation, cell activity, and survival, which ultimately regulates bone homeostasis (Kamibayashi, et al., 1995; Kollet, et al., 2006; Lee, et al., 2017a; Solomon, et al., 2018). Therefore, it which provides a crosstalk path between bone homeostasis and immunology system. Nuclear factor-κB (NF-κB), a family of inducible transcription factors that involve in many signaling pathways of different processes of the immune response, is essential in cell survival and osteoclast maturation (Scott, et al., 1997; Jimi, et al., 1998; Beedles, et al., 1999; Boyle, et al., 2003; Huang, et al., 2006; Weitzmann and Pacifici, 2006; Yao, et al., 2008). In a NF-kB knockout mice study, multinuclear osteoclasts were formed properly, while there was an increased number of osteoclast precursors, indicating the essential role of NF-κB in osteoclastogenesis (Miyazaki, et al., 2000; Xing, et al., 2002). Moreover, inflammatory cytokines have a significant impact on osteoclast activity. Classic stimuli for innate immune cells can directly regulate osteoclast differentiation. Macrophages and dendritic cells produce inflammatory cytokines after the immune activation by pattern recognition receptors (PPRs) recognize the pathogens (Li and Wu, 2021). In human and mice, the pro-inflammatory cytokines TNF-a, interleukin-1 b (IL-1b), interleukin-6 (IL-6), and interleukin-17 (IL-17) have also been recognized as pro-osteoclastogenic cytokines (Roux and Orcel, 2000; Wei, et al., 2005; Schett, 2008), known to increase bone resorption by stimulating both osteoclast activity and differentiation (Weitzmann and Pacifici, 2006). Besides, the immune response could stimulate osteoclast activity and differentiation by promoting RANKL expression (Rifas, 1999; Kwan Tat, et al., 2004; Park, et al., 2017). On the other side, anti-inflammatory cytokines such as calcitonin,

interleukin-1 or interferon gamma (IFN-γ) can inhibit osteoclast differentiation in *vitro* (Roux and Orcel, 2000). Moreover, several transcript factors have multifunctional roles in inflammatory response, osteogenesis and osteoclastogenesis. For example, OPG has been shown to be an inhibitor of TNF-related apoptosis (Neville-Webbe, et al., 2004). Smad1 is a key element that intermediates transforming growth factor-beta (TGF-β) signaling pathway and bone morphogenetic protein (BMP) pathway, which are shown to be important regulators in both osteoblast activity and bone mineralization and affect osteoclast differentiation (Tasca, et al., 2015; Tasca, et al., 2018; Zou, et al., 2021).

There are many cases have reported the inflammatory conditions can drive bone destruction and mineral loss in human and mice studies. For example, in human clinic studies, the long-term investment showed bone microarchitectural changes under infection of C virus (HCV), which increased the risk of fracture (Bedimo, et al., 2018). Acute malaria infection severely suppresses bone homeostasis, leading to increased RANKL expression and overstimulation of osteoclastogenesis which favor bone resorption (Lee, et al., 2017a). Trabecular bone microstructure is impaired in the proximal femur of human immunodeficiency virus-infected (HIV) men with normal bone mineral density (Kazakia, et al., 2018). Decreased bone mass and abnormality in trabecular and cortical microarchitecture were observed in young men infected with HIV early in life (Yin, et al., 2014). In broilers, the related report is very limited. It was reported that acute inflammatory response cause by lipopolysaccharides (LPS) injection suppressed growth performance and altered bone homeostasis, significantly decreasing body weight, breast weight and tibial breaking strength (Mireles, et al., 2005). Given all

this, studies have successfully identified osteoclast-activating immune response, and the term 'osteoimmunology' has been used to describe the close interface between bone homeostasis and immune response (Kamibayashi, et al., 1995; Solomon, et al., 2018). However, avian species carry many uniqueness in bone and immune characteristics, such as pneumatic bones, the maturation of B cells in avian species which occur in bursa of Fabricius instead of bone marrow, and the medullary bone and egg production. Therefore, avian osteoimmunological interaction is possible to be different from mammal species. There is a need for better understanding of bone strength in poultry because bone breakage and associated infections contribute to mortality, low productivity, and carcass condemnations.

Coccidiosis and Broilers Bone Integrity

Coccidias infection is one of the most economically important diseases of the poultry industry worldwide. *Eimeria*, the protozoan parasite that causes coccidiosis in many species, can infect the cells of the digestive tract and causes severe intestinal damage that leads to the intestinal lesion, inflammation, and malabsorption of nutrients (Yun, 2000). Nutrition deficiency could reduce the usability of energy, vitamin, animal acid and minerals that directly impact bone health. Energy metabolic status has a direct impact on bone formation (Dirckx, et al., 2019). Bone loss caused by *Eimeria spp.* in broilers has been linked to nutrition malabsorption, especially the reduced absorption of calcium, phosphate, several important trace minerals and essential vitamins (Turk and Stephens, 1967; Turk and Stephens, 1969; Turk and Stephens, 1970; Turk, 1973; Joyner, et al., 1975; Southern and Baker, 1983). From a nutritional aspect, coccidia infects the

duodenum and jejunum, the major sites of minerals absorption, including calcium, phosphorous, zinc, copper and magnesium (Southern and Baker, 1983; Ward, et al., 1990; Ward, et al., 1993). Serum calcium and phosphate homeostasis directly impacts bone health and is associated with bone modeling or remodeling status. Reduced calcium absorption was reported in broilers infected with *E. acervulina*, *E. necatrix*, and *E. brunetti* (Turk, 1973). *E. maxima* infection impaired calcium and phosphate status in broilers (Oikeh, et al., 2019). Other than calcium and phosphate, supplements with microminerals such as manganese, zinc, and copper modulate inflammation and improve intestinal integrity in broilers during coccidiosis (Bortoluzzi, et al., 2019; Bortoluzzi, et al., 2020). Supplements with vitamin E and selenium can reduced mortality and increased body weight gain in chickens infected with *E. tenella* (Colnago, et al., 1984). These essential trace minerals are also essential in controlling oxidative stress. Zinc and copper as antioxidants can directly stimulate osteoblastogenesis and suppresses osteoclastogenesis (Rodriguez, et al., 2002; Yamaguchi and Weitzmann, 2011; Dirckx, et al., 2019). Therefore, trace mineral deficiency has been associated with the pathophysiological status of human bone (Guo, et al., 2011). Besides dietary mineral factors, growth and maintenance of bone homeostasis require vitamins (Erasmus, et al., 1960; Panda, et al., 1964; Ruff, et al., 1974; Southern and Baker, 1983). Proper vitamin supplementation is essential to bone homeostasis have been reported deficiencies caused by coccidian protozoa infection (Allen, et al., 1998). Vitamin K supplement reduced mortality from *E. tenella* infection (Harms, et al., 1962). Vitamin K is necessary for bone formation and mineralization, and the supplement of vitamin K can improve bone quality

by increasing bone mineral content and breaking strength in broilers (Zhang, et al., 2003; Guo, et al., 2020). *In vitro* studies indicated that vitamin K stimulates osteogenesis and promotes osteoblast differentiation in human and mouse cell lines (Akbari and Rasouli-Ghahroudi, 2018). Additional vitamin C supplementation during *Eimeria* infection improved broiler weight gain (Webber and Frigg, 1991; McKee and Harrison, 1995). Vitamin C (ascorbic acid) is essential for collagen synthesis and benefits bone matrix formation (Chin and Ima-Nirwana, 2018). Ascorbic acid is one of the essential ingredients in the osteogenesis medium of MSCs cell culture, it can stimulate cell proliferation, and accelerate osteogenesis by increased collagen secretion (Langenbach and Handschel, 2013; Fujisawa, et al., 2018). Vitamin C positively affected trabecular bone formation by altering osteoblastic bone matrix gene expression (Aghajanian, et al., 2015). Vitamin C also inhibits osteoclastogenesis and activates osteoblastogenesis by mediating the WNT pathway (Choi, et al., 2019). Vitamin C deficiency accelerated bone loss and increased PPAR-γ expression (adipogenesis pathway), which indicated that the bone formation was shifted towards fat formation (Park, et al., 2012). Moreover, *Eimeria* infection also decreases the fat digestibility. Suppressing fat absorption resulted in depressing fat-soluble vitamins level (Gautier, et al., 2019; Sakkas, et al., 2019), such as Vitamin E, vitamin A and vitamin D (Turk and Stephens, 1967; Turk and Stephens, 1969; Turk and Stephens, 1970; Turk, 1973; Joyner, et al., 1975; Southern and Baker, 1983). Vitamin E and selenium supplements improved weight gain and reduced mortality with *E. tenella* infection in broilers (Colnago, et al., 1984). Vitamin D is essential for calcium absorption and bone mineralization in broilers, and the supplementation of

vitamin D can improve bone quality (Laird, et al., 2010). During the infection, osteoclastic endocrine hormones such as calcitonin, parathyroid hormone (PTH) and Vitamin D could be affected by *Eimeria* infection. However, additional supplementation of vitamin D could increase *Eimeria* replication and could negatively impact intestinal health for long-term treatment (Oikeh, et al., 2019; Sakkas, et al., 2019).

The modern broiler strain is characterized by relatively higher porosity and lower mineral content in long bones due to the selection for rapid growth rate in broiler production (Thorp, 1994; Cook, 2000). Broiler leg bone exhibits frangibility under the infection with *Eimeria* parasites and leads to poor welfare in broilers (Kestin, et al., 1992; Sakkas, et al., 2018; Oikeh, et al., 2019). With increasing concerns around farm animal welfare, and the popularity of antibiotic growth promoter (AGP) free diets, poultry bone physical abnormalities or leg weakness encounter the challenge from both animal welfare and economic aspects. A better understanding of bone homeostasis is valuable to unveil the possible solution for the industry issue. Moreover, it provides a good model to understand the relationship between inflammation and skeletal development during acute intestinal infection.

Infections of coccidia significantly reduced tibia bone ash content and adversely affected femur breaking strength (Sakkas, et al., 2019). Sporozoites of some species, especially *E. acervulina* and *E. maxima,* could decreased bone mineral content (BMC) and showed a lower bone mineral density (BMD) in infected broilers (Fetterer, et al., 2013). Besides, bone growth and structure studies demonstrated an overlap between rapid bone formation (growth period: days 4 to 11, and mineralization

period: day 4 to18) and field outbreaks of coccidiosis (normally around 3 weeks of age) (Williams, et al., 2000; Musa, et al., 2010), the retardation of growth might be associate with the suppressed bone formation during the early age. To date, research has been predominantly concerned with bone low quality attribute to the nutrition deficient (Turk, 1973; Southern and Baker, 1983; Ward, et al., 1990; Ward, et al., 1993). In contrast, relatively little data exist on the underlying mechanisms that immune response and oxidative stress during coccidia. While coccidiosis affects chickens of all ages, the negative impacts of coccidiosis was more severe in young age birds due to their immature immune system (Fatoba and Adeleke, 2018). Emerging evidence suggested the increased bone resorption was involved in the alteration of skeletal homeostasis during disease (Frost, 1994; Allen and Burr, 2014). In poultry studies, Kakhki and etc. have reported *Eimeria* had adverse effects on long bone attributes linked bone remodeling (Akbari Moghaddam Kakhki, et al., 2019). Increasing expression of TNF-α, IL-1 IL-9, IFN-γ and CD8-expressing T cells are response to *Eimeria* challenged in chickens (Mireles, et al., 2005). Those cytokines have been well understood in the human osteoimmunology, but the link between them and bone homeostasis were rarely well understood in avian species. It encouraged us to focus on the immunology response and other possible co-factors on bone integrity during pathogen infection.

Fish oil which enriches n-3 polyunsaturated fatty acids (n-3 PUFA) is widely accepted as an nature anti-inflammatory component (Calder, 2006; Kalinski, 2012; Xiang, et al., 2016), and has an intestinal barrier-protective effect in animal studies (Lauridsen, 2020; Durkin, et al., 2021). LC n-3 PUFA can be incorporated into intestinal

epithelial cell membranes, reduce the production of pro-inflammatory cytokines and induce the production of anti-inflammatory factors (Calder, 2006; Durkin, et al., 2021). DHA supplementation was shown to ease the severity of necrosis under pathogen challenges in mice (Lu, et al., 2007). EPA and DHA have been shown to reduce stress and improve barrier integrity in wean piglets or under pathogen challenges (Zhu, et al., 2016; Lee, et al., 2019; Lauridsen, 2020). In poultry studies, several investigations have shown that a dietary n-3 PUFA enriched diet significantly reduced broiler cecal lesions caused by *Eimeria tenella* (Allen, et al., 1996; Barua, et al., 2016). Moreover, several studies have reported the positive impact pf n-3 PUFA on poultry bone health (Ebeid, et al., 2011; Tompkins, et al., 2022a). Our previous studies indicated that maternal fish oil supplements benefit bone health in offspring. Therefore, with the anti-inflammatory character, the fish oil was used as nutrition supplement during coccidiosis in our study, aim to better understand the possible link between intestinal inflammation and bone homeostasis during pathogen challenge.

Oxidative Stress and Bone Integrity

Modern commercial poultry production is strictly operated based on balanced nutrition and optimized environmental conditions. However, oxidative stress can be commonly found in production systems due to nutritional factors such as feed toxins or insufficient antioxidant supplements, pathogens infection, and poor environmental conditions including heat stress, ammonia exposure, and flock density (Mishra and Jha, 2019; Ali Hassan and Li, 2021). Oxidative stress has become one of the important effects on broiler performance, healthy growth, and production quality (Celi and Chauhan, 2013;

K. Panda and Cherian, 2014; Estevez, 2015; Mishra and Jha, 2019; Surai, et al., 2019). Oxidative stress represents an unbalanced condition between the production of reactive oxygen species (ROS) and the antioxidant defense systems (Sies, et al., 2017). In broiler production, other than the management-associated physiological oxidative stress, infectious agents are other factors that robustly cause phagocytic ROS generation, which leads to severe oxidative stress in broilers (Zorov, et al., 2014; Forrester, et al., 2018). Oxidative stress was also detected during phagocytosis in *Eimeria* infection. During the robust innate response, immune cells such as macrophages and neutrophils could rapidly release of the reactive oxygen species (ROS) from different cell types, including superoxide anion (O^{-}_{2}), nitric oxide (NO) and hydrogen peroxide (H_2O_2), and implicate the oxidative burst after in contact with pathogens (Laurent, et al., 2001; Kim, et al., 2019). Coccidiosis can cause severe oxidative stress that elevates intracellular levels of ROS in not just broilers but also wild birds and rabbits (Sepp, et al., 2012; Abdel-Haleem, et al., 2017). The first line defense enzymatic antioxidants, such as catalase (CAT), superoxide dismutase (SOD), and glutathione peroxidase (GPX), are indispensable in the defense system and protect from the damage that caused by free radicals especially superoxide anion radicals during *Eimeria* infection (Georgieva, et al., 2006). A marked increase in serum NO level was detected in chicken with coccidiosis (Laurent, et al., 2001). The activities of the parasite infection and the response from immune system that cause a depletion of antioxidant enzymes, reduced glutathione (GSH) level, and increased lipid peroxidation and apoptosis of intestinal cells, affecting the health status and productivity of poultry (Gotep, et al., 2016). Meanwhile, due to the

lesion in the intestine, the absorption of certain antioxidant amino acids, such as arginine, cysteine, glutamine and glutathione, was significantly interrupted (Gómez-Osorio, et al., 2021). Several studies indicated that tibia minerals in broilers were not influenced by trace minerals supplementation during *Eimeria* infection, but trace mineral supplementing can alter the adverse effect of oxidative stress and improve bone-breaking strength (Fernandes Müller, et al., 2019; Santos, et al., 2020). In addition, the vitamin level decreased during adverse conditions of a nutritional and pathological nature (Challey, 1960). Vitamin studies showed that the supplementation of vitamin E with selenium can reduce the mortality rate with *E. tellena* infection (Allen, et al., 1998). The systemic changed ROS level could induce oxidative stress in the bone marrow and effect bone homeostasis during *Eimeria* infection (Tompkins, et al., 2022b). Studies in rodent indicated that the oxidative stress response results in an inhibition of mineralization and osteogenesis and activation of bone resorption, subsequently causing bone loss and structural changes (Basu, et al., 2001; Domazetovic, et al., 2017). Oxidation-reduction (redox) homeostasis is ubiquitous to living cells, tissues, organs, and whole systems. Oxidative stress has been associated with many bone-related diseases in humans and mammals (Reis and Ramos, 2021). The redox state changes are also related to the bone remodeling process by alternate continuous bone regeneration through the coordinated activation or inactivation of bone cells (Georgieva, et al., 2006; Georgieva, et al., 2011; Gautier, et al., 2019). However, the study focusing on the direct relationship between oxidative stress during *Eimeria* infection and bone health in broilers is limited.

Understanding oxidative stress with in *vitro*, in *vivo* and in *ovo* models are essential for understanding and dealing with challenges from poultry leg diseases. Tibial dyschondroplasia (TD) and bacterial osteomyelitis (BCO) are two of the most common skeletal abnormalities. In previous studies, BCO appears to be initiated by mechanical micro-fracturing of the growth plate, followed by colonization and distribution of opportunistic bacteria that lead to necrosis (Wideman, 2016). Although there is no direct evidence to demonstrate the link between oxidative stress and BCO pathogenesis, the pathology of osteomyelitis, a local infection of the human bone which characterized by severe inflammation, and localized bone mineral loss and structure destruction, sharing the pathogenic similarlity with chicken BCO (Grbic, et al., 2014). It has been associated with significantly increased oxidative stress levels in response to infections in chronic osteomyelitis patients, as compared to the healthy controls (Jyoti, et al., 2015; Massaccesi, et al., 2022). Besides, studies in broiler BCO also indicated the mitochondrial oxidative metabolism and dysfunction is involved in BCO model in broilers (Ferver, et al., 2021). Therefore, by gathering and analyzing all the evidences, we hypothesized that oxidative stress could potentially be one of the pathogenic co-factors involved in the chicken BCO. Moreover, tibial dyschondroplasia (TD) is another common bone abnormalities in fast-growing broilers, which is characterized by difficulty in standing, growth retardation, and tibial bone deformities with non-vascular and non-mineralized TGP (Mehmood, et al., 2017; Zhang, et al., 2019b). It is a chondrogenesis disease highly associated with inhibition of bone angiogenesis and cell apoptosis, resulting in suppressed growth plate development (Mehmood, 2018). There is an

established relationship between tibial dyschondroplasia and oxidative stress induced by thiram because thiram causes TD in broilers by reducing liver antioxidation capability and damaging liver function (Li, et al., 2007a). TD impacts bone integrity and is associated with changed morphology and decreased meat quality, which both are connected with the increased systemic activity of antioxidant enzymes (Zhang, et al., 2018; Huang, et al., 2021). Therefore, based on the current information, we also hypothesize that TD may be partially associated with systemic oxidative stress; the inhibition of osteoblast activity by oxidative stress could be another factor causing the deformation of the growth plate. But more profound studies are in need.

Moreover, H_2O_2 is a by-product of glycerol metabolism in mycoplasmas. The *M. pneumoniae* produces H_2O_2 and superoxide radicals, which induce oxidative stress in the respiratory epithelium and can directly affect bone metabolism (Shimizu, 2016). Clinical signs of infection with *M. synoviae* are more severe, and the infection of *M synoviae* is associated with joint lesions in avian species (Osorio, et al., 2007). However, more evidence is need to explain the pathogenicity of Mycoplasmas on bone mineral density and bone integrity. Although many questions remain, ever-growing numbers of observations regarding chicken bone disorders and avian bone health rapidly shape our understanding of various topics, such as metabolic regulation and pathogenesis of bone disorders in broilers (Porto, et al., 2015). The knowledge of antioxidant defense systems will serve as the guiding principle for establishing the most effective nutrition support to minimize oxidative stress. Such an approach will enhance chicken health, welfare, and product quality, increasing economic returns and the sustainability of poultry production.

With growing numbers of observations regarding chicken bone, we conducted a serial study and aimed to provide more evidences to improve chicken bone health and production quality.

The main objectives of this study were:

1: To understand the role of oxidative stress in broiler bone formation.

2: To better understand the bone homeostasis under pathogenic infection disease model.

3: To explore the multifunctional roles of bone in growth and disease.

References

Abdel-Haleem, H. M., S. M. Aboelhadid, T. Sakran, G. El-Shahawy, H. El-Fayoumi, S. Al-Quraishy, and A. S. Abdel-Baki. 2017. Gene expression, oxidative stress and apoptotic changes in rabbit ileum experimentally infected with Eimeria intestinalis. Folia Parasitol. (Praha) 64.

Aghajanian, P., S. Hall, M. D. Wongworawat, and S. Mohan. 2015. The Roles and Mechanisms of Actions of Vitamin C in Bone: New Developments. J Bone Miner Res 30:1945-1955.

Aguado, E., F. Pascaretti-Grizon, E. Goyenvalle, M. Audran, and D. Chappard. 2015. Bone mass and bone quality are altered by hypoactivity in the chicken. PLoS One 10:e0116763.

Akbari Moghaddam Kakhki, R., Z. Lu, A. Thanabalan, H. Leung, M. Mohammadigheisar, and E. Kiarie. 2019. Eimeria challenge adversely affected long bone attributes linked to increased resorption in 14-day-old broiler chickens. Poult Sci 98:1615-1621.

Akbari, S., and A. A. Rasouli-Ghahroudi. 2018. Vitamin K and Bone Metabolism: A Review of the Latest Evidence in Preclinical Studies. Biomed Res Int 2018:4629383.

Ali Hassan, N., and Z. Li. 2021. Oxidative stress in broiler chicken and its consequences on meat quality. International Journal of Life Science Research Archive 1:045-054.

Allen, M. R., and D. B. Burr. 2014. Bone Modeling and Remodeling. Pages 75-90 in Basic and Applied Bone Biology.

Allen, P. C., H. D. Danforth, and P. C. Augustine. 1998. Dietary modulation of avian coccidiosis. International Journal for Parasitology 28:1131-1140.

Almeida Paz, I. C. L., A. A. Mendes, T. S. Takita, L. C. Vulcano, P. C. Guerra, F. S. Wechsler, R. G. Garcia, S. E. Takahashi, J. Moreira, K. Pelícia, C. M. Komiyama, and R. R. Quinteiro. 2005. Comparison of techniques for tibial dyschondroplasia assessment in broiler chickens. Revista Brasileira de Ciência Avícola 7:27-31.

Applegate, T. J., and M. S. Lilburn. 2002. Growth of the femur and tibia of a commercial broiler line. Poult Sci 81:1289-1294.

Bailey, R. A., E. Souza, and S. Avendano. 2020. Characterising the Influence of Genetics on Breast Muscle Myopathies in Broiler Chickens. Front Physiol 11:1041.

Basu, S., K. Michaelsson, H. Olofsson, S. Johansson, and H. Melhus. 2001. Association between oxidative stress and bone mineral density. Biochem Biophys Res Commun 288:275-279.

Bedimo, R. J., B. Adams-Huet, J. Poindexter, G. Brown, I. Farukhi, R. Castanon, D. Turner, T. Moore, P. Tebas, and N. M. Maalouf. 2018. The Differential Effects of Human Immunodeficiency Virus and Hepatitis C Virus on Bone Microarchitecture and Fracture Risk. Clin Infect Dis 66:1442-1447.

Beedles, K. E., P. T. Sharpe, E. F. Wagner, and A. E. Grigoriadis. 1999. A putative role for c-Fos in the pathophysiology of Paget's disease. J Bone Miner Res 14 Suppl 2:21-28.

Bihan-Duval, E. L., C. Beaumont, and J. J. Colleau. 1997. Estimation of the genetic correlations between twisted legs and growth or conformation traits in broiler chickens. J Anim Breed Genet 114:239-259.

Bilkovski, R., D. M. Schulte, F. Oberhauser, M. Gomolka, M. Udelhoven, M. M. Hettich, B. Roth, A. Heidenreich, C. Gutschow, W. Krone, and M. Laudes. 2010. Role of WNT-5a in the determination of human mesenchymal stem cells into preadipocytes. J Biol Chem 285:6170-6178.

Bjornerem, A. 2016. The clinical contribution of cortical porosity to fragility fractures. Bonekey Rep 5:846.

Bolamperti, S., I. Villa, and A. Rubinacci. 2022. Bone remodeling: an operational process ensuring survival and bone mechanical competence. Bone Res 10:48.

Bortoluzzi, C., B. Lumpkins, G. F. Mathis, M. Franca, W. D. King, D. E. Graugnard, K. A. Dawson, and T. J. Applegate. 2019. Zinc source modulates intestinal inflammation and intestinal integrity of broiler chickens challenged with coccidia and Clostridium perfringens. Poult Sci 98:2211-2219.

Bortoluzzi, C., B. S. Vieira, and T. J. Applegate. 2020. Influence of Dietary Zinc, Copper, and Manganese on the Intestinal Health of Broilers Under Eimeria Challenge. Front Vet Sci 7:13.

Boyce, B. F., and L. Xing. 2008. Functions of RANKL/RANK/OPG in bone modeling and remodeling. Arch Biochem Biophys 473:139-146.

Boyce, B. F., Z. Yao, and L. Xing. 2009. Osteoclasts have multiple roles in bone in addition to bone resorption. Crit Rev Eukaryot Gene Expr 19:171-180.

Boyle, W. J., W. S. Simonet, and D. L. Lacey. 2003. Osteoclast differentiation and activation. Nature 423:337-342.

Brennan-Speranza, T. C., and A. D. Conigrave. 2015. Osteocalcin: an osteoblast-derived polypeptide hormone that modulates whole body energy metabolism. Calcif Tissue Int 96:1-10.

Çapar Akyüz, H., and E. E. Onbaşılar. 2020. Non-infectious skeletal disorders in broilers. World's Poultry Science Journal 76:611-623.

Celi, P., and S. Chauhan. Year. Oxidative stress management in farm animals: opportunities and challenges. Proc. Proceedings of the 4th International Conference on Sustainable Animal Agriculture for Developing Countries (SAADC).

Challey, J. R. J. T. J. o. P. 1960. The effect of cecal coccidiosis infections and experimental hemorrhage upon adrenal ascorbic acid levels in the chicken. 46:727-731.

Chatakun, P., R. Nunez-Toldra, E. J. Diaz Lopez, C. Gil-Recio, E. Martinez-Sarra, F. Hernandez-Alfaro, E. Ferres-Padro, L. Giner-Tarrida, and M. Atari. 2014. The effect of five proteins on stem cells used for osteoblast differentiation and proliferation: a current review of the literature. Cell Mol Life Sci 71:113-142.

Chin, K. Y., and S. Ima-Nirwana. 2018. Vitamin C and Bone Health: Evidence from Cell, Animal and Human Studies. Curr Drug Targets 19:439-450.

Choi, H. K., G. J. Kim, H. S. Yoo, D. H. Song, K. H. Chung, K. J. Lee, Y. T. Koo, and J. H. An. 2019. Vitamin C Activates Osteoblastogenesis and Inhibits Osteoclastogenesis via Wnt/beta-Catenin/ATF4 Signaling Pathways. Nutrients 11.

Clarke, B. 2008. Normal bone anatomy and physiology. Clin J Am Soc Nephrol 3 Suppl 3:S131-139.

Colnago, G. L., L. S. Jensen, and P. L. Long. 1984. Effect of selenium and vitamin E on the development of immunity to coccidiosis in chickens. Poult Sci 63:1136-1143.

Cook, M. E. 2000. Skeletal deformities and their causes: introduction. Poult Sci 79:982-984.

Cook, M. E., Y. Bai, and M. W. Orth. 1994. Factors influencing growth plate cartilage turnover. Poult Sci 73:889-896.

de Jong, I., C. Berg, A. Butterworth, and I. Estevéz. 2012. Scientific report updating the EFSA opinions on the welfare of broilers and broiler breeders. EFSA Supporting Publications 9.

de Oliveira, H. C., A. M. G. Ibelli, S. E. F. Guimaraes, M. E. Cantao, J. O. Peixoto, L. L. Coutinho, and M. C. Ledur. 2020. RNA-seq reveals downregulated osteochondral genes potentially related to tibia bacterial chondronecrosis with osteomyelitis in broilers. BMC Genet 21:58.

Dent, P. B., D. M. Brown, and R. A. Good. 1969. Ultimobranchial calcitonin in the developing chicken. Endocrinology 85:582-585.

Dilworth, B. C., and E. J. Day. 1965. Effect of varying dietary calcium: phosphorus ratios on tibia and femur composition of the chick. Poult Sci 44:1474-1479.

Dirckx, N., M. C. Moorer, T. L. Clemens, and R. C. Riddle. 2019. The role of osteoblasts in energy homeostasis. Nat Rev Endocrinol 15:651-665.

Dobnig, H., and R. T. Turner. 1995. Evidence that intermittent treatment with parathyroid hormone increases bone formation in adult rats by activation of bone lining cells. Endocrinology 136:3632-3638.

Domazetovic, V., G. Marcucci, T. Iantomasi, M. L. Brandi, and M. T. Vincenzini. 2017. Oxidative stress in bone remodeling: role of antioxidants. Clin Cases Miner Bone Metab 14:209-216.

Ducy, P., R. Zhang, V. Geoffroy, A. L. Ridall, and G. Karsenty. 1997. Osf2/Cbfa1: A Transcriptional Activator of Osteoblast Differentiation. Cell 89:747-754.

Erasmus, J., M. L. Scott, and P. P. Levine. 1960. A Relationship Between Coccidiosis and Vitamin A Nutrition in Chickens. Poultry Science 39:565-572.

Eriksen, E. F. 1986. Normal and pathological remodeling of human trabecular bone: three dimensional reconstruction of the remodeling sequence in normals and in metabolic bone disease. Endocr Rev 7:379-408.

Estevez, M. 2015. Oxidative damage to poultry: from farm to fork. Poult Sci 94:1368-1378.

Farquharson, C., and D. Jefferies. 2000. Chondrocytes and longitudinal bone growth: the development of tibial dyschondroplasia. Poult Sci 79:994-1004.

Fatoba, A. J., and M. A. Adeleke. 2018. Diagnosis and control of chicken coccidiosis: a recent update. J Parasit Dis 42:483-493.

Feng, X., and J. M. McDonald. 2011. Disorders of bone remodeling. Annu Rev Pathol 6:121-145.

Fernandes Müller, I. J., M. Ribeiro Vissotto, L. Cardoso Bittencourt, T. E. Riffel, F. Lima Kaiser, S. Palma Castro, and G. R. Hermes. 2019. Mineral supplementation: effects on bone integrity and intestinal morphometry of broiler chickens challenged with Eimeria sp. Acta Vet. Brno. 69:88-105.

Ferver, A., E. Greene, R. Wideman, and S. Dridi. 2021. Evidence of Mitochondrial Dysfunction in Bacterial Chondronecrosis With Osteomyelitis-Affected Broilers. Front Vet Sci 8:640901.

Fetterer, R. H., K. B. Miska, A. D. Mitchell, and M. C. Jenkins. 2013. The use of dual-energy X-ray absorptiometry to assess the impact of Eimeria infections in broiler chicks. Avian Dis 57:199-204.

Forrester, S. J., D. S. Kikuchi, M. S. Hernandes, Q. Xu, and K. K. Griendling. 2018. Reactive Oxygen Species in Metabolic and Inflammatory Signaling. Circ Res 122:877-902.

Franz-Odendaal, T. A., B. K. Hall, and P. E. Witten. 2006. Buried alive: how osteoblasts become osteocytes. Dev Dyn 235:176-190.

Frost, H. M. 1994. Wolff's Law and bone's structural adaptations to mechanical usage: an overview for clinicians. Angle Orthod 64:175-188.

Fujisawa, K., K. Hara, T. Takami, S. Okada, T. Matsumoto, N. Yamamoto, and I. Sakaida. 2018. Evaluation of the effects of ascorbic acid on metabolism of human mesenchymal stem cells. Stem Cell Res Ther 9:93.

Furuya, Y., K. Mori, T. Ninomiya, Y. Tomimori, S. Tanaka, N. Takahashi, N. Udagawa, K. Uchida, and H. Yasuda. 2011. Increased bone mass in mice after single injection of anti-receptor activator of nuclear factor-kappaB ligand-neutralizing antibody: evidence for bone anabolic effect of parathyroid hormone in mice with few osteoclasts. J Biol Chem 286:37023-37031.

Galindo, M., J. Pratap, D. W. Young, H. Hovhannisyan, H. J. Im, J. Y. Choi, J. B. Lian, J. L. Stein, G. S. Stein, and A. J. van Wijnen. 2005. The bone-specific expression of Runx2 oscillates during the cell cycle to support a G1-related antiproliferative function in osteoblasts. J Biol Chem 280:20274-20285.

Gautier, A. E., J. D. Latorre, P. L. Matsler, and S. J. Rochell. 2019. Longitudinal Characterization of Coccidiosis Control Methods on Live Performance and Nutrient Utilization in Broilers. Front Vet Sci 6:468.

Georgieva, N. V., M. Gabrashanska, V. Koinarski, and Z. Yaneva. 2011. Zinc Supplementation against Eimeria acervulina-Induced Oxidative Damage in Broiler Chickens. Vet. Med. Int. 2011:647124.

Georgieva, N. V., V. Koinarski, and V. Gadjeva. 2006. Antioxidant status during the course of Eimeria tenella infection in broiler chickens. Vet J 172:488-492.

Gibon, E., L. Y. Lu, K. Nathan, and S. B. Goodman. 2017. Inflammation, ageing, and bone regeneration. J Orthop Translat 10:28-35.

Gilley, A. D., H. Lester, I. Y. Pevzner, N. B. Anthony, and R. F. Wideman, Jr. 2014. Evaluating portable wire-flooring models for inducing bacterial chondronecrosis with osteomyelitis in broilers. Poult Sci 93:1354-1367.

Gómez-Osorio, L.-M., J.-J. Chaparro-Gutiérrez, and S. J. A. i. P. N. R. López-Osorio. 2021. Nutrition and Poultry Coccidiosis: Causes, Consequences and Current Strategies to Modulate the.161.

Gong, J. K., J. S. Arnold, and S. H. Cohn. 1964. Composition of Trabecular and Cortical Bone. Anat Rec 149:325-331.

González-Cerón, F., R. Rekaya, and S. E. Aggrey. 2015. Genetic relationship between leg problems and bone quality traits in a random mating broiler population. Poultry Science 94:1787-1790.

Gotep, J. G., J. T. Tanko, G. E. Forcados, I. A. Muraina, N. Ozele, B. B. Dogonyaro, O. O. Oladipo, M. S. Makoshi, O. B. Akanbi, H. Kinjir, A. L. Samuel, T. E. Onyiche, G. O. Ochigbo, O. B. Aladelokun, H. A. Ozoani, V. Z. Viyoff, C. C. Dapuliga, A. A. Atiku, P. A. Okewole, D. Shamaki, M. S. Ahmed, and C. I. Nduaka. 2016. Therapeutic and Safety Evaluation of Combined Aqueous Extracts of Azadirachta indica and Khaya senegalensis in Chickens Experimentally Infected with Eimeria Oocysts. J Parasitol Res 2016:4692424.

Grabowski, P. 2009. Physiology of bone. Endocr Dev 16:32-48.

Granquist, E. G., G. Vasdal, I. C. de Jong, and R. O. Moe. 2019. Lameness and its relationship with health and production measures in broiler chickens. Animal 13:2365-2372.

Grbic, R., D. J. Miric, B. Kisic, L. Popovic, V. Nestorovic, and A. Vasic. 2014. Sequential analysis of oxidative stress markers and vitamin C status in acute bacterial osteomyelitis. Mediators Inflamm 2014:975061.

Guo, C. H., P. J. Liu, S. Hsia, C. J. Chuang, and P. C. Chen. 2011. Role of certain trace minerals in oxidative stress, inflammation, CD4/CD8 lymphocyte ratios and lung function in asthmatic patients. Ann Clin Biochem 48:344-351.

Guo, S., J. Xv, Y. Li, Y. Bi, Y. Hou, and B. Ding. 2020. Interactive effects of dietary vitamin K3 and Bacillus subtilis PB6 on the growth performance and tibia quality of broiler chickens with sex separate rearing. Animal:1-9.

Hambli, R. 2014. Connecting mechanics and bone cell activities in the bone remodeling process: an integrated finite element modeling. Front Bioeng Biotechnol 2:6.

Han, Y., X. You, W. Xing, Z. Zhang, and W. Zou. 2018. Paracrine and endocrine actions of bone-the functions of secretory proteins from osteoblasts, osteocytes, and osteoclasts. Bone Res 6:16.

Hardy, R. S., H. Zhou, M. J. Seibel, and M. S. Cooper. 2018. Glucocorticoids and Bone: Consequences of Endogenous and Exogenous Excess and Replacement Therapy. Endocr Rev 39:519-548.

Harms, R. H., P. W. Waldroup, and D. D. Cox. 1962. Activity of Vitamin K1 and Menadione Sodium Bisulfite Complex When Measured by Mortality of Chicks with Cecal Coccidiosis. Poultry Science 41:1836-1839.

Heino, T. J., T. A. Hentunen, and H. K. Vaananen. 2002. Osteocytes inhibit osteoclastic bone resorption through transforming growth factor-beta: enhancement by estrogen. J Cell Biochem 85:185-197.

Huang, H., E. J. Chang, J. Ryu, Z. H. Lee, Y. Lee, and H. H. Kim. 2006. Induction of c-Fos and NFATc1 during RANKL-stimulated osteoclast differentiation is mediated by the p38 signaling pathway. Biochem Biophys Res Commun 351:99-105.

Huang, S., A. Kong, Q. Cao, Z. Tong, and X. Wang. 2019. The role of blood vessels in broiler chickens with tibial dyschondroplasia. Poult Sci 98:6527-6532.

Huang, S. C., Q. Q. Cao, Y. B. Cao, Y. R. Yang, T. T. Xu, K. Yue, F. Liu, Z. X. Tong, and X. B. Wang. 2021. Morinda officinalis polysaccharides improve meat quality by reducing oxidative damage in chickens suffering from tibial dyschondroplasia. Food Chem 344:128688.

Huang, W., S. Yang, J. Shao, and Y. P. Li. 2007. Signaling and transcriptional regulation in osteoblast commitment and differentiation. Front Biosci 12:3068-3092.

Hughes, D. E., A. Dai, J. C. Tiffee, H. H. Li, G. R. Mundy, and B. F. Boyce. 1996. Estrogen promotes apoptosis of murine osteoclasts mediated by TGF-beta. Nat Med 2:1132-1136.

Indo, Y., S. Takeshita, K. A. Ishii, T. Hoshii, H. Aburatani, A. Hirao, and K. Ikeda. 2013. Metabolic regulation of osteoclast differentiation and function. J Bone Miner Res 28:2392-2399.

Isojima, T., and N. A. Sims. 2021. Cortical bone development, maintenance and porosity: genetic alterations in humans and mice influencing chondrocytes, osteoclasts, osteoblasts and osteocytes. Cellular and Molecular Life Sciences 78:5755-5773.

Itoh, H., and T. Hatano. 1964. Comparison of Calcium Metabolism in Various Bones of Growing Chicks in Varying States of Vitamin D Supplementation. Poultry Science 43:70-76.

Javed, A., J. S. Bae, F. Afzal, S. Gutierrez, J. Pratap, S. K. Zaidi, Y. Lou, A. J. van Wijnen, J. L. Stein, G. S. Stein, and J. B. Lian. 2008. Structural coupling of Smad and Runx2 for execution of the BMP2 osteogenic signal. J Biol Chem 283:8412-8422.

Jimi, E., I. Nakamura, T. Ikebe, S. Akiyama, N. Takahashi, and T. Suda. 1998. Activation of NF-kappaB is involved in the survival of osteoclasts promoted by interleukin-1. J Biol Chem 273:8799-8805.

Jordan, F. T. 1981. Mycoplasma-induced arthritis in poultry. Isr J Med Sci 17:622-625.

Joyner, L. P., D. S. Patterson, S. Berrett, C. D. Boarer, F. H. Cheong, and C. C. Norton. 1975. Amino-acid malabsorption and intestinal leakage of plasma-proteins in young chicks infected with Eimeria acervulina. Avian Pathol. 4:17-33.

Jyoti, A., S. Singh, B. Mukhopadhyay, R. Gavel, and S. P. Mishra. 2015. Free radicals and antioxidant status in chronic osteomyelitis patients: a case control study. J Clin Diagn Res 9:BC08-10.

K. Panda, A., and G. Cherian. 2014. Role of Vitamin E in Counteracting Oxidative Stress in Poultry. The Journal of Poultry Science 51:109-117.

Kamibayashi, L., U. P. Wyss, T. D. V. Cooke, and B. Zee. 1995. Trabecular microstructure in the medial condyle of the proximal tibia of patients with knee osteoarthritis. Bone 17:27-35.

Kazakia, G. J., J. Carballido-Gamio, A. Lai, L. Nardo, L. Facchetti, C. Pasco, C. A. Zhang, M. Han, A. H. Parrott, P. Tien, and R. Krug. 2018. Trabecular bone microstructure is impaired in the proximal femur of human immunodeficiency virus-infected men with normal bone mineral density. Quant Imaging Med Surg 8:5-13.

Kent, G. N., R. I. Price, D. H. Gutteridge, M. Smith, J. R. Allen, C. I. Bhagat, M. P. Barnes, C. J. Hickling, R. W. Retallack, S. G. Wilson, and et al. 1990. Human lactation: forearm trabecular bone loss, increased bone turnover, and renal conservation of calcium

and inorganic phosphate with recovery of bone mass following weaning. J Bone Miner Res 5:361-369.

Kestin, S. C., T. G. Knowles, A. E. Tinch, and N. G. Gregory. 1992. Prevalence of leg weakness in broiler chickens and its relationship with genotype. Vet Rec 131:190-194.

Khosla, S., J. J. Westendorf, and M. J. Oursler. 2008. Building bone to reverse osteoporosis and repair fractures. J Clin Invest 118:421-428.

Kim, C., and D. Park. 2013. The effect of restriction of dietary calcium on trabecular and cortical bone mineral density in the rats. Journal of Exercise Nutrition and Biochemistry 17:123-131.

Kim, W. H., A. A. Chaudhari, and H. S. Lillehoj. 2019. Involvement of T Cell Immunity in Avian Coccidiosis. Front Immunol 10:2732.

Kittelsen, K. E., B. David, R. O. Moe, H. D. Poulsen, J. F. Young, and E. G. Granquist. 2017. Associations among gait score, production data, abattoir registrations, and postmortem tibia measurements in broiler chickens. Poult Sci 96:1033-1040.

Kleven, S. H. 2008. Control of avian mycoplasma infections in commercial poultry. Avian Dis 52:367-374.

Kleven, S. H., and N. J. D. o. p. Ferguson-Noel. 2008. Mycoplasma synoviae infection. 12:845-856.

Knowles, T. G., S. C. Kestin, S. M. Haslam, S. N. Brown, L. E. Green, A. Butterworth, S. J. Pope, D. Pfeiffer, and C. J. Nicol. 2008. Leg disorders in broiler chickens: prevalence, risk factors and prevention. PLoS One 3:e1545.

Kollet, O., A. Dar, S. Shivtiel, A. Kalinkovich, K. Lapid, Y. Sztainberg, M. Tesio, R. M. Samstein, P. Goichberg, A. Spiegel, A. Elson, and T. Lapidot. 2006. Osteoclasts degrade endosteal components and promote mobilization of hematopoietic progenitor cells. Nat Med 12:657-664.

Kronenberg, H. M. 2003. Developmental regulation of the growth plate. Nature 423:332-336.

Kwan Tat, S., M. Padrines, S. Theoleyre, D. Heymann, and Y. Fortun. 2004. IL-6, RANKL, TNF-alpha/IL-1: interrelations in bone resorption pathophysiology. Cytokine Growth Factor Rev 15:49-60.

Laird, E., M. Ward, E. McSorley, J. J. Strain, and J. Wallace. 2010. Vitamin D and bone health: potential mechanisms. Nutrients 2:693-724.

Langdahl, B., S. Ferrari, and D. W. Dempster. 2016. Bone modeling and remodeling: potential as therapeutic targets for the treatment of osteoporosis. Ther Adv Musculoskelet Dis 8:225-235.

Langenbach, F., and J. Handschel. 2013. Effects of dexamethasone, ascorbic acid and beta-glycerophosphate on the osteogenic differentiation of stem cells in vitro. Stem Cell Res Ther 4:117.

Laurent, F., R. Mancassola, S. Lacroix, R. Menezes, and M. Naciri. 2001. Analysis of chicken mucosal immune response to Eimeria tenella and Eimeria maxima infection by quantitative reverse transcription-PCR. Infect Immun 69:2527-2534.

Leach, R. M., Jr., and E. Monsonego-Ornan. 2007. Tibial dyschondroplasia 40 years later. Poult Sci 86:2053-2058.

Lee, K. S., H. J. Kim, Q. L. Li, X. Z. Chi, C. Ueta, T. Komori, J. M. Wozney, E. G. Kim, J. Y. Choi, H. M. Ryoo, and S. C. Bae. 2000. Runx2 is a common target of transforming growth factor beta1 and bone morphogenetic protein 2, and cooperation between Runx2 and Smad5 induces osteoblast-specific gene expression in the pluripotent mesenchymal precursor cell line C2C12. Mol Cell Biol 20:8783-8792.

Lee, M. S. J., K. Maruyama, Y. Fujita, A. Konishi, P. M. Lelliott, S. Itagaki, T. Horii, J. W. Lin, S. M. Khan, E. Kuroda, S. Akira, K. J. Ishii, and C. Coban. 2017a. Plasmodium products persist in the bone marrow and promote chronic bone loss. Sci Immunol 2.

Lee, N. K., H. Sowa, E. Hinoi, M. Ferron, J. D. Ahn, C. Confavreux, R. Dacquin, P. J. Mee, M. D. McKee, D. Y. Jung, Z. Zhang, J. K. Kim, F. Mauvais-Jarvis, P. Ducy, and G. Karsenty. 2007. Endocrine regulation of energy metabolism by the skeleton. Cell 130:456-469.

Lee, W. C., A. R. Guntur, F. Long, and C. J. Rosen. 2017b. Energy Metabolism of the Osteoblast: Implications for Osteoporosis. Endocr Rev 38:255-266.

Leibbrandt, A., and J. M. Penninger. 2008. RANK/RANKL: regulators of immune responses and bone physiology. Ann N Y Acad Sci 1143:123-150.

Lemma, S., M. Sboarina, P. E. Porporato, N. Zini, P. Sonveaux, G. Di Pompo, N. Baldini, and S. Avnet. 2016. Energy metabolism in osteoclast formation and activity. Int J Biochem Cell Biol 79:168-180.

Li, J., D. Bi, S. Pan, and Y. Zhang. 2007. Effect of diet with thiram on liver antioxidant capacity and tibial dyschondroplasia in broilers. Br Poult Sci 48:724-728.

Lorenzo, J., M. Horowitz, and Y. Choi. 2008. Osteoimmunology: interactions of the bone and immune system. Endocr Rev 29:403-440.

Mackie, E. J., Y. A. Ahmed, L. Tatarczuch, K. S. Chen, and M. Mirams. 2008. Endochondral ossification: how cartilage is converted into bone in the developing skeleton. Int J Biochem Cell Biol 40:46-62.

Maddineni, S. R., S. M. Krzysik-Walker, O. M. Ocon-Grove, S. M. Motch, G. L. Hendricks, 3rd, and R. Ramachandran. 2007. Calcitonin is expressed in the chicken pituitary gland: influence of gonadal steroids and sexual maturation. Cell Tissue Res 327:521-528.

Massaccesi, L., E. Galliera, A. Pellegrini, G. Banfi, and M. M. Corsi Romanelli. 2022. Osteomyelitis, Oxidative Stress and Related Biomarkers. Antioxidants (Basel) 11.

McKee, J. S., and P. C. Harrison. 1995. Effects of supplemental ascorbic acid on the performance of broiler chickens exposed to multiple concurrent stressors. Poult Sci 74:1772-1785.

McNamee, P. T., and J. A. Smyth. 2000. Bacterial chondronecrosis with osteomyelitis ('femoral head necrosis') of broiler chickens: a review. Avian Pathol 29:253-270.

Mehmood, K. 2018. Tetramethylpyrazine Mitigates Toxicity and Liver Oxidative Stress in Tibial Dyschondroplasia Chickens. Pakistan Veterinary Journal 38:76-80.

Mehmood, K., H. Zhang, M. K. Iqbal, M. U. Rehman, M. Shahzad, K. Li, S. Huang, F. Nabi, L. Zhang, and J. Li. 2017. In Vitro Effect of Apigenin and Danshen in Tibial Dyschondroplasia Through Inhibition of Heat-Shock Protein 90 and Vascular Endothelial Growth Factor Expressions in Avian Growth Plate Cells. Avian Dis 61:372-377.

Miller, C. J., S. Trichilo, E. Pickering, S. Martelli, P. Delisser, L. B. Meakin, and P. Pivonka. 2021. Cortical Thickness Adaptive Response to Mechanical Loading Depends on Periosteal Position and Varies Linearly With Loading Magnitude. Front Bioeng Biotechnol 9:671606.

Mireles, A. J., S. M. Kim, and K. C. Klasing. 2005. An acute inflammatory response alters bone homeostasis, body composition, and the humoral immune response of broiler chickens. Poult Sci 84:553-560.

Mishra, B., and R. Jha. 2019. Oxidative Stress in the Poultry Gut: Potential Challenges and Interventions. Front Vet Sci 6:60.

Miyazaki, T., H. Katagiri, Y. Kanegae, H. Takayanagi, Y. Sawada, A. Yamamoto, M. P. Pando, T. Asano, I. M. Verma, H. Oda, K. Nakamura, and S. Tanaka. 2000. Reciprocal role of ERK and NF-kappaB pathways in survival and activation of osteoclasts. J Cell Biol 148:333-342.

Monier-Faugere, M. C., Z. Geng, Q. Qi, I. Arnala, and H. H. Malluche. 1996. Calcitonin prevents bone loss but decreases osteoblastic activity in ovariohysterectomized beagle dogs. J Bone Miner Res 11:446-455.

Möstl, E., and R. Palme. 2002. Hormones as indicators of stress. Domestic Animal Endocrinology 23:67-74.

Musa, I. W., L. Sa`idu, I. D. Jatau, J. Adamu, M. O. Otu, and P. A. Abdu. 2010. Outbreak of Coccidiosis in 5-day Old Commercial Broiler Breeder Flock in Zaria, Nigeria. International Journal of Poultry Science 9:1112-1115.

Neville-Webbe, H. L., N. A. Cross, C. L. Eaton, R. Nyambo, C. A. Evans, R. E. Coleman, and I. Holen. 2004. Osteoprotegerin (OPG) produced by bone marrow stromal cells protects breast cancer cells from TRAIL-induced apoptosis. Breast Cancer Res Treat 86:269-279.

Oftadeh, R., M. Perez-Viloria, J. C. Villa-Camacho, A. Vaziri, and A. Nazarian. 2015. Biomechanics and mechanobiology of trabecular bone: a review. J Biomech Eng 137.

Oikeh, I., P. Sakkas, D. P. Blake, and I. Kyriazakis. 2019. Interactions between dietary calcium and phosphorus level, and vitamin D source on bone mineralization, performance, and intestinal morphology of coccidia-infected broilers1. Poult Sci 98:5679-5690.

Olivares-Navarrete, R., S. L. Hyzy, D. L. Hutton, G. R. Dunn, C. Appert, B. D. Boyan, and Z. Schwartz. 2011. Role of non-canonical Wnt signaling in osteoblast maturation on microstructured titanium surfaces. Acta Biomater 7:2740-2750.

Olson, N. O., and K. M. Kerr. 1970. A Comparison of Radiographic Lesions in Pelvic Limbs of Chickens Infected with Mycoplasma gallisepticum, Mycoplasma synoviae, or an Arthritis-Producing Virus. Avian Diseases 14.

Orth, M. W., and M. E. Cook. 1994. Avian tibial dyschondroplasia: a morphological and biochemical review of the growth plate lesion and its causes. Vet Pathol 31:403-404.

Orth, M. W., J. I. Fenton, and K. A. Chlebek-Brown. 1999. Biochemical characterization of cartilage degradation in embryonic chick tibial explant cultures. Poult Sci 78:1596-1600.

Osorio, C., O. J. Fletcher, T. Abdul-Aziz, E. Gonder, B. Tilley, and D. H. Ley. 2007. Pneumonia of Turkey Breeder Hens Associated with Mycoplasma Synoviae. Avian Diseases 51:791-796.

Ott, S. M. 2018. Cortical or Trabecular Bone: What's the Difference? Am J Nephrol 47:373-375.

Panda, B., G. F. Combs, and H. M. DeVolt. 1964. Studies on Coccidiosis and Vitamin A Nutrition of Broilers. Poultry Science 43:154-164.

Parfitt, A. M. 1994. Osteonal and hemi-osteonal remodeling: the spatial and temporal framework for signal traffic in adult human bone. J Cell Biochem 55:273-286.

Park, J. H., N. K. Lee, and S. Y. Lee. 2017. Current Understanding of RANK Signaling in Osteoclast Differentiation and Maturation. Mol Cells 40:706-713.

Park, J. K., E. M. Lee, A. Y. Kim, E. J. Lee, C. W. Min, K. K. Kang, M. M. Lee, and K. S. Jeong. 2012. Vitamin C deficiency accelerates bone loss inducing an increase in PPAR-gamma expression in SMP30 knockout mice. Int J Exp Pathol 93:332-340.

Passi, N., and A. Gefen. 2005. Trabecular bone contributes to strength of the proximal femur under mediolateral impact in the avian. J Biomech Eng 127:198-203.

Peretz, A. M., J. A. Hipp, and M. H. Heggeness. 1998. The internal bony architecture of the sacrum. Spine (Phila Pa 1976) 23:971-974.

Phibbs, D. V., P. J. Groves, and W. I. Muir. 2021. Leg health of meat chickens: impact on welfare, consumer behaviour, and the role of environmental enrichment. Animal Production Science 61.

Porto, M. L., B. P. Rodrigues, T. N. Menezes, S. L. Ceschim, D. E. Casarini, A. L. Gava, T. M. Pereira, E. C. Vasquez, B. P. Campagnaro, and S. S. Meyrelles. 2015. Reactive oxygen species contribute to dysfunction of bone marrow hematopoietic stem cells in aged C57BL/6 J mice. J Biomed Sci 22:97.

Praul, C. A., B. C. Ford, C. V. Gay, M. Pines, and R. M. Leach. 2000. Gene expression and tibial dyschondroplasia. Poult Sci 79:1009-1013.

Rath, N. C., and V. Durairaj. 2022. Avian bone physiology and poultry bone disorders. Pages 529-543 in Sturkie's Avian PhysiologyElsevier.

Reis, J., and A. Ramos. 2021. In Sickness and in Health: The Oxygen Reactive Species and the Bone. Front Bioeng Biotechnol 9:745911.

Rekaya, R., R. L. Sapp, T. Wing, and S. E. Aggrey. 2013. Genetic evaluation for growth, body composition, feed efficiency, and leg soundness. Poult Sci 92:923-929.

Riddle, R. C., and T. L. Clemens. 2017. Bone Cell Bioenergetics and Skeletal Energy Homeostasis. Physiol Rev 97:667-698.

Rifas, L. 1999. Bone and cytokines: beyond IL-1, IL-6 and TNF-alpha. Calcif Tissue Int 64:1-7.

Roberts, J. R., R. Souillard, and J. Bertin. 2011. Avian diseases which affect egg production and quality. Pages 376-393 in Improving the safety and quality of eggs and egg productsElsevier.

Rodriguez, J. P., S. Rios, and M. Gonzalez. 2002. Modulation of the proliferation and differentiation of human mesenchymal stem cells by copper. J Cell Biochem 85:92-100.

Roux, S., and P. Orcel. 2000. Bone loss. Factors that regulate osteoclast differentiation: an update. Arthritis Res 2:451-456.

Rubert, M., and C. De la Piedra. 2020. La osteocalcina: de marcador de formación ósea a hormona; y el hueso, un órgano endocrino. Revista de Osteoporosis y Metabolismo Mineral 12:146-151.

Ruff, M. D., W. M. Reid, and J. K. Johnson. 1974. Lowered blood carotenoid levels in chickens infected with coccidia. Poult Sci 53:1801-1809.

Sakkas, P., I. Oikeh, D. P. Blake, M. J. Nolan, R. A. Bailey, A. Oxley, I. Rychlik, G. Lietz, and I. Kyriazakis. 2018. Does selection for growth rate in broilers affect their resistance and tolerance to Eimeria maxima? Vet Parasitol 258:88-98.

Sakkas, P., I. Oikeh, D. P. Blake, S. Smith, and I. Kyriazakis. 2019. Dietary vitamin D improves performance and bone mineralisation, but increases parasite replication and compromises gut health in Eimeria-infected broilers. Br J Nutr 122:676-688.

Santos, A., A. D. Bakker, J. M. de Blieck-Hogervorst, and J. Klein-Nulend. 2010. WNT5A induces osteogenic differentiation of human adipose stem cells via rho-associated kinase ROCK. Cytotherapy 12:924-932.

Santos, T. S. d., P.-Y. Teng, S. Yadav, F. L. d. S. Castro, R. L. Gould, S. W. Craig, C. Chen, A. L. Fuller, R. Pazdro, J. R. Sartori, and W. K. Kim. 2020. Effects of Inorganic Zn and Cu Supplementation on Gut Health in Broiler Chickens Challenged With Eimeria spp. Frontiers in Veterinary Science 7.

Scanes, C. G. 2016. Biology of stress in poultry with emphasis on glucocorticoids and the heterophil to lymphocyte ratio. Poult Sci 95:2208-2215.

Schett, G. 2008. Review: Immune cells and mediators of inflammatory arthritis. Autoimmunity 41:224-229.

Scott, E. W., R. C. Fisher, M. C. Olson, E. W. Kehrli, M. C. Simon, and H. Singh. 1997. PU.1 Functions in a Cell-Autonomous Manner to Control the Differentiation of Multipotential Lymphoid–Myeloid Progenitors. Immunity 6:437-447.

Sepp, T., U. Karu, J. D. Blount, E. Sild, M. Manniste, and P. Horak. 2012. Coccidian infection causes oxidative damage in greenfinches. PLoS One 7:e36495.

Shimizu, T. 2016. Inflammation-inducing Factors of Mycoplasma pneumoniae. Front Microbiol 7:414.

Sies, H., C. Berndt, and D. P. Jones. 2017. Oxidative Stress. Annu Rev Biochem 86:715-748.

Solomon, L. B., D. Kitchen, P. H. Anderson, D. Yang, Y. Starczak, M. Kogawa, E. Perilli, P. J. Smitham, M. S. Rickman, D. Thewlis, and G. J. Atkins. 2018. Time dependent loss of trabecular bone in human tibial plateau fractures. J. Orthop. Res. 36:2865-2875.

Southern, L. L., and D. H. Baker. 1983. Zinc toxicity, zinc deficiency and zinc-copper interrelationship in Eimeria acervulina-infected chicks. J Nutr 113:688-696.

Soysa, N. S., and N. Alles. 2019. Positive and negative regulators of osteoclast apoptosis. Bone Rep 11:100225.

Surai, P. F., Kochish, II, V. I. Fisinin, and M. T. Kidd. 2019. Antioxidant Defence Systems and Oxidative Stress in Poultry Biology: An Update. Antioxidants (Basel) 8.

Swarthout, J. T., R. C. D'Alonzo, N. Selvamurugan, and N. C. Partridge. 2002. Parathyroid hormone-dependent signaling pathways regulating genes in bone cells. Gene 282:1-17.

Taichman, R. S. 2005. Blood and bone: two tissues whose fates are intertwined to create the hematopoietic stem-cell niche. Blood 105:2631-2639.

Takada, I., M. Mihara, M. Suzawa, F. Ohtake, S. Kobayashi, M. Igarashi, M. Y. Youn, K. Takeyama, T. Nakamura, Y. Mezaki, S. Takezawa, Y. Yogiashi, H. Kitagawa, G. Yamada, S. Takada, Y. Minami, H. Shibuya, K. Matsumoto, and S. Kato. 2007. A histone lysine methyltransferase activated by non-canonical Wnt signalling suppresses PPAR-gamma transactivation. Nat Cell Biol 9:1273-1285.

Takahashi, N., N. Udagawa, and T. Suda. 2014. Vitamin D endocrine system and osteoclasts. Bonekey Rep 3:495.

Talaty, P. N., M. N. Katanbaf, and P. Y. Hester. 2009. Variability in bone mineralization among purebred lines of meat-type chickens. Poult Sci 88:1963-1974.

Tasca, A., K. Astleford, N. C. Blixt, E. D. Jensen, R. Gopalakrishnan, and K. C. Mansky. 2018. SMAD1/5 signaling in osteoclasts regulates bone formation via coupling factors. PLoS One 13:e0203404.

Tasca, A., M. Stemig, A. Broege, B. Huang, J. Davydova, A. Zwijsen, L. Umans, E. D. Jensen, R. Gopalakrishnan, and K. C. Mansky. 2015. Smad1/5 and Smad4 expression are important for osteoclast differentiation. J Cell Biochem 116:1350-1360.

Teitelbaum, S. L. 2007. Osteoclasts: what do they do and how do they do it? Am J Pathol 170:427-435.

Teitelbaum, S. L., and F. P. Ross. 2003. Genetic regulation of osteoclast development and function. Nat Rev Genet 4:638-649.

Thakker, R. V., M. P. Whyte, J. Eisman, and T. Igarashi. 2017. Genetics of bone biology and skeletal disease. Academic Press.

Thorp, B. H. 1994. Skeletal disorders in the fowl: a review. Avian Pathol 23:203-236.

Tompkins, Y. H., P. Teng, R. Pazdro, and W. K. Kim. 2022. Long Bone Mineral Loss, Bone Microstructural Changes and Oxidative Stress After Eimeria Challenge in Broilers. Front Physiol 13:945740.

Tortelli, F., R. Tasso, F. Loiacono, and R. Cancedda. 2010. The development of tissue-engineered bone of different origin through endochondral and intramembranous ossification following the implantation of mesenchymal stem cells and osteoblasts in a murine model. Biomaterials 31:242-249.

Turk, D. E. 1973. Calcium absorption during coccidial infections in chicks. Poult Sci 52:854-857.

Turk, D. E., and J. F. Stephens. 1967. Upper intestinal tract infection produced by E. acervulina and absorption of 65Zn and 131-I-labeled oleic acid. J Nutr 93:161-165.

Turk, D. E., and J. F. Stephens. 1969. Coccidial infections of the ileum, colon, and ceca of the chick and nutrient absorption. Poult Sci 48:586-589.

Turk, D. E., and J. F. Stephens. 1970. Effects of serial inoculations with Eimeria acervulina or Eimeria necatrix upon zinc and oleic acid absorption in chicks. Poult Sci 49:523-526.

Walser, M. M., N. K. Allen, C. J. Mirocha, G. F. Hanlon, and J. A. Newman. 1982. Fusarium-induced osteochondrosis (tibial dyschondroplasia) in chickens. Vet Pathol 19:544-550.

Ward, T. L., K. L. Watkins, and L. L. Southern. 1990. Interactive effects of sodium zeolite A (Ethacal) and monensin in uninfected and Eimeria acervulina-infected chicks. Poult Sci 69:276-280.

Ward, T. L., K. L. Watkins, and L. L. Southern. 1993. Research note: interactive effects of sodium zeolite A and Eimeria acervulina infection on growth and tissue minerals in chicks. Poult Sci 72:2172-2175.

Webber, G., and M. Frigg. Year. Effect of high level of vitamin C on coccidiosis infected chickens. Proc. Roche Symp. on Anim. Nutr. and Health. Basel Village-Neuf.

Wei, J., J. Shimazu, M. P. Makinistoglu, A. Maurizi, D. Kajimura, H. Zong, T. Takarada, T. Lezaki, J. E. Pessin, E. Hinoi, and G. Karsenty. 2015. Glucose Uptake and Runx2 Synergize to Orchestrate Osteoblast Differentiation and Bone Formation. Cell 161:1576-1591.

Wei, S., H. Kitaura, P. Zhou, F. P. Ross, and S. L. Teitelbaum. 2005. IL-1 mediates TNF-induced osteoclastogenesis. Journal of Clinical Investigation 115:282-290.

Weitzmann, M. N., and R. Pacifici. 2006. Estrogen deficiency and bone loss: an inflammatory tale. Clin Invest 116:1186-1194.

Whitehead, C. C., and R. H. Fleming. 2000. Osteoporosis in Cage Layers. Poultry Science 79:1033-1041.

Wideman, R. F., Jr. 2016. Bacterial chondronecrosis with osteomyelitis and lameness in broilers: a review. Poult Sci 95:325-344.

Wideman, R. F., Jr., A. Al-Rubaye, A. Gilley, D. Reynolds, H. Lester, D. Yoho, J. M. Hughes, and I. Pevzner. 2013. Susceptibility of 4 commercial broiler crosses to lameness attributable to bacterial chondronecrosis with osteomyelitis. Poult Sci 92:2311-2325.

Wideman, R. F., Jr., J. Blankenship, I. Y. Pevzner, and B. J. Turner. 2015. Efficacy of 25-OH Vitamin D3 prophylactic administration for reducing lameness in broilers grown on wire flooring. Poult Sci 94:1821-1827.

Williams, B., S. Solomon, D. Waddington, B. Thorp, and C. Farquharson. 2000. Skeletal development in the meat-type chicken. Br Poult Sci 41:141-149.

Wu, X., M. A. McKenna, X. Feng, T. R. Nagy, and J. M. McDonald. 2003. Osteoclast apoptosis: the role of Fas in vivo and in vitro. Endocrinology 144:5545-5555.

Xing, L., and B. F. Boyce. 2005. Regulation of apoptosis in osteoclasts and osteoblastic cells. Biochem Biophys Res Commun 328:709-720.

Xing, L., T. P. Bushnell, L. Carlson, Z. Tai, M. Tondravi, U. Siebenlist, F. Young, and B. F. Boyce. 2002. NF-kappaB p50 and p52 expression is not required for RANK-expressing osteoclast progenitor formation but is essential for RANK- and cytokine-mediated osteoclastogenesis. J Bone Miner Res 17:1200-1210.

Yamaguchi, M., and M. N. Weitzmann. 2011. Zinc stimulates osteoblastogenesis and suppresses osteoclastogenesis by antagonizing NF-kappaB activation. Mol Cell Biochem 355:179-186.

Yao, W., H. Zhang, X. Jiang, K. Mehmood, M. Iqbal, A. Li, J. Zhang, Y. Wang, M. Waqas, Y. Shen, and J. Li. 2018. Effect of Total Flavonoids of Rhizoma drynariae on Tibial Dyschondroplasia by Regulating BMP-2 and Runx2 Expression in Chickens. Front Pharmacol 9:1251.

Yao, Z., L. Xing, C. Qin, E. M. Schwarz, and B. F. Boyce. 2008. Osteoclast precursor interaction with bone matrix induces osteoclast formation directly by an interleukin-1-mediated autocrine mechanism. J Biol Chem 283:9917-9924.

Yin, M. T., E. Lund, J. Shah, C. A. Zhang, M. Foca, N. Neu, K. K. Nishiyama, B. Zhou, X. E. Guo, J. Nelson, D. L. Bell, E. Shane, and S. M. Arpadi. 2014. Lower peak bone mass and abnormal trabecular and cortical microarchitecture in young men infected with HIV early in life. AIDS 28:345-353.

Yun, C. 2000. Intestinal immune responses to coccidiosis. Developmental & Comparative Immunology 24:303-324.

Zhang, C., D. Li, F. Wang, and T. Dong. 2003. Effects of dietary vitamin K levels on bone quality in broilers. Arch Tierernahr 57:197-206.

Zhang, H., K. Mehmood, X. Jiang, Z. Li, W. Yao, J. Zhang, X. Tong, Y. Wang, A. Li, M. Waqas, M. Iqbal, and J. Li. 2019. Identification of differentially expressed MiRNAs profile in a thiram-induced tibial dyschondroplasia. Ecotoxicol Environ Saf 175:83-89.

Zhang, H., K. Mehmood, K. Li, M. U. Rehman, X. Jiang, S. Huang, L. Wang, L. Zhang, X. Tong, F. Nabi, W. Yao, M. K. Iqbal, M. Shahzad, and J. Li. 2018. Icariin Ameliorate Thiram-Induced Tibial Dyschondroplasia via Regulation of WNT4 and VEGF Expression in Broiler Chickens. Front Pharmacol 9:123.

Zhang, H., Y. Wang, K. Mehmood, Y. F. Chang, Z. Tang, and Y. Li. 2020. Treatment of tibial dyschondroplasia with traditional Chinese medicines: "Lesson and future directions". Poult Sci 99:6422-6433.

Zhang, Q., I. R. Badell, E. M. Schwarz, K. E. Boulukos, Z. Yao, B. F. Boyce, and L. Xing. 2005. Tumor necrosis factor prevents alendronate-induced osteoclast apoptosis in vivo by stimulating Bcl-xL expression through Ets-2. Arthritis Rheum 52:2708-2718.

Zhou, R., Q. Guo, Y. Xiao, Q. Guo, Y. Huang, C. Li, and X. Luo. 2021. Endocrine role of bone in the regulation of energy metabolism. Bone Res 9:25.

Zomorodian, E., and M. Baghaban Eslaminejad. 2012. Mesenchymal stem cells as a potent cell source for bone regeneration. Stem Cells Int 2012:980353.

Zorov, D. B., M. Juhaszova, and S. J. Sollott. 2014. Mitochondrial reactive oxygen species (ROS) and ROS-induced ROS release. Physiol Rev 94:909-950.

Zou, M. L., Z. H. Chen, Y. Y. Teng, S. Y. Liu, Y. Jia, K. W. Zhang, Z. L. Sun, J. J. Wu, Z. D. Yuan, Y. Feng, X. Li, R. S. Xu, and F. L. Yuan. 2021. The Smad Dependent TGF-beta and BMP Signaling Pathway in Bone Remodeling and Therapies. Front Mol Biosci 8:593310.

CHAPTER 2

LONG BONE MINERAL LOSS, BONE MICROSTRUCTURAL CHANGES AND OXIDATIVE STRESS AFTER *EIMERIA* CHALLENGE IN BROILERS [1]

[1] Y. H. Tompkins, P. Teng, R. Pazdro, and W. K. Kim. Published on *Frontiers in Physiology*

Abstract

The objective of this study was to evaluate the impact of coccidiosis on bone quality and antioxidant status in the liver and bone marrow of broiler chickens. A total of 360 13-day old male broilers (Cobb500) were randomly assigned to different groups (negative control, low, medium-low, medium-high, and highest dose groups) and orally gavaged with different concentrations of *Eimeria* oocysts solution. Broiler tibia and tibia bone marrow were collected at 6 days post-infection (6 dpi) for bone 3-D structural analyses and the gene expression related to osteogenesis, oxidative stress, and adipogenesis using micro-computed tomography (micro-CT) and real-time qPCR analysis, respectively. Metaphyseal bone mineral density and content were reduced in response to the increase of *Eimeria* challenge dose, and poor trabecular bone traits were observed in the high inoculation group. However, there were no significant structural changes in metaphyseal cortical bone. Medium-high *Eimeria* challenge dose significantly increased level of peroxisome proliferator-activated receptor gamma (*PPARG*, $p < 0.05$) and decreased levels of bone gamma-carboxyglutamate protein coding gene (*BGLAP*, $p < 0.05$) and fatty acid synthase coding gene (*FASN*, $p < 0.05$) in bone marrow. An increased mRNA level of superoxide dismutase type 1 (*SOD1*, $p < 0.05$) and heme oxygenase 1 (*HMOX1*, $p < 0.05$), and increased enzyme activity of SOD ($p < 0.05$) were found in bone marrow of *Eimeria* challenged groups compared with that of non-infected control. Similarly, enzyme activity of SOD and the mRNA level of *SOD1*, *HMOX1* and aflatoxin aldehyde reductase (*AKE7A2*) were increased in the liver of infected broilers ($p < 0.05$), whereas glutathione (GSH) content was lower in the

medium-high challenge group ($p < 0.05$) compared with non-challenged control. Moreover, the mRNA expression of catalase (*CAT*) and nuclear factor kappa B1 (*NFKB1*) showed dose-depend response in the liver, where expression of *CAT* and *NFKB1* was upregulated in the low challenge group but decreased with the higher *Eimeria* challenge dosage ($p < 0.05$). In conclusion, high challenge dose of *Eimeria* infection negatively affected the long bone development. The structural changes of tibia and decreased mineral content were mainly located at the trabecular bone of metaphyseal area. The change of redox and impaired antioxidant status following the *Eimeria* infection were observed in the liver and bone marrow of broilers.

Keyword: *Eimeria*, bone health, bone mineral loss, bone quality, oxidative stress, broiler bone

Introduction

Avian coccidiosis is one of the top prevalent enteric diseases in the poultry industry. Especially in the modern broiler production, the high-density, small confinement, warm, and humid animal housing accelerate the dispersal, transmission, and outbreak of coccidiosis, making this issue hard to eradicate (Chapman 2014; Blake et al., 2020). Coccidiosis is a parasite disease caused by parasites of the genus *Eimeria* that can cause intestinal damage leading to inflammation and nutrient malabsorption (Gautier et al., 2019). The infection with *Eimeria* spp. results in growth retardation and mortality, which creates 13 billion dollars in losses by its detriment to production and increases the cost (Amerah and Ravindran, 2015). The prevention and control of coccidiosis outbreaks are not only achieved by careful management practices, but also the use of in-feed anticoccidial drugs or vaccines, alone or in combination. However, because of the market demand, the use of antibiotic-free diets leads to numerous challenges, such as control and treatment of enteric and systemic diseases (Dalloul and Lillehoj, 2006; Blake and Tomley, 2014; Cervantes, 2015). Other than anorexia or nutrient malabsorption, the pathogenicity of coccidiosis is also associated with the response from immune system which generates reactive oxygen species (ROS) in chicken (Georgieva et al., 2006; Georgieva et al., 2011; Gautier et al., 2019). The parasite infection causes an imbalance between endogenous antioxidant defense and free radical production, which leads to depletion of antioxidant enzymes and reduction of glutathione (GSH) level (Surai, 2019). The unbalanced status results in increased lipid peroxidation and DNA damage which can cause apoptosis of intestinal cells and affect the health status and productivity of poultry

(Estevez, 2015; Mishra and Jha, 2019). The first lines of antioxidant defense system including catalase (CAT), superoxide dismutase (SOD), and glutathione peroxidase (GPX) are indispensable for protecting the body from the damage caused by free radicals, especially superoxide anion radicals, during *Eimeria* infection (Georgieva et al., 2006). Dietary manipulations, such as optimizing amino acids profile or adding dietary supplements are potential strategies to support broilers against coccidiosis induced oxidative stress (Arczewska-Wlosek et al., 2018; Gautier et al., 2019). In broilers, nutrient supplements such as vitamins, antioxidants, and trace minerals can alleviate the negative effect caused by oxidative stress (Arczewska-Wlosek et al., 2018; Santos et al., 2020).

Meanwhile, the incidence of physical abnormalities in bone of broilers has been noted. Because the fast-growing broilers are characterized by poor calcification and high porosity of long bone, severe duodenum and upper jejunum damage caused by *Eimeria* infection intensifies the bone health issues in the modern poultry industry (Sakkas et al., 2018; Oikeh et al., 2019). Bone mineral loss caused by *Eimeria* spp. in broilers has been previously linked to nutrition malabsorption, especially the reduced absorption of calcium, phosphate, and several important trace minerals for optimal bone growth (Turk and Stephens, 1967; Turk and Stephens, 1969; Turk and Stephens, 1970; Turk, 1973; Joyner et al., 1975). Recent studies have revealed a more profound understanding in regards to bone loss after *Eimeria* infection, where suppressed fat absorption resulted in depressed levels of fat-soluble vitamins; thus, an increase in bone resorption level was detected (Akbari Moghaddam Kakhki et al., 2019; Sakkas et al., 2019). Studies in human

and mice also indicated that oxidative stress response caused by gastrointestinal infection could lead to inhibition of mineralization and osteogenesis, and activation of bone resorption, subsequently causing bone loss and structural changes (Basu et al., 2001; Domazetovic et al., 2017). Bone architectural organization is an independent marker that can precisely reflect bone turnover, however, how does the *Eimeria* infection change biomechanical properties on the specific bone region has not been documented extensively to date, and the etiology behind it is not fully understood (Brandi, 2009; Henkelmann et al., 2017). We reported that the increasing infection severity of *Eimeria* spp. linearly reduced nutrient digestibility and body weight of birds. The increased gut permeability and lesion scores in response to the graded levels of *Eimeria* infection were also found and presented in our recent publication (Teng, et al., 2020a). The objective of this study was to further evaluate the negative impact of coccidiosis on bone traits in broiler chickens. A new approach, micro-CT scanning and analyses, was taken in assessing the three-dimensional structure to provide in-depth and comprehensive understanding the pathogenetic mechanisms of bone disorders with acute intestinal pathogen infections in avian species.

Materials and Methods

Ethics Statement

All experiments followed the guidelines of the Institutional Animal Care and Use Committee and was conducted at the Poultry Research Farm, University of Georgia, Athens, GA. The protocol was approved by the Institutional Animal Care and Use Committee at the University of Georgia.

Experimental Design

Management and diet formulation as previously described (Teng et al., 2020). Briefly, a total of 360 male broiler chicks were randomly allocated to five treatments with six replicates and twelve birds per cage. The birds were gavaged with 1 mL of water for a control and 1 mL of different concentrations of *Eimeria* solutions for challenge groups at 13 days of age. Mixed *Eimeria* spp. oocyst solutions were pre-prepared for the Low group as the lowest challenge dose with 6,250 oocysts of *E. maxima*, 6,250 oocysts of *E. tenella* and 31,250 oocysts of *E. acervulina*; the Med-low group as the medium-low challenge dose with 12,500 oocysts of *E. maxima*, 12,500 oocysts of *E. tenella* and 62,500 oocysts of *E. acervulina*; the Med-high group as the medium-high challenge dose with 25,000 oocysts of *E. maxima*, 25,000 oocysts of *E. tenella* and 125,000 oocysts of *E. acervulina*; and the High group as the highest challenge dose with 50,000 oocysts of *E. maxima*, 50,000 oocysts of *E. tenella*, and 250,000 oocysts of *E. acervulina* (Table 2.1). All chicks were raised under the same environmental conditions according to the Cobb 500 broiler management guide (Cobb 2019). All chicks were fed the same basal diet and allowed to consume feed and water on an *ad libitum* basis. Starter (0-12 d of age) and grower (13-19 days of age) diets were formulated to meet Cobb 500 nutrient requirements as previously described (Teng et al., 2020).

A total of 30 birds (1 bird per replicate cage) were selected and euthanized by cervical dislocation at 6 dpi (19 days of age), and tibia bone and liver samples were collected and snap-frozen in liquid nitrogen and kept in -80°C until processing.

Antioxidant study by Enzyme-linked immunosorbent assay (ELISA)

SOD and CAT enzyme activities in the liver and bone marrow of 30 samples (6 samples per treatment group) were analyzed using superoxide dismutase assay and catalase assay kits (Cayman chemical, Superoxide dismutase assay kit, item No. 706002, Catalase Assay Kit, item No. 707002, AnnArbor, MI, USA), following the manufacturer's instructions. Approximately 100 mg of each sample was homogenized in 1mL of cold sample buffer (20 mM HEPES buffer, pH 7.2, 2 mM EGTA, 10 mM mannitol, and 70 mM sucrose). The homogenized sample was centrifuged at 1,500 x g for five minutes at 4°C, and the supernatant was collected for analyses. All supernatant samples were diluted by using the sample buffer before the ELISA assays. Samples were measured by spectrophotometer (SpectraMax ABS Plus, Softmax Pro 7 software, Molecular devices, San Jose, CA) at wavelength of 450 nm for SOD activity assay, and at 540 nm for CAT assay. For protein quantification assay (Pierce BCA Protein Assay Kit, Ref. 23227, Thermo Scientific, Rockford, IL, USA), the supernatants were diluted before the assay, and Bovine Serum Albumin (2 mg/mL) was used as the protein standard, and enzyme activity was normalized to the total protein content for the final calculation. The protein samples were diluted and placed in duplicate and read in a spectrophotometer (SpectraMax, San Jose, CA) at wavelength of 562 nm.

High-performance liquid chromatography (HPLC)

High-performance liquid chromatography (HPLC) setting and reading for measuring antioxidative parameters were as previously described (Gould et al., 2018). Immediately after collecting liver and tibia marrow samples, all samples were snap-

frozen in liquid nitrogen. Within 24 hours, all harvested tissues were homogenized in PBS containing 10 mM diethylenetriaminepentaacetic acid (DTPA) and promptly acidified as previously described (Park et al., 2010). Samples were stored at -80°C for HPLC analyses. Briefly, glutathione (GSH) and glutathione disulfide (GSSG) were quantified in each sample by HPLC coupled with electrochemical detection (Dionex Ultimate 3000, Thermo Scientific, Waltham, MA, USA). The cell was set at + 1600 mV with a cleaning potential of + 1900 mV between the samples. The mobile phase consisted of 4.0% acetonitrile, 0.1% pentafluoropropionic acid, and 0.02% ammonium hydroxide. The flow rate was maintained at 0.5 mL/min, and injection volumes were set at 2.0 µL for bone marrow samples. Peaks were quantified using external GSH and GSSG standards and the Chromeleon Chromatography Data System Software (Dionex Version 7.2, Thermo Scientific, Germering, Germany). Total glutathione was determined by calculating GSH + 2GSSG, and levels of total glutathione, GSH, and GSSG were all standardized to total protein content (Pierce BCA Protein Assay Kit). The protein samples were diluted and placed in duplicate and read in a spectrophotometer (SpectraMax, San Jose, CA) at wavelength of 562 nm.

Micro-Computed Tomography (micro-CT)

To evaluate bone morphologic changes in the broiler, 30 samples (6 samples per treatment group) were randomly chosen for micro-Computed Tomography (micro-CT) microarchitectural scanning. The right tibias were scanned according to a standard protocol at 80 kV and128 µA, and a 0.5 mm aluminum filter, and analyses were performed with a SkyScan 1172 (SkyScan, Kontich, Belgium). The scanned images were

captured with a 360° complete rotation and an 18 min of acquisition time at 26 μm pixel size. 2-D images were transferred to CTAn software (CTAn, SkyScan, Aartselaar, Belgium) for structure construction and quantification as previously described (Chen and Kim, 2020). Trabecular and cortical bones of the metaphysis were analyzed. The analysis parameters are listed in Table 2.2. All images were post-operated to isolate trabecular bone from cortical bone and preserve its morphology using a threshold of 800 manually. Average bone mineral content (BMC), bone mineral density (BMD), and bone micro-architectural parameters of each treatment group were taken from the same region of interest (ROI). The whole bone length and bone diaphysis width were measured by using CTAn ruler tool which measures straight line distance. Controlling the location, 4 measurements were conducted on each sample by using CTAn ruler tool, the mean thickness of cortical bone was used for statistical analysis.

Real-time qPCR analysis for gene expression in the bone marrow

Right tibia bones were opened, and bone marrow samples were collected and stored at -80°C until RNA isolation (n = 6). Bone marrow and liver total RNA were extracted by using Qiazol reagents (Quiagen, Germantown, MD, USA) according to the manufacturer's instructions. Nano-Drop 1000 Spectrophotometer (ThermoFisher Scientific, Pittsburgh, PA, USA) was used to determine the quantity of extracted RNA. The cDNA was synthesized from total RNA (2000 ng) using high-capacity cDNA reverse transcription kits (Thermo Fisher Scientific, Waltham, MA, USA). Real-time reverse transcription polymerase chain reaction (Real-time RT-PCR) was used to measure mRNA expression. Primers were designed using the Primer-BLAST program

(https://www.ncbi.nlm.nih.gov/tools/primer-blast/). The specificity of primers was validated by PCR product sequencing and previously published (Table 2.3). Primer quality was verified through melting curve analysis and gel electrophoresis in this study. Real-time qPCR was performed on an Applied Biosystems StepOnePlus (Thermo Fisher Scientific, Waltham, MA, USA) with iTaq Universal SYBR Green Supermix (BioRad, Hercules, CA, USA) using the following conditions for all genes: 95°C for 10 minutes followed 40 cycles at 95°C for 15 seconds, annealing temperature (Table 2.3) for 20 seconds, and extending at 72°C for one minute.

The geometric means of glyceraldehyde-3-phosphate dehydrogenase (*GAPDH*) and actin beta (*ACTB*) were used as housekeeping genes for normalization, and the stability of the housekeeping genes was confirmed by their consistent Ct values among the treatments ($p > 0.1$) (Vandesompele et al., 2002). Details of primer sequences used for the experiment are presented in Table 2.3. Peroxisome proliferator-activated receptor gamma (*PPARG*), fatty acid synthase (*FASN*), adipose tissue fatty acid binding protein 4 (*FABP4*) and sterol regulatory element-binding transcription factor 1 (*SREBP1*) were used as early markers of adipogenic differentiation and fatty acid synthesis, and bone gamma-carboxyglutamate protein (*BGLAP*) and runt-related transcription factor 2 (*RUNX2*) were used as osteogenic marker genes in the bone marrow. Nuclear factor kappa B subunit 1 (*NFKB1*) and antioxidant enzyme protein coding genes including catalase (*CAT*), superoxide dismutase type 1(*SOD1*), glutathione peroxidase 1 (*GPX1*), heme oxygenase 1 (*HMOX1*), and aflatoxin aldehyde reductase (*AKR7A2*) were used to determine the antioxidant enzyme activity and oxidative stress status (Lee et al., 2018).

Samples were run in triplicate, and relative gene expression data were analyzed using the $2^{-\Delta\Delta Ct}$ (Livak and Schmittgen, 2001). The mean ΔCt of each marker gene from the control group was used to calculate the ΔΔCt value, and $2^{-\Delta\Delta Ct}$ expression levels were normalized to 1 for the control group, and expression levels of the other treatment groups were presented as fold change relative to the control group.

Statistical analysis

All experimental data were expressed as mean with standard errors of the means (SEM). Data were tested for homogeneity of variances and normality of studentized residuals. The differences between the treatment groups were analyzed by one-way ANOVA, and the means were analyzed statistically by Tukey's test using JMP Pro14 (SAS Institute, Cary, NC, USA). A $p \leq 0.05$ was considered statistically significant, and $0.05 \leq p \leq 0.1$ were also presented to show the trending toward statistical significance (Thiese, Ronna, and Ott 2016; Serdar et al., 2021). To evaluate the effects of increasing oocysts inoculation doses on responses of each parameter, the linear and quadratic regression were analyzed using an ordered logistic regression model with inoculated number of oocytes as a fixed factor and broiler per pen as the experimental unit. The comparisons between non-challenge control and pooled challenged groups (Low, Med-low, Med-high, and High) were calculated by unpaired *t*-test with Welch's correction. Pair wise correlations (JMP Pro14) were evaluated for bone micro-CT and antioxidant variables. Statistical significance was set at $p \leq 0.05$.

Results

Bone microstructural changes in response to increasing doses of *Eimeria* oocysts

There were no statistically significant differences in the whole tibia length, tibia diaphysis width and the thickness of cortical bone among treatment groups at 6 dpi (Table 2.4). And all the micro-CT results are presented in Table 2.5. For the total bone structure of metaphysis, the lowest BMC (ANOVA, $p = 0.025$; linear regression, $p = 0.012$, $R^2 = 0.205$), BMD (ANOVA, $p = 0.002$; linear regression, $p < 0.001$, $R^2 = 0.342$), and the lowest bone volume fraction (BV/TV; ANOVA, $p = 0.023$) ratio were detected in the High group in response to increased challenge dose.

The microstructure changes in metaphysis were mainly attributed to impaired trabecular bone traits caused by higher *Eimeria* challenge dosage, including lower BMC (Figure 2.1; ANOVA, $p = 0.001$; linear regression, $p < 0.001$, $R^2 = 0.362$), lower BMD (ANOVA, $p < 0.001$; linear regression, $p < 0.001$, $R^2 = 0.402$), smaller bone surface (BS; ANOVA, $p = 0.048$), lower trabecular number (Tb. N; ANOVA, $p = 0.025$; linear regression, $p = 0.021$, $R^2 = 0.177$), lower connectivity density (Conn. Dn; ANOVA, $p = 0.035$; linear regression, $p = 0.014$, $R^2 = 0.243$), and higher rating structure model index (SMI; ANOVA, $p = 0.002$; linear regression, $p < 0.001$, $R^2 = 0.387$), higher rating of trabecular pattern factor (Tb. pf; ANOVA, $p = 0.029$; linear regression, $p = 0.003$, $R^2 = 0.268$). However, the microstructure of metaphyseal cortical bone was not significantly affected by *Eimeria* infection (ANOVA, $p > 0.050$).

Gene expression changes of bone formation and adipogenic markers in the bone marrow

The expression of protein coding genes that are involved in bone formation or adipocyte differentiation was measured (Figure 2.2). For bone growth gene markers, results showed a significant downregulation of *BGLAP* with increased inoculation levels (ANOVA, $p = 0.020$; linear regression, $p = 0.029$, $R^2 = 0.396$), where the lowest level of *BGLAP* was detected in the Med-High group. The mRNA expression of *RUNX2* was not affected by different doses of *Eimeria* oocysts challenge (ANOVA, $p > 0.100$). For adipogenic gene expression, the expression of *PPARG* was significantly increased by the Med-high dose of challenge when compared with the Control, the Low and the Med-low groups (Figure 2.2; ANOVA, $p = 0.047$). The expression of *SREBP1* (Figure 2.2; ANOVA, $p = 0.056$; linear regression, $p = 0.008$, $R^2 = 0.226$), *FABP4* (Figure 2.2; ANOVA, $p = 0.057$; linear regression, $p = 0.004$, $R^2 = 0.279$), and *FASN* (ANOVA, $p = 0.013$; linear regression, $p = 0.005$, $R^2 = 0.261$) were down-regulated in response to graded inoculation doses.

Antioxidant status in the bone marrow in response to *Eimeria* challenge

In the bone marrow, SOD enzyme activity increased in response to graded levels of oocysts challenge and showed the highest response to the Med-high challenge dose (Table 2.6; ANOVA, $p = 0.027$). However, the CAT enzyme activity was not significantly affected by the *Eimeria* challenge (Table 2.6; $p > 0.050$) in bone marrow. The bone marrow GSSG levels did not significantly changed by *Eimeria* infection, but it exhibited a negative response to increasing inoculation doses (Table 2.6; ANOVA, $p > 0.050$; linear regression,

$p = 0.039$, $R^2 = 0.150$). However, there were no significant differences in total glutathione content (GSH + 2GSSG), GSH content or GSH/GSSG ratios among the treatment groups (Table 2.6).

Additionally, mRNA expression of *CAT* was positively correlated with higher inoculation doses of the mixed *Eimeria* oocysts in bone marrow (Figure 2.3; ANOVA, $p > 0.050$; linear regression, $p = 0.040$, $R^2 = 0.124$), whereas there were no significant differences in expression of *HMOX1*, *SOD1*, *GPX1* or *NFKB1* among the treatments in bone marrow (Figure 2.3; ANOVA, $p > 0.050$; linear regression, $p > 0.050$). By pooling all infected groups (Low, Med-low, Med-high, and High) together and compared with the non-infected Control, *Eimeria* infection significantly increased the mRNA level of *SOD1* ($p = 0.036$) and *HMOX1* ($p = 0.006$).

Antioxidant status in the liver in response to *Eimeria* challenge

In the liver, CAT activity was not significantly affected by *Eimeria* infection (ANOVA, $p > 0.050$), but the activity of CAT was negatively correlated to the higher challenge dose of *Eimeria* oocysts (Table 2.7; linear, $p = 0.043$, $R^2 = 0.143$). GSH content was significantly decreased by *Eimeria* infection and the lowest GSH content was observed in the Med-High group (Table 2.7; ANOVA, $p = 0.036$). By comparing infected groups (Low, Med-low, Med-high, High) with the non-infected Control, a significant higher SOD activity ($p < 0.001$) and numeric lower GSH content ($p = 0.091$) were detected in pooled *Eimeria*-infected groups.

Additionally, the expression of genes coding for front-line antioxidant enzymes was measured (Figure 2.4). The gene expression of antioxidant gene showed a dose

dependent manner. More specifically, the Low challenge dose significantly increased the mRNA expression of CAT when compared with the Control, and the expression level was decreased with the high challenge dose of *Eimeria* oocysts (Figure 2.4; ANOVA, p = 0.006; linear regression, p = 0.004, R^2 = 0.144). The highest inoculation dose of *Eimeria* oocysts upregulated the expression of *AKR7A2* (ANOVA, p = 0.006; linear regression, p = 0.002, R^2 = 0.434). The low challenge dose of *Eimeria* oocysts resulted in significantly higher *NFKB1* expression, compared to the Med-high and the High group (ANOVA, p = 0.002; linear regression, p = 0.006, R^2 = 0.263). No significant differences in the expression of *SOD1*, *GPX1*, and *HMOX1* were evident among the challenge doses (p > 0.100). By comparing infected groups with the non-infected Control, a significant higher level of *SOD1* (p = 0.036) and a numeric higher level of *HMOX1* (p = 0.083) were detected in the *Eimeria*-infected groups.

Correlation between antioxidant enzymes level and bone parameters

Pearson correlation analyses revealed a positive correlation between the liver *GPX1* mRNA level and bone marrow *BGLAP* mRNA level (R^2 = 0.197, p = 0.026; Figure 2.5A); between bone marrow *GPX1* mRNA and bone marrow *FASN* mRNA expression (R^2 = 0.171, p = 0.029; Figure 2.5B); and between bone marrow *GPX1* mRNA and bone marrow *FABP4* mRNA expression (R^2 = 0.212, p = 0.016; Figure 2.5C). Meanwhile, bone marrow *CAT* mRNA level was negatively correlated with tibia metaphyseal BMD (R^2 = 0.190, p = 0.016; Figure 2.5D) and trabecular BMD (R^2 = 0.217, p = 0.009; Figure 2.5E).

Discussion

Based on current data, we concluded that high challenge dose of *Eimeria* infection negatively affected the long bone development. The structural changes of tibia and decreased mineral content were mainly located at the trabecular bone of metaphyseal area. The change of redox and impaired antioxidant status following the *Eimeria* infection were observed in the liver and bone marrow of broilers. Compared with the slower growing strains of broilers, bone formation and turnover are extremely rapid in the modern strains (Yair et al., 2017), that fast body weight gain places challenges to bone health in the modern broiler industry (Edwards, 2000; Fleming, 2008; Wideman, 2016; (Schmidt et al., 2009; Alrubaye et al., 2020). The rapid bone growth results in decreased mineral density, increased cortical porosity, and altered biomechanical properties of long bone in the modern broiler strains (Williams et al., 2004), that is partly responsible for broiler leg bone disorder that restricts the growth of broiler. Long bone homeostasis is closely associated intrinsic and extrinsic factors including nutrition status, physical stress (mechanical loading), immune status, hormonal status, genetics, management, and age of animals (Fleming, 2008; Rokavec and Semrov, 2020; Cao et al., 2021). Therefore, we propose that bone traits can be used as a dynamic indicator for growth and health status of poultry.

Bone is made up of two components: the organic matrix and the inorganic matrix (Rath and Durairaj, 2022). Crystals of calcium phosphate make up the bulk of the inorganic matrix, which is eventually counted as bone mineral content. The inorganic mineral content is the major component of the bone that provides stiffness and strength to

the bone (Eliaz and Metoki, 2017), where quantitate bone mineral content is the easiest and most common way to reflect the bone health status. To date, researchers have conventionally focused on the changes in bone mineral content and density after *Eimeria* infection (Fetterer et al., 2013; Oikeh et al., 2019; Akbari Moghaddam Kakhki et al., 2019). Bone microarchitecture is a predictor for evaluating bone quality and health independent of bone mineral content (Chen and Kim, 2020; Brandi, 2009). However, few data exist on the poultry bone microstructure changes after *Eimeria* infection. Micro-CT is a precise and non-destructive evaluation approach that can provide a comprehensive overview of the morphological and architectural characteristics in poultry bones (Chen and Kim, 2020). In the current study, micro-CT was used in assessing the three-dimensional structure, which provides in-depth understanding behind the relationship between changes of bone traits and *Eimeria* infection. We mainly evaluated those parameters representing metaphyseal bone traits to reflect earlier bone changes under *Eimeria spp.* infection, because acute trabecular bone loss following infectious diseases or bone damage occurred almost exclusively within the metaphyseal compartment in human and poultry (Mubarak et al., 2009; Raehtz et al., 2018). Consistent with previous findings (Akbari Moghaddam Kakhki et al., 2019; Oikeh et al., 2019), the present results showed that a significant reduction in tibia metaphyseal bone mineral content and bone mineral density in the *Eimeria*-challenged groups, especially in the High challenge group of broilers as compared to the non-infected Control, demonstrated the impaired metaphyseal trabecular microstructure under parasite infection. The organization of the trabecular bone is not only a key to bone strength but also plays an important role in

metabolic function (Seifert and Watkins, 1997). The trabecular bones are organized as a lattice structure that provides larger surface areas for osteoclast attachment, showing a higher turnover rate during bone resorption compared with cortical bones in rodent or human study (Baron et al., 1984; Qiu et al., 2019). Previous studies in mouse displayed a decreased total bone BV/TV, trabecular BV/TV, and trabecular BS, which indicated an accelerated trabecular bone turnover (Boskey and Imbert, 2017). As for both whole metaphyseal structure and trabecular bone structure in the current study, there were no statistical changes in bone mass (BV or TV) with different *Eimeria*-challenge dosages, whereas the total bone BMD and trabecular bone BMD were negatively correlated with increased inoculation doses of oocysts, and BMC decreased correspondingly. In the present study, the lower bone mineral content and density, and changed ratio of BV/TV at metaphyseal trabecular bone could be the outcome of trabecular bone remodeling in the High dose of *Eimeria* challenge group. Trabecular microstructure assay in this study also showed significant decreases in trabecular number (Tb. N) and connectivity density (Conn. Dn), and significant increases in SMI in tibia metaphyseal trabecular bone by *Eimeria* spp. challenge. The similar alteration of bone microstructures is also known in human bone microfracture, where small fractions that resulted from trauma, physical stress, or infection (Prat-Fabregat and Camacho-Carrasco, 2016; Solomon et al., 2018). Bone trabecular microstructure traits such as SMI was designed to estimate the rod or plate-like trabecular geometry which describes the trabecular network (Hildebrand and Ruegsegger, 1997). Evaluation of SMI across human and rat studies suggests that higher SMI values represent a rod-like trabecular structure that indicates a poor weight-bearing

ability; this structure could be observed in osteoporosis disease models (Borah et al., 2004; Akhter et al., 2007). Higher SMI values and lower numbers of trabeculae indicated a poor trabecular bone architecture in human (Greenwood et al., 2015). As for the current study, a higher SMI and lower number of trabeculae pointed out the poor-quality of the trabecular bone in *Eimeria* challenge groups, indicating that the bone mineral loss might have happened before any observation of phenotype abnormality of tibia bone during the *Eimeria* infection. At 19 days of age, the body weight of the broiler has yet to cause mechanical trauma on the tibia, thereby the immune response, nutrient deficiency or immune response associated energy cost resulted in the long bone structure abnormality and bone mineral loss. Although changes in bone microstructure during *Eimeria* infection may not necessarily cause bone damage during growth, it potentially enhances the risk of bone damage and the susceptibility to bone disease, with certain mechanical triggering and severe intestinal bacterial infection (Prisby et al., 2014; Wideman, 2016). Moreover, in the current study, the mRNA expression of bone related proteins in bone marrow is also in line with the micro-CT morphological observation. A reciprocal relationship between a key osteogenic marker, *BGLAP,* and a key adipogenic marker, *PPARG* was observed in the Med-high group that were challenged with second highest dose of *Eimeria* oocytes. Bone marrow adipose tissue content has adverse effects on bone quality and can serve as a relevant marker of a compromised bone integrity (Hardouin et al., 2016; Sundh et al., 2016; Kim et al., 2017). Previous studies indicated that higher *PPARG* expression could direct the mesenchymal stem cells (MSCs) differentiated into adipocytes instead of osteoblasts in *vitro* (Hu et al., 2018; Shockley et al., 2009). In the

present study, the suppressed expression of *BGLAP* and increased expression of *PPARG* both indicated the impetus of fat growth instead of bone formation during *Eimeria* infection, confirming the negative impact of *Eimeria* infection on bone health from mRNA level. However, by *Eimeria* infection and intestinal damage, the dietary lipid malabsorption and low nutrient levels in high challenge dosage groups might predispose the suppression of fatty acid synthesis by decreasing the expression of *FASN* in bone marrow.

Broiler bone majorly develops in the first 3 weeks of life (Lilburn, 1994; Williams et al., 2000), which overlaps with the timeline when the oocyst shedding rapid accumulated (Chapman et al., 2016). For the etiology of bone loss after *Eimeria* infection, other than the main factors such as physical stress or nutritional deficiency, accumulating data documented the interaction between immune response, oxidative stress and bone mineral loss due to the crosstalk between the skeletal and the immune systems, and the important biological role of ROS in a variety of physiological systems (Takayanagi, 2007; Lorenzo et al., 2008). Reactive species play an important role in immune response. As for innate immunity, immune cells such as macrophages and neutrophils (heterophils in avian species) utilized phagocytic oxidative burst to destruct pathogens (Lauridsen, 2019; Mishra and Jha, 2019). However, unregulated ROS can damage host tissue homeostasis (Costantini and Moller 2009; Rehman et al., 2018). Coccidiosis can cause severe oxidative stress that elevates intracellular levels of reactive oxygen species (ROS) in broiler and other species (Sepp et al., 2012; Abdel-Haleem et al., 2017). *In vitro* studies in human and mouse cells have shown that ROS is an

important activator for various cell signaling pathways, mediated MSCs differentiation and cell fate (Yang et al., 2013; Atashi et al., 2015). Accumulating evidence suggesting the alteration of the redox state causes systemic changes that can coordinate osteoblast differentiation or osteoclast activity that relat to the bone remodeling process in human and animal models (Domazetovic et al., 2017; Schreurs et al., 2020; Sheppard et al., 2022). The supplementation of trace minerals can alleviate the negative effect of oxidative stress and optimize the bone quality in human and broilers (Santos et al., 2020; Savaram Venkata et al., 2021). Infection with *E. tenella* or *E. acervulina* could increase serum CAT activity while it decreases serum GPX activity in broilers (Georgieva et al., 2006). In the present study, the changes in antioxidant enzyme activity and level of mRNA expression in the liver and bone marrow displayed a systemic oxidative stress in broilers after *Eimeria* infection. Moreover, significantly lower GSH levels were observed in the liver of *Eimeria* infected birds. The decreased defensive antioxidant abilities in higher *Eimeria* challenge dosage groups could partially be related to reduced intestinal absorption of antioxidants (Georgieva et al., 2006; Abdel-Haleem et al., 2017; Mishra and Jha, 2019). Moreover, in the present study, the mRNA expression pf *HMOX1* was upregulated by *Eimeria* infection. HMOX plays essential roles against oxidative stress by balancing body's systemic iron homeostasis and inflammation response (Immenschuh et al., 2010; Otterbein and Choi, 2000). *In vitro* studies have shown that upregulated *HMOX*1 inhibited the maturation and mineralization of osteoblasts (Lin et al., 2010), and HMOX enzyme was involved in the response of bone marrow macrophages to RANKL, which is an essential pathway for osteoclast formation (Florczyk-Soluch et al., 2018).

Thus, the increased mRNA expression of *HMOX1* in bone marrow may be associated with oxidative- or inflammation-induced bone loss by either increasing the activity of osteoclast formation, inhibiting maturation of osteoblast, or both.

Unlike previous results that enzymatic antioxidant SOD was remarkably decreased in chicken serum in most cases of *Eimeria* spp. infection (Georgieva et al., 2006), we found the enzyme activity of SOD and mRNA expression of *SOD1* were significantly increased in the liver and bone marrow.

Previous researchers have established that SOD has immunomodulatory function, and SOD3 is reported to downregulate several signaling cascades including nuclear factor kappa B (NFKB) transcription factors, thereby constraining the inflammatory responses in MSCs (Sah et al., 2020). In the present study, significantly downregulated mRNA expression of NFKB1 was coupled with upregulated mRNA expression of *SOD1* in the liver, indicating the constraining of inflammatory responses. SODs also play significant role in MSCs differentiation and function (Nightingale et al., 2012; Shi et al., 2019). An *in vitro* study of human MSCs reported that the expression of *SOD3* was significantly increased under adipogenic differentiation, and overexpression of *SOD3* in MSCs promoted adipogenic differentiation of MSCs *in vitro* instead of osteogenic differentiation (Nightingale et al., 2012). Therefore, the increased SOD enzyme activity, increased mRNA expression of *SOD1*, and increased expression of *PPARG* both in the present study indicated that oxidative stress caused by *Eimeria* infection tilts the balance of MSC lineage specific differentiation in bone marrow more toward the adipogeneic differentiation.

Another crucial enzyme antioxidant, catalase (CAT), has been described as an important enzyme implicated in inflammation conditions (Georgieva et al., 2006). In present study, mRNA expression and activity of *CAT* were negatively correlated with higher challenge dose of *Eimeria* spp. in the liver. The Low group showed a higher level of *CAT* mRNA expression when compared with the Control, but higher *Eimeria* infection dosage did not change the expression of *CAT* in the liver. In bone marrow, mRNA expression of *CAT* was positively correlated with higher challenge dose of *Eimeria* spp. in bone marrow, where this result is similar with other studies that *Eimeria* infection decreased serum GPX activity but increased serum CAT activity (Georgieva, Koinarski, and Gadjeva 2006; Georgieva et al., 2011). However, the enzyme activity of CAT in bone marrow was not affected by *Eimeria* spp. infection at 6 dpi, suggested that bone marrow is not a CAT active site during *Eimeria* infection, but lower level of *Eimeria* infection can stimulate synthesis of enzymatic antioxidant in bone marrow (Zhang, et al., 2019a). The high dose of inoculation might lead to apoptotic cell death that negatively impacts on protein level and mRNA level of CAT (Saha et al., 2020). Furthermore, the correlation analysis indicated that liver *GPX1* mRNA expression is positively correlated with bone marrow *BGLAP* mRNA expression, whereas bone marrow *CAT* mRNA expression was negatively correlated with tibia metaphysis BMD, emphasizing that the negative impact of *Eimeria* infection on bone quality might be associated with the occurrence of oxidative stress. However, while nutritional factors and animal husbandry play significant roles in determining antioxidant status and bone homeostasis**,** in *vitro* animal model is hard to provide direct evidence to explain the interaction between

oxidative stress and bone remodeling in broilers. Further studies require comprehensive in *vitro* and in *ovo* investigation, which is necessary to confirm the functional significance of antioxidants in bone homeostasis, especially under parasite challenge models.

Recent studies also indicated that the immune status of individuals promoted the process of osteoclastic bone resorption that resulted in bone mineral loss, which is defined as osteoimmunology (Kamibayashi et al., 1995, Solomon et al., 2018). For example, in human clinical studies, the long-term investigation showed bone microarchitectural changes under infection of C virus (HCV), which increased the risk of fracture (Bedimo et al., 2018). Acute malaria infection severely suppresses bone homeostasis, which leads to increased RANKL expression and overstimulation of osteoclastogenesis which favors bone resorption (Lee et al., 2017). Trabecular bone microstructure is impaired in the proximal femur of human immunodeficiency virus-infected (HIV) men with normal bone mineral density (Kazakia et al., 2018). Decreased bone mass and abnormality in trabecular and cortical microarchitecture were observed in young men infected with HIV early in life (Yin et al., 2014). Related reports are very limited in poultry studies. Studies of acute inflammatory response caused by lipopolysaccharides (LPS) injection suppressed growth performance and altered bone homeostasis, which significantly decreased body weight and tibia breaking strength (Mireles et al., 2005). Immunosuppressive doses of dexamethasone triggered high incidences of turkey osteomyelitis complex in turkey poults and bone lesions in broilers (Wideman and Pevzner, 2012). All those studies indicated the link between health status

and bone remodeling in broilers, suggesting immune status must be considered as another critical factor in the pathogenesis of bone abnormities under intestinal parasite infection.

References

Abdel-Haleem, H. M., S. M. Aboelhadid, T. Sakran, G. El-Shahawy, H. El-Fayoumi, S. Al-Quraishy, and A. S. Abdel-Baki. (2017). Gene expression, oxidative stress and apoptotic changes in rabbit ileum experimentally infected with *Eimeria* intestinalis. Folia Parasitol. (Praha) 64.

Adhikari, R., Chen, C., Kim, W. K. (2020). Effect of 20(S)-hydroxycholesterol on multilineage differentiation of mesenchymal stem cells isolated from compact bones in Chicken. Genes (Basel), 11(11). doi:10.3390/genes11111360.

Akbari Moghaddam Kakhki, R., Z. Lu, A. Thanabalan, H. Leung, M. Mohammadigheisar and E. Kiarie (2019). *Eimeria* challenge adversely affected long bone attributes linked to increased resorption in 14-day-old broiler chickens. Poult Sci 98(4): 1615-1621.

Akhter, M. P., J. M. Lappe, K. M. Davies and R. R. Recker (2007). Transmenopausal changes in the trabecular bone structure. Bone 41(1): 111-116.

Allen, P. C. (1987). Effect of *Eimeria acervulina* infection on chick (*Gallus domesticus*) high density lipoprotein composition. Comp. Biochem. Physiol. B 87(2): 313-319.

Amerah, A. M. and V. Ravindran (2015). Effect of coccidia challenge and natural betaine supplementation on performance, nutrient utilization, and intestinal lesion scores of broiler chickens fed suboptimal level of dietary methionine. Poult Sci 94(4): 673-680.

Arczewska-Wlosek, A., S. Swiatkiewicz, K. Ognik and D. Jozefiak (2018). Effect of dietary crude protein level and supplemental herbal extract blend on selected blood variables in broiler chickens vaccinated against coccidiosis. Animals (Basel) 8(11).

Alrubaye, A. A. K., N. S. Ekesi, A. Hasan, D. A. Koltes, R. F. Wideman, Jr., and D. D. Rhoads. (2020). Chondronecrosis with osteomyelitis in broilers: further defining a bacterial challenge model using standard litter flooring and protection with probiotics. Poult Sci 99: 6474-80.

Atashi, F., A. Modarressi, and M. S. Pepper. 2015. The role of reactive oxygen species in mesenchymal stem cell adipogenic and osteogenic differentiation: a review, Stem Cells Devs 24: 1150-63.

Bouxsein, M. L., S. K. Boyd, B. A. Christiansen, R. E. Guldberg, K. J. Jepsen, and R. Muller. (2010). Guidelines for assessment of bone microstructure in rodents using micro-computed tomography. J Bone Miner Res 25:1468-1486.

Brandi, M. L. (2009). Microarchitecture, the key to bone quality. Rheumatology (Oxford) 48 Suppl 4: iv3-8.

Baron, R., R. Tross and A. Vignery (1984). Evidence of sequential remodeling in rat trabecular bone: morphology, dynamic histomorphometry, and changes during skeletal maturation. Anat Rec 208(1): 137-145.

Basu, S., K. Michaelsson, H. Olofsson, S. Johansson and H. Melhus (2001). Association between oxidative stress and bone mineral density. Biochem Biophys Res Commun 288(1): 275-279.

Bedimo, R. J., B. Adams-Huet, J. Poindexter, G. Brown, I. Farukhi, R. Castanon, D. Turner, T. Moore, P. Tebas and N. M. Maalouf. (2018). The differential effects of human immunodeficiency virus and hepatitis c virus on bone microarchitecture and fracture risk. Clin Infect Dis 66(9): 1442-1447.

Blake, D. P. and F. M. Tomley (2014). Securing poultry production from the ever-present Eimeria challenge. Trends Parasitol 30(1): 12-19.

Blake, D. P., J. Knox, B. Dehaeck, B. Huntington, T. Rathinam, V. Ravipati, S. Ayoade, W. Gilbert, A. O. Adebambo, I. D. Jatau, M. Raman, D. Parker, J. Rushton, and F. M. Tomley. (2020). Re-calculating the cost of coccidiosis in chickens. Vet. Res 51:115.

Borah, B., T. E. Dufresne, P. A. Chmielewski, T. D. Johnson, A. Chines and M. D. Manhart (2004). Risedronate preserves bone architecture in postmenopausal women with osteoporosis as measured by three-dimensional microcomputed tomography. Bone 34(4): 736-746.

Boskey, A. L. and L. Imbert (2017). Bone quality changes associated with aging and disease: a review. Ann N Y Acad Sci 1410(1): 93-106.

Cao, S., T. Li, Y. Shao, L. Zhang, L. Lu, R. Zhang, S. Hou, X. Luo and X. Liao (2021). Regulation of bone phosphorus retention and bone development possibly by related hormones and local bone-derived regulators in broiler chicks. J Anim Sci Biotechnol 12(1): 88.

Cervantes, H. M. (2015). Antibiotic-free poultry production: Is it sustainable? J Appl Poult Res 24 (1): 91-97.

Chapman, H. D. (2014). Milestones in avian coccidiosis research: a review. Poult Sci 93:501-511.

Chen, C., and W. K. Kim. (2020). The application of micro-CT in egg-laying hen bone analysis: introducing an automated bone separation algorithm. Poult Sci 99:5175-5183.

Costantini, D., and A. P. Moller. (2009). Does immune response cause oxidative stress in birds? A meta-analysis. Comp biochem physiol, Mol amp; integr physiol 153: 339-44.

Dalloul, R. A. and H. S. Lillehoj (2006). Poultry coccidiosis: recent advancements in control measures and vaccine development. Expert Rev Vaccines 5(1): 143-163.

Domazetovic, V., G. Marcucci, T. Iantomasi, M. L. Brandi, and M. T. Vincenzini. (2017). Oxidative stress in bone remodeling: role of antioxidants. Clin Cases Miner Bone Metab 14:209-216.

Edwards, H. M., Jr. (2000). Nutrition and skeletal problems in poultry. Poult Sci 79(7): 1018-1023.

Estevez, M. (2015). Oxidative damage to poultry: from farm to fork. Poult Sci 94:1368-1378.

Florczyk-Soluch, U., E. Jozefczuk, J. Stepniewski, K. Bukowska-Strakova, M. Mendel, M. Viscardi, W. N. Nowak, A. Jozkowicz, and J. Dulak. (2018). Various roles of heme oxygenase-1 in response of bone marrow macrophages to RANKL and in the early stage of osteoclastogenesis. Sci Rep 8:10797.

Eliaz, N. and N. Metoki (2017). Calcium Phosphate Bioceramics: A Review of Their History, Structure, Properties, Coating Technologies and Biomedical Applications. Materials (Basel) 10(4).

Fleming, R. H. (2008). Nutritional factors affecting poultry bone health. Proc Nutr Soc 67(2): 177-183.

Gautier, A. E., J. D. Latorre, P. L. Matsler, and S. J. Rochell. (2019). Longitudinal Characterization of Coccidiosis Control Methods on Live Performance and Nutrient Utilization in Broilers. Front Vet Sci 6:468.

Georgieva, N. V., V. Koinarski, and V. Gadjeva. (2006). Antioxidant status during the course of Eimeria tenella infection in broiler chickens. Vet. J. 172:488-492.

Georgieva, N. V., M. Gabrashanska, V. Koinarski, and Z. Yaneva. (2011). Zinc Supplementation against Eimeria acervulina-Induced Oxidative Damage in Broiler Chickens. Vet. Med. Int. 2011:647124.

Gould, R. L., Y. Zhou, C. L. Yakaitis, K. Love, J. Reeves, W. Kong, E. Coe, Y. Xiao and R. Pazdro (2018). Heritability of the aged glutathione phenotype is dependent on tissue of origin. Mamm Genome 29 (9-10): 619-631.

Greenwood, C., J. G. Clement, A. J. Dicken, J. P. Evans, I. D. Lyburn, R. M. Martin, K. D. Rogers, N. Stone, G. Adams and P. Zioupos (2015). The micro-architecture of human cancellous bone from fracture neck of femur patients in relation to the structural integrity and fracture toughness of the tissue. Bone Rep 3: 67-75.

Hu, L., C. Yin, F. Zhao, A. Ali, J. Ma, and A. Qian. (2018). Mesenchymal Stem Cells: Cell Fate Decision to Osteoblast or Adipocyte and Application in Osteoporosis Treatment. Int. J. Mol. Sci. 19.

Henkelmann, R., K.-H. Frosch, R. Glaab, H. Lill, C. Schoepp, D. Seybold, C. Josten and P. Hepp (2017). Infection following fractures of the proximal tibia – a systematic review of incidence and outcome. BMC Musculoskelet Disord 18 (1): 481.

Hildebrand, T. and P. Ruegsegger (1997). Quantification of Bone Microarchitecture with the Structure Model Index. Comput Methods Biomech Biomed Engin 1(1): 15-23.

Immenschuh, S., E. Baumgart-Vogt, and S. Mueller. (2010). Heme oxygenase-1 and iron in liver inflammation: a complex alliance, Curr Drug Targets 11(12): 1541-1550.

Joyner, L. P., D. S. Patterson, S. Berrett, C. D. Boarer, F. H. Cheong and C. C. Norton (1975). Amino-acid malabsorption and intestinal leakage of plasma-proteins in young chicks infected with *Eimeria acervulina*. Avian Pathol 4(1): 17-33.

Kamibayashi, L., U. P. Wyss, T. D. V. Cooke and B. Zee (1995). Trabecular microstructure in the medial condyle of the proximal tibia of patients with knee osteoarthritis. Bone 17(1): 27-35.

Kazakia, G. J., J. Carballido-Gamio, A. Lai, L. Nardo, L. Facchetti, C. Pasco, C. A. Zhang, M. Han, A. H. Parrott, P. Tien and R. Krug (2018). Trabecular bone microstructure is impaired in the proximal femur of human immunodeficiency virus-infected men with normal bone mineral density. Quant Imaging Med Surg 8(1): 5-13.

Lauridsen, C. (2019). From oxidative stress to inflammation: redox balance and immune system, Poult Sci 98: 4240-46.

Lee, M. S. J., K. Maruyama, Y. Fujita, A. Konishi, P. M. Lelliott, S. Itagaki, T. Horii, J. W. Lin, S. M. Khan, E. Kuroda, S. Akira, K. J. Ishii and C. Coban (2017). Plasmodium products persist in the bone marrow and promote chronic bone loss. Sci Immunol 2(12). doi: 10.1126/sciimmunol.aam8093

Lee, Y., S. H. Lee, S. J. Lee, U. D. Gadde, S. T. Oh, H. Han, and H. S. Lillehoj (2018). Effects of dietary allium hookeri root on growth performance and antioxidant activity in young broiler chickens. Res. Vet. Sci. 118:345-350.

Lin, T. H., C. H. Tang, S. Y. Hung, S. H. Liu, Y. M. Lin, W. M. Fu, and Yang, R. S. (2010). Upregulation of heme oxygenase-1 inhibits the maturation and mineralization of osteoblasts. J. Cell. Physiol. 222:757-768.

Mireles, A. J., S. M. Kim, and K. C. Klasing. (2005). An acute inflammatory response alters bone homeostasis, body composition, and the humoral immune response of broiler chickens. Poult Sci 84:553-560.

Mishra, B., and R. Jha. (2019). Oxidative stress in the poultry gut: potential challenges and interventions. Front Vet Sci 6:60.

Mubarak, S. J., J. R. Kim, E. W. Edmonds, M. E. Pring, and T. P. Bastrom. (2009). Classification of proximal tibial fractures in children, J Pediatr Orthop 3: 191-197.

Oh, S., Lillehoj, H. S., Lee, Y., Bravo, D., & Lillehoj, E. P. (2019). Dietary antibiotic growth promoters down-regulate intestinal inflammatory cytokine expression in chickens challenged with lps or co-infected with eimeria maxima and clostridium perfringens. Front Vet Sci, 6, 420. doi:10.3389/fvets.2019.00420.

Oikeh, I., P. Sakkas, D. P. Blake and I. Kyriazakis (2019). Interactions between dietary calcium and phosphorus level, and vitamin D source on bone mineralization, performance, and intestinal morphology of coccidia-infected broilers1. Poult Sci 98(11): 5679-5690.

Otterbein, L. E., and A. M. Choi. (2000). Heme oxygenase: colors of defense against cellular stress. Am. J. Physiol. Lung Cell Mol. Physiol. 279: L1029-1037.

Park, H. J., E. Mah and R. S. Bruno (2010). Validation of high-performance liquid chromatography-boron-doped diamond detection for assessing hepatic glutathione redox status. Anal Biochem 407(2): 151-159.

Prat-Fabregat, S. and P. Camacho-Carrasco (2016). Treatment strategy for tibial plateau fractures: an update. EFORT Open Rev 1(5): 225-232.

Preston-Mafham, R. A. and A. H. Sykes (1970). Changes in body weight and intestinal absorption during infections with *Eimeria acervulina* in the chicken. Parasitology 61(3): 417-424.

Prisby, R., Menezes, T., Campbell, J., Benson, T., Samraj, E., Pevzner, I., & Wideman, R. F., Jr. (2014). Kinetic examination of femoral bone modeling in broilers. Poult Sci, 93(5). 1122-1129. doi:10.3382/ps.2013-03778

Qiu, Y., C. Tang, M. Serrano-Sosa, J. Hu, J. Zhu, G. Tang, C. Huang and M. Huang (2019). Bone microarchitectural parameters can detect oxytocin induced changes prior to bone density on mitigating bone deterioration in rabbit osteoporosis model using micro-CT. BMC Musculoskelet Disord 20(1): 560.

Rath, N. C., and V. Durairaj. (2022). “Avian bone physiology and poultry bone disorders” in Sturkie's Avian Physiology (San Diego: Academic Press), 529-543.

Raehtz, S., B. M. Hargis, V. A. Kuttappan, R. Pamukcu, L. R. Bielke, and L. R. McCabe. (2018) High Molecular Weight Polymer Promotes Bone Health and Prevents Bone Loss Under Salmonella Challenge in Broiler Chickens, Front Physiol, 9: 384.

Rehman, Z. U., C. Meng, Y. Sun, A. Safdar, R. H. Pasha, M. Munir, and C. Ding. (2018) Oxidative Stress in Poultry: Lessons from the Viral Infections, Oxid Med Cell Longev, 2018: 5123147.

Saha, S., B. Buttari, E. Panieri, E. Profumo, and L. Saso (2020). An Overview of Nrf2 Signaling Pathway and Its Role in Inflammation, Molecules, 25.

Sakkas, P., I. Oikeh, D. P. Blake, M. J. Nolan, R. A. Bailey, A. Oxley, I. Rychlik, G. Lietz and I. Kyriazakis (2018). Does selection for growth rate in broilers affect their resistance and tolerance to *Eimeria maxima*? Vet Parasitol 258: 88-98.

Sakkas, P., I. Oikeh, D. P. Blake, S. Smith and I. Kyriazakis (2019). Dietary vitamin D improves performance and bone mineralisation, but increases parasite replication and compromises gut health in *Eimeria*-infected broilers. Br J Nutr 122(6): 676-688.

Santos, T. S. d., P.-Y. Teng, S. Yadav, F. L. d. S. Castro, R. L. Gould, S. W. Craig, C. Chen, A. L. Fuller, R. Pazdro, J. R. Sartori and W. K. Kim (2020). Effects of inorganic Zn and Cu supplementation on gut health in broiler chickens challenged with *Eimeria* spp. Front Vet Sci 7:230

Schmidt, C. J., M. E. Persia, E. Feierstein, B. Kingham, and W. W. Saylor (2009). Comparison of a modern broiler line and a heritage line unselected since the 1950s, Poult Sci, 88: 2610-9.

Serdar, C. C., M. Cihan, D. Yucel, and M. A. Serdar. 2021. 'Sample size, power and effect size revisited: simplified and practical approaches in pre-clinical, clinical and laboratory studies', *Biochemia Medica: Casopis Hrvatskoga Drustva Medicinskih Biokemicara*, 31: 010502.

Seifert, M. F. and B. A. Watkins (1997). Role of dietary lipid and antioxidants in bone metabolism. Nutr Res 17(7): 1209-1228.

Sepp, T., U. Karu, J. D. Blount, E. Sild, M. Manniste and P. Horak (2012). Coccidian infection causes oxidative damage in greenfinches. PLoS One 7(5): e36495. doi: 10.1371/journal.pone.0036495

Sharma, V. D. and M. A. Fernando (1975). Effect of *Eimeria acervulina* infection on nutrient retention with special reference to fat malabsorption in chickens. Can J Comp Med 39(2): 146-154.

Sheppard, A. J., A. M. Barfield, S. Barton, and Y. Dong. (2022). Understanding reactive Oxygen species in bone regeneration: a glance at potential therapeutics and bioengineering applications, Front Bioeng Biotechnol, 10: 836764.

Shockley, K. R., O. P. Lazarenko, P. J. Czernik, C. J. Rosen, G. A. Churchill, and B. Lecka-Czernik. 2009. *PPARgamma2* nuclear receptor controls multiple regulatory pathways of osteoblast differentiation from marrow mesenchymal stem cells. J Cell Biochem 106: 232-246.

Solomon, L. B., D. Kitchen, P. H. Anderson, D. Yang, Y. Starczak, M. Kogawa, E. Perilli, P. J. Smitham, M. S. Rickman, D. Thewlis and G. J. Atkins (2018). Time dependent loss of trabecular bone in human tibial plateau fractures. J Orthop Res 36(11): 2865-2875.

Su, S., Wang, Y., Chen, C., Suh, M., Azain, M., Kim, W. K. (2020). Fatty acid composition and regulatory gene expression in late-term embryos of ACRB and COBB broilers. Front Vet Sci, *7*, 317. doi:10.3389/fvets.2020.00317.

Surai, P. F., Kochish, II, V. I. Fisinin, and M. T. Kidd. (2019). Antioxidant Defence Systems and Oxidative Stress in Poultry Biology: An Update, Antioxidants (Basel), 8.

Turk, D. E. (1973). Calcium absorption during coccidial infections in chicks. Poult Sci 52(3): 854-857.

Turk, D. E. and J. F. Stephens (1967). Upper intestinal tract infection produced by *E. acervulina* and absorption of 65Zn and 131-I-labeled oleic acid. J Nutr, 93(2): 161-165.

Turk, D. E. and J. F. Stephens (1969). Coccidial infections of the ileum, colon, and ceca of the chick and nutrient absorption. Poult Sci, 48(2): 586-589.

Turk, D. E. and J. F. Stephens (1970). Effects of serial inoculations with *Eimeria acervulina* or *Eimeria necatrix* upon zinc and oleic acid absorption in chicks. Poult Sci, 49(2): 523-526.

Teng, P. Y., S. Yadav, F. L. S. Castro, Y. H. Tompkins, A. L. Fuller, and W. K. Kim (2020). Graded *Eimeria* challenge linearly regulated growth performance, dynamic change of gastrointestinal permeability, apparent ileal digestibility, intestinal morphology, and tight junctions of broiler chickens. Poult Sci, 99:4203-4216.

Thiese, M. S., B. Ronna, and U. Ott (2016). P value interpretations and considerations, J Thorac Dis, 8: E928-E31.

Vandesompele, J., K. De Preter, F. Pattyn, B. Poppe, N. Van Roy, A. De Paepe, and F. Speleman (2002). Accurate normalization of real-time quantitative RT-PCR data by geometric averaging of multiple internal control genes, Genome Biol, 3: RESEARCH0034.

Wideman, R. F., Jr., and Pevzner, I. (2012). Dexamethasone triggers lameness associated with necrosis of the proximal tibial head and proximal femoral head in broilers. Poult Sci, 91(10), 2464-2474

Wideman, R. F., Jr. (2016). Bacterial chondronecrosis with osteomyelitis and lameness in broilers: a review. Poult Sci, 95(2), 325-344.

Yair, R., A. Cahaner, Z. Uni, and R. Shahar (2017). Maternal and genetic effects on broiler bone properties during incubation period, Poult Sci, 96: 2301-11.

Yang, Y., A. V. Bazhin, J. Werner, and S. Karakhanova (2013). Reactive oxygen species in the immune system, Int Rev Immunol, 32: 249-70.

Yin, M. T., E. Lund, J. Shah, C. A. Zhang, M. Foca, N. Neu, K. K. Nishiyama, B. Zhou, X. E. Guo, J. Nelson, D. L. Bell, E. Shane and S. M. Arpadi (2014). Lower peak bone mass and abnormal trabecular and cortical microarchitecture in young men infected with HIV early in life. AIDS, 28(3): 345-353.

Zhang, F., Peng, W., Zhang, J., Dong, W., Yuan, D., Zheng, Y., & Wang, Z. (2019). New strategy of bone marrow mesenchymal stem cells against oxidative stress injury via Nrf2 pathway: oxidative stress preconditioning. J. Cell. Biochem., 120(12), 19902-19914. doi:10.1002/jcb.29298

Tables

Table 2.1 *Eimeria* spp. challenge dosage (Unit: oocysts/ chick).

Treatment group[1]	*E. maxima*	*E. tenella*	*E. acervulina*	Total concentration	Challenge dosage
Control	0	0	0	0	Non-challenge
Low	6,250	6,250	31,250	43,750	Lowest challenge dose
Med-low	12,500	12,500	62,500	87,500	Medium-low challenge dose
Med-high	25,000	25,000	125,000	175,000	Medium-high challenge dose
High	50,000	50,000	250,000	350,000	Highest challenge dose

[1]Low, the lowest challenge dose; Med-low, the medium-low challenge dose; Med-high, the medium-high challenge dose; High, the highest challenge dose.

Table 2.2: Definition and description of bone microstructure by using micro-CT method (Bouxsein et al., 2010).

Abbreviation	variable	Unit	Description
BMC	Bone mineral content	g	The amount of the solid objects (bone minerals that mostly included calcium and phosphorous) within the region of interest.
BMD	Bone mineral density	g/mm^2	The ratio of bone minerals within a mixed bone-soft tissue region
TV	Total volume	mm^3	Volume of the entire region of interest
BV	Bone volume	mm^3	Volume of the region segmented as bone
BS	Bone surface	mm^2	Surface area of all solid objects (bone tissue) within the total tissue volume
BV/TV	Bone volume fraction	%	Ratio of the solid objects (bone tissue) volume to the total volume of the region of interest
BS/BV	Specific bone surface	mm^2/mm^3	Ratio of the segmented bone surface to the mineralized bone volume
BS/TV	Bone surface density	%	Ratio of the segmented bone surface to the total volume of the region of interest
Tb. N	Trabecular number	1/mm	Measure of the average number of trabeculae per unit length
Tb. Th	Trabecular thickness	mm	Mean thickness of trabeculae osseous structure. It assessed using direct 3D methods
Tb. Sp	Trabecular spacing	mm	Mean space between trabeculae (marrow space), assessed using direct 3D methods
SMI	Structure model index	-	An indicator of the structure of trabeculae; Parallel plates was defined as 0 and and cylindrical rods was rated as 3
Tb.pf	Trabecular pattern factor	1/mm	Describes quantitatively trabecular connectivity
Conn. Dn	Connectivity density	$1/mm^3$	A measure of the degree of connectivity of trabeculae normalized by TV

Po (op)	Cortical porosity (open pore)	%	In a given cortical region, the volume of open pores (Po.V, mm^3) ÷ total volume of cortical bone compartment (Ct.V, mm^3)
Po.V(op)	Open pore volume	mm^3	The volume of the open pores
Po.V(tot)	Total pore volume	mm^3	The volume of all pores
Po (tot)	Total cortical porosity	%	In a given cortical region, the volume of pores (Po.V, mm^3) ÷ total volume of cortical bone compartment (Ct.V, mm^3)

Table 2.3: Nucleotide sequences of the primers used for real-time qPCR.

Gene[1]	Primer sequence (5'-3')	Product length (bp)	Annealing temperature (°C)	Accession #	Gene references
GAPDH	F-GCTAAGGCTGTGGGGAAAGT R-TCAGCAGCAGCCTTCACTAC	161	55	NM_204305.1	Su et al., 2020
ACTB	F-CAACACAGTGCTGTCTGGTGGTA R-ATCGTACTCCTGCTTGCTGATCC	205	61	NM_205518.1	Teng et al., 2020
NFKB1	F-GAAGGAATCGTACCGGGAACA R-CTCAGAGGGCCTTGTGACAGTAA	131	59	XM_015285418.2	Su et al., 2020
RUNX2	F-ACTTTGACAATAACTGTCCT R-GACCCCTACTCTCATACTGG	192	60	XM_015285081.2	Adhikari, et al, 2020
PPARG	F-GAGCCCAAGTTTGAGTTTGC R-TCTTCAATGGGCTTCACATTT	131	58	XM_025154400.1	Chen et al., 2021
FASN	F-AGAGGCTTTGAAGCTCGGAC R-GGTGCCTGAATACTTGGGCT	127	60	NM_205155.3	Su et al., 2020
FABP4	F-GCAGAAGTGGGATGGCAAAG R-GTTCGCCTTCGGATCAGTCC	153	60	NM_204290.1	Chen et al., 2021
BGLAP	F-GGATGCTCGCAGTGCTAAAG	142	57	NM_205387.3	Adhikari, et al, 2020

	R-CTCACACACCTCTCGTTGGG				
SOD1	F-ATTACCGGCTTGTCTGATGG	173	58	NM_205064.1	(Oh, et al., 2019)
	R-CCTCCCTTTGCAGTCACATT				
CAT	F-ACTGCAAGGCGAAAGTGTTT	222	60	NM_001031215.1	(Oh, et al., 2019)
	R-GGCTATGGATGAAGGATGGA				
AKR7A2	F-CAAACTGCAGGGTTCTCTTG	234	60	NM_205344.1	Lee et al., 2018
	R-GAAGTAGTTGGGGCAGTCGT				
HMOX1	F-CTGGAGAAGGGTTGGCTTTCT	166	60	XM_417628.2	(Oh, et al., 2019)
	R-GAAGCTCTGCCTTTGGCTGTA				
GPX1	F-AACCAATTCGGGCACCAG	122	60	NM_001277853.2	(Oh, et al., 2019)
	R-CCGTTCACCTCGCACTTCTC				

[1] GAPDH: glyceraldehyde-3-phosphate dehydrogenase; ACTB: actin beta; PPARG: peroxisome proliferator-activated receptor gamma; FASN: fatty acid synthase; SREBP1: sterol regulatory element-binding transcription factor 1; BGLAP: bone gamma-carboxyglutamate protein; RUNX2: runt-related transcription factor 2; FABP4: adipose tissue fatty acid binding protein 4; NFKB1: nuclear factor kappa B subunit 1; CAT: catalase; SOD1: superoxide dismutase type 1; GPX1: glutathione peroxidase 1; HMOX1: heme oxygenase 1; and AKR7A2: aflatoxin aldehyde reductase

Table 2.4: Tibia length, width, and cortical bone thickness.

Unit (mm)	Bone length	Bone width	Cortical bone thickness[1]
Control	54.497	4.959	0.841
Low	54.436	4.969	0.850
Med-low	55.413	4.958	0.898
Med-High	55.109	4.969	0.841
High	55.092	5.086	0.873
SEM	0.244	0.051	0.021
ANOVA	0.226	0.925	0.836

[1]Cortical thickness: a mean thickness of cortical mid-shaft.

Table 2.5: Tibial metaphysis microstructure changes with increasing challenge dose of mixed *Eimeria spp*. oocysts.

	Items[1*]	Unit	Control	Low	Med-low	Med-high	High	SEM	ANOVA
Total	BMC	g	61.244 ^{ab}	70.906 ^{a}	68.282 ^{ab}	67.241 ^{ab}	51.567 ^{b}	2.139	0.025
	BMD	g/mm$_2$	0.209 ^{a}	0.209 ^{a}	0.215 ^{a}	0.213 ^{a}	0.170 ^{b}	0.004	0.002
	TV	mm^3	295.216	339.192	318.777	312.631	303.064	6.177	0.284
	BV	mm^3	89.331	100.332	108.552	101.309	85.588	3.196	0.134
	BS	mm^2	1260.402	1419.550	1415.952	1333.981	1116.761	48.366	0.250
	BV/TV	%	29.590 ^{ab}	29.628 ^{ab}	34.105 ^{a}	32.069 ^{ab}	28.161 ^{b}	0.667	0.023
	BS/BV	mm^2/mm^3	14.018	14.114	13.047	13.281	13.025	0.224	0.360
	BS/TV	%	4.160	4.171	4.454	4.236	3.671	0.105	0.202
Trabecular	BMC	g	2.812^{a}	2.646 ^{a}	1.839^{a} ^{b}	2.462^{a}	1.087^{b}	0.161	0.001
	BMD	g/mm$_2$	0.087^{a}	0.096 ^{a}	0.068^{a} ^{b}	0.083^{a}	0.038^{b}	0.005	<0.001
	TV	mm^3	178.487	205.576	174.901	178.060	188.858	3.882	0.065
	BV	mm^3	5.802	7.704	6.717	6.086	4.863	0.331	0.073
	BS	mm^2	295.527^{a}	385.188^{ab}	340.596 ^{ab}	321.624 ^{ab}	258.360 ^{b}	14.230	0.048
	BV/TV	%	3.238	3.710	3.863	3.424	2.590 72	0.156	0.075
	BS/BV	mm^2/mm^3	52.046	50.578	50.831	52.900	54.140	0.643	0.394
	Tb. N	1/mm	0.389 ^{ab}	0.435 ^{ab}	0.464 ^{a}	0.421 ^{ab}	0.310 ^{b}	0.017	0.025
	Tb. Th	mm	0.082	0.085	0.083	0.081	0.083	0.001	0.846
	Tb. Sp	mm	2.848	2.513	2.364	2.376	2.935	0.087	0.100

	SMI	-	2.622[b]	2.617[b]	2.577[b]	2.661[ab]	2.759[a]	0.017	0.002
	Tb.pf	1/mm	18.814[ab]	18.238[ab]	17.943[b]	19.635[ab]	21.084[a]	0.360	0.029
	Conn. Dn	$1/mm^3$	10.158[ab]	11.076[a]	11.852[ab]	10.389[ab]	8.077[b]	0.407	0.035
Cortical	BMC	g	44.029	47.190	51.033	46.949	41.989	1.388	0.306
	BMD	g/mm^2	0.412	0.401	0.404	0.402	0.409	0.876	0.876
	TV	mm^3	108.061	118.168	126.627	117.158	103.270	3.955	0.386
	BV	mm^3	79.177	87.435	93.899	87.243	78.179	2.614	0.298
	BV/TV	%	73.945	74.158	74.263	74.701	76.121	0.537	0.741
	Po (op)	%	25.951	25.736	25.604	25.171	23.763	0.536	0.737
	Po.V(op)	mm^3	28.767	30.605	32.559	29.757	24.971	1.455	0.589
	Po.V(tot)	mm^3	28.884	30.733	32.727	29.915	25.091	1.462	0.588
	Po (tot)	%	26.055	25.842	25.738	25.299	23.879	0.537	0.741

[1]Low, the lowest challenge dose; Med-low, the medium-low challenge dose; Med-high, the medium-high challenge dose; High, the highest challenge dose.

[*]BMC, bone mineral content; BMD, bone mineral density; TV, total bone volume; BV, bone volume (TV minus bone marrow volume); BS, bone surface area; BV/TV, bone volume/ total volume; BS/BV, bone surface/ total volume; BS/TV, bone surface/ total volume; Tb. N, trabecular number; Tb.Th, trabecular bone thickness; Tb. Sp, trabecular spacing; SMI, structural model index; Tb.Pf, trabecular pattern factor; Conn. Dn, connectivity density; Po.V (tot), total volume of pore space; Po. V(op), volume of open

pore; Po (tot), porosity rate (percent). [a, ab, b] Treatments with different letters means a significantly difference between treatments by using Tukey's HSD test, $P < 0.05$, N = 6.

Table 2.6: Superoxide dismutase activity (SOD, U/g bone marrow), catalase activity (CAT, U/g bone marrow), GSH (µM/g), GSSG (µM/g) and GSH/GSSG ratio (µM/ µM) concentrations in bone marrow at 6 dpi.

Items[1*]	Unit	Control	Low	Med-low	Med-High	High	SEM	ANOVA	Non-challenge vs challenge[2]
GSH	µM/g	18.145	20.891	19.154	14.762	15.318	1.260	0.495	0.469
GSSG	µM/g	0.487	0.506	0.613	0.360	0.353	0.034	0.069	0.224
GSH + 2GSSG	µM/g	19.119	21.903	20.379	15.482	16.025	1.296	0.452	0.453
GSH/GSSG	µM/µM	5.093	5.002	5.137	4.574	4.470	0.288	0.935	0.244
CAT	U/g	32.290	30.271	26.408	27.419	44.407	3.124	0.386	0.937
SOD	U/g	4.574 bc	4.385 c	5.616 ab	5.892 a	5.434[a] bc	0.188	0.027	0.488

[1]Low, the lowest challenge dose; Med-low, the medium-low challenge dose; Med-high, the medium-high challenge dose; High, the highest challenge dose.

[2]The comparisons between non-challenge control and pooled challenged groups (Low, Med-low, Med-high, and High) were calculated by unpaired *t*-test with Welch's correction. [*]GSH: glutathione content; GSSG: oxidized glutathione content; GSH + 2GSSG: the total glutathione level; GSH/GSSG: the ratio of reduced glutathione content to oxidized glutathione content; CAT: catalase activity; SOD: superoxide dismutase. [a, ab, abc, c] Treatments with different letters means a significantly difference between treatments by using Tukey's HSD test, $p < 0.05$, N = 6.

Table 2.7 Superoxide dismutase activity (SOD, U/g), catalase activity (CAT, U/g) and GSH content (µM/g) in the liver at 6 dpi.

Items [1*]	Unit	Control	Low	Med-low	Med-high	High	SEM	ANOVA	Non-challenge vs challenge [2]
SOD	U/g	3891.0	16676.5	10079.2	13335.7	13097.8	60.4	0.166	< 0.001
CAT	U/g	6749.8	6851.56	4361.84	5402.07	5253.27	2029.01	0.778	0.594
GSH	µM/g	11.562 [a]	7.876 [ab]	6.710 [ab]	6.374 [b]	7.688 [ab]	0.600	0.036	0.091

[1]Low, the lowest challenge dose; Med-low, the medium-low challenge dose; Med-high, the medium-high challenge dose; High, the highest challenge dose.

*GSH: glutathione content; CAT: catalase activity; and SOD: superoxide dismutase.

[2]The comparisons between non-challenge control and pooled challenged groups (Low, Med-low, Med-high, and High) were calculated by unpaired *t*-test with Welch's correction**.**

[a, ab, b] Treatments with different letters means a significantly difference between treatments by using Tukey's HSD test, $p < 0.05$, N = 6.

Figures

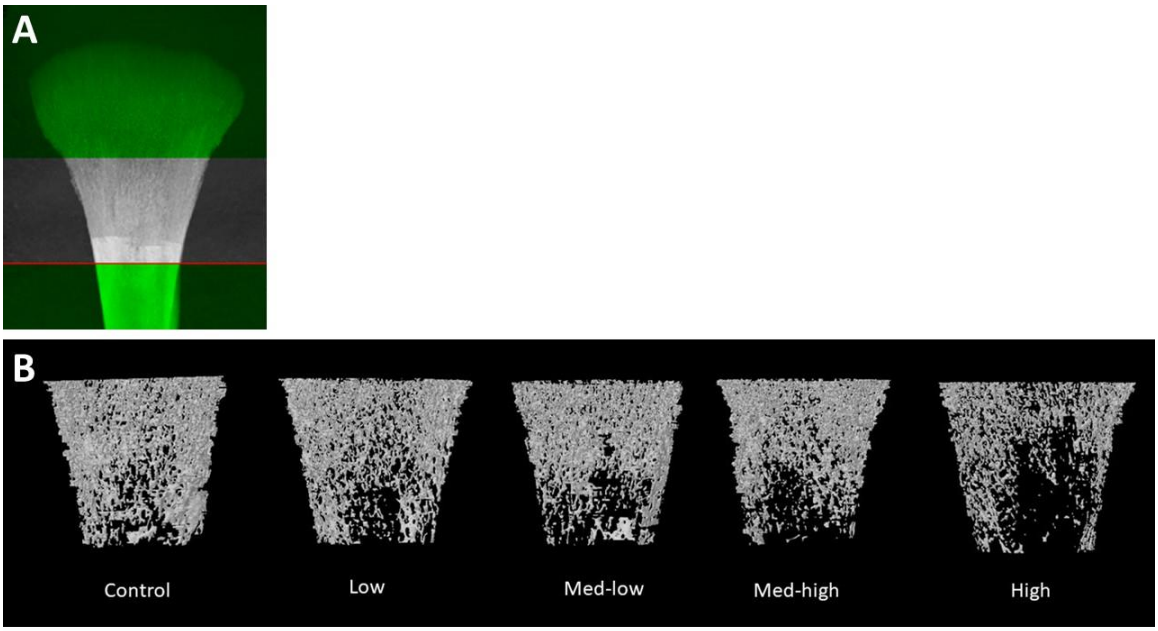

Figure 2.1: (**A**) The selection of metaphyseal region of interest. (**B**) Representative reconstructed 2D images of broiler tibia metaphysis at 6 dpi (19 days of age). Metaphyseal structure analysis showed a lower bone mineral content and density coupled with impaired trabecular bone traits following the higher inoculation doses of *Eimeria*. The negative impact of Eimeria infection on bone traits was mainly located at metaphyseal trabecular bone.

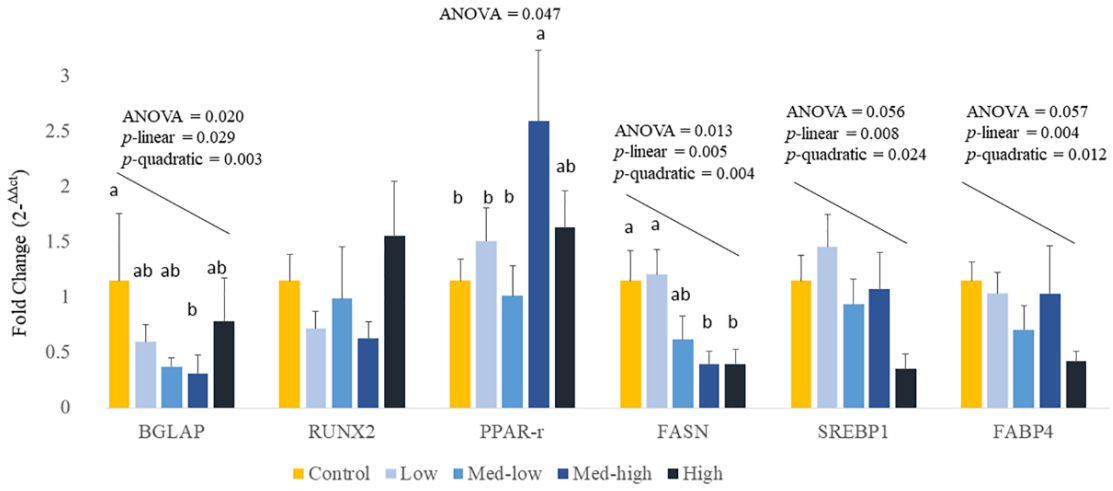

Figure 2.2 Effects of increasing oocysts dose of *Eimeria* mix on osteogenesis, adipogenesis and fatty acid synthesis gene expression in bone marrow of broilers. Low, the lowest challenge dose; Med-low, the medium-low challenge dose; Med-high, the medium-high challenge dose; High, the highest challenge dose. BGLAP: bone gamma-carboxyglutamate protein; RUNX2: runt-related transcription factor 2; PPARG: peroxisome proliferator-activated receptor gamma; FASN: fatty acid synthase; SREBP1: sterol regulatory element-binding transcription factor 1; FABP4: adipose tissue fatty acid binding protein 4.

[a, ab, b] Treatments with different letters means a significantly difference between treatments by using Tukey's HSD test, $p < 0.05$, N = 6.

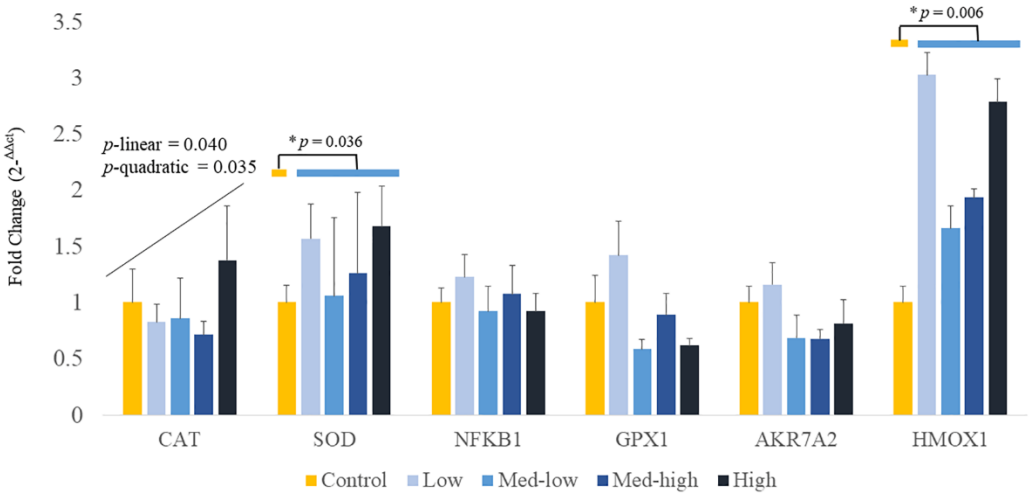

Figure 2.3 Effects of increasing oocysts dose of *Eimeria* mix on the expression of antioxidant-related transcript genes in bone marrow of broilers. Low, the lowest challenge dose; Med-low, the medium-low challenge dose; Med-high, the medium-high challenge dose; High, the highest challenge dose. CAT: catalase; SOD1: superoxide dismutase 1; NFKB1: nuclear factor kappa B subunit 1; GPX1: glutathione peroxidase 1; HMOX1: heme oxygenase 1; and AKR7A2: aflatoxin aldehyde reductase.

[a, ab, b] Treatments with different letters means a significantly difference between treatments by using Tukey's HSD test, $p < 0.05$, $N = 6$. [*] a significant difference between non-challenge control and pooled challenge groups (Low, Med-low, Med-high, and High) by using Welch's *t*-test, $p < 0.05$.

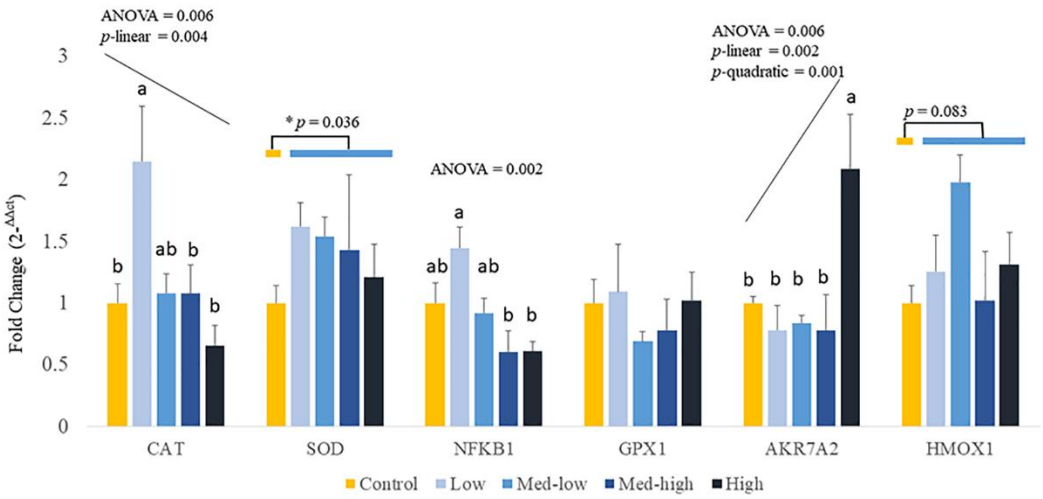

Figure 2.4 Effects of increasing oocysts dose of *Eimeria* mix on antioxidant-related transcripts gene expression in the liver of broilers. Low, the lowest challenge dose; Med-low, the medium-low challenge dose; Med-high, the medium-high challenge dose; High, the highest challenge dose. CAT: catalase; SOD1: superoxide dismutase 1; NFKB1: nuclear factor kappa B subunit 1; GPX1: glutathione peroxidase 1; HMOX1: heme oxygenase 1; and AKR7A2: aflatoxin aldehyde reductase.

[a, ab, b] Treatments with different letters means a significantly difference between treatments by using Tukey's HSD test, $p < 0.05$, N = 6. [*] a significant difference between non-challenge control and pooled challenge groups (Low, Med-low, Med-high, and High) by using Welch's *t*-test, $p < 0.05$

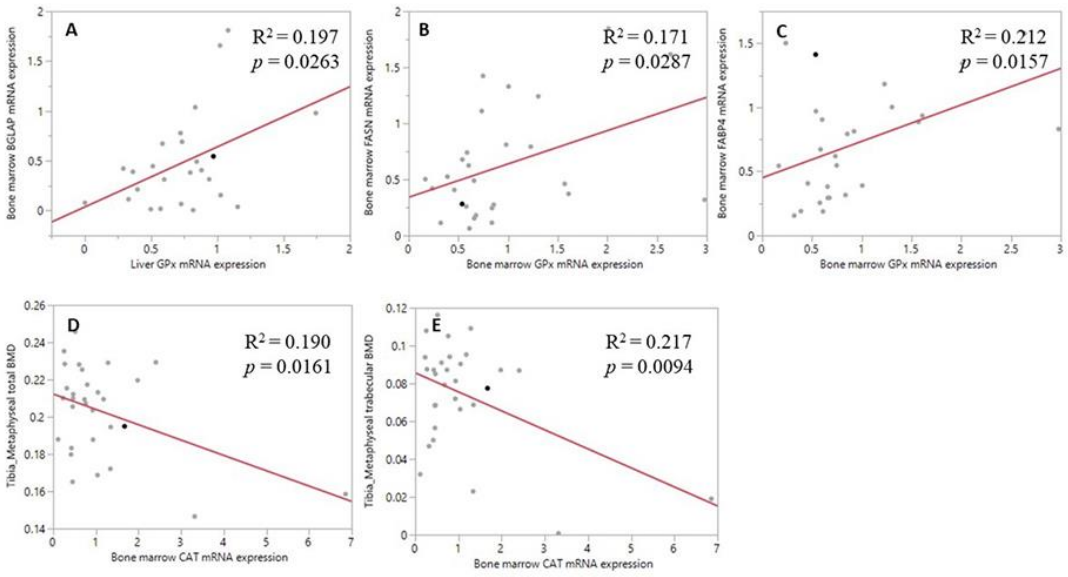

Figure 2.5: Correlation of antioxidant enzyme mRNA expression and bone related parameters. (**A**) The positive correlation between liver *GPX1* mRNA level and the bone marrow *BGLAP* mRNA expression; (**B**) The positive correlation between bone marrow *GPX1* mRNA expression and the bone marrow *FASN* mRNA expression; (**C**) The positive correlation between bone marrow *GPX1* mRNA expression and the bone marrow *FABP4* mRNA expression; (**D**) The negative correlation between bone marrow *CAT* mRNA expression and tibia metaphyseal total BMD; (**E**) The negative correlation between bone marrow *CAT* mRNA expression and tibia metaphyseal trabecular BMD.

CHAPTER 3

REDUCED BONE FORMATION AND INCREASED BONE RESORPTION DRIVE BONE LOSS IN *EIMERIA* INFECTED BROILERS [2]

[2] Yuguo Hou Tompkins, Janghan Choi, Po-Yun Teng, Masayoshi Yamada, Toshie Sugiyama, Woo Kyun Kim. Submitted to *Scientific Reports*

Abstract

Coccidiosis is an economically significant disease in the global poultry industry, but little is known about the mechanisms of bone defects caused by coccidiosis; thus, the study focused on effects of coccidiosis on the bone homeostasis of young broiler chickens. A total of 480 male Cobb500 broilers were randomly allocated into four treatment groups, including an uninfected control consuming diet *ad libitum*, two infected groups were orally gavaged with two different concentrations of sporulated *Eimeria* oocysts, and an uninfected pair-fed group fed the same amount of feed as the high *Eimeria*-infected group consumed. Growth performance and feed intake were recorded, and samples were collected on 6 days post infection. Results indicated that coccidiosis increased systemic oxidative status and elevated immune response in bone marrow, suppressing bone growth rate ($P < 0.05$) and increasing bone resorption ($P < 0.05$) which led to lower bone mineral density ($P < 0.05$) and mineral content ($P < 0.05$) under *Eimeria* infection. With the same amount of feed intake, the uninfected pair-fed group showed a distinguished bone formation rate and bone resorption level compared with the *Eimeria* infected groups. In conclusion, inflammatory immune response and oxidative stress in broilers after *Eimeria* infection were closely associated with altered bone homeostasis, highlighting the role of inflammation and oxidative stress in broiler bone homeostasis during coccidiosis.

Keywords: Broiler, Coccidiosis, *Eimeria*, bone resorption, bone formation, osteoimmunology

Introduction

Coccidiosis induced by protozoan parasites, *Eimeria spp.*, causes a sizeable economic impact in the poultry industry worldwide(Blake, et al., 2020). ***Eimeria spp.*** infect enterocytes and cause severe digestive tract damage, leading to inflammation and malabsorption of nutrients(Yun, 2000; Teng, et al., 2020a; Teng, et al., 2021). Coccidiosis affects chickens of all ages, although the negative impact of coccidiosis was more severe at younger ages owing to the immature immune system (Fatoba and Adeleke, 2018). Furthermore, because the modern broiler chicken is characterized by relatively higher porosity and lower mineral content in long bones (Thorp, 1994; Cook, 2000), broiler chickens' leg bones might be more frangible under the infection with *Eimeria spp*.(Kestin, et al., 1992; Sakkas, et al., 2018; Oikeh, et al., 2019). Coccidiosis significantly reduced tibia bone ash content and adversely affected femur breaking strength (Sakkas, et al., 2019). Sporozoites of some species, especially *E. acervulina* and *E. maxima*, also decreased bone mineral content (BMC) and showed lower bone mineral density (BMD) in infected broilers (Fetterer, et al., 2013). Bone mineral loss caused by *Eimeria spp.* in broiler chickens has been linked to nutrition imbalance and malabsorption with significantly reduced absorption of essential minerals and vitamins (Turk and Stephens, 1969; Turk, 1973; Joyner, et al., 1975; Southern and Baker, 1983; Gautier, et al., 2019). Other than the nutritional factors, emerging evidence suggests that bone homeostasis is mediated by oxidative stress and immune response under disease conditions(Frost, 1994; Allen and Burr, 2014). It has been shown that oxidative stress is a negative impact factor of osteoblast activity in broilers during

Eimeria infection, and there is a potential link between oxidative stress and lower bone quality (Tompkins, et al., 2022b). Moreover, the activity of osteoclasts can be another factor to mediate skeletal homeostasis during pathogen infection (Hambli, 2014; Prisby, et al., 2014). Osteoclasts, unique multinuclear cells, originate from hematopoietic stem cells in bone marrow(Holtrop and King, 1977), are located on the surface of the bone (Teitelbaum, 2007). Osteoclast highly express tartrate-resistant acid phosphatase (TRAP, TRAPase) (Fukushima, et al., 1991).The expression and activity of TRAP enzyme was not only considered as a histochemical biomarker of osteoclasts activity but also considered as an important messenger between skeleton homeostasis and the immune system (Hayman, 2008). Bone marrow also serves as the cradle of hematopoiesis and a reservoir of growth factors and cytokines(Wu, et al., 2010). Many inflammatory cytokines trigger osteoclastic bone resorption by mediating osteoclast formation, cell activity, and lifespan, which ultimately leads to bone mineral loss (Kamibayashi, et al., 1995; Kollet, et al., 2006; Lee, et al., 2017a; Solomon, et al., 2018). The crosstalk between bone homeostasis and immunity was referred as osteoimmunology (Lorenzo, et al., 2008). Receptor activator of nuclear factor kappa B (RANK) is essential in activating the nuclear factor kappa B (NFKB) pathway and the c-Fos (*FOS*, Fos proto-oncogene) pathway by mediating the expression of intracellular promoter nuclear factor of activated T cell (NFATC1) that stimulates the differentiation of osteoclasts(Scott, et al., 1997; Jimi, et al., 1998; Beedles, et al., 1999; Takayanagi, et al., 2002; Boyle, et al., 2003; Huang, et al., 2006; Weitzmann and Pacifici, 2006; Yao, et al., 2008; Nakashima and Takayanagi, 2011). NFKB ligand (RANKL) is a critical cytokine produced mainly in osteoblasts and

regulates osteoclast formation (Taichman, 2005; Lorenzo, et al., 2008). The binding of RANKL to its receptor RANK on the surface of osteoclast progenitor cells triggers the differentiation of osteoclast precursors into osteoclasts, which increases the number of osteoclasts on their bone surfaces (Park, et al., 2017). Besides, pro-osteoclastogenic cytokines produced by macrophages include tumor necrosis factor-α (TNF-α; tumor necrosis factor-α-like in chicken), interleukin-1β (IL1B), and interleukin-6 (IL6) are essential cytokines in mediating osteoclast activity (Rifas, 1999; Kwan Tat, et al., 2004; Wei, et al., 2005; Schett, 2008; Park, et al., 2017). Meanwhile, those cytokines are excessively released in response to *Eimeria* infection (Byrnes, et al., 1993; Lillehoj, 1998; Hong, et al., 2006). Moreover, several transcript factors have multiple roles in inflammatory response, osteogenesis, and osteoclastogenesis. For example, osteoprotegerin (OPG) has been shown to be an inhibitor of TNF-related apoptosis (Neville-Webbe, et al., 2004). It is produced by osteoblast lineage cells and acts as a natural decoy receptor for RANKL, negatively regulating RANK-RANKL signaling and reducing bone resorption. The ratio of RANKL/OPG was used as a biomarker that indicates the occurrence of bone remodeling (Boyce and Xing, 2008). Modulating the expression of OPG/RANKL can affect the activity of osteoblasts, osteoclastogenesis, and osteoclast activity. SMAD1 is a key element that intermediates transforming growth factor-beta signaling and the bone morphogenetic protein (BMP) signaling pathway that are essential in osteoblast activity, bone mineralization, and osteoclast differentiation (Tasca, et al., 2015; Tasca, et al., 2018; Zou, et al., 2021).

In poultry studies, Kakhki et al., (2019) have reported *Eimeria spp.* had adverse effects on long bone homeostasis, which is attributed to bone remodeling status(Akbari Moghaddam Kakhki, et al., 2019). However, the biomechanical properties of specific bone homeostasis and its precise etiology remain to be fully elucidated. Based on the aforementioned information, we hypothesized that broiler bone health during the coccidiosis is not simply caused by nutritional deficiency but also associated with inflammatory immune responses and oxidative stress in the broiler chicken. Thus, the study was conducted to better understand bone homeostasis in broiler chickens and the relationship between inflammation/oxidative stress and skeletal development during acute *Eimeria* infection.

Results

Performance variables and intestinal permeability

On 5 days post-infection (dpi), the Control and the pair-fed (PF) groups showed no sign of intestinal damage, whereas a higher concentration of FITC-d in the serum was detected in the *Eimeria* challenged groups, which revealed damage to the gut epithelium owing to the *Eimeria* infection. Feed restriction in the PF group did not cause intestinal lesions. The high challenge group (High) had higher gastrointestinal permeability than the Control or PF ($P < 0.05$; Figure 3.1). The average daily feed intake (ADFI) was recorded during the trial (Table 3.2). There were no differences in ADFI between the PF and the High (High) ($P > 0.05$). From 4 to 6 dpi, *Eimeria* infection significantly decreased ADFI in the Low ($P < 0.05$) and High ($P < 0.05$) groups when compared to the uninfected Control group. The result of the cumulative feed consumed (FI), body weight

gain (BWG), and feed conversion ratio (FCR) clearly showed that *Eimeria* infection adversely affected all performance parameters ($P < 0.05$; Table 3.2). The low dose of *Eimeria* infection significantly reduced BWG and increased FCR ($P < 0.05$) in broilers compared with the Control during the whole acute challenge period (0-6 dpi); however, it did not significantly alter the FI during the infection. The high dose of *Eimeria* infection significantly reduced BWG ($P < 0.05$) and FI ($P < 0.001$), and increased FCR ($P < 0.001$) compared with the Control or Low group. Significantly lower BWG ($P < 0.05$), lower cumulative FI ($P < 0.05$), and higher FCR ($P < 0.05$) were observed in the PF group compared with the Control. Besides, the PF group showed a 16.21% higher BWG ($P > 0.05$) and significantly lower FCR ($P < 0.05$) when compared with the High.

Bone mineral density was reduced in the *Eimeria*-infected groups

Bone morphology parameters were analyzed in diaphysis and metaphysis sections using microCT (Table 3.3). Tibia diaphyseal BMC was significantly reduced in the High and PF groups ($P < 0.05$), and diaphyseal BMD was reduced in the Low ($P < 0.05$), High ($P < 0.05$) and PF groups ($P < 0.05$) compared with the Control. Tibia metaphyseal BMD (total) was significantly reduced in the Low ($P < 0.05$) and the High ($P < 0.05$), whereas there was no significant difference between the PF group ($P > 0.05$) and the Control. Trabecular BMD and the number of trabecular bone (Tb. N) at metaphyseal regions were significantly reduced in the Low, High, and PF groups ($P < 0.05$) compared to the Control. However, metaphyseal total BMC, metaphyseal trabecular BMC, metaphyseal cortical BMD, and metaphyseal cortical BMC were not affected by *Eimeria* infection or feed restriction.

***Eimeria*-infected broilers exhibited suppression in bone formation**

The distance between double layers of calcein bands was measured at the diaphysis of the tibia and femurs to evaluate bone growth rate (Figure 3.2; Table 2.4). From 0 to 4 dpi (mild infection period), the femoral growth rate was significantly decreased in the High and PF groups compared to the Control, whereas the tibial growth rate was not significantly changed during 0-4 dpi. From 4 to 8 dpi (severe infection period), tibial and femoral growth was significantly reduced in the Low group ($P < 0.05$) and the High group ($P < 0.05$), however, it was not changed in the PF group ($P > 0.05$) when compared with the Control.

By adding data together from both injection stages, during 0-8 dpi, the Low, High, and PF treatment groups showed a significant decrease in bone formation (only femur), whereas the High group had the lowest bone growth rate ($P < 0.05$), followed by the Low ($P < 0.05$) and PF ($P < 0.05$) when compared with the Control. Compared with the Control, tibial growth in the Low and High groups was significantly reduced ($P < 0.05$) by the *Eimeria* challenge. However, the tibial growth of the PF group was not statistically different compared to the Control or infected groups ($P > 0.05$).
Relative mRNA expression of *BGLAP* was significantly reduced in the High group when compared with the Control ($P < 0.05$; Figure 3.3), confirming that the severe infection of *Eimeria* adversely affected long bone growth. However, the expression of other bone formation markers was not significantly changed among the treatments. Moreover, higher cumulative FI was linearly correlated with higher femoral bone formation rate ($R^2 = 0.4655$, $P = 0.010$), but not in tibia ($P > 0.05$). The tibial bone growth rate was

highly correlated with metaphyseal trabecular BMD ($R^2 = 0.710$, $P < 0.001$). Tibial bone growth rate (by calcein injection method) was positively correlated with tibial diaphysis BMD ($R^2 = 0.4308$, $P = 0.032$).

Eimeria infected broilers exhibited an increased bone resorption

The number of osteoclasts per bone surface (N. Ocl/BS) in the Low and High groups was significantly higher than in the Control ($P < 0.05$; Figure 3.4a and 3.4b). *Eimeria* challenge increased the formation of TRAP-positive cells and bone resorption activity on the surface of tibia metaphysis trabecular bone. Meanwhile, an increased serum level of RANKL was observed in the Low ($P < 0.05$; Figure 3.4c), whereas the High and PF serum levels of RANKL had numeric increasing compared to the Control ($P > 0.05$). Moreover, the mRNA expression of *NFATC1* was significantly decreased in the PF ($P < 0.05$; Figure 3.4d), and expression of *TNFRSF11B* (*OPG*) and *TNF* (tumor necrosis factor-like*)* was significantly increased in the High ($P < 0.001$) when compared with the Control. However, there were no significant changes in the expression of *NFKB1*, *RANKL*, *FOS*, *ACP5*(*TRAP*), *IL1B*, and *SMAD1* among the treatments. A higher ratio of *RANKL*/*OPG* was observed in the Low ($P < 0.05$) and the PF ($P < 0.05$) when compared with the High (Figure 3.5). Together, results suggest that *Eimeria* infection resulted in bone remodeling along with higher osteoclast number and activity in broilers. There was a negative correlation between *TNF* and metaphyseal BMD ($R^2 = 0.419$, $P = 0.030$).

Eimeria infection increased lipid peroxidation and decreased antioxidant capacity, and the correlation between redox status and bone parameters

The total antioxidant capacity of serum in the *Eimeria spp*. infected broilers (the Low and High groups) decreased significantly at 6 dpi compared with the non-infected Control ($P < 0.05$; Figure 3.6a). Meanwhile, the total antioxidant capacity of serum in the PF group showed a numeric decrease compared with the Control, but the change was not statistically significant. In contrast to the antioxidant parameters in serum, the level of MDA in the liver was significantly increased by *Eimeria* infection compared with the Control and PF groups ($P < 0.01$; Figure 3.6b) at 6 dpi.

Pearson correlation analyses revealed a negative correlation of the liver TBAR level with femur growth rate ($R^2 = 0.249$, $P = 0.005$) and between the liver TBAR level and tibia growth rate ($R^2 = 0.330$, $P = 0.001$). There was a positive correlation between serum total antioxidant capacity and metaphysis bone mineral density ($R^2 = 0.219$, $P = 0.0182$); and a negative correlation between the liver TBAR level and metaphysis bone mineral density ($R^2 = 0.391$, $P < 0.001$). Meanwhile, bone marrow *BGLAP* mRNA level was negatively correlated with the liver TBAR level ($R^2 = 0.130$, $P = 0.031$) and positively correlated with serum total antioxidant capacity ($R^2 = 0.227$, $P = 0.004$).

Discussion

With increasing concerns around farm animal welfare, poultry bone abnormalities have become one of the significant challenges for the poultry industry. Bone is an essential multifunctional organ that not only provides static functions such as structural support and internal organ protection but also acts as a dynamic endocrine organ that

releases hormones for mineral homeostasis, acid-base balance, and reservoir of energy and minerals (Guntur and Rosen, 2012; Suchacki, et al., 2017). However, for a long time, bone health in broiler production yet gained enough attention until recently because more research suggests that current commercial broiler chicken breeds grow fast to heavyweight that predisposes the chickens to leg weakness and skeletal abnormalities (Bradshaw, et al., 2002; Hartcher and Lum, 2019). With coccidiosis so widespread, the *Eimeria*-challenge model was chosen as a disease model to understand the possible link between intestinal parasite infection and bone health in the current study. With a mild infection, broilers was able to compensate for growth loss partially at later stage after recover from coccidiosis, even so, the growth potential remains severely compromised (Lillehoj, 1998). Uncoupling bone remodeling may not be apparent at early growth but may show up later in the market age, resulting in clinically leg bone abnormality, eventually decreasing the market value (Waldenstedt, 2006). Thus, the early stage of bone health is vital in broiler growth performance and critical in product profitability. The etiology of leg abnormalities under intestinal infection is generally complex. The factors that affect bone metabolism during infection include but are not limited to nutrition, immunity and physical stress. *Eimeria* infection could affect epithelium cells directly by mediating nutrition transporter activity or indirectly by causing apoptosis of cells and damaging the integrity of the intestine (Kong, et al., 2018; Teng, et al., 2020a; Yadav, et al., 2020). The damage to the digestive tract can cause malabsorption of nutrients, the deficiency of macronutrients including carbohydrates, crude protein, lipid, and minerals, and is associated with a bone remodeling imbalance that increases markers

of bone resorption and decreases markers of bone formation (Nattiv, et al., 2007; MacDonell, et al., 2016; Papageorgiou, et al., 2018). Bone also serves as a minerals and energy reservoir, playing a role in maintaining glucose and phosphorus level within a narrow range in blood (Zhou, et al., 2021). Long-term calcium deficiency is a potential risk factor for osteoporosis and bone fracture (Nordin and Morris, 1989; Imari, et al., 2020). Depleting dietary calcium and phosphate could increase bone resorption and decrease bone mineral density (Akesson, et al., 1998; Zhang, et al., 2019c), but increased calcium intake alone is insufficient to compensate for the severe bone mineral loss under acute disease conditions (Reid, et al., 1995). Besides, protein deficiency could significantly decrease BMD and cancellous bone mass, reducing bone strength(Turk, 1973; Southern and Baker, 1983; Bourrin, et al., 2000). FI is positively correlated with the bone formation rate (de Paula and Rosen, 2013). Lower energy, essential amino acid or mineral level can subsequently decrease osteoblastic activity suppressing bone formation. Moreover, nutrition deficiency could modify the plasma levels of certain essential hormones, such as growth hormone and insulin-like growth factor (Bruggeman, et al., 1997; Buyse, et al., 2000), and elevated plasma stress hormones such as corticosterone (de Jong, et al., 2002; Shini and Kaiser, 2009; Almeida, et al., 2017; Iyasere, et al., 2017; Bowling, et al., 2018). Endocrine changes can directly mediate bone remodeling by regulating the activity of osteoblasts or osteoclasts, and those variables should also be considered in the experimental design. In order to permit a clear interpretation of the results and limit the variables of nutrient and endocrine factors, the pair-feeding method was incorporated in this study. Pair-feeding is a technique to

determine the effect of treatment on growth that is independent of nutritional factors. It has been widely used in the animal *in vivo* study model and was particularly well adapted to a study of energy, protein, and mineral intake deficiency (Mitchell and Beadles, 1930; Walker, 2015). In the current study, the amount of feed provided to the uninfected PF group was matched with the High group. However, the growth performance in the PF group was numerically higher than in the High group but not significant. The growth difference between the two groups reflected the metabolic cost of immune activation, oxidative stress, and other factors, rather than feed intake difference. Comparing the High group and the PF group, it provided more direct evidence to find the possible link between immune response/oxidative stress and bone metabolism.

Moreover, the micro-CT analyses revealed more specific details of bone structural changes. A significant drop in BMD was observed in bone metaphysis and diaphysis in both *Eimeria*-infected groups. Furthermore, the PF group and the infected Low and High groups showed different responses in the metaphysis and diaphysis sections. For example, the diaphysis is the mid-section (shaft) of a long bone and is the primary site of radial growth in young animals (Sanchez-Rodriguez, et al., 2019). The diaphysis is made up of cortical bone, which has higher mineral content and density, and less water content when compared with trabecular bone, providing structural strength (Gong, et al., 1964). According to the current results, a significant decrease in BMD, BMC, and bone growth rate was observed in the diaphysis section. Both infected groups and the PF groups showed suppression of bone formation over this site. The PF group had the lowest diaphyseal BMC compared with the other groups. Lowest metaphyseal BMD was

observed in the High group. It showed that bone metabolic activity appears site-specific during *Eimeria* infection, and bone mineral loss occurs distinctly in the proximal tibia metaphysis and diaphysis. Moreover, trabecular bones are metabolically more active than cortical bone, which not only contributes to the strength of the bone but also serves as a source of calcium for the body because trabecular bones are remodeled more rapidly during physiological processes (Whitehead and Fleming, 2000; Passi and Gefen, 2005; Kim and Park, 2013). Cortical bone loss occurs slower than trabecular loss due to the fact that less surface per unit of bone matrix volume is available for bone remodeling (Harada and Rodan, 2003). Nutrient deficiency, stress, and infectious skeletal disorders could cause bone mass loss and decrease bone quality by altering the trabecular bone microarchitecture (Aguado, et al., 2015; Kierończyk, et al., 2017). In human and mouse research, the rate of bone turnover is more rapid in trabecular bone with a larger surface area than in cortical bone (Kent, et al., 1990). The current results showed that the bone mineral loss at the metaphysis section mainly occurred in the trabecular bone structure. Larger bone endo-surface could provide broader space for osteoblast or osteoclast attachment in trabecular bone. We hypothesized that bone resorption happens more frequently around the trabecular bone. Also, the tibial growth rate was highly correlated with tibial trabecular BMD instead of BMC, which indicates metaphysis trabecular bone BMD is more suited to evaluate early biochemical changes of bone during pathogen infection in broilers. Total mineral content (BMC) or bone ash weight may not accurately reflect the metabolic change of bone during infection.

Metabolic changes can be further assessed by different methods focusing on bone formation and resorption individually. Calcein labeling was used in the current study to visualize the newly formatted bone, and the RT-qPCR method was used to examine the bone formation-related marker genes in the bone marrow. The calcein labeling method is commonly used to assess bone growth, which directly visualizes bone growth *in vivo*. According to the results, by correlating FI with bone formation in each group, the Low group had significantly higher FI compared with the PF group; however, the bone formation rate was significantly lower than the PF ($P < 0.05$), which is in agreement with the findings of the microstructure analysis. With the same amount of FI, the PF group has a 4.71% higher BMD than the High group ($P < 0.05$). With a similar amount of FI ($P > 0.05$) between the Control and Low groups, diaphyseal BMD in the Low group was significantly lower than in the Control group. Based on the current results, even though provided with the same amount of feed, the *Eimeria*-challenged chickens had worse bone health status than the PF group, suggesting that apart from nutrition deficiency, other factors may be involved in bone homeostasis in both direct and indirect manners. In our previous studies, we have reported the changed redox status in broilers on 6 dpi after *Eimeria spp.* challenge(Tompkins, et al., 2022b). Oxidative stress has been acknowledged as a major contributor to the immune response. The increased production of ROS is an inflammatory response that functions for the recruitment and activation of immune cells that lead to pathogen killing(Georgieva, et al., 2006). ROS production is involved in mineral homeostasis and contributes to bone remodeling by promoting bone resorption and suppressing bone formation. Human and mice studies have found a tight

association between oxidative stress and pathogenesis of the bone disorder, that the redox state changes are related to the bone modeling and remodeling processes(Mody, 2001; Bai, et al., 2004). The redox state can directly impact osteoblast activity that regulates bone formation rate(Domazetovic, et al., 2017). Oxidative stress suppressed the osteoblastic differentiation process of primary bone marrow stem cells(Bai, et al., 2004). In the current study, the oxidative stress (increased TBAR level and decreased total antioxidant capacity) was negatively correlated with bone growth rate and mRNA expression of *BGLAP*. This result was consistent with our previous finding(Tompkins, et al., 2022b), that decreased bone quality was associated with systemic oxidative stress in broiler during *Eimeria* infection. Oxidative stress can be a co-factor involved in loss of osteoblastic activity that ultimately led to poor bone quality.

Eimeria infection can cause a complex host immune responses, encompassing both cellular and humoral mechanisms during infection(Lillehoj, 1998). Studies indicated that humoral immunity and antibodies produced by B cells were increased during severe *Eimeria* infection(Kim, et al., 2019). Different from other species, the bursa of Fabricius, a unique central immune organ of birds located near the cloaca, is the location of B lymphocyte differentiation and maturation instead of bone marrow(Ifrah, et al., 2017). Fully differentiated B lymphocytes migrate to peripheral lymphoid organs to participate in immune responses, such as producing antibodies and participating in humoral immunity(Masteller and Thompson, 1994; Lillehoj, 1998). B cell-produced proteins such as RANKL and OPG are critical for bone metabolism(Li, et al., 2007b; Onal, et al., 2012; Li, et al., 2014; Titanji, et al., 2014; Titanji, 2017). B lineage cells produce more than

60% of total OPG in bone marrow(Li, et al., 2014). Mice that were injected with RANKL inhibitor resulted in a larger bone mass(Furuya, et al., 2011). According to our study, an increased mRNA expression of *OPG* in bone marrow indicated that the system was actively producing more OPG, but the source of OPG remains unknown. The drastically higher expression of *OPG* in bone marrow may be related to a negative feedback loop, that increased *OPG* subsequently affects osteoclastogenesis(Brandstrom, et al., 1998). We hypothesize that the bone marrow could actively reduce or inhibit highly-elevated osteoclast activity by increased expression of *OPG*, then preserving minerals for bone homeostasis during *Eimeria* infection. A similar pattern of expression was observed in gene expression of tight junction protein during acute *Eimeria* infection, that *Eimeria* infection damaged intestine integrity, but tight junction protein gene expression was significantly elevated to repair the damage (Teng, et al., 2021).

Bone marrow not only contains different cell types that perform bone formation and resorption but also serves as the cradle of hematopoiesis and a reservoir of growth factors and cytokines, providing an ideal environment for communicating between bone metabolism and the immune system. Essentially all the units that participate in cellular immunity can influence bone cells, particularly impacting the activity and formation of osteoclasts (Yun, 2000; Zaiss, et al., 2010; Kim, et al., 2019). The cytokines IL-1β, IL-6, and TNF-α are known to increase bone resorption by stimulating both osteoclast activity and differentiation in mammals (Kwan Tat, et al., 2004). The number of osteoclast precursors increases under inflammatory conditions, characterized by high levels of the potent inflammatory cytokine TNF-α (Li, et al., 2004; Yao, et al., 2006). The current

study found significantly higher mRNA expression of *TNF* (tumor necrosis factor-like) in the High group than in the other groups. Meanwhile, activation of osteoclast formation was detected in the High group over the metaphysis trabecular bone. It is important to mention that, with the same amount of FI, the expression of *TNF* was relatively low in the PF group compared with the High, as well as the number of osteoclast and enzyme activity of RANKL was relatively higher in the High group than the PF group. Based on the comparison between the High group and the PF group, we concluded that the increased osteoclastic bone resorption is associated with the activation of immune response in broiler chickens during *Eimeria* infection. Moreover, NFKB is involved in many signaling pathways and plays an important role in osteoclast formation and survival rate(Jimi, et al., 1998; Miyazaki, et al., 2000; Xing, et al., 2002). NFKB ligand (RANKL), one of the most critical molecules that regulate osteoclast formation, provides the crosstalk between bone and immune systems (Taichman, 2005; Lorenzo, et al., 2008). The binding of RANKL to its receptor RANK triggers osteoclast precursors to differentiate into osteoclasts, which increases the number of osteoclasts on their bone surfaces (Rucci, et al., 2007; Pivonka, et al., 2010; Park, et al., 2017). In the present study, the High group showed the lowest level of *RANKL*/*OPG*, indicating that the negative feedback loop was turned on because less osteoclastic activity was in need to preserve the minerals for bone structure and support (Logar, et al., 2007). The different expressions of the *RANKL*/*OPG* ratio between the Low and the High indicated the bone homeostasis is infection-dose-dependent during coccidiosis. However, with the difference in B-cell development in avian species, immunity, particularly humoral immunity, might

interact with bone metabolism differently from mammals. How osteoimmunology plays a role in avian bone homeostasis needs more profound studies.

Taken together, delayed bone development in the parasite-challenged groups was attributable to an uncoupling of osteoblast and osteoclast activity, whereby increased bone resorption and decreased bone formation were closely associated with immune response/oxidative stress during *Eimeria* infection. With the long-held notion that the central pathophysiology of bone disorder was nutrition deficiency and physical stress during *Eimeria* infection, we demonstrated that bone disorder is also closely connected with bone modeling and remodeling which are associated with immune response/oxidative stress. Both nutrition and concurrent diseases will influence the occurrence of leg disorders. Further study on osteoimmunology needs to address bone disorder issues and will further lead to a more precise understanding of the mechanism underlying the pathogenesis of bone mineral loss and bone disease in broilers, eventually improving animal production and welfare in the future.

Materials and Methods

Ethics Statement

The experiment followed the guideline of the Institutional Animal Care and Use Committee and was conducted at the Poultry Research Farm, University of Georgia, Athens, GA. The protocol was approved by the Institutional Animal Care and Use Committee at the University of Georgia (ethical approval code: A2021 12-012).

Experimental Design

The study was carried out in compliance with the ARRIVE guidelines. A total of 480 one-day-old male broiler chickens (Cobb 500) were randomly distributed into four treatment groups with ten replicates and twelve birds per cage. Experimental groups included uninfected controls (Control) fed diet *ad libitum* (gavaged with water), a low *Eimeria*-infected group (Low) fed diet *ad libitum* (gavaged with 50,000 oocysts of *E. maxima*, 50,000 oocysts of *E. tenella*, and 250,000 oocysts of *E. acervulina*), a severely *Eimeria*-infected group (High) fed diet *ad libitum* diet (gavaged with 12,500 oocysts of *E. maxima*; 12,500 oocysts of *E. tenella*; 62,500 oocysts of *E. acervulina*), and an uninfected pair-fed group (PF; gavaged with water) that fed the same amount of feed as the High group consumed. Starter (0-14 d of age) and grower (15-20 d of age) diets were formulated following Cobb500 broiler management guide(Cobb, 2019). All chicks were raised under the same house, feeding, and environmental management conditions based on the broiler management guide (Cobb, 2019). Chicks were allowed to consume water on an *ad libitum* basis, and daily feed intake was measured during the study. On 6 days post infection (dpi), one bird per replicate was randomly selected to collect tissue samples. The tissue samples were snap-frozen in liquid nitrogen and kept in -80°C until future processing.

Gut Permeability

The gut permeability was measured on 5 dpi by the method used in our previous study (Teng, et al., 2020a; Teng, et al., 2020b). Briefly, fluorescein isothiocyanate dextran (FITC-d; MW 4000; Sigma-Aldrich, Ontario, Canada) was dissolved in distilled

water and made into 2.2 mg/mL solution. One bird per cage was randomly selected and gavaged with 1 mL of FITC-d solution. Two hours after inoculation, the blood was collected from birds and kept in the dark at room temperature for clotting. The clotted blood was centrifuged at 1,500 *g* for 15 min to serum collection. The standard curve solution was made from a serial dilution of FITC-d stock (2.2 mg/mL). Dilution buffer was made from the pooled serum of non-infection birds with the basal diet. Sample and standard solutions were loaded into black 96-well plates, and FITC-d concentrations were measured by a spectrophotometer (SpectraMax M5; Molecular Devices, San Jose, CA). The excitation wavelength was set at 485 nm, and the emission wavelength was set at 528 nm.

Micro-Computed Tomography (Micro-CT)

A total of 40 samples (one bird per cage) were randomly collected to evaluate 3-D bone morphologic changes in the broiler. The proximal and shaft of the tibia were assessed by Micro-Computed Tomography (Micro-CT). The scanning process was performed according to our previous publications (Tompkins, et al., 2022a; Tompkins, et al., 2022b), with setting as 83 kV, 121 µA, and a 0.5 mm aluminum filter, the pixel size as 26 µm with 360° complete rotation, and 42 minutes of acquisition time. Scanning was performed with SkyScan 1172 (SkyScan, Kontich, Belgium). 2-D images were transferred to CTAn software (CTAn, SkyScan) for structure construction and quantification. The metaphyseal region of interest (ROI) was post-operated to automatically separate trabecular bone from cortical bone and preserve its morphology using a threshold of 800. Average bone mineral density (BMD), bone mineral content

(BMC), and bone micro-architectural parameters of each group were taken from the same ROI. Cortical and trabecular bone parameters were quantified and analyzed separately. The following parameters were quantified: total volume (TV), bone volume (BV), bone surface (BS), bone volume per tissue volume (BV/ TV), and trabecular number (Tb. N)(Tompkins, et al., 2022b).

Calcein Labeling

For dynamic histomorphometry measures of bone formation, calcein (Cat no. C0875, Sigma Aldrich, St. Louis, MO) was dissolved in a 1 M sodium hydroxide solution and then mixed with sterilized distilled water to make the 2.0% working solution. The birds were injected with the calcein solution intraperitoneally at 20 mg/kg of body weight. On day 4 after the first injection of calcein, the birds were injected again as previously described. Bone samples were collected on 4 days after the second injection. The muscle was removed immediately, and bones were preserved in 70% ethanol. Upon analysis, a thin slice of bone was taken from mid-diaphysis by a circular saw (Ryobi, Anderson, SC, USA), sanded each bone slice down by using sandpaper then mounted on a glass slide. Calcein has a high calcium affinity and translates into a relatively broad fluorescent band. A fluorescence microscope (Leica DC500 camera, Leica Microsystems Inc., Buffalo Groove, IL) was used to visualize new bone formation and determine the distance between the two calcein labels on the bones. Eight measurements at different angles were performed using ImageJ software (National Institutes of Health, Bethesda, MD, USA). The average values were calculated for data analysis.

Serum Receptor Activator of Nuclear Factor Kappa B Ligand Enzyme-linked Immunosorbent Assay (RANKL ELISA)

Chicken RANKL concentrations were measured by commercially available kits (MyBioSource, San Diego, CA, USA). All procedures were performed according to the manufacturer's protocol. The method was two-site sandwich ELISA, the pre-coated antibody was Chicken PRM1 monoclonal antibody and the detecting antibody was polyclonal antibody with biotin labeled. A standard curve was created, and the RANKL concentration of the examined samples was calculated and expressed in pg/ml. Background OD values were subtracted from the calculation, and the color depth was directly proportional to the amount of RANKL in the sample.

Tartrate-resistant Acid Phosphatase Staining (TRAP Staining)

All tibia bones were collected at 6 dpi. After removing the muscle tissue, tibias were fixed in 4% PBS-buffered formaldehyde at 4°C for three days and then moved into 70% ethanol for preservation. Tibial tuberosity was used as a landmark to cut the bone slides by the circular saw. The bone slides were demineralized with 10% ethylenediaminetetraacetic acid (EDTA) at 4°C for 13 days. Each bone slide was equally cut into four pieces perpendicularly. The samples were then embedded in paraffin and cut into 4 µm sections using Leitz 1512 rotary microtome (Leica Microsystems, Wetzlar, Germany). The paraffin sections were stained with tartrate-resistant acid phosphatase (TRAP) solution prepared by mixing acetate buffer (pH 5.0), naphthol AS-MX phosphate (Sigma Chemical, St. Louis, MO, USA), Fast Red Violet LB Salt (Sigma), and 50 mM sodium tartrate (Sigma). The sections were counterstained with hematoxylin (Sigma).

Osteoclasts were defined in this study as TRAP-positive cells with three or more nuclei. Bone circumference was measured using ImageJ software (National Institutes of Health, Bethesda, MD, USA).

Lipid Peroxidation and Antioxidant Status Assay

Chicken total antioxidant capacity in serum was analyzed using a QuantiChrom antioxidant assay kit (BioAssay Systems, Hayward, CA, USA), and the level of liver lipid peroxidation was determinated by using QuantiChro TBARS Assay Kit (BioAssay Systems, Hayward, CA, USA). Serum was collected, centrifuged, and then kept at -80°C. A liver sample from one bird per cage was collected, snap-frozen in liquid nitrogen, and then kept at -80°C. Liver samples were homogenized and centrifuged in the assay buffer, and all assay procedures were performed according to the manufacturer's protocols. The protein concentration was measured by protein quantification assay (Pierce™ BCA Protein Assay Kit, Thermo Scientific, Rockford, IL, United States) following the procedure indicated in our previous publication (Tompkins, et al., 2022b).

Real-time Quantitative PCR Analysis of Gene Expression in Bone Marrow

Bone marrow from femur bones was extracted, snap-frozen in liquid nitrogen, and stored immediately at -80°C until RNA isolation (N = 10). Bone marrow total RNA was extracted using Qiazol reagent (Qiagen, USA) according to the manufacturer's instruction. A Nano-Drop 1000 Spectrophotometer (ThermoFisher Scientific, Pittsburgh, PA) was used to determine the quantity of RNA. The cDNA was synthesized from total RNA (2000 ng) using high-capacity cDNA reverse transcription kits (Thermo Fisher Scientific, Waltham, MA).

Real-time reverse transcription polymerase chain reaction (RT-qPCR) was performed to measure mRNA expression. Primers were designed using the Primer-BLAST program (https://www.ncbi.nlm.nih.gov/tools/primer-blast/). The specificity of primers was validated by melting curve analysis and gel electrophoresis. RT-qPCR was performed on an Applied Biosystems StepOnePlus™ (Thermo Fisher Scientific, Waltham, MA) with iTaq™ Universal SYBR Green Supermix (BioRad, Hercules, CA) using the following conditions for all genes: 95°C for 10 minutes followed by 40 cycles at 95°C for 15 seconds, annealing temperature for 20 seconds, and extending at 72°C for 1 minute.

The geometric mean of *18S, HBMS* and *GAPDH* were used for normalization(Vandesompele, et al., 2002). The stability of housekeeping genes were confirmed by their consistent Ct values among the treatments ($P > 0.1$)(Stephens, et al., 2011). *BGLAP*, *RUNX2*, *SPP1*, *BMP2*, and *ALP* were used as genetic markers of bone formation in the bone marrow(Chen, et al., 2021). *NFKB, RANKL, FOS, ACP5*, *NFATC1, IL1B, TNF, SMAD1*, and *TNFRSF11B* (*OPG*)(Paludo, et al., 2017) were used as the genetic markers for osteoclastic activity in the bone marrow. Details of primer sequences used for the experiment are presented in Table 3.1. Moreover, the ratio of *OPG*/*RANKL* in bone marrow was calculated. Samples were run in triplicate, and relative gene expression data were analyzed using the $2^{-\Delta\Delta Ct}$. The mean ΔCt of each marker gene from the control group was used to calculate the ΔΔCt value, and $2^{-\Delta\Delta Ct}$ expression levels were normalized to 1 for the control group. Expression levels of the treatment groups were presented as fold change.

Statistical Analysis

All experimental data were expressed as mean with standard error of the means (SEM). Data were tested for homogeneity of variances and normality of studentized residuals. The differences among the treatment groups were analyzed by one-way ANOVA, whereas the means were analyzed statistically by Tukey's test using JMP Pro14 (SAS Institute, Inc., Cary, NC). Statistical significance was set at $P < 0.05$, and $0.05 \leq p \leq 0.1$ were also presented to show the trending toward statistical significance (Thiese, et al., 2016). Pair wise correlations (JMP Pro14) were evaluated for all bone and growth variables.

References

Abdel-Haleem, H. M., S. M. Aboelhadid, T. Sakran, G. El-Shahawy, H. El-Fayoumi, S. Al-Quraishy, and A. S. Abdel-Baki. 2017. Gene expression, oxidative stress and apoptotic changes in rabbit ileum experimentally infected with Eimeria intestinalis. Folia Parasitol. (Praha) 64.

Aghajanian, P., S. Hall, M. D. Wongworawat, and S. Mohan. 2015. The Roles and Mechanisms of Actions of Vitamin C in Bone: New Developments. J Bone Miner Res 30:1945-1955.

Aguado, E., F. Pascaretti-Grizon, E. Goyenvalle, M. Audran, and D. Chappard. 2015. Bone mass and bone quality are altered by hypoactivity in the chicken. PLoS One 10:e0116763.

Akbari Moghaddam Kakhki, R., Z. Lu, A. Thanabalan, H. Leung, M. Mohammadigheisar, and E. Kiarie. 2019. Eimeria challenge adversely affected long bone attributes linked to increased resorption in 14-day-old broiler chickens. Poult Sci 98:1615-1621.

Akbari, S., and A. A. Rasouli-Ghahroudi. 2018. Vitamin K and Bone Metabolism: A Review of the Latest Evidence in Preclinical Studies. Biomed Res Int 2018:4629383.

Akesson, K., K. H. Lau, P. Johnston, E. Imperio, and D. J. Baylink. 1998. Effects of short-term calcium depletion and repletion on biochemical markers of bone turnover in young adult women. J Clin Endocrinol Metab 83:1921-1927.

Ali Hassan, N., and Z. Li. 2021. Oxidative stress in broiler chicken and its consequences on meat quality. International Journal of Life Science Research Archive 1:045-054.

Allen, M. R., and D. B. Burr. 2014. Bone Modeling and Remodeling. Pages 75-90 in Basic and Applied Bone Biology.

Allen, P. C., H. D. Danforth, and P. C. Augustine. 1998. Dietary modulation of avian coccidiosis. International Journal for Parasitology 28:1131-1140.

Allen, P. C., H. D. Danforth, and O. A. Levander. 1996. Diets high in n-3 fatty acids reduce cecal lesion scores in chickens infected with Eimeria tenella. Poult Sci 75:179-185.

Almeida, M., M. R. Laurent, V. Dubois, F. Claessens, C. A. O'Brien, R. Bouillon, D. Vanderschueren, and S. C. Manolagas. 2017. Estrogens and Androgens in Skeletal Physiology and Pathophysiology. Physiol Rev 97:135-187.

Almeida Paz, I. C. L., A. A. Mendes, T. S. Takita, L. C. Vulcano, P. C. Guerra, F. S. Wechsler, R. G. Garcia, S. E. Takahashi, J. Moreira, K. Pelícia, C. M. Komiyama, and R. R. Quinteiro. 2005. Comparison of techniques for tibial dyschondroplasia assessment in broiler chickens. Revista Brasileira de Ciência Avícola 7:27-31.

Applegate, T. J., and M. S. Lilburn. 2002. Growth of the femur and tibia of a commercial broiler line. Poult Sci 81:1289-1294.

Bai, X. C., D. Lu, J. Bai, H. Zheng, Z. Y. Ke, X. M. Li, and S. Q. Luo. 2004. Oxidative stress inhibits osteoblastic differentiation of bone cells by ERK and NF-kappaB. Biochem Biophys Res Commun 314:197-207.

Bailey, R. A., E. Souza, and S. Avendano. 2020. Characterising the Influence of Genetics on Breast Muscle Myopathies in Broiler Chickens. Front Physiol 11:1041.

Barua, M., G. Buddha Das, K. Islam, S. Chowdhury, M. Emran Hoss, B. Kanti Nath, and M. Shafiqul I. 2016. Effect of Fish Oil on Performance, Coccidiosis Prevention and Serum Lipid Profile in Broiler. Asian Journal of Poultry Science 11:20-30.

Basu, S., K. Michaelsson, H. Olofsson, S. Johansson, and H. Melhus. 2001. Association between oxidative stress and bone mineral density. Biochem Biophys Res Commun 288:275-279.

Bedimo, R. J., B. Adams-Huet, J. Poindexter, G. Brown, I. Farukhi, R. Castanon, D. Turner, T. Moore, P. Tebas, and N. M. Maalouf. 2018. The Differential Effects of Human Immunodeficiency Virus and Hepatitis C Virus on Bone Microarchitecture and Fracture Risk. Clin Infect Dis 66:1442-1447.

Beedles, K. E., P. T. Sharpe, E. F. Wagner, and A. E. Grigoriadis. 1999. A putative role for c-Fos in the pathophysiology of Paget's disease. J Bone Miner Res 14 Suppl 2:21-28.

Bihan-Duval, E. L., C. Beaumont, and J. J. Colleau. 1997. Estimation of the genetic correlations between twisted legs and growth or conformation traits in broiler chickens. J Anim Breed Genet 114:239-259.

Bilkovski, R., D. M. Schulte, F. Oberhauser, M. Gomolka, M. Udelhoven, M. M. Hettich, B. Roth, A. Heidenreich, C. Gutschow, W. Krone, and M. Laudes. 2010. Role of WNT-5a in the determination of human mesenchymal stem cells into preadipocytes. J Biol Chem 285:6170-6178.

Bjornerem, A. 2016. The clinical contribution of cortical porosity to fragility fractures. Bonekey Rep 5:846.

Blake, D. P., J. Knox, B. Dehaeck, B. Huntington, T. Rathinam, V. Ravipati, S. Ayoade, W. Gilbert, A. O. Adebambo, I. D. Jatau, M. Raman, D. Parker, J. Rushton, and F. M. Tomley. 2020. Re-calculating the cost of coccidiosis in chickens. Vet Res 51:115.

Bolamperti, S., I. Villa, and A. Rubinacci. 2022. Bone remodeling: an operational process ensuring survival and bone mechanical competence. Bone Res 10:48.

Bortoluzzi, C., B. Lumpkins, G. F. Mathis, M. Franca, W. D. King, D. E. Graugnard, K. A. Dawson, and T. J. Applegate. 2019. Zinc source modulates intestinal inflammation and intestinal integrity of broiler chickens challenged with coccidia and Clostridium perfringens. Poult Sci 98:2211-2219.

Bortoluzzi, C., B. S. Vieira, and T. J. Applegate. 2020. Influence of Dietary Zinc, Copper, and Manganese on the Intestinal Health of Broilers Under Eimeria Challenge. Front Vet Sci 7:13.

Bourrin, S., A. Toromanoff, P. Ammann, J. P. Bonjour, and R. Rizzoli. 2000. Dietary protein deficiency induces osteoporosis in aged male rats. J Bone Miner Res 15:1555-1563.

Bowling, M., R. Forder, R. J. Hughes, S. Weaver, and P. I. Hynd. 2018. Effect of restricted feed intake in broiler breeder hens on their stress levels and the growth and immunology of their offspring. Transl Anim Sci 2:263-271.

Boyce, B. F., and L. Xing. 2008. Functions of RANKL/RANK/OPG in bone modeling and remodeling. Arch Biochem Biophys 473:139-146.

Boyce, B. F., Z. Yao, and L. Xing. 2009. Osteoclasts have multiple roles in bone in addition to bone resorption. Crit Rev Eukaryot Gene Expr 19:171-180.

Boyle, W. J., W. S. Simonet, and D. L. Lacey. 2003. Osteoclast differentiation and activation. Nature 423:337-342.

Bradshaw, R. H., R. D. Kirkden, and D. M. Broom. 2002. A Review of the Aetiology and Pathology of Leg Weakness in Broilers in Relation to Welfare. Avian and Poultry Biology Reviews 13:45-103.

Brandstrom, H., K. B. Jonsson, O. Vidal, S. Ljunghall, C. Ohlsson, and O. Ljunggren. 1998. Tumor necrosis factor-alpha and -beta upregulate the levels of osteoprotegerin mRNA in human osteosarcoma MG-63 cells. Biochem Biophys Res Commun 248:454-457.

Brennan-Speranza, T. C., and A. D. Conigrave. 2015. Osteocalcin: an osteoblast-derived polypeptide hormone that modulates whole body energy metabolism. Calcif Tissue Int 96:1-10.

Bruggeman, V., D. Vanmontfort, R. Renaville, D. Portetelle, and E. Decuypere. 1997. The effect of food intake from two weeks of age to sexual maturity on plasma growth hormone, insulin-like growth factor-I, insulin-like growth factor-binding proteins, and thyroid hormones in female broiler breeder chickens. Gen Comp Endocrinol 107:212-220.

Buyse, J., E. Decuypere, V. M. Darras, L. M. Vleurick, E. R. Kuhn, and J. D. Veldhuis. 2000. Food deprivation and feeding of broiler chickens is associated with rapid and interdependent changes in the somatotrophic and thyrotrophic axes. Br Poult Sci 41:107-116.

Byrnes, S., R. Eaton, and M. Kogut. 1993. In vitro interleukin-1 and tumor necrosis factor-alpha production by macrophages from chickens infected with either Eimeria maxima or Eimeria tenella. International Journal for Parasitology 23:639-645.

Calder, P. C. 2006. n-3 polyunsaturated fatty acids, inflammation, and inflammatory diseases. Am J Clin Nutr 83:1505S-1519S.

Çapar Akyüz, H., and E. E. Onbaşılar. 2020. Non-infectious skeletal disorders in broilers. World's Poultry Science Journal 76:611-623.

Celi, P., and S. Chauhan. Year. Oxidative stress management in farm animals: opportunities and challenges. Proc. Proceedings of the 4th International Conference on Sustainable Animal Agriculture for Developing Countries (SAADC).

Challey, J. R. J. T. J. o. P. 1960. The effect of cecal coccidiosis infections and experimental hemorrhage upon adrenal ascorbic acid levels in the chicken. 46:727-731.

Chatakun, P., R. Nunez-Toldra, E. J. Diaz Lopez, C. Gil-Recio, E. Martinez-Sarra, F. Hernandez-Alfaro, E. Ferres-Padro, L. Giner-Tarrida, and M. Atari. 2014. The effect of five proteins on stem cells used for osteoblast differentiation and proliferation: a current review of the literature. Cell Mol Life Sci 71:113-142.

Chen, C., D. L. White, B. Marshall, and W. K. Kim. 2021. Role of 25-Hydroxyvitamin D3 and 1,25-Dihydroxyvitamin D3 in Chicken Embryo Osteogenesis, Adipogenesis, Myogenesis, and Vitamin D3 Metabolism. Front Physiol 12:637629.

Chin, K. Y., and S. Ima-Nirwana. 2018. Vitamin C and Bone Health: Evidence from Cell, Animal and Human Studies. Curr Drug Targets 19:439-450.

Choi, H. K., G. J. Kim, H. S. Yoo, D. H. Song, K. H. Chung, K. J. Lee, Y. T. Koo, and J. H. An. 2019. Vitamin C Activates Osteoblastogenesis and Inhibits Osteoclastogenesis via Wnt/beta-Catenin/ATF4 Signaling Pathways. Nutrients 11.

Clarke, B. 2008. Normal bone anatomy and physiology. Clin J Am Soc Nephrol 3 Suppl 3:S131-139.

Cobb. 2019. Cobb 500 broiler performance and nutrient supplement guide. . Siloam Springs (AR): Cobb-Vantress.

Colnago, G. L., L. S. Jensen, and P. L. Long. 1984. Effect of selenium and vitamin E on the development of immunity to coccidiosis in chickens. Poult Sci 63:1136-1143.

Cook, M. E. 2000. Skeletal deformities and their causes: introduction. Poult Sci 79:982-984.

Cook, M. E., Y. Bai, and M. W. Orth. 1994. Factors influencing growth plate cartilage turnover. Poult Sci 73:889-896.

de Jong, I., C. Berg, A. Butterworth, and I. Estevéz. 2012. Scientific report updating the EFSA opinions on the welfare of broilers and broiler breeders. EFSA Supporting Publications 9.

de Jong, I. C., S. van Voorst, D. A. Ehlhardt, and H. J. Blokhuis. 2002. Effects of restricted feeding on physiological stress parameters in growing broiler breeders. Br Poult Sci 43:157-168.

de Oliveira, H. C., A. M. G. Ibelli, S. E. F. Guimaraes, M. E. Cantao, J. O. Peixoto, L. L. Coutinho, and M. C. Ledur. 2020. RNA-seq reveals downregulated osteochondral genes

potentially related to tibia bacterial chondronecrosis with osteomyelitis in broilers. BMC Genet 21:58.

de Paula, F. J., and C. J. Rosen. 2013. Bone Remodeling and Energy Metabolism: New Perspectives. Bone Res 1:72-84.

Dent, P. B., D. M. Brown, and R. A. Good. 1969. Ultimobranchial calcitonin in the developing chicken. Endocrinology 85:582-585.

Dilworth, B. C., and E. J. Day. 1965. Effect of varying dietary calcium: phosphorus ratios on tibia and femur composition of the chick. Poult Sci 44:1474-1479.

Dirckx, N., M. C. Moorer, T. L. Clemens, and R. C. Riddle. 2019. The role of osteoblasts in energy homeostasis. Nat Rev Endocrinol 15:651-665.

Dobnig, H., and R. T. Turner. 1995. Evidence that intermittent treatment with parathyroid hormone increases bone formation in adult rats by activation of bone lining cells. Endocrinology 136:3632-3638.

Domazetovic, V., G. Marcucci, T. Iantomasi, M. L. Brandi, and M. T. Vincenzini. 2017. Oxidative stress in bone remodeling: role of antioxidants. Clin Cases Miner Bone Metab 14:209-216.

Ducy, P., R. Zhang, V. Geoffroy, A. L. Ridall, and G. Karsenty. 1997. Osf2/Cbfa1: A Transcriptional Activator of Osteoblast Differentiation. Cell 89:747-754.

Durkin, L. A., C. E. Childs, and P. C. Calder. 2021. Omega-3 Polyunsaturated Fatty Acids and the Intestinal Epithelium-A Review. Foods 10.

Ebeid, T., A. Fayoud, S. Abou El-Soud, Y. Eid, and M. El-Habbak. 2011. The effect of omega-3 enriched meat production on lipid peroxidation, antioxidative status, immune

response and tibia bone characteristics in Japanese quail . Czech Journal of Animal Science 56:314-324.

Erasmus, J., M. L. Scott, and P. P. Levine. 1960. A Relationship Between Coccidiosis and Vitamin A Nutrition in Chickens. Poultry Science 39:565-572.

Eriksen, E. F. 1986. Normal and pathological remodeling of human trabecular bone: three dimensional reconstruction of the remodeling sequence in normals and in metabolic bone disease. Endocr Rev 7:379-408.

Estevez, M. 2015. Oxidative damage to poultry: from farm to fork. Poult Sci 94:1368-1378.

Farquharson, C., and D. Jefferies. 2000. Chondrocytes and longitudinal bone growth: the development of tibial dyschondroplasia. Poult Sci 79:994-1004.

Fatoba, A. J., and M. A. Adeleke. 2018. Diagnosis and control of chicken coccidiosis: a recent update. J Parasit Dis 42:483-493.

Feng, X., and J. M. McDonald. 2011. Disorders of bone remodeling. Annu Rev Pathol 6:121-145.

Fernandes Müller, I. J., M. Ribeiro Vissotto, L. Cardoso Bittencourt, T. E. Riffel, F. Lima Kaiser, S. Palma Castro, and G. R. Hermes. 2019. Mineral supplementation: effects on bone integrity and intestinal morphometry of broiler chickens challenged with Eimeria sp. Acta Vet. Brno. 69:88-105.

Ferver, A., E. Greene, R. Wideman, and S. Dridi. 2021. Evidence of Mitochondrial Dysfunction in Bacterial Chondronecrosis With Osteomyelitis-Affected Broilers. Front Vet Sci 8:640901.

Fetterer, R. H., K. B. Miska, A. D. Mitchell, and M. C. Jenkins. 2013. The use of dual-energy X-ray absorptiometry to assess the impact of Eimeria infections in broiler chicks. Avian Dis 57:199-204.

Forrester, S. J., D. S. Kikuchi, M. S. Hernandes, Q. Xu, and K. K. Griendling. 2018. Reactive Oxygen Species in Metabolic and Inflammatory Signaling. Circ Res 122:877-902.

Franz-Odendaal, T. A., B. K. Hall, and P. E. Witten. 2006. Buried alive: how osteoblasts become osteocytes. Dev Dyn 235:176-190.

Frost, H. M. 1994. Wolff's Law and bone's structural adaptations to mechanical usage: an overview for clinicians. Angle Orthod 64:175-188.

Fujisawa, K., K. Hara, T. Takami, S. Okada, T. Matsumoto, N. Yamamoto, and I. Sakaida. 2018. Evaluation of the effects of ascorbic acid on metabolism of human mesenchymal stem cells. Stem Cell Res Ther 9:93.

Fukushima, O., P. J. Bekker, and C. V. Gay. 1991. Ultrastructural localization of tartrate-resistant acid phosphatase (purple acid phosphatase) activity in chicken cartilage and bone. Am J Anat 191:228-236.

Furuya, Y., K. Mori, T. Ninomiya, Y. Tomimori, S. Tanaka, N. Takahashi, N. Udagawa, K. Uchida, and H. Yasuda. 2011. Increased bone mass in mice after single injection of anti-receptor activator of nuclear factor-kappaB ligand-neutralizing antibody: evidence for bone anabolic effect of parathyroid hormone in mice with few osteoclasts. J Biol Chem 286:37023-37031.

Galindo, M., J. Pratap, D. W. Young, H. Hovhannisyan, H. J. Im, J. Y. Choi, J. B. Lian, J. L. Stein, G. S. Stein, and A. J. van Wijnen. 2005. The bone-specific expression of Runx2 oscillates during the cell cycle to support a G1-related antiproliferative function in osteoblasts. J Biol Chem 280:20274-20285.

Gautier, A. E., J. D. Latorre, P. L. Matsler, and S. J. Rochell. 2019. Longitudinal Characterization of Coccidiosis Control Methods on Live Performance and Nutrient Utilization in Broilers. Front Vet Sci 6:468.

Georgieva, N. V., M. Gabrashanska, V. Koinarski, and Z. Yaneva. 2011. Zinc Supplementation against Eimeria acervulina-Induced Oxidative Damage in Broiler Chickens. Vet. Med. Int. 2011:647124.

Georgieva, N. V., V. Koinarski, and V. Gadjeva. 2006. Antioxidant status during the course of Eimeria tenella infection in broiler chickens. Vet J 172:488-492.

Gibon, E., L. Y. Lu, K. Nathan, and S. B. Goodman. 2017. Inflammation, ageing, and bone regeneration. J Orthop Translat 10:28-35.

Gilley, A. D., H. Lester, I. Y. Pevzner, N. B. Anthony, and R. F. Wideman, Jr. 2014. Evaluating portable wire-flooring models for inducing bacterial chondronecrosis with osteomyelitis in broilers. Poult Sci 93:1354-1367.

Gómez-Osorio, L.-M., J.-J. Chaparro-Gutiérrez, and S. J. A. i. P. N. R. López-Osorio. 2021. Nutrition and Poultry Coccidiosis: Causes, Consequences and Current Strategies to Modulate the.161.

Gong, J. K., J. S. Arnold, and S. H. Cohn. 1964. Composition of Trabecular and Cortical Bone. Anat Rec 149:325-331.

González-Cerón, F., R. Rekaya, and S. E. Aggrey. 2015. Genetic relationship between leg problems and bone quality traits in a random mating broiler population. Poultry Science 94:1787-1790.

Gotep, J. G., J. T. Tanko, G. E. Forcados, I. A. Muraina, N. Ozele, B. B. Dogonyaro, O. O. Oladipo, M. S. Makoshi, O. B. Akanbi, H. Kinjir, A. L. Samuel, T. E. Onyiche, G. O. Ochigbo, O. B. Aladelokun, H. A. Ozoani, V. Z. Viyoff, C. C. Dapuliga, A. A. Atiku, P. A. Okewole, D. Shamaki, M. S. Ahmed, and C. I. Nduaka. 2016. Therapeutic and Safety Evaluation of Combined Aqueous Extracts of Azadirachta indica and Khaya senegalensis in Chickens Experimentally Infected with Eimeria Oocysts. J Parasitol Res 2016:4692424.

Grabowski, P. 2009. Physiology of bone. Endocr Dev 16:32-48.

Granquist, E. G., G. Vasdal, I. C. de Jong, and R. O. Moe. 2019. Lameness and its relationship with health and production measures in broiler chickens. Animal 13:2365-2372.

Grbic, R., D. J. Miric, B. Kisic, L. Popovic, V. Nestorovic, and A. Vasic. 2014. Sequential analysis of oxidative stress markers and vitamin C status in acute bacterial osteomyelitis. Mediators Inflamm 2014:975061.

Guntur, A. R., and C. J. Rosen. 2012. Bone as an endocrine organ. Endocr Pract 18:758-762.

Guo, C. H., P. J. Liu, S. Hsia, C. J. Chuang, and P. C. Chen. 2011. Role of certain trace minerals in oxidative stress, inflammation, CD4/CD8 lymphocyte ratios and lung function in asthmatic patients. Ann Clin Biochem 48:344-351.

Guo, S., J. Xv, Y. Li, Y. Bi, Y. Hou, and B. Ding. 2020. Interactive effects of dietary vitamin K3 and Bacillus subtilis PB6 on the growth performance and tibia quality of broiler chickens with sex separate rearing. Animal:1-9.

Hambli, R. 2014. Connecting mechanics and bone cell activities in the bone remodeling process: an integrated finite element modeling. Front Bioeng Biotechnol 2:6.

Han, Y., X. You, W. Xing, Z. Zhang, and W. Zou. 2018. Paracrine and endocrine actions of bone-the functions of secretory proteins from osteoblasts, osteocytes, and osteoclasts. Bone Res 6:16.

Harada, S., and G. A. Rodan. 2003. Control of osteoblast function and regulation of bone mass. Nature 423:349-355.

Hardy, R. S., H. Zhou, M. J. Seibel, and M. S. Cooper. 2018. Glucocorticoids and Bone: Consequences of Endogenous and Exogenous Excess and Replacement Therapy. Endocr Rev 39:519-548.

Harms, R. H., P. W. Waldroup, and D. D. Cox. 1962. Activity of Vitamin K1 and Menadione Sodium Bisulfite Complex When Measured by Mortality of Chicks with Cecal Coccidiosis. Poultry Science 41:1836-1839.

Hartcher, K. M., and H. K. Lum. 2019. Genetic selection of broilers and welfare consequences: a review. World's Poultry Science Journal 76:154-167.

Hayman, A. R. 2008. Tartrate-resistant acid phosphatase (TRAP) and the osteoclast/immune cell dichotomy. Autoimmunity 41:218-223.

Heino, T. J., T. A. Hentunen, and H. K. Vaananen. 2002. Osteocytes inhibit osteoclastic bone resorption through transforming growth factor-beta: enhancement by estrogen. J Cell Biochem 85:185-197.

Holtrop, M. E., and G. J. King. 1977. The Ultrastructure of the Osteoclast and its Functional Implications. Clinical Orthopaedics and Related Research &NA;.

Hong, Y. H., H. S. Lillehoj, S. H. Lee, R. A. Dalloul, and E. P. Lillehoj. 2006. Analysis of chicken cytokine and chemokine gene expression following Eimeria acervulina and Eimeria tenella infections. Vet Immunol Immunopathol 114:209-223.

Huang, H., E. J. Chang, J. Ryu, Z. H. Lee, Y. Lee, and H. H. Kim. 2006. Induction of c-Fos and NFATc1 during RANKL-stimulated osteoclast differentiation is mediated by the p38 signaling pathway. Biochem Biophys Res Commun 351:99-105.

Huang, S., A. Kong, Q. Cao, Z. Tong, and X. Wang. 2019. The role of blood vessels in broiler chickens with tibial dyschondroplasia. Poult Sci 98:6527-6532.

Huang, S. C., Q. Q. Cao, Y. B. Cao, Y. R. Yang, T. T. Xu, K. Yue, F. Liu, Z. X. Tong, and X. B. Wang. 2021. Morinda officinalis polysaccharides improve meat quality by reducing oxidative damage in chickens suffering from tibial dyschondroplasia. Food Chem 344:128688.

Huang, W., S. Yang, J. Shao, and Y. P. Li. 2007. Signaling and transcriptional regulation in osteoblast commitment and differentiation. Front Biosci 12:3068-3092.

Hughes, D. E., A. Dai, J. C. Tiffee, H. H. Li, G. R. Mundy, and B. F. Boyce. 1996. Estrogen promotes apoptosis of murine osteoclasts mediated by TGF-beta. Nat Med 2:1132-1136.

Ifrah, M. E., B. Perelman, A. Finger, and Z. Uni. 2017. The role of the bursa of Fabricius in the immune response to vaccinal antigens and the development of immune tolerance in chicks (Gallus domesticus) vaccinated at a very young age. Poult Sci 96:51-57.

Imari, Z. K., A. Hassanabadi, and H. Nassiri Moghaddam. 2020. Response of broiler chickens to calcium and phosphorus restriction: Effects on growth performance, carcase traits, tibia characteristics and total tract retention of nutrients. Italian Journal of Animal Science 19:929-939.

Indo, Y., S. Takeshita, K. A. Ishii, T. Hoshii, H. Aburatani, A. Hirao, and K. Ikeda. 2013. Metabolic regulation of osteoclast differentiation and function. J Bone Miner Res 28:2392-2399.

Isojima, T., and N. A. Sims. 2021. Cortical bone development, maintenance and porosity: genetic alterations in humans and mice influencing chondrocytes, osteoclasts, osteoblasts and osteocytes. Cellular and Molecular Life Sciences 78:5755-5773.

Itoh, H., and T. Hatano. 1964. Comparison of Calcium Metabolism in Various Bones of Growing Chicks in Varying States of Vitamin D Supplementation. Poultry Science 43:70-76.

Iyasere, O. S., A. P. Beard, J. H. Guy, and M. Bateson. 2017. Elevated levels of the stress hormone, corticosterone, cause 'pessimistic' judgment bias in broiler chickens. Sci Rep 7:6860.

Javed, A., J. S. Bae, F. Afzal, S. Gutierrez, J. Pratap, S. K. Zaidi, Y. Lou, A. J. van Wijnen, J. L. Stein, G. S. Stein, and J. B. Lian. 2008. Structural coupling of Smad and Runx2 for execution of the BMP2 osteogenic signal. J Biol Chem 283:8412-8422.

Jimi, E., I. Nakamura, T. Ikebe, S. Akiyama, N. Takahashi, and T. Suda. 1998. Activation of NF-kappaB is involved in the survival of osteoclasts promoted by interleukin-1. J Biol Chem 273:8799-8805.

Jordan, F. T. 1981. Mycoplasma-induced arthritis in poultry. Isr J Med Sci 17:622-625.

Joyner, L. P., D. S. Patterson, S. Berrett, C. D. Boarer, F. H. Cheong, and C. C. Norton. 1975. Amino-acid malabsorption and intestinal leakage of plasma-proteins in young chicks infected with Eimeria acervulina. Avian Pathol. 4:17-33.

Jyoti, A., S. Singh, B. Mukhopadhyay, R. Gavel, and S. P. Mishra. 2015. Free radicals and antioxidant status in chronic osteomyelitis patients: a case control study. J Clin Diagn Res 9:BC08-10.

K. Panda, A., and G. Cherian. 2014. Role of Vitamin E in Counteracting Oxidative Stress in Poultry. The Journal of Poultry Science 51:109-117.

Kalinski, P. 2012. Regulation of immune responses by prostaglandin E2. J Immunol 188:21-28.

Kamibayashi, L., U. P. Wyss, T. D. V. Cooke, and B. Zee. 1995. Trabecular microstructure in the medial condyle of the proximal tibia of patients with knee osteoarthritis. Bone 17:27-35.

Kazakia, G. J., J. Carballido-Gamio, A. Lai, L. Nardo, L. Facchetti, C. Pasco, C. A. Zhang, M. Han, A. H. Parrott, P. Tien, and R. Krug. 2018. Trabecular bone microstructure is impaired in the proximal femur of human immunodeficiency virus-infected men with normal bone mineral density. Quant Imaging Med Surg 8:5-13.

Kent, G. N., R. I. Price, D. H. Gutteridge, M. Smith, J. R. Allen, C. I. Bhagat, M. P. Barnes, C. J. Hickling, R. W. Retallack, S. G. Wilson, and et al. 1990. Human lactation: forearm trabecular bone loss, increased bone turnover, and renal conservation of calcium and inorganic phosphate with recovery of bone mass following weaning. J Bone Miner Res 5:361-369.

Kestin, S. C., T. G. Knowles, A. E. Tinch, and N. G. Gregory. 1992. Prevalence of leg weakness in broiler chickens and its relationship with genotype. Vet Rec 131:190-194.

Khosla, S., J. J. Westendorf, and M. J. Oursler. 2008. Building bone to reverse osteoporosis and repair fractures. J Clin Invest 118:421-428.

Kierończyk, B., M. Rawski, D. Józefiak, and S. Świątkiewicz. 2017. Infectious and non-infectious factors associated with leg disorders in poultry – a review. Annals of Animal Science 17:645-669.

Kim, C., and D. Park. 2013. The effect of restriction of dietary calcium on trabecular and cortical bone mineral density in the rats. Journal of Exercise Nutrition and Biochemistry 17:123-131.

Kim, W. H., A. A. Chaudhari, and H. S. Lillehoj. 2019. Involvement of T Cell Immunity in Avian Coccidiosis. Front Immunol 10:2732.

Kittelsen, K. E., B. David, R. O. Moe, H. D. Poulsen, J. F. Young, and E. G. Granquist. 2017. Associations among gait score, production data, abattoir registrations, and postmortem tibia measurements in broiler chickens. Poult Sci 96:1033-1040.

Kleven, S. H. 2008. Control of avian mycoplasma infections in commercial poultry. Avian Dis 52:367-374.

Kleven, S. H., and N. J. D. o. p. Ferguson-Noel. 2008. Mycoplasma synoviae infection. 12:845-856.

Knowles, T. G., S. C. Kestin, S. M. Haslam, S. N. Brown, L. E. Green, A. Butterworth, S. J. Pope, D. Pfeiffer, and C. J. Nicol. 2008. Leg disorders in broiler chickens: prevalence, risk factors and prevention. PLoS One 3:e1545.

Kokabu, S., T. Katagiri, T. Yoda, and V. Rosen. 2012. Role of Smad phosphatases in BMP-Smad signaling axis-induced osteoblast differentiation. Journal of Oral Biosciences 54:73-78.

Kollet, O., A. Dar, S. Shivtiel, A. Kalinkovich, K. Lapid, Y. Sztainberg, M. Tesio, R. M. Samstein, P. Goichberg, A. Spiegel, A. Elson, and T. Lapidot. 2006. Osteoclasts degrade endosteal components and promote mobilization of hematopoietic progenitor cells. Nat Med 12:657-664.

Kong, S., Y. H. Zhang, and W. Zhang. 2018. Regulation of Intestinal Epithelial Cells Properties and Functions by Amino Acids. Biomed Res Int 2018:2819154.

Kronenberg, H. M. 2003. Developmental regulation of the growth plate. Nature 423:332-336.

Kwan Tat, S., M. Padrines, S. Theoleyre, D. Heymann, and Y. Fortun. 2004. IL-6, RANKL, TNF-alpha/IL-1: interrelations in bone resorption pathophysiology. Cytokine Growth Factor Rev 15:49-60.

Laird, E., M. Ward, E. McSorley, J. J. Strain, and J. Wallace. 2010. Vitamin D and bone health: potential mechanisms. Nutrients 2:693-724.

Langdahl, B., S. Ferrari, and D. W. Dempster. 2016. Bone modeling and remodeling: potential as therapeutic targets for the treatment of osteoporosis. Ther Adv Musculoskelet Dis 8:225-235.

Langenbach, F., and J. Handschel. 2013. Effects of dexamethasone, ascorbic acid and beta-glycerophosphate on the osteogenic differentiation of stem cells in vitro. Stem Cell Res Ther 4:117.

Laurent, F., R. Mancassola, S. Lacroix, R. Menezes, and M. Naciri. 2001. Analysis of chicken mucosal immune response to Eimeria tenella and Eimeria maxima infection by quantitative reverse transcription-PCR. Infect Immun 69:2527-2534.

Lauridsen, C. 2020. Effects of dietary fatty acids on gut health and function of pigs pre- and post-weaning. J Anim Sci 98.

Leach, R. M., Jr., and E. Monsonego-Ornan. 2007. Tibial dyschondroplasia 40 years later. Poult Sci 86:2053-2058.

Lee, A. V., L. You, S. Y. Oh, Z. Li, A. Code, C. Zhu, R. E. Fisher-Heffernan, T. R. H. Regnault, C. F. M. De Lange, L. A. Huber, and N. A. Karrow. 2019. Health Benefits of Supplementing Nursery Pig Diets with Microalgae or Fish Oil. Animals (Basel) 9.

Lee, K. S., H. J. Kim, Q. L. Li, X. Z. Chi, C. Ueta, T. Komori, J. M. Wozney, E. G. Kim, J. Y. Choi, H. M. Ryoo, and S. C. Bae. 2000. Runx2 is a common target of transforming growth factor beta1 and bone morphogenetic protein 2, and cooperation between Runx2 and Smad5 induces osteoblast-specific gene expression in the pluripotent mesenchymal precursor cell line C2C12. Mol Cell Biol 20:8783-8792.

Lee, M. S. J., K. Maruyama, Y. Fujita, A. Konishi, P. M. Lelliott, S. Itagaki, T. Horii, J. W. Lin, S. M. Khan, E. Kuroda, S. Akira, K. J. Ishii, and C. Coban. 2017a. Plasmodium products persist in the bone marrow and promote chronic bone loss. Sci Immunol 2.

Lee, N. K., H. Sowa, E. Hinoi, M. Ferron, J. D. Ahn, C. Confavreux, R. Dacquin, P. J. Mee, M. D. McKee, D. Y. Jung, Z. Zhang, J. K. Kim, F. Mauvais-Jarvis, P. Ducy, and G. Karsenty. 2007. Endocrine regulation of energy metabolism by the skeleton. Cell 130:456-469.

Lee, W. C., A. R. Guntur, F. Long, and C. J. Rosen. 2017b. Energy Metabolism of the Osteoblast: Implications for Osteoporosis. Endocr Rev 38:255-266.

Leibbrandt, A., and J. M. Penninger. 2008. RANK/RANKL: regulators of immune responses and bone physiology. Ann N Y Acad Sci 1143:123-150.

Lemma, S., M. Sboarina, P. E. Porporato, N. Zini, P. Sonveaux, G. Di Pompo, N. Baldini, and S. Avnet. 2016. Energy metabolism in osteoclast formation and activity. Int J Biochem Cell Biol 79:168-180.

Li, D., and M. Wu. 2021. Pattern recognition receptors in health and diseases. Signal Transduct Target Ther 6:291.

Li, J., D. Bi, S. Pan, and Y. Zhang. 2007a. Effect of diet with thiram on liver antioxidant capacity and tibial dyschondroplasia in broilers. Br Poult Sci 48:724-728.

Li, P., E. M. Schwarz, R. J. O'Keefe, L. Ma, R. J. Looney, C. T. Ritchlin, B. F. Boyce, and L. Xing. 2004. Systemic tumor necrosis factor alpha mediates an increase in peripheral CD11bhigh osteoclast precursors in tumor necrosis factor alpha-transgenic mice. Arthritis Rheum 50:265-276.

Li, Y., M. Terauchi, T. Vikulina, S. Roser-Page, and M. N. Weitzmann. 2014. B Cell Production of Both OPG and RANKL is Significantly Increased in Aged Mice. Open Bone J 6:8-17.

Li, Y., G. Toraldo, A. Li, X. Yang, H. Zhang, W. P. Qian, and M. N. Weitzmann. 2007b. B cells and T cells are critical for the preservation of bone homeostasis and attainment of peak bone mass in vivo. Blood 109:3839-3848.

Lillehoj, H. S. 1998. Role of T lymphocytes and cytokines in coccidiosis. International Journal for Parasitology 28:1071-1081.

Logar, D. B., R. Komadina, J. Prezelj, B. Ostanek, Z. Trost, and J. Marc. 2007. Expression of bone resorption genes in osteoarthritis and in osteoporosis. J Bone Miner Metab 25:219-225.

Lorenzo, J., M. Horowitz, and Y. Choi. 2008. Osteoimmunology: interactions of the bone and immune system. Endocr Rev 29:403-440.

Lu, J., T. Jilling, D. Li, and M. S. Caplan. 2007. Polyunsaturated fatty acid supplementation alters proinflammatory gene expression and reduces the incidence of necrotizing enterocolitis in a neonatal rat model. Pediatr Res 61:427-432.

MacDonell, R., M. W. Hamrick, and C. M. Isales. 2016. Protein/amino-acid modulation of bone cell function. Bonekey Rep 5:827.

Mackie, E. J., Y. A. Ahmed, L. Tatarczuch, K. S. Chen, and M. Mirams. 2008. Endochondral ossification: how cartilage is converted into bone in the developing skeleton. Int J Biochem Cell Biol 40:46-62.

Maddineni, S. R., S. M. Krzysik-Walker, O. M. Ocon-Grove, S. M. Motch, G. L. Hendricks, 3rd, and R. Ramachandran. 2007. Calcitonin is expressed in the chicken pituitary gland: influence of gonadal steroids and sexual maturation. Cell Tissue Res 327:521-528.

Massaccesi, L., E. Galliera, A. Pellegrini, G. Banfi, and M. M. Corsi Romanelli. 2022. Osteomyelitis, Oxidative Stress and Related Biomarkers. Antioxidants (Basel) 11.

Masteller, E. L., and C. B. Thompson. 1994. B cell development in the chicken. Poult Sci 73:998-1011.

McKee, J. S., and P. C. Harrison. 1995. Effects of supplemental ascorbic acid on the performance of broiler chickens exposed to multiple concurrent stressors. Poult Sci 74:1772-1785.

McNamee, P. T., and J. A. Smyth. 2000. Bacterial chondronecrosis with osteomyelitis ('femoral head necrosis') of broiler chickens: a review. Avian Pathol 29:253-270.

Mehmood, K. 2018. Tetramethylpyrazine Mitigates Toxicity and Liver Oxidative Stress in Tibial Dyschondroplasia Chickens. Pakistan Veterinary Journal 38:76-80.

Mehmood, K., H. Zhang, M. K. Iqbal, M. U. Rehman, M. Shahzad, K. Li, S. Huang, F. Nabi, L. Zhang, and J. Li. 2017. In Vitro Effect of Apigenin and Danshen in Tibial Dyschondroplasia Through Inhibition of Heat-Shock Protein 90 and Vascular Endothelial Growth Factor Expressions in Avian Growth Plate Cells. Avian Dis 61:372-377.

Miller, C. J., S. Trichilo, E. Pickering, S. Martelli, P. Delisser, L. B. Meakin, and P. Pivonka. 2021. Cortical Thickness Adaptive Response to Mechanical Loading Depends

on Periosteal Position and Varies Linearly With Loading Magnitude. Front Bioeng Biotechnol 9:671606.

Mireles, A. J., S. M. Kim, and K. C. Klasing. 2005. An acute inflammatory response alters bone homeostasis, body composition, and the humoral immune response of broiler chickens. Poult Sci 84:553-560.

Mishra, B., and R. Jha. 2019. Oxidative Stress in the Poultry Gut: Potential Challenges and Interventions. Front Vet Sci 6:60.

Mitchell, H. H., and J. R. Beadles. 1930. The Paired-Feeding Method in Nutrition Experiments and Its Application to the Problem of Cystine Deficiencies in Food Proteins. The Journal of Nutrition 2:225-243.

Miyazaki, T., H. Katagiri, Y. Kanegae, H. Takayanagi, Y. Sawada, A. Yamamoto, M. P. Pando, T. Asano, I. M. Verma, H. Oda, K. Nakamura, and S. Tanaka. 2000. Reciprocal role of ERK and NF-kappaB pathways in survival and activation of osteoclasts. J Cell Biol 148:333-342.

Mody, N. 2001. Oxidative stress modulates osteoblastic differentiation of vascular and bone cells. Free Radical Biology and Medicine 31:509-519.

Monier-Faugere, M. C., Z. Geng, Q. Qi, I. Arnala, and H. H. Malluche. 1996. Calcitonin prevents bone loss but decreases osteoblastic activity in ovariohysterectomized beagle dogs. J Bone Miner Res 11:446-455.

Möstl, E., and R. Palme. 2002. Hormones as indicators of stress. Domestic Animal Endocrinology 23:67-74.

Musa, I. W., L. Sa`idu, I. D. Jatau, J. Adamu, M. O. Otu, and P. A. Abdu. 2010. Outbreak of Coccidiosis in 5-day Old Commercial Broiler Breeder Flock in Zaria, Nigeria. International Journal of Poultry Science 9:1112-1115.

Nakashima, T., and H. Takayanagi. 2011. New regulation mechanisms of osteoclast differentiation. Ann N Y Acad Sci 1240:E13-18.

Nattiv, A., A. B. Loucks, M. M. Manore, C. F. Sanborn, J. Sundgot-Borgen, M. P. Warren, and M. American College of Sports. 2007. American College of Sports Medicine position stand. The female athlete triad. Med Sci Sports Exerc 39:1867-1882.

Neville-Webbe, H. L., N. A. Cross, C. L. Eaton, R. Nyambo, C. A. Evans, R. E. Coleman, and I. Holen. 2004. Osteoprotegerin (OPG) produced by bone marrow stromal cells protects breast cancer cells from TRAIL-induced apoptosis. Breast Cancer Res Treat 86:269-279.

Nordin, B. E., and H. A. Morris. 1989. The calcium deficiency model for osteoporosis. Nutr Rev 47:65-72.

Oftadeh, R., M. Perez-Viloria, J. C. Villa-Camacho, A. Vaziri, and A. Nazarian. 2015. Biomechanics and mechanobiology of trabecular bone: a review. J Biomech Eng 137.

Oh, S., H. S. Lillehoj, Y. Lee, D. Bravo, and E. P. Lillehoj. 2019. Dietary Antibiotic Growth Promoters Down-Regulate Intestinal Inflammatory Cytokine Expression in Chickens Challenged With LPS or Co-infected With Eimeria maxima and Clostridium perfringens. Front Vet Sci 6:420.

Oikeh, I., P. Sakkas, D. P. Blake, and I. Kyriazakis. 2019. Interactions between dietary calcium and phosphorus level, and vitamin D source on bone mineralization,

performance, and intestinal morphology of coccidia-infected broilers1. Poult Sci 98:5679-5690.

Olivares-Navarrete, R., S. L. Hyzy, D. L. Hutton, G. R. Dunn, C. Appert, B. D. Boyan, and Z. Schwartz. 2011. Role of non-canonical Wnt signaling in osteoblast maturation on microstructured titanium surfaces. Acta Biomater 7:2740-2750.

Olson, N. O., and K. M. Kerr. 1970. A Comparison of Radiographic Lesions in Pelvic Limbs of Chickens Infected with Mycoplasma gallisepticum, Mycoplasma synoviae, or an Arthritis-Producing Virus. Avian Diseases 14.

Onal, M., J. Xiong, X. Chen, J. D. Thostenson, M. Almeida, S. C. Manolagas, and C. A. O'Brien. 2012. Receptor activator of nuclear factor kappaB ligand (RANKL) protein expression by B lymphocytes contributes to ovariectomy-induced bone loss. J Biol Chem 287:29851-29860.

Orth, M. W., and M. E. Cook. 1994. Avian tibial dyschondroplasia: a morphological and biochemical review of the growth plate lesion and its causes. Vet Pathol 31:403-404.

Orth, M. W., J. I. Fenton, and K. A. Chlebek-Brown. 1999. Biochemical characterization of cartilage degradation in embryonic chick tibial explant cultures. Poult Sci 78:1596-1600.

Osorio, C., O. J. Fletcher, T. Abdul-Aziz, E. Gonder, B. Tilley, and D. H. Ley. 2007. Pneumonia of Turkey Breeder Hens Associated with Mycoplasma Synoviae. Avian Diseases 51:791-796.

Ott, S. M. 2018. Cortical or Trabecular Bone: What's the Difference? Am J Nephrol 47:373-375.

Paludo, E., A. M. G. Ibelli, J. O. Peixoto, F. C. Tavernari, C. A. V. Lima-Rosa, J. R. C. Pandolfi, and M. C. Ledur. 2017. The involvement of RUNX2 and SPARC genes in the bacterial chondronecrosis with osteomyelitis in broilers. Animal 11:1063-1070.

Panda, B., G. F. Combs, and H. M. DeVolt. 1964. Studies on Coccidiosis and Vitamin A Nutrition of Broilers. Poultry Science 43:154-164.

Papageorgiou, M., E. Dolan, K. J. Elliott-Sale, and C. Sale. 2018. Reduced energy availability: implications for bone health in physically active populations. Eur J Nutr 57:847-859.

Parfitt, A. M. 1994. Osteonal and hemi-osteonal remodeling: the spatial and temporal framework for signal traffic in adult human bone. J Cell Biochem 55:273-286.

Park, J. H., N. K. Lee, and S. Y. Lee. 2017. Current Understanding of RANK Signaling in Osteoclast Differentiation and Maturation. Mol Cells 40:706-713.

Park, J. K., E. M. Lee, A. Y. Kim, E. J. Lee, C. W. Min, K. K. Kang, M. M. Lee, and K. S. Jeong. 2012. Vitamin C deficiency accelerates bone loss inducing an increase in PPAR-gamma expression in SMP30 knockout mice. Int J Exp Pathol 93:332-340.

Passi, N., and A. Gefen. 2005. Trabecular bone contributes to strength of the proximal femur under mediolateral impact in the avian. J Biomech Eng 127:198-203.

Peretz, A. M., J. A. Hipp, and M. H. Heggeness. 1998. The internal bony architecture of the sacrum. Spine (Phila Pa 1976) 23:971-974.

Phibbs, D. V., P. J. Groves, and W. I. Muir. 2021. Leg health of meat chickens: impact on welfare, consumer behaviour, and the role of environmental enrichment. Animal Production Science 61.

Pivonka, P., J. Zimak, D. W. Smith, B. S. Gardiner, C. R. Dunstan, N. A. Sims, T. J. Martin, and G. R. Mundy. 2010. Theoretical investigation of the role of the RANK-RANKL-OPG system in bone remodeling. J Theor Biol 262:306-316.

Porto, M. L., B. P. Rodrigues, T. N. Menezes, S. L. Ceschim, D. E. Casarini, A. L. Gava, T. M. Pereira, E. C. Vasquez, B. P. Campagnaro, and S. S. Meyrelles. 2015. Reactive oxygen species contribute to dysfunction of bone marrow hematopoietic stem cells in aged C57BL/6 J mice. J Biomed Sci 22:97.

Praul, C. A., B. C. Ford, C. V. Gay, M. Pines, and R. M. Leach. 2000. Gene expression and tibial dyschondroplasia. Poult Sci 79:1009-1013.

Prisby, R., T. Menezes, J. Campbell, T. Benson, E. Samraj, I. Pevzner, and R. F. Wideman, Jr. 2014. Kinetic examination of femoral bone modeling in broilers. Poult Sci 93:1122-1129.

Rath, N. C., and V. Durairaj. 2022. Avian bone physiology and poultry bone disorders. Pages 529-543 in Sturkie's Avian PhysiologyElsevier.

Reid, I. R., R. W. Ames, M. C. Evans, G. D. Gamble, and S. J. Sharpe. 1995. Long-term effects of calcium supplementation on bone loss and fractures in postmenopausal women: A randomized controlled trial. The American Journal of Medicine 98:331-335.

Reis, J., and A. Ramos. 2021. In Sickness and in Health: The Oxygen Reactive Species and the Bone. Front Bioeng Biotechnol 9:745911.

Rekaya, R., R. L. Sapp, T. Wing, and S. E. Aggrey. 2013. Genetic evaluation for growth, body composition, feed efficiency, and leg soundness. Poult Sci 92:923-929.

Riddle, R. C., and T. L. Clemens. 2017. Bone Cell Bioenergetics and Skeletal Energy Homeostasis. Physiol Rev 97:667-698.

Rifas, L. 1999. Bone and cytokines: beyond IL-1, IL-6 and TNF-alpha. Calcif Tissue Int 64:1-7.

Roberts, J. R., R. Souillard, and J. Bertin. 2011. Avian diseases which affect egg production and quality. Pages 376-393 in Improving the safety and quality of eggs and egg productsElsevier.

Rodriguez, J. P., S. Rios, and M. Gonzalez. 2002. Modulation of the proliferation and differentiation of human mesenchymal stem cells by copper. J Cell Biochem 85:92-100.

Roux, S., and P. Orcel. 2000. Bone loss. Factors that regulate osteoclast differentiation: an update. Arthritis Res 2:451-456.

Rubert, M., and C. De la Piedra. 2020. La osteocalcina: de marcador de formación ósea a hormona; y el hueso, un órgano endocrino. Revista de Osteoporosis y Metabolismo Mineral 12:146-151.

Rucci, N., A. Rufo, M. Alamanou, and A. Teti. 2007. Modeled microgravity stimulates osteoclastogenesis and bone resorption by increasing osteoblast RANKL/OPG ratio. J Cell Biochem 100:464-473.

Ruff, M. D., W. M. Reid, and J. K. Johnson. 1974. Lowered blood carotenoid levels in chickens infected with coccidia. Poult Sci 53:1801-1809.

Sakkas, P., I. Oikeh, D. P. Blake, M. J. Nolan, R. A. Bailey, A. Oxley, I. Rychlik, G. Lietz, and I. Kyriazakis. 2018. Does selection for growth rate in broilers affect their resistance and tolerance to Eimeria maxima? Vet Parasitol 258:88-98.

Sakkas, P., I. Oikeh, D. P. Blake, S. Smith, and I. Kyriazakis. 2019. Dietary vitamin D improves performance and bone mineralisation, but increases parasite replication and compromises gut health in Eimeria-infected broilers. Br J Nutr 122:676-688.

Sanchez-Rodriguez, E., C. Benavides-Reyes, C. Torres, N. Dominguez-Gasca, A. I. Garcia-Ruiz, S. Gonzalez-Lopez, and A. B. Rodriguez-Navarro. 2019. Changes with age (from 0 to 37 D) in tibiae bone mineralization, chemical composition and structural organization in broiler chickens. Poult Sci 98:5215-5225.

Santos, A., A. D. Bakker, J. M. de Blieck-Hogervorst, and J. Klein-Nulend. 2010. WNT5A induces osteogenic differentiation of human adipose stem cells via rho-associated kinase ROCK. Cytotherapy 12:924-932.

Santos, T. S. d., P.-Y. Teng, S. Yadav, F. L. d. S. Castro, R. L. Gould, S. W. Craig, C. Chen, A. L. Fuller, R. Pazdro, J. R. Sartori, and W. K. Kim. 2020. Effects of Inorganic Zn and Cu Supplementation on Gut Health in Broiler Chickens Challenged With Eimeria spp. Frontiers in Veterinary Science 7.

Scanes, C. G. 2016. Biology of stress in poultry with emphasis on glucocorticoids and the heterophil to lymphocyte ratio. Poult Sci 95:2208-2215.

Schett, G. 2008. Review: Immune cells and mediators of inflammatory arthritis. Autoimmunity 41:224-229.

Scott, E. W., R. C. Fisher, M. C. Olson, E. W. Kehrli, M. C. Simon, and H. Singh. 1997. PU.1 Functions in a Cell-Autonomous Manner to Control the Differentiation of Multipotential Lymphoid–Myeloid Progenitors. Immunity 6:437-447.

Sepp, T., U. Karu, J. D. Blount, E. Sild, M. Manniste, and P. Horak. 2012. Coccidian infection causes oxidative damage in greenfinches. PLoS One 7:e36495.

Shimizu, T. 2016. Inflammation-inducing Factors of Mycoplasma pneumoniae. Front Microbiol 7:414.

Shini, S., and P. Kaiser. 2009. Effects of stress, mimicked by administration of corticosterone in drinking water, on the expression of chicken cytokine and chemokine genes in lymphocytes. Stress 12:388-399.

Sies, H., C. Berndt, and D. P. Jones. 2017. Oxidative Stress. Annu Rev Biochem 86:715-748.

Solomon, L. B., D. Kitchen, P. H. Anderson, D. Yang, Y. Starczak, M. Kogawa, E. Perilli, P. J. Smitham, M. S. Rickman, D. Thewlis, and G. J. Atkins. 2018. Time dependent loss of trabecular bone in human tibial plateau fractures. J. Orthop. Res. 36:2865-2875.

Southern, L. L., and D. H. Baker. 1983. Zinc toxicity, zinc deficiency and zinc-copper interrelationship in Eimeria acervulina-infected chicks. J Nutr 113:688-696.

Soysa, N. S., and N. Alles. 2019. Positive and negative regulators of osteoclast apoptosis. Bone Rep 11:100225.

Stephens, A. S., S. R. Stephens, and N. A. Morrison. 2011. Internal control genes for quantitative RT-PCR expression analysis in mouse osteoblasts, osteoclasts and macrophages. BMC Res Notes 4:410.

Suchacki, K. J., F. Roberts, A. Lovdel, C. Farquharson, N. M. Morton, V. E. MacRae, and W. P. Cawthorn. 2017. Skeletal energy homeostasis: a paradigm of endocrine discovery. J Endocrinol 234:R67-R79.

Surai, P. F., Kochish, II, V. I. Fisinin, and M. T. Kidd. 2019. Antioxidant Defence Systems and Oxidative Stress in Poultry Biology: An Update. Antioxidants (Basel) 8.

Swarthout, J. T., R. C. D'Alonzo, N. Selvamurugan, and N. C. Partridge. 2002. Parathyroid hormone-dependent signaling pathways regulating genes in bone cells. Gene 282:1-17.

Taichman, R. S. 2005. Blood and bone: two tissues whose fates are intertwined to create the hematopoietic stem-cell niche. Blood 105:2631-2639.

Takada, I., M. Mihara, M. Suzawa, F. Ohtake, S. Kobayashi, M. Igarashi, M. Y. Youn, K. Takeyama, T. Nakamura, Y. Mezaki, S. Takezawa, Y. Yogiashi, H. Kitagawa, G. Yamada, S. Takada, Y. Minami, H. Shibuya, K. Matsumoto, and S. Kato. 2007. A histone lysine methyltransferase activated by non-canonical Wnt signalling suppresses PPAR-gamma transactivation. Nat Cell Biol 9:1273-1285.

Takahashi, N., N. Udagawa, and T. Suda. 2014. Vitamin D endocrine system and osteoclasts. Bonekey Rep 3:495.

Takayanagi, H., S. Kim, T. Koga, H. Nishina, M. Isshiki, H. Yoshida, A. Saiura, M. Isobe, T. Yokochi, J.-i. Inoue, E. F. Wagner, T. W. Mak, T. Kodama, and T. Taniguchi. 2002. Induction and Activation of the Transcription Factor NFATc1 (NFAT2) Integrate RANKL Signaling in Terminal Differentiation of Osteoclasts. Developmental Cell 3:889-901.

Talaty, P. N., M. N. Katanbaf, and P. Y. Hester. 2009. Variability in bone mineralization among purebred lines of meat-type chickens. Poult Sci 88:1963-1974.

Tasca, A., K. Astleford, N. C. Blixt, E. D. Jensen, R. Gopalakrishnan, and K. C. Mansky. 2018. SMAD1/5 signaling in osteoclasts regulates bone formation via coupling factors. PLoS One 13:e0203404.

Tasca, A., M. Stemig, A. Broege, B. Huang, J. Davydova, A. Zwijsen, L. Umans, E. D. Jensen, R. Gopalakrishnan, and K. C. Mansky. 2015. Smad1/5 and Smad4 expression are important for osteoclast differentiation. J Cell Biochem 116:1350-1360.

Teitelbaum, S. L. 2007. Osteoclasts: what do they do and how do they do it? Am J Pathol 170:427-435.

Teitelbaum, S. L., and F. P. Ross. 2003. Genetic regulation of osteoclast development and function. Nat Rev Genet 4:638-649.

Teng, P. Y., J. Choi, Y. Tompkins, H. Lillehoj, and W. Kim. 2021. Impacts of increasing challenge with Eimeria maxima on the growth performance and gene expression of biomarkers associated with intestinal integrity and nutrient transporters. Vet Res 52:81.

Teng, P. Y., S. Yadav, F. L. S. Castro, Y. H. Tompkins, A. L. Fuller, and W. K. Kim. 2020a. Graded Eimeria challenge linearly regulated growth performance, dynamic change of gastrointestinal permeability, apparent ileal digestibility, intestinal morphology, and tight junctions of broiler chickens. Poult Sci 99:4203-4216.

Teng, P. Y., S. Yadav, T. S. Dos Santos, A. L. Fuller, and W. K. Kim. 2020b. 2-Nitro-1-propanol improved nutrient digestibility and oocyst shedding but not growth performance of Eimeria-challenged broilers. Poult Sci 99:4314-4322.

Thakker, R. V., M. P. Whyte, J. Eisman, and T. Igarashi. 2017. Genetics of bone biology and skeletal disease. Academic Press.

Thiese, M. S., B. Ronna, and U. Ott. 2016. P value interpretations and considerations. J Thorac Dis 8:E928-E931.

Thorp, B. H. 1994. Skeletal disorders in the fowl: a review. Avian Pathol 23:203-236.

Titanji, K. 2017. Beyond Antibodies: B Cells and the OPG/RANK-RANKL Pathway in Health, Non-HIV Disease and HIV-Induced Bone Loss. Front Immunol 8:1851.

Titanji, K., A. Vunnava, A. N. Sheth, C. Delille, J. L. Lennox, S. E. Sanford, A. Foster, A. Knezevic, K. A. Easley, M. N. Weitzmann, and I. Ofotokun. 2014. Dysregulated B cell expression of RANKL and OPG correlates with loss of bone mineral density in HIV infection. PLoS Pathog 10:e1004497.

Tompkins, Y. H., C. Chen, K. M. Sweeney, M. Kim, B. H. Voy, J. L. Wilson, and W. K. Kim. 2022a. The effects of maternal fish oil supplementation rich in n-3 PUFA on offspring-broiler growth performance, body composition and bone microstructure. PLoS One 17:e0273025.

Tompkins, Y. H., P. Teng, R. Pazdro, and W. K. Kim. 2022b. Long Bone Mineral Loss, Bone Microstructural Changes and Oxidative Stress After Eimeria Challenge in Broilers. Front Physiol 13:945740.

Tortelli, F., R. Tasso, F. Loiacono, and R. Cancedda. 2010. The development of tissue-engineered bone of different origin through endochondral and intramembranous ossification following the implantation of mesenchymal stem cells and osteoblasts in a murine model. Biomaterials 31:242-249.

Turk, D. E. 1973. Calcium absorption during coccidial infections in chicks. Poult Sci 52:854-857.

Turk, D. E., and J. F. Stephens. 1967. Upper intestinal tract infection produced by E. acervulina and absorption of 65Zn and 131-I-labeled oleic acid. J Nutr 93:161-165.

Turk, D. E., and J. F. Stephens. 1969. Coccidial infections of the ileum, colon, and ceca of the chick and nutrient absorption. Poult Sci 48:586-589.

Turk, D. E., and J. F. Stephens. 1970. Effects of serial inoculations with Eimeria acervulina or Eimeria necatrix upon zinc and oleic acid absorption in chicks. Poult Sci 49:523-526.

Vandesompele, J., K. De Preter, F. Pattyn, B. Poppe, N. Van Roy, A. De Paepe, and F. Speleman. 2002. Accurate normalization of real-time quantitative RT-PCR data by geometric averaging of multiple internal control genes. Genome Biol 3:RESEARCH0034.

Waldenstedt, L. 2006. Nutritional factors of importance for optimal leg health in broilers: A review. Animal Feed Science and Technology 126:291-307.

Walker, B. R. 2015. Dietary regulation of cortisol production and metabolism in humans. Endocrine Abstracts.

Walser, M. M., N. K. Allen, C. J. Mirocha, G. F. Hanlon, and J. A. Newman. 1982. Fusarium-induced osteochondrosis (tibial dyschondroplasia) in chickens. Vet Pathol 19:544-550.

Ward, T. L., K. L. Watkins, and L. L. Southern. 1990. Interactive effects of sodium zeolite A (Ethacal) and monensin in uninfected and Eimeria acervulina-infected chicks. Poult Sci 69:276-280.

Ward, T. L., K. L. Watkins, and L. L. Southern. 1993. Research note: interactive effects of sodium zeolite A and Eimeria acervulina infection on growth and tissue minerals in chicks. Poult Sci 72:2172-2175.

Webber, G., and M. Frigg. Year. Effect of high level of vitamin C on coccidiosis infected chickens. Proc. Roche Symp. on Anim. Nutr. and Health. Basel Village-Neuf.

Wei, J., J. Shimazu, M. P. Makinistoglu, A. Maurizi, D. Kajimura, H. Zong, T. Takarada, T. Lezaki, J. E. Pessin, E. Hinoi, and G. Karsenty. 2015. Glucose Uptake and Runx2 Synergize to Orchestrate Osteoblast Differentiation and Bone Formation. Cell 161:1576-1591.

Wei, S., H. Kitaura, P. Zhou, F. P. Ross, and S. L. Teitelbaum. 2005. IL-1 mediates TNF-induced osteoclastogenesis. Journal of Clinical Investigation 115:282-290.

Weitzmann, M. N., and R. Pacifici. 2006. Estrogen deficiency and bone loss: an inflammatory tale. Clin Invest 116:1186-1194.

Whitehead, C. C., and R. H. Fleming. 2000. Osteoporosis in Cage Layers. Poultry Science 79:1033-1041.

Wideman, R. F., Jr. 2016. Bacterial chondronecrosis with osteomyelitis and lameness in broilers: a review. Poult Sci 95:325-344.

Wideman, R. F., Jr., A. Al-Rubaye, A. Gilley, D. Reynolds, H. Lester, D. Yoho, J. M. Hughes, and I. Pevzner. 2013. Susceptibility of 4 commercial broiler crosses to lameness attributable to bacterial chondronecrosis with osteomyelitis. Poult Sci 92:2311-2325.

Wideman, R. F., Jr., J. Blankenship, I. Y. Pevzner, and B. J. Turner. 2015. Efficacy of 25-OH Vitamin D3 prophylactic administration for reducing lameness in broilers grown on wire flooring. Poult Sci 94:1821-1827.

Williams, B., S. Solomon, D. Waddington, B. Thorp, and C. Farquharson. 2000. Skeletal development in the meat-type chicken. Br Poult Sci 41:141-149.

Wu, M., G. Chen, and Y. P. Li. 2016. TGF-beta and BMP signaling in osteoblast, skeletal development, and bone formation, homeostasis and disease. Bone Res 4:16009.

Wu, X., M. A. McKenna, X. Feng, T. R. Nagy, and J. M. McDonald. 2003. Osteoclast apoptosis: the role of Fas in vivo and in vitro. Endocrinology 144:5545-5555.

Wu, Z., L. Rothwell, J. R. Young, J. Kaufman, C. Butter, and P. Kaiser. 2010. Generation and characterization of chicken bone marrow-derived dendritic cells. Immunology 129:133-145.

Xiang, J., C. Wan, R. Guo, and D. Guo. 2016. Is Hydrogen Peroxide a Suitable Apoptosis Inducer for All Cell Types? Biomed Res Int 2016:7343965.

Xing, L., and B. F. Boyce. 2005. Regulation of apoptosis in osteoclasts and osteoblastic cells. Biochem Biophys Res Commun 328:709-720.

Xing, L., T. P. Bushnell, L. Carlson, Z. Tai, M. Tondravi, U. Siebenlist, F. Young, and B. F. Boyce. 2002. NF-kappaB p50 and p52 expression is not required for RANK-

expressing osteoclast progenitor formation but is essential for RANK- and cytokine-mediated osteoclastogenesis. J Bone Miner Res 17:1200-1210.

Yadav, S., P. Y. Teng, T. Souza Dos Santos, R. L. Gould, S. W. Craig, A. Lorraine Fuller, R. Pazdro, and W. K. Kim. 2020. The effects of different doses of curcumin compound on growth performance, antioxidant status, and gut health of broiler chickens challenged with Eimeria species. Poult Sci 99:5936-5945.

Yamaguchi, M., and M. N. Weitzmann. 2011. Zinc stimulates osteoblastogenesis and suppresses osteoclastogenesis by antagonizing NF-kappaB activation. Mol Cell Biochem 355:179-186.

Yao, W., H. Zhang, X. Jiang, K. Mehmood, M. Iqbal, A. Li, J. Zhang, Y. Wang, M. Waqas, Y. Shen, and J. Li. 2018. Effect of Total Flavonoids of Rhizoma drynariae on Tibial Dyschondroplasia by Regulating BMP-2 and Runx2 Expression in Chickens. Front Pharmacol 9:1251.

Yao, Z., P. Li, Q. Zhang, E. M. Schwarz, P. Keng, A. Arbini, B. F. Boyce, and L. Xing. 2006. Tumor necrosis factor-alpha increases circulating osteoclast precursor numbers by promoting their proliferation and differentiation in the bone marrow through up-regulation of c-Fms expression. J Biol Chem 281:11846-11855.

Yao, Z., L. Xing, C. Qin, E. M. Schwarz, and B. F. Boyce. 2008. Osteoclast precursor interaction with bone matrix induces osteoclast formation directly by an interleukin-1-mediated autocrine mechanism. J Biol Chem 283:9917-9924.

Yin, M. T., E. Lund, J. Shah, C. A. Zhang, M. Foca, N. Neu, K. K. Nishiyama, B. Zhou, X. E. Guo, J. Nelson, D. L. Bell, E. Shane, and S. M. Arpadi. 2014. Lower peak bone

mass and abnormal trabecular and cortical microarchitecture in young men infected with HIV early in life. AIDS 28:345-353.

Yun, C. 2000. Intestinal immune responses to coccidiosis. Developmental & Comparative Immunology 24:303-324.

Zaiss, M. M., B. Frey, A. Hess, J. Zwerina, J. Luther, F. Nimmerjahn, K. Engelke, G. Kollias, T. Hunig, G. Schett, and J. P. David. 2010. Regulatory T cells protect from local and systemic bone destruction in arthritis. J Immunol 184:7238-7246.

Zhang, C., D. Li, F. Wang, and T. Dong. 2003. Effects of dietary vitamin K levels on bone quality in broilers. Arch Tierernahr 57:197-206.

Zhang, F., W. Peng, J. Zhang, W. Dong, D. Yuan, Y. Zheng, and Z. Wang. 2019a. New strategy of bone marrow mesenchymal stem cells against oxidative stress injury via Nrf2 pathway: oxidative stress preconditioning. J. Cell. Biochem. 120:19902-19914.

Zhang, H., K. Mehmood, X. Jiang, Z. Li, W. Yao, J. Zhang, X. Tong, Y. Wang, A. Li, M. Waqas, M. Iqbal, and J. Li. 2019b. Identification of differentially expressed MiRNAs profile in a thiram-induced tibial dyschondroplasia. Ecotoxicol Environ Saf 175:83-89.

Zhang, H., K. Mehmood, K. Li, M. U. Rehman, X. Jiang, S. Huang, L. Wang, L. Zhang, X. Tong, F. Nabi, W. Yao, M. K. Iqbal, M. Shahzad, and J. Li. 2018. Icariin Ameliorate Thiram-Induced Tibial Dyschondroplasia via Regulation of WNT4 and VEGF Expression in Broiler Chickens. Front Pharmacol 9:123.

Zhang, H., Y. Wang, K. Mehmood, Y. F. Chang, Z. Tang, and Y. Li. 2020. Treatment of tibial dyschondroplasia with traditional Chinese medicines: "Lesson and future directions". Poult Sci 99:6422-6433.

Zhang, L., T. He, M. Li, J. Hu, and X. Piao. 2019c. Effects of dietary calcium and phosphorus levels and supplementation of 25-hydroxycholecalciferol on performance and bone properties of broiler starters. Arch Anim Nutr 73:445-456.

Zhang, Q., I. R. Badell, E. M. Schwarz, K. E. Boulukos, Z. Yao, B. F. Boyce, and L. Xing. 2005. Tumor necrosis factor prevents alendronate-induced osteoclast apoptosis in vivo by stimulating Bcl-xL expression through Ets-2. Arthritis Rheum 52:2708-2718.

Zhou, R., Q. Guo, Y. Xiao, Q. Guo, Y. Huang, C. Li, and X. Luo. 2021. Endocrine role of bone in the regulation of energy metabolism. Bone Res 9:25.

Zhu, H., Y. Liu, S. Chen, X. Wang, D. Pi, W. Leng, F. Chen, J. Zhang, and P. Kang. 2016. Fish oil enhances intestinal barrier function and inhibits corticotropin-releasing hormone/corticotropin-releasing hormone receptor 1 signalling pathway in weaned pigs after lipopolysaccharide challenge. Br J Nutr 115:1947-1957.

Zomorodian, E., and M. Baghaban Eslaminejad. 2012. Mesenchymal stem cells as a potent cell source for bone regeneration. Stem Cells Int 2012:980353.

Zorov, D. B., M. Juhaszova, and S. J. Sollott. 2014. Mitochondrial reactive oxygen species (ROS) and ROS-induced ROS release. Physiol Rev 94:909-950.

Zou, M. L., Z. H. Chen, Y. Y. Teng, S. Y. Liu, Y. Jia, K. W. Zhang, Z. L. Sun, J. J. Wu, Z. D. Yuan, Y. Feng, X. Li, R. S. Xu, and F. L. Yuan. 2021. The Smad Dependent TGF-beta and BMP Signaling Pathway in Bone Remodeling and Therapies. Front Mol Biosci 8:593310.

Tables

Table 3.1: Nucleotide sequences of the primers used for real-time RT-PCR.

	Primer sequence (5'-3')	Product length (bp)	Annealing temperature (°C)	Accession #
GAPDH	F-GCTAAGGCTGTGGGGAAAGT R-TCAGCAGCAGCCTTCACTAC	161	55	NM_204305.1
RNA18S1	F-AGCCTGCGGCTTAATTTGAC R-CAACTAAGAACGGCCATGCA	121	56.5	AF_173612.1
HMBS	F-GGCTGGGAGAATCGCATAGG R-TCCTGCAGGGCAGATACCAT	131	59	XM_004947916.3
SPP1	F-GCCCAACATCAGAGCGTAGA R-ACGGGTGACCTCGTTGTTTT	204	57	NM_204535.4
BMP2	F-TCAGCTCAGGCCGTTGTTAG R-GTCATTCCACCCCACGTCAT	163	57	XM_025148488.1
RUNX2	F-ACTTTGACAATAACTGTCCT R-GACCCCTACTCTCATACTGG	192	60	XM_015285081.2
ALP	F-CGACCACTCACACGTCTTCA R-CGATCTTATAGCCAGGGCCG	140	58	NM_205360.1
BGLAP	F-GGATGCTCGCAGTGCTAAAG R-CTCACACACCTCTCGTTGGG	142	57	NM_205387.3
NFKB1	F-GAAGGAATCGTACCGGGAAC A	131	59	XM_015285418.2

	R-CTCAGAGGGCCTTGTGACAGTAA			
FOS	F-CTTCGACGAGCTGCTTTTCT R-TGGAGGTGTAGGTGCTAGGG	191	60	NM_205508.1
TNFRSF11B	F-ACGCTTGTGCTCTTGGACAT R-CAGCGTAGTACTGGTCTGGG	193	60	NM_001033641.1
TNFSF11	F-ACACGCCCTTTGAAAATCAG R-GCAAAAGGTTGCTTCTCTGG	196	60	XM_015275777.2
ACP5	F-GCTTCCAGGAGACCTTCGAG R-CAGGCGGAGGCTGTAGTAGT	170	61	XM_040693093.1
NFATC1	F-CAGTCCTGCAGTCCAACTCA R-TCCTCAGGTTCTCGCTTGAT	173	60	XM_040663226.1
SMAD1	F-GTTTTGTAAAGGGTTGGGGAGC R-AATGCAGGAGCTTGGGACCTTA	174	61	XM_040698719.1
IL1B	F-AGATGAAGCGGGTCAGCTC R-GCATCAAGGGCTACAAGCTC	120	59	XM_015297469.2
TNF	F-CGTGGTTCGAGTCGCTGTAT R-CCGTGCAGGTCGAGGTAC	100	60	XM_040694846.2

[1] GAPDH: glyceraldehyde-3-phosphate dehydrogenase; HMBS: hydroxymethylbilane synthase; RNA18S1: RNA, 18S ribosomal 1; ACP5: TRAP, acid phosphatase 5, tartrate resistant; TNFSF11: RANKL,TNF superfamily member 11; TNF: tumor necrosis factor-like; NFATC1:nuclear factor of activated T cells 1; TNFRSF11B: OPG, TNF receptor superfamily 11; TNF: tumor necrosis factor-like; NFATC1:nuclear factor

of activated T cells 1; TNFRSF11B: OPG, TNF receptor superfamily member 11b; IL1B: interleukin 1 beta; BGLAP: bone gamma-carboxyglutamate protein; RUNX2: runt-related transcription factor 2; ALP: alkaline phosphatase; SPP1: secreted phosphoprotein 1; BMP2: bone morphogenetic protein 2; FOS: Fos proto-oncogene, AP-1 transcription factor subunit; NFKB1: nuclear factor kappa B subunit 1; SMAD1: SMAD family member 1.

Table 3.2: Average daily feed intake (ADFI), cumulative feed intake (FI), body weight gain (BWG, kg) and feed conversion ratio (FCR) from 0 to 6 dpi.

ADFI (g) / Treatments[1]	1 dpi	2 dpi	3 dpi	4 dpi	5 dpi	6 dpi
Control	126.01	95.42	104.23	108.19[a]	86.38 [a]	96.68[a]
Low	134.75	103.97	107.01	86.89[b]	68.09[b]	64.51[b]
High	133.40	101.93	100.40	75.22[b]	42.18[c]	44.89[c]
PF	127.27	93.33	93.333	76.36[b]	42.42[c]	46.82[c]
SEM	1.6601	2.3237	2.1636	2.9236	3.5585	3.8577
P-value	0.158	0.316	0.128	< 0.001	< 0.001	< 0.001

Treatmemts	0-6 dpi		
	FI	BWG	FCR
Control	617.753[a]	352.59[a]	1.77031[c]
Low	566.531[a]	250.432[b]	2.32316[b]
High	499.474[b]	178.061[c]	2.92614[a]
PF	480.379[b]	206.937[bc]	2.35415[b]
SEM	12.0978	12.8636	0.08879
P-value	< 0.001	< 0.001	< 0.001

[1]Control: uninfected controls fed diet *ad libitum* and gavaged with water; Low: low *Eimeria*-infected group fed diet *ad libitum* and gavaged with 50,000 oocysts of *E. maxima*, 50,000 oocysts of *E. tenella*, and 250,000 oocysts of *E. acervulina*; High: severely *Eimeria*-infected group fed diet *ad libitum* diet and gavaged with 12,500 oocysts of *E. maxima*; 12,500 oocysts of *E. tenella*; 62,500 oocysts of *E. acervulina*; PF: an uninfected pair-fed group that fed the same amount of feed as the High group, gavaged with water.

[a, ab, b, c] Treatments with different letters means a significantly difference between treatments by using Tukey's HSD test, $P < 0.05$, N = 10.

Table 3.3: Femur bone metaphysis and diaphysis structure in broiler chickens at 6 dpi.

	Section		Unit	Control[1]	Low	High	PF	SEM	*P*-value
Metaphysis	Total	BMC[2]	g	149.403	137.218	117.639	132.312	6.984	0.469
		BMD	g/mm^2	0.288^{a}	0.233^{b}	0.239^{b}	0.243^{ab}	0.009	0.017
		TV	mm^3	579.742	606.012	534.340	559.222	22.068	0.704
		BV	mm^3	315.092	359.677	301.793	335.881	20.723	0.783
	Cortical	BMD	g/mm^2	0.556	0.511	0.522	0.492	0.0136	0.449
		BMC	g	84.366	97.495	86.034	95.740	4.9120	0.325
	Trabecular	BMD	g/mm^2	0.519^{a}	0.398^{b}	0.392^{b}	0.411^{b}	0.0135	<0.001
		BMC	g	4.339	4.286	3.304	5.483	0.4082	0.294
		BS	mm^2	403.078	410.676	317.433	443.159	37.1790	0.660
		Tb.N	-	11.325^{a}	9.1304^{b}	9.236^{b}	8.2574^{b}	0.2855	0.004
Diaphysis	Total	BMC	g	136.838^{a}	120.375^{ab}	104.044^{b}	96.318^{b}	4.8538	0.013
		BMD	g/mm^2	1.028^{a}	0.902^{b}	0.912^{b}	0.898^{b}	0.0130	<0.001
		BV	mm^3	133.672	133.649	114.335	107.172	4.8897	0.126

[1]Control: uninfected controls fed diet *ad libitum* and gavaged with water; Low: low *Eimeria*-infected group fed diet *ad libitum* and gavaged with 50,000 oocysts of *E. maxima*, 50,000 oocysts of *E. tenella*, and 250,000 oocysts of *E. acervulina*; High:

severely *Eimeria*-infected group fed diet *ad libitum* diet and gavaged with 12,500 oocysts of *E. maxima*; 12,500 oocysts of *E. tenella*; 62,500 oocysts of *E. acervulina*; PF: an uninfected pair-fed group that fed the same amount of feed as the High group, gavaged with water.

[2]BMC, bone mineral content; BMD, bone mineral density; TV, total bone volume; BV, bone volume (TV minus bone marrow volume); BS, bone surface area; Tb. N, trabecular number.

[a, ab, b,] Treatments with different letters means a significantly difference between treatments by using Tukey's HSD test, $P < 0.05$, N = 10.

Table 3.4: Bone growth rate measured by calcein injection method.

Femur: unit (mm)			
Treatment[1]	0-4 dpi	4-8 dpi	0-8 dpi
Control	0.253[a]	0.212[a]	0.479[a]
Low	0.175[ab]	0.081[b]	0.219[bc]
High	0.157[b]	0.032[b]	0.190[c]
PF	0.145[b]	0.157[a]	0.300[b]
SEM	0.0132	0.0143	0.0241
P-value	0.014	< 0.001	< 0.001
Tibia: unit (mm)			
Treatment[1]	0-4 dpi	4-8 dpi	0-8 dpi
Control	0.208	0.186[a]	0.387[a]
Low	0.128	0.030[b]	0.147[b]
High	0.115	0.036[b]	0.152[b]
PF	0.125	0.140[a]	0.270[ab]
SEM	0.0177	0.0158	0.0285
P-value	0.197	< 0.001	0.002

[1] Control, control group; Low, the lower challenge dose; High, the high challenge dose; PF, pair-feeding group, paired with the High group; [2] unit: mm; [a, ab, b, bc, c] Treatments with different letters means a significantly difference between treatments by using Tukey's HSD test, $P < 0.05$, N = 10.

Figures

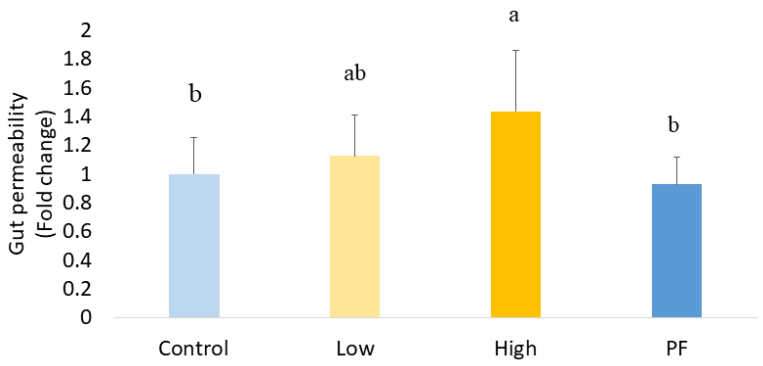

Figure 3.1: Gut permeability at 5 dpi. Higher concentration of FITC-d in the serum revealed more severe damage to the gut epithelium owing to the *Eimeria* challenge.

[a, ab, b] Treatments with different letters means a significantly difference between treatments by using Tukey's HSD test, $P < 0.05$, N = 10. The relatively level of FITC-d in serum was presented as fold change.

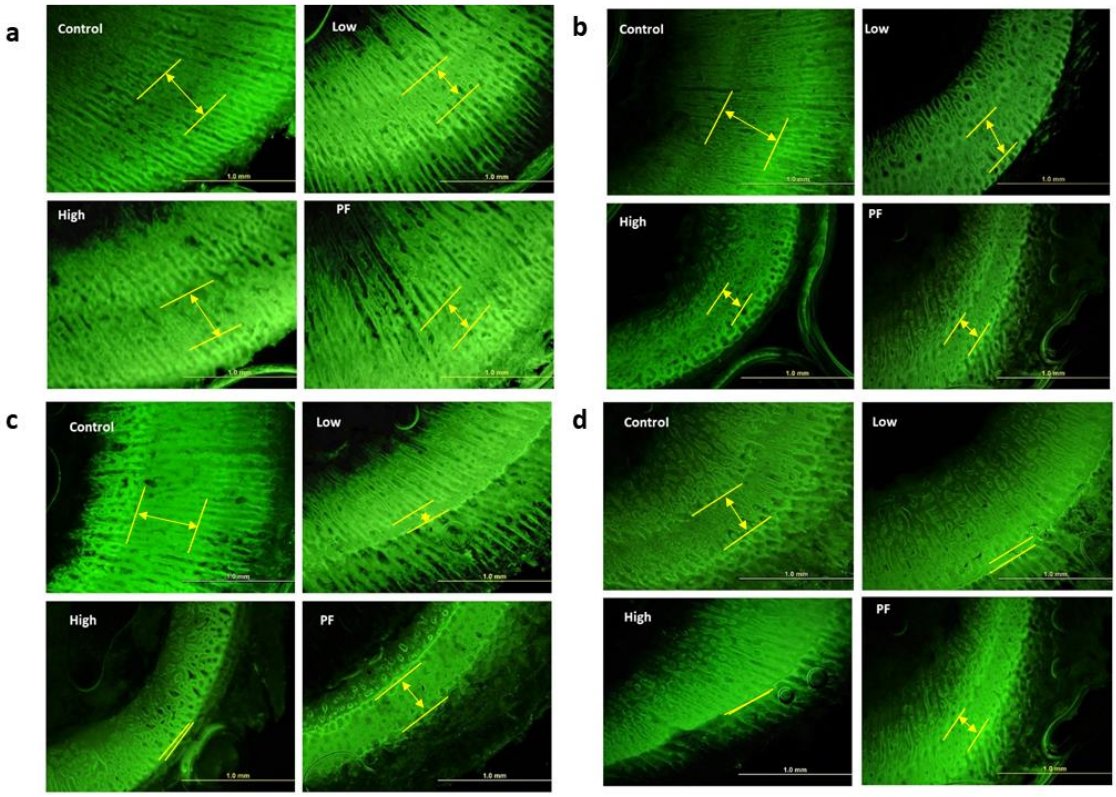

Figure 3.2: Fluorescence image of the femoral or tibial cross-section of broilers (measurement data shown as Table 4). Bone formation was visualized by double calcein labeling in the femoral bone and tibia bone, respectively. Representative picture **a**: femoral bone at 0-4 dpi; **b**: tibial bone at 0-4; **c**: femoral bone at 4-8 dpi; **d**: tibial bone at 4-8 dpi; Photos were taken at 4x objective. The yellow scale bar is 1 mm in length. The yellow lines marked the distance between two calcein injections.

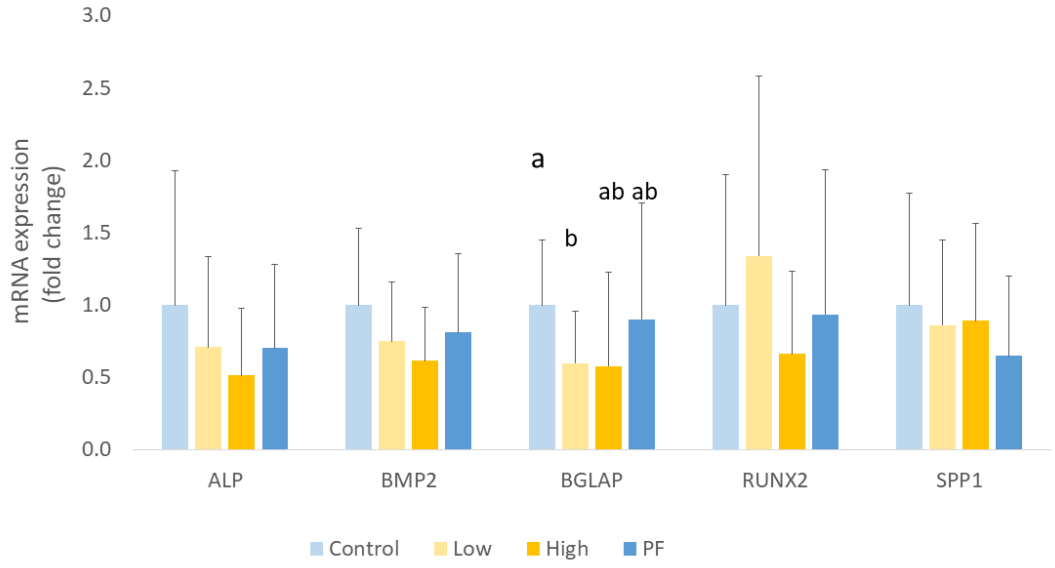

Figure 3.3: Osteogenesis-related gene expression in broilers bone marrow of different treatment groups. Control, non-challenge control group; Low, the low challenge dose of *Eimeria*; High, the high challenge dosage of *Eimeria*; PF, pair-feeding group that paired with High group.

[a, ab, b] Treatments with different letters means a significantly difference between treatments by using Tukey's HSD test, $P = 0.002$, N = 10.

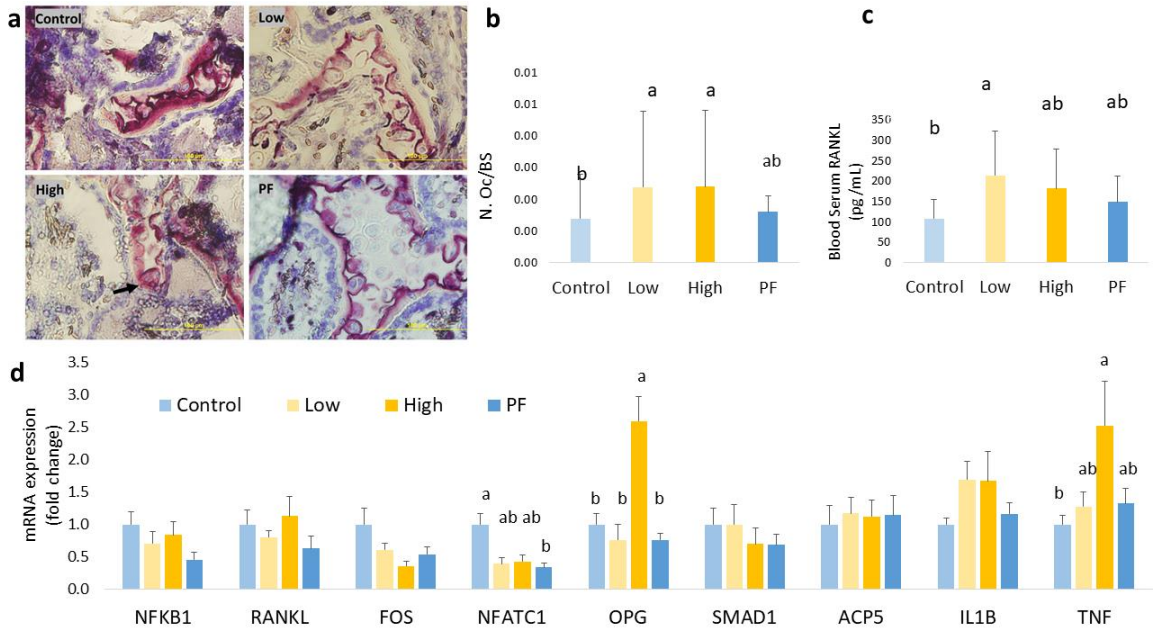

Figure 3.4. *Eimeria* infection increases osteoclast formation.

a: Illustration of TRAP staining at tibial metaphysis section. Osteoclasts were defined in this study as TRAP-positive cells with three or more nuclei. Osteoclast was indicated with arrow. Photos were taken at 10x objective. The yellow scale bar is 100 μm in length.

b: Number of osteoclasts (N. Oc) were counted and bone circumference (BS) were measured. The increased ratio of N. Oc/BS indicated an increased formation of osteoclast activity at metaphysis section in *Eimeria* infected groups ($P = 0.004$).

c: Serum level of RANKL in broilers at 6 dpi. The low group has higher level of RANKL than the Control group ($P = 0.047$).

d: Osteoclastogenesis-related gene expression in broilers bone marrow of different treatment groups.

[a, ab, b] Treatments with different letters means a significantly difference between treatments by using Tukey's HSD test, $P < 0.050$, N = 10. Control, non-challenge control group; Low, the low challenge dose of *Eimeria*; High, the high challenge dosage of *Eimeria*; PF, pair-feeding group that paired with High group.

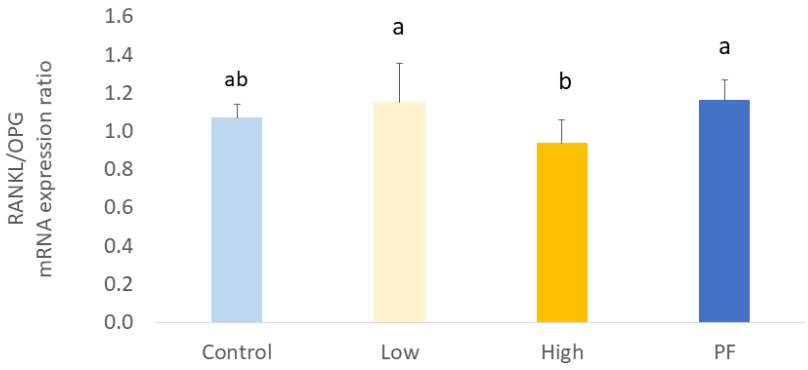

Figure 3.5: mRNA expression ratio of *RANKL*/*OPG* in bone marrow. Higher rate of *RANKL*/*OPG* indicated bone remodeling status.

[a, ab, b] Treatments with different letters means a significantly difference between treatments by using Tukey's HSD test, $P = 0.005$, N = 10. Control, non-challenge control group; Low, the low challenge dose of *Eimeria*; High, the high challenge dosage of Eimeria; PF, pair-feeding group that paired with High group.

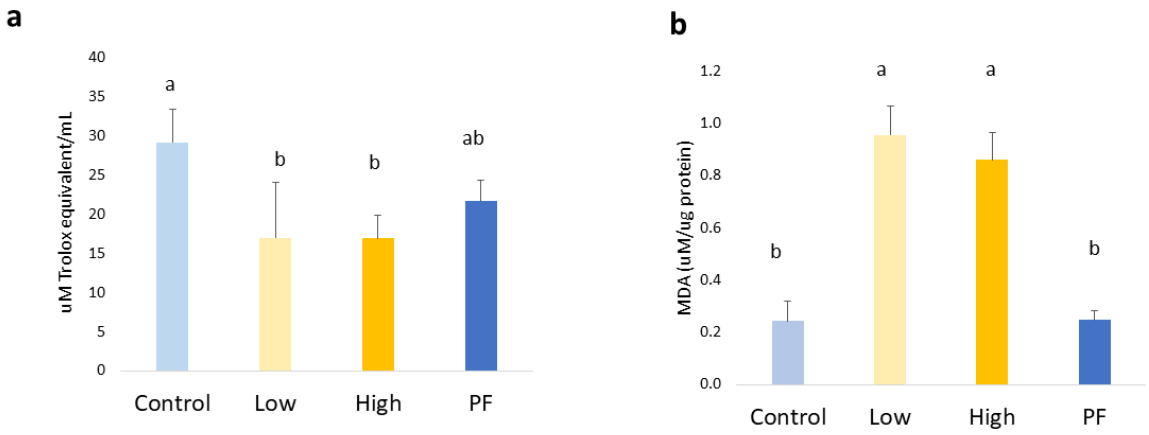

Figure 3.6: Oxidative status at 6 dpi. **a:** serum total antioxidant capacity was measured by antioxidant assay kit, that coccidial infection significantly decreased the antioxidant capacity ($P = 0.001$). **b**: liver lipid peroxidation was measured by TBAR assay kit, that coccidial infection significantly elevated lipid peroxidation in liver ($P < 0.001$). Control, non-challenge control group; Low, the low challenge dose of Eimeria; High, the high challenge dosage of Eimeria; PF, pair-feeding group that paired with High group. [a, ab, b] Treatments with different letters means a significantly difference between treatments by using Tukey's HSD test, $P < 0.05$, N = 10.

CHAPTER 4

HYDROGEN PEROXIDE-INDUCED OXIDATIVE STRESS INHIBIT OSTEOGENESIS AND MINERALIZATION IN BROILER CHICKEN COMPACT BONES DERIVED MESENCHYMAL STEM CELLS [3]

[3] Y. H. Tompkins, G. Liu, W. K. Kim. Submitted to *International Journal of Molecular Sciences*

Abstract

To understand the interaction between oxidative stress and bone metabolism, an *in vitro* model with induced oxidative stress was used. Chicken primary mesenchymal stem cells (MSCs) were continuously exposed to hydrogen peroxide (H_2O_2) to induce oxidative stress for 14 days of differentiation. Our analysis revealed that reactive oxygen species (ROS)-induced adipogenesis/osteogenesis lineage imbalance, and H_2O_2-induced oxidative stress negatively regulated osteogenic differentiation by modulating mRNA expression levels of osteogenesis-related genes, collagen type I, bone morphogenic protein 2, and osteocalcin. Furthermore, *in vitro* mineralization was decreased. In contrast, long-term H_2O_2 exposure promoted adipogenic differentiation. H_2O_2 treatment increased intracellular ROS production and altered antioxidant enzyme gene expression, and the long-term oxidative stress upregulated pro-apoptotic *CASP8* gene expression. These results indicate that long-term oxidative stress impaired chicken MSCs osteogenic differentiation but promoted adipogenic differentiation.

Keywords: broiler bone health, oxidative stress, chicken MSCs, cellular ROS, *in vitro*

Introduction

Modern commercial poultry production is strictly operated based on balanced nutrition and optimized environmental conditions. However, oxidative stress is ubiquitous in broiler production systems. For example, anti-nutritional factors, such as feed toxins or antioxidant deficiency, pathogens infection, and poor environmental conditions including heat stress, ammonia exposure, and flock density, can induce oxidative stress in broilers (Puppel, et al., 2015; Mishra and Jha, 2019; Ali Hassan and Li, 2021; Chauhan, et al., 2021; Pintus and Ros-Santaella, 2021). Oxidative stress has been reported as a negative factor on broiler performance, healthy growth, and production quality (Celi and Chauhan, 2013; K. Panda and Cherian, 2014; Estevez, 2015; Mishra and Jha, 2019; Surai, et al., 2019), representing an unbalanced condition between the production of reactive oxygen species (ROS) and the antioxidant defense systems (Sies, et al., 2017). In broiler production, other than the management-associated physiological oxidative stress, infectious agents are other key factors that cause robustly phagocytic ROS generation, which leads to severe oxidative stress in broilers (Zorov, et al., 2014; Forrester, et al., 2018).

There is an ongoing interest in using mesenchymal stem cells (MSCs) as a study model to understand cell physiology and disease etiology (Svoradova, et al., 2021), and the effect of oxidative stress on mammal MSCs has been well noted (Denu and Hematti, 2016). The classic ROS family members, such as superoxide anion, hydrogen peroxide (H_2O_2), and singlet oxygen, have been extensively studied for health effects linked to its presence (Sharma, et al., 2012). H_2O_2 is a non-radical ROS, a most common endogenous

byproduct of mitochondrial respiration that is present in avian systems (Ojano-Dirain, et al., 2007). Cellular H_2O_2 exposure has been widely used for assessing susceptibility to oxidative stress in *in vitro* models (Bai, et al., 2004; Liu, et al., 2004). At a cellular level, ROS level is tightly regulated by the antioxidant defense system and is critical for MSCs multipotency (Atashi, et al., 2015). There are evidences showing that a low basal level of ROS is a critical mediator in pathophysiological responses (Maraldi, et al., 2015), whereas differentiated MSCs presented a higher intracellular ROS production which is essential for cell survival and early differentiation (Kim, et al., 2010; Hu, et al., 2018). H_2O_2 is also an effective apoptosis inducer, the high concentration of H_2O_2 commonly induced apoptosis or cellular senescence in cell lines (Lin, et al., 2016a). However, the corresponding dose ranges for the apoptosis responses differs by cell types, due to the different cellular antioxidant activities and contents (Ko, et al., 2012; Xiang, et al., 2016). The uncontrollable high level of ROS not only impair the cell membrane fluidity and permeability but is also responsible for oxidation damage of DNA, RNA, protein, and lipid damage in mitochondria, which results in cellular senescence including cell dysfunction, cellular injury and cell apoptosis (Denu and Hematti, 2016). Given that a high level of ROS is cytotoxic, cells develop antioxidant defenses to convert severe free radicals into non-toxic molecules (Sies, et al., 2017). For cellular homeostasis, endogenous scavengers are mainly divided into two categories, enzymatic proteins, including superoxide dismutases (SOD), glutathione peroxidase (GPx), and catalases (CAT), and non-enzymatic antioxidants, such as vitamins and trace minerals which are mainly derived from dietary sources (Hu, et al., 2018). All those antioxidant defenses

work together for controlling intracellular ROS-related stress by removing and converting excessive ROS (Estevez, 2015; Denu and Hematti, 2016).

A relatively high level of ROS can directly interact with critical signaling molecules in essential osteogenic pathways, which negatively impacts bone homeostasis (Atashi, et al., 2015). Thus, Oxidative stress induced by ROS over-production has been considered as a pathogenic factor involved in human skeletal disorders (Bai, et al., 2004; Liu, et al., 2004; Sharma, et al., 2015). Moreover, in response to oxidative stress, ROS can activate extracellular signal-regulated kinases that modulate nuclear factor kappa light chain enhancer of activated B cells (NF-κB) and NF-E2 p45-related factor 2 (NRF2) signaling pathways, which are not only critical in regulating inflammation and cellular redox status, but also directly mediate bone homeostasis by regulating osteoblast or osteoclast differentiation and activity (Hyeon, et al., 2013; Sun, et al., 2015; Yuan, et al., 2017).

Oxidative stress is also a main consequence of stress and immune responses that act as a co-factor on performance and physiologic decline in broiler production (Mishra and Jha, 2019). In our previous study, an up-regulated oxidative stress, decreased antioxidant level, and poor bone integrity were detected in broilers that were challenged with *Eimeria spp*., which are the major parasites damage the intestine of the broilers (Tompkins, et al., 2022). However, the response of chickens MSCs to oxidative stress is not well-understood, and how ROS affects avian osteoblastic differentiation is unknown. Understanding of ROS's impact on MSC terminal fate and differentiation capacity is important to develop novel strategies for preventing, anticipating or reverting oxidative

stress-induced leg problems in chicken production. Therefore, in the current study, H_2O_2 was used as a stimulator of oxidative stress in MSC culture. This study aimed to investigate the effects of H_2O_2 on osteogenic differentiation of chicken MSCs isolated from broiler compact bones.

Material and Method

Ethics Statement

The study was carried out in compliance with the ARRIVE guidelines. All experiments protocols and animal use were approved by the Institutional Animal Care and Use Committee at the University of Georgia, Athens, GA.

Isolation of broiler MSCs

MSCs were isolated according to previously described methods (Adhikari, et al., 2018). Briefly, legs from one-day old chicks were obtained after cervical dislocation. The leg tissue was soaked in alcohol within a minute and then dried with Kimwipes (Kimberly Clark, Irving, TX, USA). Muscle was removed, and long bones were harvested. The long bones were kept in high glucose Dulbecco's Modified Eagle's medium (DMEM; contains 4.5 g/L glucose, 25 mM HEPES, sodium pyruvate, and without L-glutamine; 15-018-cv, Corning, Corning, NY, USA) until muscle and cartilage tissues were completely removed using a scalpel and scissors in a bio-safety cabinet (NuAire, Plymouth, MN, USA). The bones were placed in washing buffer to cut off the metaphysis. Only tibia diaphysis and femur diaphysis were kept for cell isolation. Washing buffer contained 2% fetal bovine serum (FBS) (Hyclone Laboratories Inc., Logan, UT) in Dulbecco's phosphate-buffer saline (PBS) (Corning). The bones were

cracked with a scalpel, bone marrow was flushed out with washing buffer, and bone marrow was discarded. The bones were chopped into small fragments and then suspended in a 50 mL tube containing 10 mL digestion medium made of 100 IU/mL penicillin, 100 ug/mL streptomycin, 0.25% collagenase (Sigma-Aldrich, St. Louis, MO, USA), 20% FBS, and high glucose DMEM. The tubes were placed in a 37°C incubated orbital shaker at 180 rpm for 60 min (VWR, Radnor, PA, USA). The digested bone solution was filtered with a 40 μm cell strainer (Thermo Fisher Scientific, Waltham, MA, USA) set over a 50 mL tube to remove the bone fragments, and then the filtered medium was centrifuged at 1,200 rpm for 10 min. The supernatant was discarded, the cell pellet was resuspended with 20 mL growth medium which contained DMEM with 10% FBS, 100 U/mL penicillin, 100 μg/mL streptomycin, and 0.292 mg/mL L-glutamine (Thermo Fisher Scientific), and 10 mL resuspend cells were plated in a 100 mm cell culture dishes (Corning). Cells were incubated at 37°C in a humidified incubator (NuAire) containing 5% CO_2. Half of the medium was replaced by fresh growth medium after 24 h of culture, and then the culture medium was changed every two days. For cell passing, once the cells reached 80% confluency, the cells were washed twice with 5 mL pre-warmed PBS, dissociated with 1.5 mL 0.1% Trypsin-EDTA (Corning) for 2 min at 37°C, and subcultured with cell density of 25,000 cells/cm^2 in 100 mm cell culture dishes.

Proliferation and viability of cultured chicken MSCs with H_2O_2 exposure

The viability of cells was determined using cellular 3-(4,5-dimethylthiazol-2-yl)-2,5-diphenyltetrazolium bromide (MTT) kits (Cayman Chemical, Ann Arbor, MI, USA). The treatment of MSCs with various concentrations of H_2O_2 (50, 100, 200, 400, and 800

nM; H_2O_2, 30% (w/w) solution, Sigma-Aldrich) during culture were also examined. MSCs cultured without H_2O_2 but PBS was used as the control. Experiments were carried out in 96-well culture plates. After the cells were incubated with different levels of H_2O_2 treatments for 6, 24, and 48 h, DMEM with 10% MTT was added and incubated for 4 h, and then the culture medium was completely discarded. The formed formazan was dissolved with 100 µL dimethyl sulfoxide (DMSO; Sigma-Aldrich) to develop a purple color, and the plates were then placed on an orbital shaker (VWR) with low speed for 5 min. The absorbance was measured at 570 nm using a microplate reader (BioTek, Winooski, VT, USA).

Osteogenic differentiation

MSC cells were expanded to passage 4 for osteogenic differentiation study. After selecting the proper concentration for H_2O_2 treatment based on the MTT assay, the cells were seeded at a density of 8×10^4 cells per well in 24-well cell culture plates (Corning), and cultured in growth medium at 37°C in the cell culture incubator (NuAire) until 100 % confluency. Then the cells were treated with osteogenic differentiation medium containing high glucose DMEM with 10^{-7} M dexamethasone (Sigma-Aldrich), 10mM β-glycerophosphate (Sigma-Aldrich), 50 µg/mL ascorbate (Sigma-Aldrich), 5% FBS, and 100 U/mL penicillin, 100 µg/mL streptomycin, and 0.292 mg/mL L-glutamine (Thermo Fisher Scientific) for osteogenic differentiation. Cells that were cultured in growth medium were used as the negative control. Culture medium was replaced with fresh pre-warmed differentiation medium daily. The cells were differentiation for 6 h, 24 h, 48 h, 72 h, 96 h, 5 days, 6 days, 10 days and 14 days.

Intracellular reactive oxygen species (ROS) detection

The intracellular ROS levels were examined using DCFDA/H_2DCFDA cellular ROS assay kits (Abcam Cambridge, MA, USA) as described by the manufacturer. In brief, 3×10^3 cells were seeded in a black clear-flat-bottom 96-well microplate and allowed to adhere overnight. After the corresponding treatments, medium was removed, 100 µL/well of 1× washing buffer was added to wash off the residual, and then 100 µL/well of the diluted DCFDA solution was added to stain for 45 min at 37°C in the culture incubator. After removing DCFDA solution, the cells were rinsed with washing buffer for once, then 100 µL/well washing buffer was added for microplate measurement. The fluorescence density was measured at an excitation wavelength of 485 nm and an emission wavelength of 535 nm by using a microplate reader (Spectramax M5, Molecular Devices, San Jose, CA). Images were acquired in 10× magnification using a fluorescence microscope (Keyence bz-X8000, Keyence Corp., Osaka, Japan).

Alizarin red S staining and mineral deposit quantification

The degree of mineralization of chicken MSCs was determined in a 24-well plate using Alizarin red S staining (Adhikari, et al., 2018). In brief, cells were exposed to H_2O_2 in osteogenic differentiation medium for 6, 10, and 14 days. Cells were fixed with 10% neutral buffered formalin for 1 h and then stained with 0.2% Alizarin red S (Sigma-Aldrich, St. Louis, MO) in distilled water for 45 min at room temperature. After rinsing with distilled water, images of cell culture plates were captured in 2× magnification using a microscope with a camera (Keyence bz-x8000, Keyence). The mineralized nodules were labeled as dark red spots. In order to quantify the mineral deposition, the stained

cells were solubilized with 200 µL of 10% acetic acid per well and incubated for 30 min with low-speed shaking on an orbital shaker (VWR). After the monolayer was loosely attached, the cells were gently scraped from the plate and transferred to a 1.5 mL microcentrifuge tube. The microcentrifuge tubes containing the cells were then vortexed vigorously for 40 s and heated to 85°C for 10 min. The tubes were transferred on ice to cool down for 5 min and then centrifuged at 20,000 g for 15 min. After that, 150 µL of the supernatant was aliquot to a new 1.5 mL microcentrifuge tube, and the pH was neutralized with 60 µL 10% ammonium hydroxide. After supernatant neutralization, 50 µL of each sample was loaded into an opaque-walled transparent bottom 96-well plate and read at OD 405 nm using a microplate reader (BioTek) for Alizarin red S staining quantification (Serguienko, et al., 2018).

Von Kossa staining

The degree of mineralization of chicken MSCs was determined in a 24-well plate using the von Kossa staining (Chijimatsu, et al., 2017; Adhikari, et al., 2018). Cells were exposed to H_2O_2 in osteogenic medium and stained after 6, 10, and 14 days of osteogenic differentiation. Briefly, cell culture plates were washed three times with PBS and then fixed with 0.1% glutaraldehyde (G5882, Sigma-Aldrich) in PBS (pH 7.0) for 15 min at room temperature. After discarding the fixation buffer, the cells were washed three times with distilled water and then incubated in 5% silver nitrate (Sigma-Aldrich) for 30 min. After the silver nitrate solution was discarded, the cells were washed with distilled water at least three times, air-dried, and exposed to bright light until black color has developed in the areas of calcification. Images of cell culture plates were captured in 2×

magnification using a microscope with a camera (Keyence bz-x8000, Keyence). Mineralized nodules were observed as dark brown to black spots. The stained plates were quantified with the area fractions using the ImageJ program (National Institutes of Health, Bethesda, MD, USA). Three images from each well were analyzed, and the area fraction mean from each well was used for statistical analysis.

RNA isolation, cDNA synthesis, and real-time polymerase chain reaction (qRT-PCR) analysis

Cellular total RNA was extracted using Qiazol reagents (Qiagen, Germantown, MD, USA) according to the manufacturer's instructions. Nano-Drop 1000 Spectrophotometer (ThermoFisher Scientific) was used to determine the quantity of extracted RNA. The cDNA was synthesized from 2000 ng of total RNA using high-capacity cDNA reverse transcription kits (Thermo Fisher Scientific). Quantitative real-time reverse transcription polymerase chain reaction (qRT-PCR) was used to measure mRNA expression. Primers were designed using the Primer-BLAST program (https://www.ncbi.nlm.nih.gov/tools/primer-blast/). The specificity of primers was validated by PCR product sequencing, details of primer sequences used for the experiment are presented in Table 4.1. Primer quality was verified through melting curve analysis and gel electrophoresis in this study. The qRT-PCR was performed on an Applied Biosystems StepOnePlus™ (Thermo Fisher Scientific) with iTaq™ Universal SYBR Green Supermix (BioRad, Hercules, CA, USA) using the following conditions for all genes: 95°C for 10 min followed 40 cycles at 95°C for 15 s, annealing temperature (Table 4.1) for 20 s, and extending at 72°C for 1 min.

The geometric means of hydroxymethylbilane synthase (*HMBS*), 18S ribosomal RNA (*18S rRNA*), and actin beta (*ACTB*) were used as housekeeping genes for normalization. The stability of the housekeeping genes was confirmed by their consistent Ct values among the treatments ($p > 0.1$) and also assessed by statistical algorithms by software program NormFinder (Version 0.953; https://moma.dk/normfinder-software) (Andersen, et al., 2004; Wan, et al., 2011). Peroxisome proliferator-activated receptor gamma (*PPARG*), adipose tissue fatty acid binding protein 4 (*FABP4*), and CCAAT enhancer binding protein alpha (*CEBPA*) were used as early markers of adipogenic differentiation, and alkaline phosphatase-biomineralization associated (*ALPL*), bone gamma-carboxyglutamate protein (*BGLAP*), runt-related transcription factor 2 (*RUNX2*), secreted phosphoprotein 1 (*SPP1*), collagen type I alpha 2 chain (*COL1A2*), bone–specific alkaline phosphatase (*ALP*), and bone morphogenetic protein 2 (*BMP2*) were used as osteogenic marker genes in the bone marrow. Nuclear factor kappa B subunit 1 (*NFKB1*) and antioxidant enzyme protein coding genes including catalase (*CAT*), superoxide dismutase type 1 (*SOD1*), superoxide dismutase type 2 (*SOD2*), glutathione peroxidase 1 (*GPX1*), glutathione S-transferase alpha 2 (*GSTA2*), and nitric oxide synthase 2 (*NOS2*) were used to determine the antioxidant enzyme activity and oxidative stress status. Pro-apoptotic marker genes, such as Caspase 3 (*CASP3*), Caspase 8 (*CASP8*), and Caspase 6 (*CASP6*), were used to assess the cell apoptosis. Samples were run in triplicate, and relative gene expression data were analyzed using the $2^{-\Delta\Delta Ct}$ (Livak and Schmittgen, 2001). The mean ΔCt of each marker gene from the control group was used to calculate the ΔΔCt value, and $2^{-\Delta\Delta Ct}$ expression mean of control group were

normalized to 1, and expression levels of the other treatment groups were presented as fold changes relative to the control group.

Statistical analysis

All experimental data were expressed as means with standard errors of the means (SEM). Data were tested for homogeneity of variances and normality of studentized residuals. The differences between the treatment groups were analyzed by one-way ANOVA, and the means were analyzed statistically by Tukey's test using JMP Pro14 (SAS Institute, Cary, NC, USA). Statistical significance was set as $p \leq 0.05$, and $0.05 \leq p \leq 0.1$ was also presented to show the trend toward statistical significance (Thiese, et al., 2016; Serdar, et al., 2021).

Results

Cell viability, cell apoptosis, and intracellular ROS production with exogenous H_2O_2 exposure

Cell viability was measured by MTT assay after H_2O_2 exposure (Figure 4.1). H_2O_2 treatment decreased the viability of chicken MSCs in a dose-dependent manner. Chicken MSCs culture with different concentrations (50 to 800 nM) of H_2O_2 in osteogenic differentiation medium for 6 h showed a non-cytotoxic effect ($p > 0.05$; Figure 4.1A). At 24 h of treatment, 800 nM of H_2O_2 significantly reduced the cell viability ($p < 0.05$; Figure 4.1B) by approximately 70% compared with the untreated control. After 48 h, 800 nM of H_2O_2 reduced the cell by approximately 90% compared with the untreated control ($p < 0.05$; Figure 4.1 C). No statistically significant change in cell viability was observed on treatment concentrations lower than 800 nM. Thus, the

final treatment concentrations at 100, 200, and 400 nM of H_2O_2 were selected as the treatment doses for the following experiments.

Intracellular ROS production after H_2O_2 exposure were monitored by cellular DCFDA assay (Figure 4.2). A surge of intracellular ROS production was detected in 100, 200, and 400 nM H_2O_2-treated chicken MSCs after 6 h ($p < 0.05$; Figure 4.2B), where 100 nM of H_2O_2 showed the highest up-regulated ROS response compared with the other groups ($p < 0.05$; Figure 4.2B). After 12 h of H_2O_2 exposure, 100 nM of H_2O_2 induced a greater fluorescent signal than 400 nM H_2O_2 ($p < 0.05$; Figure 4.2B). However, the intracellular ROS signal was not significantly changed by H_2O_2 treatment after 24 and 48 h of H_2O_2 exposure. Based on the current data, the effective treatment duration is 12 h after exogenous H_2O_2 exposure. The H_2O_2 treatment medium was set to be changed every 24 h to ensure the persistent stress effect on the cellular level by H_2O_2 treatment. With such a low concentration of H_2O_2 treatment, mRNA expression of pro-apoptotic markers, including *CASP-3*, *CASP-6* and *CASP-8*, have remained unchanged in chicken MSCs during the early differentiation stage (6 h to day 5) ($p > 0.05$; Figure 4.3), indicating that the effect of H_2O_2 on osteogenic differentiation of MSCs was not attributed to a cytotoxic effect which causes cell apoptosis at the early differentiation stage. However, 200 nM H_2O_2 significantly increased mRNA expression of *CASP-8* compared to the control on day 6 ($p < 0.05$; Figure 4.3), and 400 nM H_2O_2 numerically increased expression of *CASP-8* ($p < 0.05$; Figure 4.3), but neither of the higher treatment doses changed the expression of *CASP-3* or *CASP*-6 on day 6.

Effect of H_2O_2 on osteogenesis in chicken MSCs

Chicken MSCs were treated with various concentrations of H_2O_2 in osteogenic differentiation medium for 14 days, and then the cells showed a dose-depended manner on their differentiation (Figure 4.4). In the beginning of differentiation, there was a significant down-regulation of *SPP1* ($p < 0.05$), and numerically decreased mRNA expression of *BMP2* ($p = 0.053$) was observed after 6 h of H_2O_2 treatment. In the following days, there were no changes in mRNA expression of osteogenesis marker genes (*BGLAP*, *SPP1*, *BMP2*, *Col1A2, ALP RUNX2*; $p > 0.05$) at 24, 48 or 72 h. After 96 h of treatment, the cells exposure to 400 nM H_2O_2 showed a significantly higher mRNA expression of *ALP* ($p < 0.05$), *BGLAP* ($p < 0.05$) and *SPP1* ($p < 0.05$), and 400 nM H_2O_2 tended to increase the expression of *BMP2* ($p = 0.0917$) and *Col1A2* ($p = 0.060$) but did not affect the expression of *RUNX2* ($p > 0.05$). After 5 days of H_2O_2 exposure, the mRNA expression of *BGLAP* ($p < 0.05$), *ALP* ($p < 0.05$) and *Col1A2* ($p < 0.05$) was suppressed by 200 nM H_2O_2 compared with the control. In contrast, the mRNA expression of *BGLAP* was upregulated by 400 nM H_2O_2 ($p < 0.05$), and the expression of *ALP* was numerically increased. After 6 days of daily treatment, mRNA expression of *ALP* ($p < 0.05$), *BGLAP* ($p < 0.05$) and *Col1A2* ($p < 0.05$) was reduced by H_2O_2 treatments, and *SPP1* showed a decreasing trend ($p = 0.066$). Due to unstable housekeeping genes expression on day 10 and day 14, the mRNA expression results were not included over those time points.

In parallel with the mRNA expression mentioned above, the inhibition of osteogenic differentiation was characterized by a reduction in mineral accumulation in a

dose-dependent manner on 6 days (Figure 4.5A), 10 days (Figure 4.5B) and 14 days (Figure 4.5C) of differentiation. The effects of H_2O_2 on the mineralization were visualized using Alizarin red staining (Figure 4.5). OD value density result showed a significant decrease in mineral deposition with higher H_2O_2 treatment concentrations, where 400 nM of H_2O_2 significantly reduced the OD value by 30 % compared to the control after 6 days of H_2O_2 exposure ($p < 0.05$; Figure 4.5A). There were no statistically significant changes after 10 and 14 days of differentiation, but smaller mineralized crystals were observed with a higher dose of H_2O_2 treatment, and 400 nM of H_2O_2 led a decrease in mineralization by 20 and 40% ($p > 0.05$; Figure 4.5B-C).

The extracellular calcium (black crystals) content was quantified by von Kossa staining (Figure 4.6). After 6 days of differentiation, there were smaller and less extensive crystals and less mineralized matrix with the higher doses of H_2O_2 treatment. The colorimetric analysis showed a significant decrease of OD density with 400 nM H_2O_2 treatment ($p < 0.05$; Figure 4.6A). After 10 days of H_2O_2 treatment, a lower number of mineralized nodules and smaller size of crystals were observed with higher concentrations of H_2O_2 treatment; the optical density showed a dose-dependent manner that 200 and 400 nM H_2O_2 led to a significant decrease in mineralization, and the least mineral deposition was observed in 400 nM H_2O_2 group (OD value; $p < 0.05$; Figure 4.6B). After 14 day of differentiation, 400 nM H_2O_2 significantly suppressed mineralization compared with the other groups (OD value; $p < 0.05$; Figure 4.6C).

Effect of H_2O_2 on adipogenesis in chicken MSCs

During differentiation, the expression of *PPARG* showed different patterns at different stages of differentiation. Decreases of *PPARG* expression with the higher H_2O_2 treatment doses were observed at 6 h ($p < 0.05$; Figure 4.7). Afterward, H_2O_2 reduced the expression of *PPARG* ($p = 0.053$; Figure 4.7), *CEBPA* ($p < 0.05$) and *FABP4* ($p < 0.05$) after 24 h of differentiation. In contrast, with prolonged treatment periods, 400 nM H_2O_2 significantly elevated the expression of *PPARG* ($p < 0.05$) and *FABP4* ($p < 0.05$) after 96 h of treatment. A similar expression pattern was observed after 5 days of H_2O_2 treatment, where 400 nM H_2O_2 significantly increased the expression of *PPARG* ($p < 0.05$), *CEBPA* ($p < 0.05$) and *FABP4* ($p < 0.05$) compared with the control. After 6 days of H_2O_2 treatment, 200 and 400 nM H_2O_2 treatments increased the expression of *PPARG* ($p < 0.05$; Figure 4.7), and 400 nM H_2O_2 treatment drastically increased the expression of *FABP4* ($p < 0.05$; Figure 4.7). However, 100 nM H_2O_2 reduced expression of *CEBPA* ($p < 0.05$; Figure 4.7) compared with the control.

Altered gene expression of antioxidant enzyme in response to extracellular H_2O_2 exposure

There was no significant change of expression in antioxidant enzyme mRNA after 6 h of differentiation, except for expression of *NOS2* which showed a trend of decreasing with higher H_2O_2 treatment doses ($p = 0.087$; Figure 4.8). At 24 h of treatment, the mRNA expression of *SOD1* was decreased by the highest concentration of H_2O_2 (400 nM) ($p < 0.05$; Figure 4.8). At 48 h of treatment, 100 nM H_2O_2 augmented the expression of *CAT* compared with the control. After 5 days of treatment and differentiation, 400 nM

H_2O_2 upregulated the mRNA expression of *GPX1* compared with the control ($p < 0.05$). 200 nM H_2O_2 significantly increased mRNA expression of *CAT* compared with 400 nM H_2O_2 treatment group ($p < 0.05$). After 6 days of H_2O_2 treatment, 400 nM H_2O_2 significantly upregulated mRNA expression of *SOD2* compared with 100 nM H_2O_2 group ($p < 0.05$). There was a trend of increasing in the expression of *NRF2* with 200 and 400 nM H_2O_2 treatments ($p = 0.077$).

Discussion

Cell fate with the presence of oxidative stress can vary depending on the cell types, treatment intensity, duration, dosage, and the cell differentiation status (Ryu, et al., 2015; Denu and Hematti, 2016). Moreover, several studies have pointed out that undifferentiated stem cells have superior antioxidant defense than differentiated cells; For example, the undifferentiated MSCs are known to have relatively low levels of intracellular ROS and high levels of glutathione in the human cell line (Valle-Prieto and Conget, 2010). Studies have shown that mouse embryonic stem cells exhibit high antioxidant activity and stress-resistance, but several antioxidant and cellular resistance genes were downregulated during differentiation (Saretzki, et al., 2004). Under normal circumstances during mineralization, MSCs differentiate and their expression of mineralization factors increases (Blair, et al., 2017). The size of mineral crystals increases during bone mineralization, and the collagen fibers become more organized and condensed (Blair, et al., 2017). Studies on other cell types indicated that H_2O_2 solutions have a significant effect on collagen production (Nashchekina, et al., 2021), as previous studies reported the increased activities of oxidative stress was linked to decreased

collagen synthesis in fibroblasts (Siwik, et al., 2001), human cartilage (Altindag, et al., 2007), and chick embryo tissue culture (Ramp, et al., 1987). Moreover, the chicken embryo tissue culture also indicated that multiple exposures to H_2O_2 markedly inhibited collagen synthesis (Ramp, et al., 1987). In this report, the exogenous H_2O_2 (100 to 400 nM) suppressed the osteoblastic mineralization of chicken compact bone-derived MSCs, manifested by reduced osteogenic differentiation gene markers and less mineral deposition. The decreased expression of *Col1A2* after 6 days of H_2O_2 treatment supported the hypothesis that H_2O_2-induced oxidative stress can directly interrupt type 1 collagen production. Moreover, the concentration of H_2O_2 in the present study is much lower than the H_2O_2 doses used in humans and mice stem cell studies (Halliwell, et al., 2000; Nouri, et al., 2019), demonstrating that chicken compact bone derived MSCs are relatively sensitive to oxidative stress compared with cell types in chicken (chicken cardiomyocytes: 0.2 mM H_2O_2 (Jiang, et al., 2005; Wan, et al., 2016); chicken cardiac cells, 0.2 to 2.0 mM H_2O_2 ; and chicken epithelial cells, 300 μM H_2O_2 (Lin, et al., 2016b)). Interestingly, a previous study indicated ROS production did not influence the aging process of avian fibroblast cells (Strecker, et al., 2010). Nevertheless, by comparing 78 free-living avian species' blood redox state markers, relatively long-lived bird species had high levels of antioxidants status (especially total antioxidant status and total glutathione) and low levels of ROS (Xia and Møller, 2018). With the rapid growth and relatively short lifespan of broilers, it can be assumed that oxidative stress in broiler production may occur in a great extent. Because chicken MSCs-differentiated osteoblasts

are particularly susceptible to oxidative stress, the negative impact of oxidative stress on bone homeostasis can be a key factor in skeleton abnormality.

MSCs can differentiate into different cell phenotype types, which are controlled by several transcription factors, including *PPARG*, *RUNX2* and *SOX9*, which regulate adipogenesis, osteogenesis and chondrogenesis, respectively (Bi, et al., 1999; Rosen, et al., 2002; Robert, et al., 2020). In particular, adipogenesis and osteogenesis showed a reciprocal relationship (Takada, et al., 2007; Robert, et al., 2020); In human and mouse primary MSCs *PPARG2* insufficiency resulted in increased osteogenesis of osteoblast (Akune, et al., 2004; Takada, et al., 2007), whereas depletion of *RUNX2* promoted adipogenesis (Enomoto, et al., 2004). Meanwhile, ROS level in MSCs plays an essential role in manipulating the differentiation potential (Ho, et al., 2013; Denu and Hematti, 2016). It was reported that mRNA expression of antioxidant enzymes such as *SOD, CAT*, and *GPX* was upregulated during adipogenesis in human MSCs (Higuchi, et al., 2013; Ho, et al., 2013). The present study showed that prolonged exposure to H_2O_2 increased cellular oxidative stress status and increased the expression of adipogenic differentiation marker at the later differentiation stage was coupled with decreased mineralization. This result is parallel with previous studies reporting that H_2O_2 exposure altered the differentiation potential in human and mouse MSCs or cell line (Ho, et al., 2013; Lin, et al., 2018). Besides, by analyzing genome-wide gene expression profiling, Menssen and et al. (Menssen, et al., 2011) reported an upregulated *CASP8* level during adipogenic differentiation in human bone marrow-derived MSCs. Therefore, the spiked expression of *CASP8* on day 6 might have been resulted from adipogenic differentiation of chicken

MSCs, instead of apoptosis directly caused by H_2O_2-induced oxidative stress. Moreover, the effect of H_2O_2 treatment on regulating cell differentiation has been observed in different types of cells. The sub-lethal doses of oxidative stress induced morphological alteration (46, 48, 49). For example, prolonged H_2O_2 treatment activated NF-κB transcriptional activity while stimulating brown adipogenesis during myogenesis in mice satellite cells (Morozzi, et al., 2017). Therefore, at least in part, oxidative stress is a factor for the dysfunction of bone tissue, not only by causing cell death, but also by interrupting MSCs differentiation capacity and decreasing the osteogenic ability directly.

In the current study, several osteogenic differentiation markers were significantly upregulated with the highest H_2O_2 treatment dose after 4 and 5 days of treatment, and then drastically dropped after 6 days of treatment. We made several hypotheses to explain the up and down regulated expression patterns. Firstly, studies pointed out that the cellular effects of ROS may differ depending on the cell differentiation stage due to the difference between progenitor cells and mature cells (Khalid, et al., 2020). For example, during the initial differentiation process, MSCs commit to pre-osteoblasts while actively proliferating (Infante and Rodriguez, 2018). Over the later stage of differentiation, the pre-osteoblasts can further mature into non-proliferating osteoblasts that start matrix secretion, maturation, and mineralization (Infante and Rodriguez, 2018). Studies showed that H_2O_2 treatment could significantly enhance bone marrow MSCs proliferation and migration ability (Rosova, et al., 2008; Pendergrass, et al., 2013). Human and mouse studies revealed a low level of intracellular ROS and high levels of antioxidant in undifferentiated MSCs (Hu, et al., 2018). In contrast, differentiated MSCs show a higher

ROS grade and lower activity of antioxidative enzymes (Hu, et al., 2018). Therefore, it is important to distinguish the multifunctional roles of ROS in pre-osteoblast differentiation and osteoblast maturation. Secondly, we hypothesize that ROS over-production mediated the cell cycle and caused cell prematurity. ROS is a fundamental signal in many signaling metabolisms (Ray, et al., 2012; Shadel and Horvath, 2015). The low level of ROS allowed reversible oxidative modifications until the ROS production overwhelms its antioxidant capacity, which leads to severe cellular damage (Diebold and Chandel, 2016). Redox status plays a vital role in the cell cycle, and accumulated intracellular ROS can force MSCs to undergo cellular senescence, substantially interrupting stem cells differentiation (Ben-Porath and Weinberg, 2004; Bonab, et al., 2006; Brandl, et al., 2011; Ho, et al., 2013). The changed expression of *GPX*, *CAT* and *SOD2* indicated the altered oxidation-reduction status in the present study. Interestingly, *SOD2* is required for regulating mitochondrial stress and plays a vital role in osteoblastogenesis (Gao, et al., 2018). *SOD2* upregulation helped reduce mRNA over-expression of *PPARG and FABP-4* in diabetic mouse models (Sen, et al., 2015). As for the current study, the increased expression of *SOD2* indicated that cells were actively suppressing adipogenic differentiation under oxidative stress. Based on the aforementioned information, we speculated that long-term cultured cells with higher levels of exogenous H_2O_2 stimulated intracellular ROS production and promoted pre-osteoblast commitment at the early differentiation stage. However, the accumulated ROS level accelerated the cell prematurity and cell apoptosis, decreasing mineral accrual at the later stage. However, the

detailed molecular mechanisms of ROS on the avian cell cycle remains largely unexplored, and more evidences are needed.

Another hypothesis is the exogenous H_2O_2 stimulated regeneration response. It is well-established that H_2O_2 is a ROS signaling intermediate response to tissue injury (Sanchez-de-Diego, et al., 2019). The presence of ROS activates signaling that regulate osteogenic differentiation of stem cells, which mediates vital pathways' response, such as Wnt or TGF/BMP pathways, to be involved in fracture healing and tissue repairment (Gloire, et al., 2006; Gough and Cotter, 2011; Wang, et al., 2017; Sheppard, et al., 2022). MSCs has the ability to migrate to the sites in response to various stimuli, including cytokines or growth factors after tissue injury, and then MSCs can differentiate into tissue-specific cell types at those sites to repair the damaged region (Merimi, et al., 2021). ROS can regulate the activation of BMPs and RUNX2 pathways in MSCs during the repair process by mediating the activity of NF-κB signaling (Ding, et al., 2009; Mandal, et al., 2011). Therefore, in the present study, the increased expression of bone formation marks *ALP*, *SPP1* and *BGLAP* after 5 days of differentiation possibly implied that the high ROS level stimulated cell repair-response, which recruited MSCs to be differentiated into osteoblasts to maintain cell population and homeostasis. However, with the continuous oxidative stress, the MSCs committed apoptosis and ultimately reduced the mineralization.

Oxidative stress has been associated with many bone-related diseases in humans and mammals (Reis and Ramos, 2021). It has been reported that at least 30% of birds showed poor locomotion during the fast growth period of broilers (Knowles, et al., 2008;

Wideman, 2016; Kittelsen, et al., 2017; Zhang, et al., 2020), which interfered with chicken' accessibility to feed and water, predominantly reducing the growth and causing an economic loss in production. Generally, cultured cells have higher throughput and shorter turnaround times than *in vivo* study models (Dawson, et al., 2014). The response of avian stem cells to different stress stimuli has been widely used in the context of growth and physiology (Ali Hassan and Li, 2021; Xu, et al., 2022). Thus, understanding of oxidative stress in a cell model is essential for a better understanding of the bone pathogenic process in chickens. Tibial dyschondroplasia (TD) and bacterial osteomyelitis (BCO) are two of the most common skeletal abnormalities in the broiler industry and result in deformed bones and lameness (Hartcher and Lum, 2019). Previous studies indicated that BCO was initiated by mechanical micro-fracturing, then followed by bacterial colonization and bone degradation, eventually leading to necrosis (Wideman, 2016). Mitochondrial dysfunction and apoptosis are also involved in broiler BCO (Ferver, et al., 2021). Although there is no direct evidence to demonstrate the link between oxidative stress and BCO pathogenesis, in human studies, higher oxidative stress levels in response to local infection have been reported in chronic osteomyelitis patients (Jyoti, et al., 2015; Massaccesi, et al., 2022). The pathology of osteomyelitis is characterized by localized inflammation, bone mineral loss and structural damage, which share similarities with broiler BCO (Grbic, et al., 2014). Furthermore, the recent femoral necrosis pathogenicity study reported an abnormally increased lipid metabolism and decreased bone formation in the chicken femoral head necrosis disease model (Fan, et al., 2021). Therefore, by gathering all the evidence above, we proposed that oxidative stress could potentially be one of the

pathogenic co-factors involved in chicken bone necrosis. Moreover, tibial dyschondroplasia (TD) is another common bone abnormality in fast-growing broilers, which is characterized by tibial bone deformities with non-vascular and non-mineralized growth plates (Mehmood, et al., 2017; Zhang, et al., 2019). It is a chondrogenesis-related growth plate development disease highly associated with premature and apoptosis of cells (Mehmood, 2018). There is an established relationship between tibial dyschondroplasia and oxidative stress induced by thiram, which reduced liver antioxidation capability and damages liver function (Li, et al., 2007). Altered systemic antioxidant activity was reported in broilers with TD (Zhang, et al., 2018; Huang, et al., 2021). Although currently osteoblast function has not been illustrated in details in broiler TD model, osteoblasts are responsible for the type I collagen matrix formation surrounding the vasculature buds, and osteoblast and osteocyte have direct association with chondrocyte maturation and hypotrophy (Findlay and Atkins, 2014; Zhang, et al., 2020). Based on the information mentioned above, we hypothesize that TD may be partially associated with systemic oxidative stress. Studies reported that mycoplasma (M.) can produce H_2O_2 and superoxide radicals, which induce oxidative stress in the respiratory epithelium and can directly affect bone metabolism (Shimizu, 2016). Clinical signs of *M. synoviae* infection included joint lesions in avian species (Osorio, et al., 2007). These results provide evidence to explain the pathogenicity of mycoplasmas on bone integrity, supporting our current results that high level and long-term effect of H_2O_2 negatively regulated osteoblast cell activity.

Although many questions remain, ever-growing numbers of observations regarding chicken bone disorders and avian bone health rapidly shape our understanding

of various topics, such as metabolic regulation and the pathogenesis of bone disorders in broilers (Porto, et al., 2015). The knowledge of ROS generation and antioxidant defense systems has generated a great deal of interest due to its potential application in animal production but remains to be profoundly explored in chicken stem cell models.

Conclusion

The ROS concentration is in a dynamic equilibrium and is modulated by cellular processes that produce and eliminate ROS. Cellular effects of ROS may differ depending on the cell differentiation stages. Treatment with H_2O_2 altered cellular antioxidant enzyme gene expression, and long-term treatment of H_2O_2 inhibited the osteogenic biomineralization and decreased osteogenic differentiation markers expression in chicken MSCs. The impaired osteogenic differentiation potential is associated with a greater potential for adipogenesis in chicken MSCs with oxidative stress, highlighting that cellular oxidative stress caused by exogenous H_2O_2 accumulation modulate stem cell differentiation capacity.

References

Adhikari, R., C. Chen, E. Waters, F. D. West, and W. K. Kim. 2018. Isolation and Differentiation of Mesenchymal Stem Cells From Broiler Chicken Compact Bones. Front Physiol 9:1892.

Akune, T., S. Ohba, S. Kamekura, M. Yamaguchi, U. I. Chung, N. Kubota, Y. Terauchi, Y. Harada, Y. Azuma, K. Nakamura, T. Kadowaki, and H. Kawaguchi. 2004. PPARgamma insufficiency enhances osteogenesis through osteoblast formation from bone marrow progenitors. J Clin Invest 113:846-855.

Ali Hassan, N., and Z. Li. 2021. Oxidative stress in broiler chicken and its consequences on meat quality. International Journal of Life Science Research Archive 1:045-054.

Altindag, O., O. Erel, N. Aksoy, S. Selek, H. Celik, and M. Karaoglanoglu. 2007. Increased oxidative stress and its relation with collagen metabolism in knee osteoarthritis. Rheumatol Int 27:339-344.

Andersen, C. L., J. L. Jensen, and T. F. Orntoft. 2004. Normalization of real-time quantitative reverse transcription-PCR data: a model-based variance estimation approach to identify genes suited for normalization, applied to bladder and colon cancer data sets. Cancer Res 64:5245-5250.

Atashi, F., A. Modarressi, and M. S. Pepper. 2015. The role of reactive oxygen species in mesenchymal stem cell adipogenic and osteogenic differentiation: a review. Stem Cells Dev 24:1150-1163.

Bai, X. C., D. Lu, J. Bai, H. Zheng, Z. Y. Ke, X. M. Li, and S. Q. Luo. 2004. Oxidative stress inhibits osteoblastic differentiation of bone cells by ERK and NF-kappaB. Biochem Biophys Res Commun 314:197-207.

Ben-Porath, I., and R. A. Weinberg. 2004. When cells get stressed: an integrative view of cellular senescence. J Clin Invest 113:8-13.

Bi, W., J. M. Deng, Z. Zhang, R. R. Behringer, and B. de Crombrugghe. 1999. Sox9 is required for cartilage formation. Nat Genet 22:85-89.

Blair, H. C., Q. C. Larrouture, Y. Li, H. Lin, D. Beer-Stoltz, L. Liu, R. S. Tuan, L. J. Robinson, P. H. Schlesinger, and D. J. Nelson. 2017. Osteoblast Differentiation and Bone Matrix Formation In Vivo and In Vitro. Tissue Eng Part B Rev 23:268-280.

Bonab, M. M., K. Alimoghaddam, F. Talebian, S. H. Ghaffari, A. Ghavamzadeh, and B. Nikbin. 2006. Aging of mesenchymal stem cell in vitro. BMC Cell Biol 7:14.

Brandl, A., M. Meyer, V. Bechmann, M. Nerlich, and P. Angele. 2011. Oxidative stress induces senescence in human mesenchymal stem cells. Exp Cell Res 317:1541-1547.

Celi, P., and S. Chauhan. Year. Oxidative stress management in farm animals: opportunities and challenges. Proc. Proceedings of the 4th International Conference on Sustainable Animal Agriculture for Developing Countries (SAADC).

Chauhan, S. S., V. P. Rashamol, M. Bagath, V. Sejian, and F. R. Dunshea. 2021. Impacts of heat stress on immune responses and oxidative stress in farm animals and nutritional strategies for amelioration. Int J Biometeorol 65:1231-1244.

Chijimatsu, R., M. Ikeya, Y. Yasui, Y. Ikeda, K. Ebina, Y. Moriguchi, K. Shimomura, D. A. Hart, Y. Hideki, and N. Norimasa. 2017. Characterization of Mesenchymal Stem Cell-

Like Cells Derived From Human iPSCs via Neural Crest Development and Their Application for Osteochondral Repair. Stem Cells Int 2017:1960965.

Dawson, J. I., J. Kanczler, R. Tare, M. Kassem, and R. O. Oreffo. 2014. Concise review: bridging the gap: bone regeneration using skeletal stem cell-based strategies - where are we now? Stem Cells 32:35-44.

Denu, R. A., and P. Hematti. 2016. Effects of Oxidative Stress on Mesenchymal Stem Cell Biology. Oxid Med Cell Longev 2016:2989076.

Diebold, L., and N. S. Chandel. 2016. Mitochondrial ROS regulation of proliferating cells. Free Radic Biol Med 100:86-93.

Ding, J., O. Ghali, P. Lencel, O. Broux, C. Chauveau, J. C. Devedjian, P. Hardouin, and D. Magne. 2009. TNF-alpha and IL-1beta inhibit RUNX2 and collagen expression but increase alkaline phosphatase activity and mineralization in human mesenchymal stem cells. Life Sci 84:499-504.

Enomoto, H., T. Furuichi, A. Zanma, K. Yamana, C. Yoshida, S. Sumitani, H. Yamamoto, M. Enomoto-Iwamoto, M. Iwamoto, and T. Komori. 2004. Runx2 deficiency in chondrocytes causes adipogenic changes in vitro. J Cell Sci 117:417-425.

Estevez, M. 2015. Oxidative damage to poultry: from farm to fork. Poult Sci 94:1368-1378.

Fan, R., K. Liu, and Z. Zhou. 2021. Abnormal Lipid Profile in Fast-Growing Broilers With Spontaneous Femoral Head Necrosis. Front Physiol 12:685968.

Ferver, A., E. Greene, R. Wideman, and S. Dridi. 2021. Evidence of Mitochondrial Dysfunction in Bacterial Chondronecrosis With Osteomyelitis-Affected Broilers. Front Vet Sci 8:640901.

Findlay, D. M., and G. J. Atkins. 2014. Osteoblast-chondrocyte interactions in osteoarthritis. Curr Osteoporos Rep 12:127-134.

Forrester, S. J., D. S. Kikuchi, M. S. Hernandes, Q. Xu, and K. K. Griendling. 2018. Reactive Oxygen Species in Metabolic and Inflammatory Signaling. Circ Res 122:877-902.

Gao, J., Z. Feng, X. Wang, M. Zeng, J. Liu, S. Han, J. Xu, L. Chen, K. Cao, J. Long, Z. Li, W. Shen, and J. Liu. 2018. SIRT3/SOD2 maintains osteoblast differentiation and bone formation by regulating mitochondrial stress. Cell Death Differ 25:229-240.

Gloire, G., S. Legrand-Poels, and J. Piette. 2006. NF-kappaB activation by reactive oxygen species: fifteen years later. Biochem Pharmacol 72:1493-1505.

Gough, D. R., and T. G. Cotter. 2011. Hydrogen peroxide: a Jekyll and Hyde signalling molecule. Cell Death Dis 2:e213.

Grbic, R., D. J. Miric, B. Kisic, L. Popovic, V. Nestorovic, and A. Vasic. 2014. Sequential analysis of oxidative stress markers and vitamin C status in acute bacterial osteomyelitis. Mediators Inflamm 2014:975061.

Halliwell, B., M. V. Clement, and L. H. Long. 2000. Hydrogen peroxide in the human body. FEBS Letters 486:10-13.

Hartcher, K. M., and H. K. Lum. 2019. Genetic selection of broilers and welfare consequences: a review. World's Poultry Science Journal 76:154-167.

Higuchi, M., G. J. Dusting, H. Peshavariya, F. Jiang, S. T. Hsiao, E. C. Chan, and G. S. Liu. 2013. Differentiation of human adipose-derived stem cells into fat involves reactive oxygen species and Forkhead box O1 mediated upregulation of antioxidant enzymes. Stem Cells Dev 22:878-888.

Ho, P. J., M. L. Yen, B. C. Tang, C. T. Chen, and B. L. Yen. 2013. H2O2 accumulation mediates differentiation capacity alteration, but not proliferative decline, in senescent human fetal mesenchymal stem cells. Antioxid Redox Signal 18:1895-1905.

Hu, C., L. Zhao, C. Peng, and L. Li. 2018. Regulation of the mitochondrial reactive oxygen species: Strategies to control mesenchymal stem cell fates ex vivo and in vivo. J Cell Mol Med 22:5196-5207.

Huang, S. C., Q. Q. Cao, Y. B. Cao, Y. R. Yang, T. T. Xu, K. Yue, F. Liu, Z. X. Tong, and X. B. Wang. 2021. Morinda officinalis polysaccharides improve meat quality by reducing oxidative damage in chickens suffering from tibial dyschondroplasia. Food Chem 344:128688.

Hyeon, S., H. Lee, Y. Yang, and W. Jeong. 2013. Nrf2 deficiency induces oxidative stress and promotes RANKL-induced osteoclast differentiation. Free Radic Biol Med 65:789-799.

Infante, A., and C. I. Rodriguez. 2018. Osteogenesis and aging: lessons from mesenchymal stem cells. Stem Cell Res Ther 9:244.

Jiang, B., W. Xiao, Y. Shi, M. Liu, and X. Xiao. 2005. Heat shock pretreatment inhibited the release of Smac/DIABLO from mitochondria and apoptosis induced by hydrogen

peroxide in cardiomyocytes and C2C12 myogenic cells. Cell Stress Chaperones 10:252-262.

Jyoti, A., S. Singh, B. Mukhopadhyay, R. Gavel, and S. P. Mishra. 2015. Free radicals and antioxidant status in chronic osteomyelitis patients: a case control study. J Clin Diagn Res 9:BC08-10.

K. Panda, A., and G. Cherian. 2014. Role of Vitamin E in Counteracting Oxidative Stress in Poultry. The Journal of Poultry Science 51:109-117.

Khalid, S., H. Yamazaki, M. Socorro, D. Monier, E. Beniash, and D. Napierala. 2020. Reactive oxygen species (ROS) generation as an underlying mechanism of inorganic phosphate (Pi)-induced mineralization of osteogenic cells. Free Radic Biol Med 153:103-111.

Kim, K. S., H. W. Choi, H. E. Yoon, and I. Y. Kim. 2010. Reactive oxygen species generated by NADPH oxidase 2 and 4 are required for chondrogenic differentiation. J Biol Chem 285:40294-40302.

Kittelsen, K. E., B. David, R. O. Moe, H. D. Poulsen, J. F. Young, and E. G. Granquist. 2017. Associations among gait score, production data, abattoir registrations, and postmortem tibia measurements in broiler chickens. Poult Sci 96:1033-1040.

Knowles, T. G., S. C. Kestin, S. M. Haslam, S. N. Brown, L. E. Green, A. Butterworth, S. J. Pope, D. Pfeiffer, and C. J. Nicol. 2008. Leg disorders in broiler chickens: prevalence, risk factors and prevention. PLoS One 3:e1545.

Ko, E., K. Y. Lee, and D. S. Hwang. 2012. Human umbilical cord blood-derived mesenchymal stem cells undergo cellular senescence in response to oxidative stress. Stem Cells Dev 21:1877-1886.

Li, J., D. Bi, S. Pan, and Y. Zhang. 2007. Effect of diet with thiram on liver antioxidant capacity and tibial dyschondroplasia in broilers. Br Poult Sci 48:724-728.

Lin, C. H., N. T. Li, H. S. Cheng, and M. L. Yen. 2018. Oxidative stress induces imbalance of adipogenic/osteoblastic lineage commitment in mesenchymal stem cells through decreasing SIRT1 functions. J Cell Mol Med 22:786-796.

Lin, X., S. Jiang, Z. Jiang, C. Zheng, and Z. Gou. 2016a. Effects of equol on H2 O2-induced oxidative stress in primary chicken intestinal epithelial cells. Poultry Science 95:1380-1386.

Lin, X., S. Jiang, Z. Jiang, C. Zheng, and Z. Gou. 2016b. Effects of equol on H2O2-induced oxidative stress in primary chicken intestinal epithelial cells. Poult Sci 95:1380-1386.

Liu, A. L., Z. M. Zhang, B. F. Zhu, Z. H. Liao, and Z. Liu. 2004. Metallothionein protects bone marrow stromal cells against hydrogen peroxide-induced inhibition of osteoblastic differentiation. Cell Biol Int 28:905-911.

Livak, K. J., and T. D. Schmittgen. 2001. Analysis of relative gene expression data using real-time quantitative PCR and the 2(-Delta Delta C(T)) Method. Methods 25:402-408.

Mandal, C. C., S. Ganapathy, Y. Gorin, K. Mahadev, K. Block, H. E. Abboud, S. E. Harris, G. Ghosh-Choudhury, and N. Ghosh-Choudhury. 2011. Reactive oxygen species

derived from Nox4 mediate BMP2 gene transcription and osteoblast differentiation. Biochem J 433:393-402.

Maraldi, T., C. Angeloni, E. Giannoni, and C. Sell. 2015. Reactive Oxygen Species in Stem Cells. Oxid Med Cell Longev 2015:159080.

Massaccesi, L., E. Galliera, A. Pellegrini, G. Banfi, and M. M. Corsi Romanelli. 2022. Osteomyelitis, Oxidative Stress and Related Biomarkers. Antioxidants (Basel) 11.

Mehmood, K. 2018. Tetramethylpyrazine Mitigates Toxicity and Liver Oxidative Stress in Tibial Dyschondroplasia Chickens. Pakistan Veterinary Journal 38:76-80.

Mehmood, K., H. Zhang, M. K. Iqbal, M. U. Rehman, M. Shahzad, K. Li, S. Huang, F. Nabi, L. Zhang, and J. Li. 2017. In Vitro Effect of Apigenin and Danshen in Tibial Dyschondroplasia Through Inhibition of Heat-Shock Protein 90 and Vascular Endothelial Growth Factor Expressions in Avian Growth Plate Cells. Avian Dis 61:372-377.

Menssen, A., T. Haupl, M. Sittinger, B. Delorme, P. Charbord, and J. Ringe. 2011. Differential gene expression profiling of human bone marrow-derived mesenchymal stem cells during adipogenic development. BMC Genomics 12:461.

Merimi, M., R. El-Majzoub, L. Lagneaux, D. Moussa Agha, F. Bouhtit, N. Meuleman, H. Fahmi, P. Lewalle, M. Fayyad-Kazan, and M. Najar. 2021. The Therapeutic Potential of Mesenchymal Stromal Cells for Regenerative Medicine: Current Knowledge and Future Understandings. Front Cell Dev Biol 9:661532.

Mishra, B., and R. Jha. 2019. Oxidative Stress in the Poultry Gut: Potential Challenges and Interventions. Front Vet Sci 6:60.

Morozzi, G., S. Beccafico, R. Bianchi, F. Riuzzi, I. Bellezza, I. Giambanco, C. Arcuri, A. Minelli, and R. Donato. 2017. Oxidative stress-induced S100B accumulation converts myoblasts into brown adipocytes via an NF-kappaB/YY1/miR-133 axis and NF-kappaB/YY1/BMP-7 axis. Cell Death Differ 24:2077-2088.

Nashchekina, Y., P. Nikonov, N. Mikhailova, and A. Nashchekin. 2021. Collagen Scaffolds Treated by Hydrogen Peroxide for Cell Cultivation. Polymers (Basel) 13.

Nouri, F., S. N. Nematollahi-Mahani, and A. M. Shari fi. 2019. Preconditioning of Mesenchymal Stem Cells with Non-Toxic Concentration of Hydrogen Peroxide Against Oxidative Stress Induced Cell Death: The Role of Hypoxia-Inducible Factor-1. Adv Pharm Bull 9:76-83.

Ojano-Dirain, C., N. B. Tinsley, T. Wing, M. Cooper, and W. G. Bottje. 2007. Membrane potential and H2O2 production in duodenal mitochondria from broiler chickens (Gallus gallus domesticus) with low and high feed efficiency. Comp Biochem Physiol A Mol Integr Physiol 147:934-941.

Osorio, C., O. J. Fletcher, T. Abdul-Aziz, E. Gonder, B. Tilley, and D. H. Ley. 2007. Pneumonia of Turkey Breeder Hens Associated with Mycoplasma Synoviae. Avian Diseases 51:791-796.

Pendergrass, K. D., A. V. Boopathy, G. Seshadri, K. Maiellaro-Rafferty, P. L. Che, M. E. Brown, and M. E. Davis. 2013. Acute preconditioning of cardiac progenitor cells with hydrogen peroxide enhances angiogenic pathways following ischemia-reperfusion injury. Stem Cells Dev 22:2414-2424.

Pintus, E., and J. L. Ros-Santaella. 2021. Impact of Oxidative Stress on Male Reproduction in Domestic and Wild Animals. Antioxidants (Basel) 10.

Porto, M. L., B. P. Rodrigues, T. N. Menezes, S. L. Ceschim, D. E. Casarini, A. L. Gava, T. M. Pereira, E. C. Vasquez, B. P. Campagnaro, and S. S. Meyrelles. 2015. Reactive oxygen species contribute to dysfunction of bone marrow hematopoietic stem cells in aged C57BL/6 J mice. J Biomed Sci 22:97.

Puppel, K., A. Kapusta, and B. Kuczynska. 2015. The etiology of oxidative stress in the various species of animals, a review. J Sci Food Agric 95:2179-2184.

Ramp, W. K., R. R. Arnold, J. E. Russell, and J. M. Yancey. 1987. Hydrogen peroxide inhibits glucose metabolism and collagen synthesis in bone. J Periodontol 58:340-344.

Ray, P. D., B. W. Huang, and Y. Tsuji. 2012. Reactive oxygen species (ROS) homeostasis and redox regulation in cellular signaling. Cell Signal 24:981-990.

Reis, J., and A. Ramos. 2021. In Sickness and in Health: The Oxygen Reactive Species and the Bone. Front Bioeng Biotechnol 9:745911.

Robert, A. W., B. H. Marcon, B. Dallagiovanna, and P. Shigunov. 2020. Adipogenesis, Osteogenesis, and Chondrogenesis of Human Mesenchymal Stem/Stromal Cells: A Comparative Transcriptome Approach. Front Cell Dev Biol 8:561.

Rosen, E. D., C. H. Hsu, X. Wang, S. Sakai, M. W. Freeman, F. J. Gonzalez, and B. M. Spiegelman. 2002. C/EBPalpha induces adipogenesis through PPARgamma: a unified pathway. Genes Dev 16:22-26.

Rosova, I., M. Dao, B. Capoccia, D. Link, and J. A. Nolta. 2008. Hypoxic preconditioning results in increased motility and improved therapeutic potential of human mesenchymal stem cells. Stem Cells 26:2173-2182.

Ryu, J. M., H. J. Lee, Y. H. Jung, K. H. Lee, D. I. Kim, J. Y. Kim, S. H. Ko, G. E. Choi, Chai, II, E. J. Song, J. Y. Oh, S. J. Lee, and H. J. Han. 2015. Regulation of Stem Cell Fate by ROS-mediated Alteration of Metabolism. Int J Stem Cells 8:24-35.

Sanchez-de-Diego, C., J. A. Valer, C. Pimenta-Lopes, J. L. Rosa, and F. Ventura. 2019. Interplay between BMPs and Reactive Oxygen Species in Cell Signaling and Pathology. Biomolecules 9.

Saretzki, G., L. Armstrong, A. Leake, M. Lako, and T. von Zglinicki. 2004. Stress defense in murine embryonic stem cells is superior to that of various differentiated murine cells. Stem Cells 22:962-971.

Sen, S., C. C. Domingues, C. Rouphael, C. Chou, C. Kim, and N. Yadava. 2015. Genetic modification of human mesenchymal stem cells helps to reduce adiposity and improve glucose tolerance in an obese diabetic mouse model. Stem Cell Res Ther 6:242.

Serdar, C. C., M. Cihan, D. Yucel, and M. A. Serdar. 2021. Sample size, power and effect size revisited: simplified and practical approaches in pre-clinical, clinical and laboratory studies. Biochem Med (Zagreb) 31:010502.

Serguienko, A., M. Y. Wang, and O. Myklebost. 2018. Real-Time Vital Mineralization Detection and Quantification during In Vitro Osteoblast Differentiation. Biol Proced Online 20:14.

Shadel, G. S., and T. L. Horvath. 2015. Mitochondrial ROS signaling in organismal homeostasis. Cell 163:560-569.

Sharma, P., A. B. Jha, R. S. Dubey, and M. Pessarakli. 2012. Reactive Oxygen Species, Oxidative Damage, and Antioxidative Defense Mechanism in Plants under Stressful Conditions. Journal of Botany 2012:1-26.

Sharma, T., N. Islam, J. Ahmad, N. Akhtar, and M. Beg. 2015. Correlation between bone mineral density and oxidative stress in postmenopausal women. Indian J Endocrinol Metab 19:491-497.

Sheppard, A. J., A. M. Barfield, S. Barton, and Y. Dong. 2022. Understanding Reactive Oxygen Species in Bone Regeneration: A Glance at Potential Therapeutics and Bioengineering Applications. Front Bioeng Biotechnol 10:836764.

Shimizu, T. 2016. Inflammation-inducing Factors of Mycoplasma pneumoniae. Front Microbiol 7:414.

Sies, H., C. Berndt, and D. P. Jones. 2017. Oxidative Stress. Annu Rev Biochem 86:715-748.

Siwik, D. A., P. J. Pagano, and W. S. Colucci. 2001. Oxidative stress regulates collagen synthesis and matrix metalloproteinase activity in cardiac fibroblasts. Am J Physiol Cell Physiol 280:C53-60.

Strecker, V., S. Mai, B. Muster, S. Beneke, A. Burkle, J. Bereiter-Hahn, and M. Jendrach. 2010. Aging of different avian cultured cells: lack of ROS-induced damage and quality control mechanisms. Mech Ageing Dev 131:48-59.

Sun, Y. X., A. H. Xu, Y. Yang, and J. Li. 2015. Role of Nrf2 in bone metabolism. J Biomed Sci 22:101.

Surai, P. F., Kochish, II, V. I. Fisinin, and M. T. Kidd. 2019. Antioxidant Defence Systems and Oxidative Stress in Poultry Biology: An Update. Antioxidants (Basel) 8.

Svoradova, A., V. Zmrhal, E. Venusova, and P. Slama. 2021. Chicken Mesenchymal Stem Cells and Their Applications: A Mini Review. Animals (Basel) 11.

Takada, I., M. Suzawa, K. Matsumoto, and S. Kato. 2007. Suppression of PPAR transactivation switches cell fate of bone marrow stem cells from adipocytes into osteoblasts. Ann N Y Acad Sci 1116:182-195.

Thiese, M. S., B. Ronna, and U. Ott. 2016. P value interpretations and considerations. J Thorac Dis 8:E928-E931.

Tompkins, Y. H., P. Teng, R. Pazdro, and W. K. Kim. 2022. Long Bone Mineral Loss, Bone Microstructural Changes and Oxidative Stress After Eimeria Challenge in Broilers. Frontiers in Physiology 13.

Valle-Prieto, A., and P. A. Conget. 2010. Human mesenchymal stem cells efficiently manage oxidative stress. Stem Cells Dev 19:1885-1893.

Wan, C., J. Xiang, Y. Li, and D. Guo. 2016. Differential Gene Expression Patterns in Chicken Cardiomyocytes during Hydrogen Peroxide-Induced Apoptosis. PLoS One 11:e0147950.

Wan, H., W. Yuan, M. Ruan, Q. Ye, R. Wang, Z. Li, G. Zhou, Z. Yao, J. Zhao, S. Liu, and Y. Yang. 2011. Identification of reference genes for reverse transcription quantitative

real-time PCR normalization in pepper (Capsicum annuum L.). Biochem Biophys Res Commun 416:24-30.

Wang, T., X. Zhang, and D. D. Bikle. 2017. Osteogenic Differentiation of Periosteal Cells During Fracture Healing. J Cell Physiol 232:913-921.

Wideman, R. F., Jr. 2016. Bacterial chondronecrosis with osteomyelitis and lameness in broilers: a review. Poult Sci 95:325-344.

Xia, C., and A. P. Møller. 2018. Long-lived birds suffer less from oxidative stress. Avian Research 9.

Xiang, J., C. Wan, R. Guo, and D. Guo. 2016. Is Hydrogen Peroxide a Suitable Apoptosis Inducer for All Cell Types? Biomed Res Int 2016:7343965.

Xu, J., G. M. Strasburg, K. M. Reed, and S. G. Velleman. 2022. Thermal stress and selection for growth affect myogenic satellite cell lipid accumulation and adipogenic gene expression through mechanistic target of rapamycin pathway. J Anim Sci 100.

Yuan, Z., J. Zhang, Y. Huang, Y. Zhang, W. Liu, G. Wang, Q. Zhang, G. Wang, Y. Yang, H. Li, and G. Chen. 2017. NRF2 overexpression in mesenchymal stem cells induces stem-cell marker expression and enhances osteoblastic differentiation. Biochem Biophys Res Commun 491:228-235.

Zhang, H., K. Mehmood, X. Jiang, Z. Li, W. Yao, J. Zhang, X. Tong, Y. Wang, A. Li, M. Waqas, M. Iqbal, and J. Li. 2019. Identification of differentially expressed MiRNAs profile in a thiram-induced tibial dyschondroplasia. Ecotoxicol Environ Saf 175:83-89.

Zhang, H., K. Mehmood, K. Li, M. U. Rehman, X. Jiang, S. Huang, L. Wang, L. Zhang, X. Tong, F. Nabi, W. Yao, M. K. Iqbal, M. Shahzad, and J. Li. 2018. Icariin Ameliorate

Thiram-Induced Tibial Dyschondroplasia via Regulation of WNT4 and VEGF Expression in Broiler Chickens. Front Pharmacol 9:123.

Zhang, H., Y. Wang, K. Mehmood, Y. F. Chang, Z. Tang, and Y. Li. 2020. Treatment of tibial dyschondroplasia with traditional Chinese medicines: "Lesson and future directions". Poult Sci 99:6422-6433.

Zorov, D. B., M. Juhaszova, and S. J. Sollott. 2014. Mitochondrial reactive oxygen species (ROS) and ROS-induced ROS release. Physiol Rev 94:909-950.

Tables

Table 4.1. Nucleotide sequences of the primers used for quantitative real-time RT-PCR.

Gene[1]	Primer sequence (5'-3')	Product length (bp)	Annealing temperature (°C)	Accession #
18S rRNA	F-AGCCTGCGGCTTAATTTGAC R-CAACTAAGAACGGCCATGCA	121	56.5	AF_173612.1
HMBS	F-GGCTGGGAGAATCGCATAGG R-TCCTGCAGGGCAGATACCAT	131	59	XM_004947916.3
ACTB	F-CAACACAGTGCTGTCTGGTGGTA R-ATCGTACTCCTGCTTGCTGATCC	205	61	NM_205518.1
CEBPA	F-CCTACGGCTACAGAGAGGCT R-GAAATCGAAATCCCCGGCCA	206	60	NM_001031459.1
PPARG	F-GAGCCCAAGTTTGAGTTTGC R-TCTTCAATGGGCTTCACATTT	131	58	XM_025154400.1
FABP4	F-GCAGAAGTGGGATGGCAAAG R-GTTCGCCTTCGGATCAGTCC	153	60	NM_204290.1
ALPL	F-CGACCACTCACACGTCTTCA R-CGATCTTATAGCCAGGGCCG	140	60	NM_205360.1
RUNX2	F-ACTTTGACAATAACTGTCCT R-GACCCCTACTCTCATACTGG	192	60	XM_015285081.2
BGLAP	F-GGATGCTCGCAGTGCTAAAG R-CTCACACACCTCTCGTTGGG	142	57	NM_205387.3
SPP1	F-GCCCAACATCAGAGCGTAGA R-ACGGGTGACCTCGTTGTTTT	204	57	NM_204535.4
BMP2	F-TCAGCTCAGGCCGTTGTTAG R-GTCATTCCACCCCACGTCAT	163	57	XM_025148488.1
COL1A2	F- CTGGTGAAAGCGGTGCTGTT R-CACCAGTGTCACCTCTCAGAC	222	60	NM_001079714.2
SOD2	F- GCCACCTACGTGAACAACCT R- AGTCACGTTTGATGGCTTCC	140	61	NM_204211.2
SOD1	F-ATTACCGGCTTGTCTGATGG R-CCTCCCTTTGCAGTCACATT	173	58	NM_205064.1
CAT	F-ACTGCAAGGCGAAAGTGTTT R-GGCTATGGATGAAGGATGGA	222	60	NM_001031215.1

GSTA2	F- GAGTCAATTCGGTGGCTGTT R- TGCTCTGCACCATCTTCATC	157	59	XM_046913335.1
NOS2	F-CCTGTACTGAAGGTGGCTATTGG R-AGGCCTGTGAGAGTGTGCAA	66	58	NM_204961.2
GPX1	F-AACCAATTCGGGCACCAG R-CCGTTCACCTCGCACTTCTC	122	60	NM_001277853.2
NFR2	F- GAGCCCATGGCCTTTCCTAT R- CACAGAGGCCCTGACTCAAA	210	59	XM_046907885.1
CASP3	F-TGGTATTGAAGCAGACAGTGGA R- GGAGTAGTAGCCTGGAGCAGTAGA	103	60	XM_015276122.2
CASP8	F-ATTTGGCTGGCATCATCTGT R-ACTGCTTCCCTGGCTTTTG	146	59	NM_204592.4
CASP6	F-AAACCTACACCAACCACCACA R-TTCTGTCTGCCAAAGTCCCA	196	60	NM_001396146.1

[1]18S rRNA:18S ribosomal RNA; HMBS: hydroxymethylbilane synthase; ACTB: actin beta; PPARG: peroxisome proliferator-activated receptor gamma; C/EBPα: CCAAT/enhancer-binding protein alpha; FABP4: fatty acid binding protein 4; SPP1: secreted phosphoprotein, osteopontin; BMP2: bone morphogenetic protein 2; BGLAP: bone gamma-carboxyglutamic acid-containing protein (osteocalcin). RUNX2: runt-related transcription factor 2; ALPL: alkaline phosphatase, biomineralization associated; COL1A2: collagen type I alpha 2 chain; NFKB1: nuclear factor kappa B subunit 1; CAT: catalase; SOD1: superoxide dismutase 1; SOD2: superoxide dismutase 2; GPX1: glutathione peroxidase 1; NOS2: nitric oxide synthase 2; NFR2: GA binding protein transcription factor alpha subunit (GABP2); GSTA2: glutathione S-transferase alpha 2; CASP3: caspase 3; CASP6: caspase 6; CASP8: caspase 8.

Figures

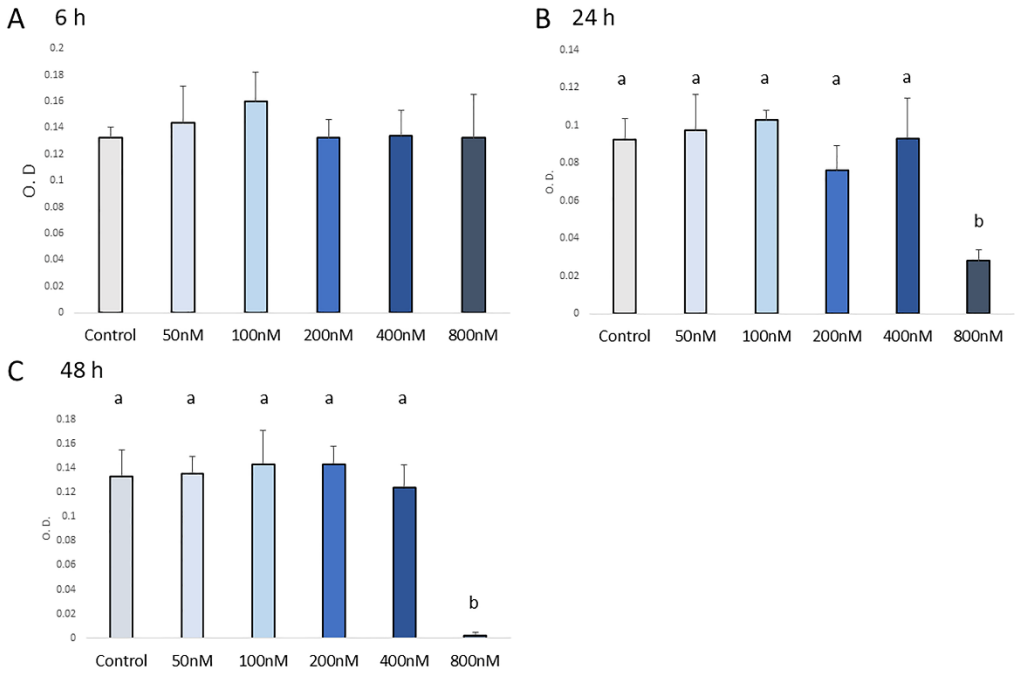

Figure 4.1: Effects of H_2O_2 on the cell viability. Cells were treated with the indicated concentrations of H_2O_2 for 6 h, 24 h and 48 h. The graphs show cellular growth changes, as assessed by MTT assays. MTT assay showed that exposure to concentrations higher than 400 nM of H_2O_2 can reduce cell viability, the appropriate H_2O_2 concentration was screened out, and final treatment concentrations as 100 nM, 200 nM and 400 nM of H_2O_2 was selected as the treatments dose for the following experiments.

[a, b] Treatments with different letters means a significantly difference between treatments by using Tukey's HSD test, $p < 0.05$, data are shown as mean ± SEM of four independent replicates (n=4).

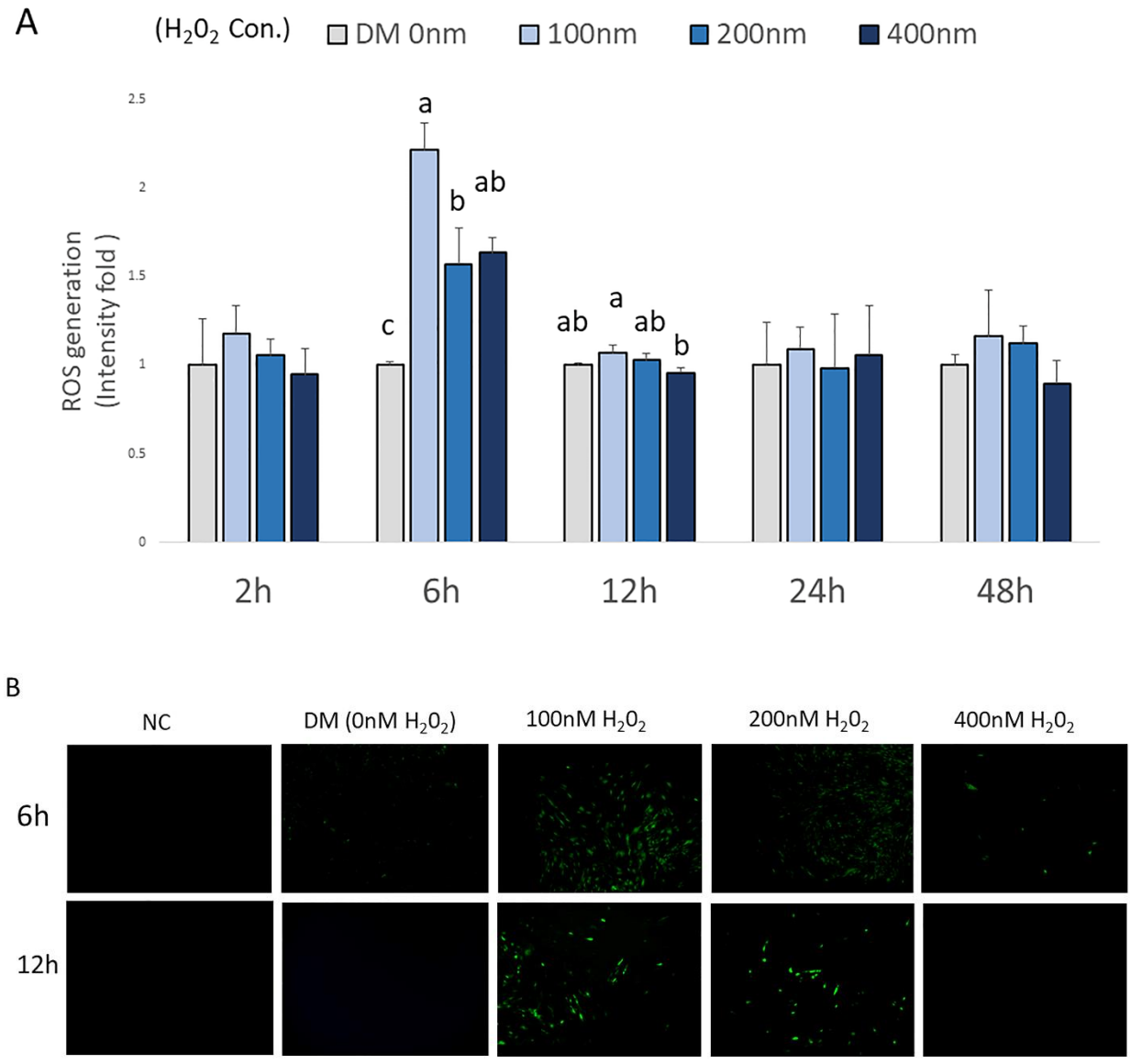

Figure 4.2: Effects of H_2O_2-induced reactive oxygen species (ROS) production in chicken MSCs. Exponentially growing cells were treated with the indicated concentrations of H_2O_2 for 2 h, 6 h, 12 h, 24 h and 48 h. ROS levels in MSCs were measured using a DCFDA/H2DCFDA cellular ROS assay kit. (A) Quantitative analysis was performed by measuring fluorescence intensity. Each value represents the mean ± SEM of three

independent replicates (n = 3). [a, ab, b, c] Treatments with different letters means a significantly difference between treatments by using Tukey's HSD test, $p < 0.05$. (B) Figures were selected as representative image from DCFDA/H_2DCFDA cellular ROS assay.

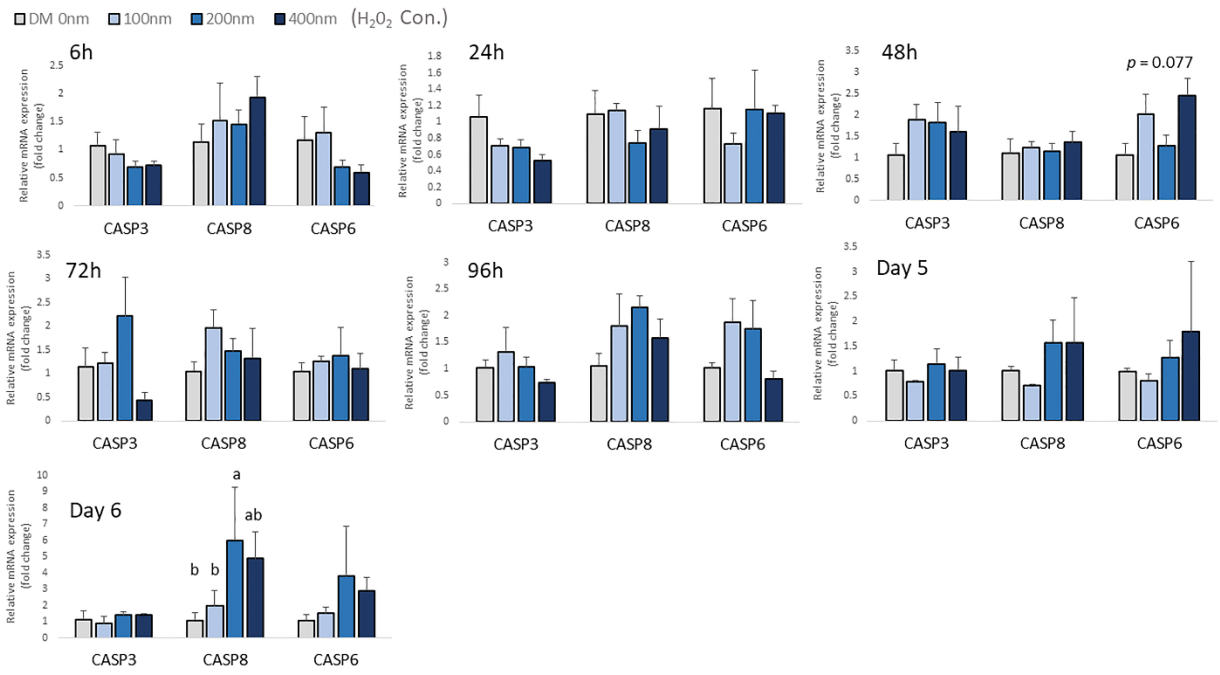

Figure 4.3: Effects of H_2O_2 on mRNA expression of apoptosis markers in chicken MSCs. Differentiation cells were treated with the indicated concentrations of H_2O_2 for 6h, 24 h, 48 h, 72 h, 96 h, 5 days and 6 days. Each value represents the mean ± SEM of three independent experiments (n = 3). $^{a, ab, b, c}$ Treatments with different letters means a significantly difference between treatments by using Tukey's HSD test, $p < 0.05$.

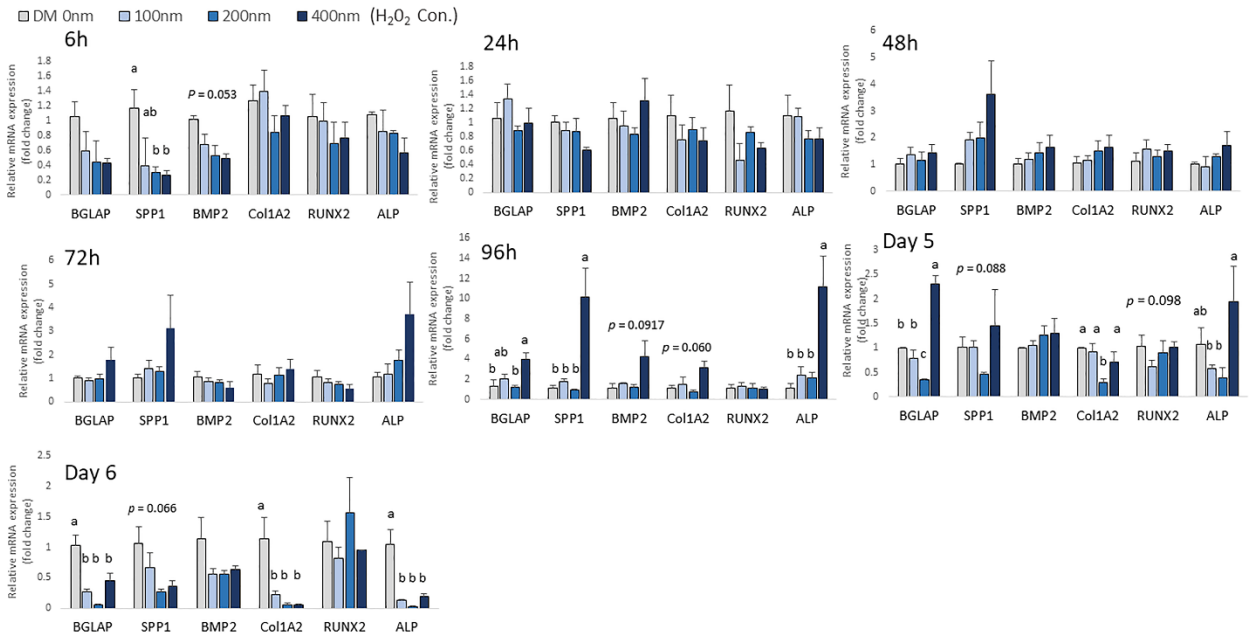

Figure 4.4: Effects of H_2O_2 on mRNA expression of osteogenic differentiation markers in chicken MSCs. Cells were treated with the indicated concentrations of H_2O_2 in differentiation medium for 6 h, 24 h, 48 h, 72 h, 96 h, 5 days and 6 days. Each value represents the mean ± SEM of three independent experiments (n = 3).

a, ab, b, c Treatments with different letters means a significantly difference between treatments by using Tukey's HSD test, $p < 0.05$.

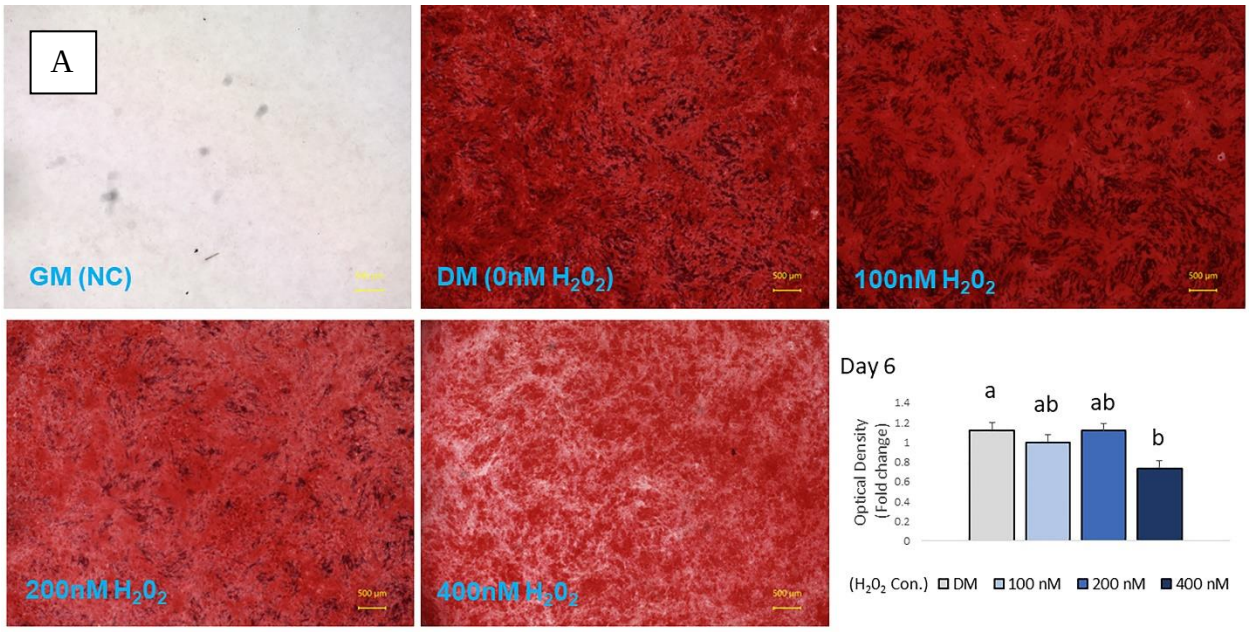
A
GM (NC)
DM (0nM H_2O_2)
100nM H_2O_2
200nM H_2O_2
400nM H_2O_2
Day 6
Optical Density (Fold change)
a
ab
ab
b
(H_2O_2 Con.) DM 100 nM 200 nM 400 nM

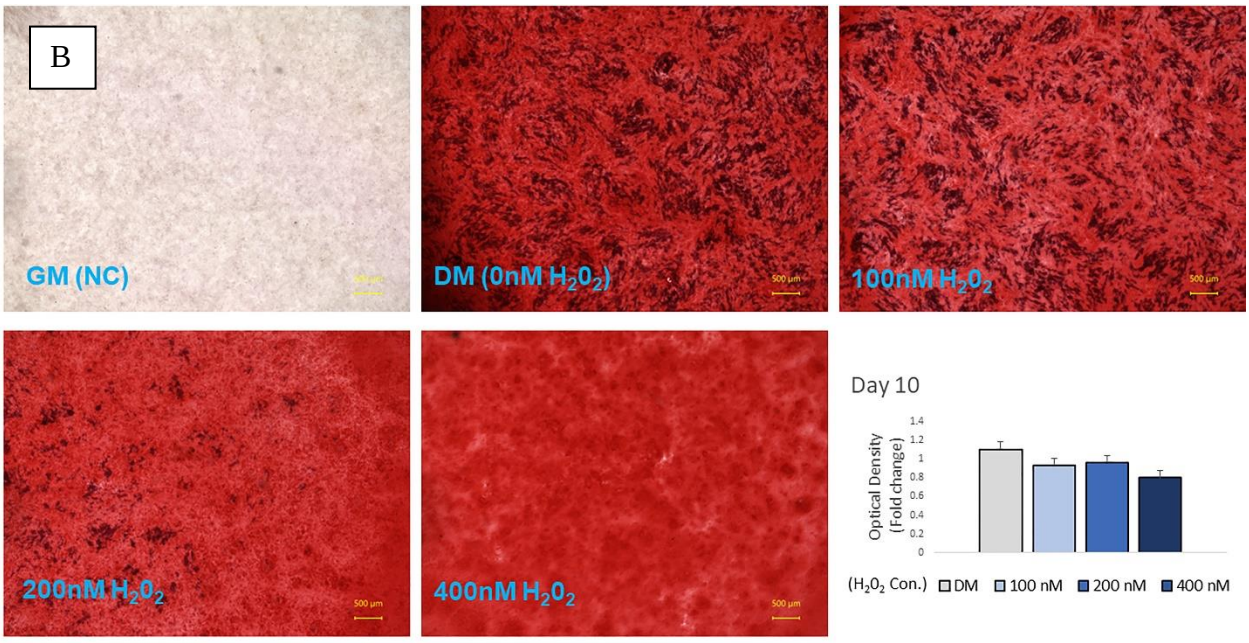
B
GM (NC)
DM (0nM H_2O_2)
100nM H_2O_2
200nM H_2O_2
400nM H_2O_2
Day 10
Optical Density (Fold change)
(H_2O_2 Con.) DM 100 nM 200 nM 400 nM

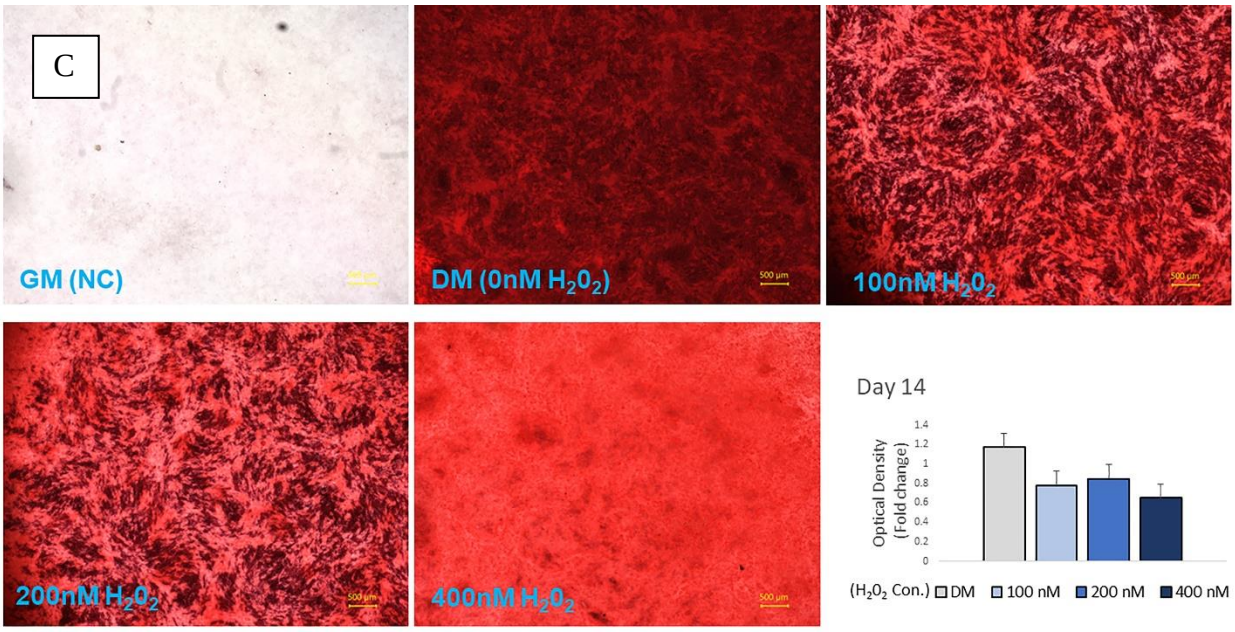

Figure 4.5. Alizarin red S staining for mineralization on day 6 (A), day 10 (B) and day 14 (C). Images were randomly acquired in 2× magnification. The calcified nodules appeared bright red in color. Mineral deposit quantification was conducted, each value represents the mean ± SEM of three independent experiments (n = 3).

[a, ab, b] Treatments with different letters means a significantly difference between treatments by using Tukey's HSD test, $p < 0.05$.

A

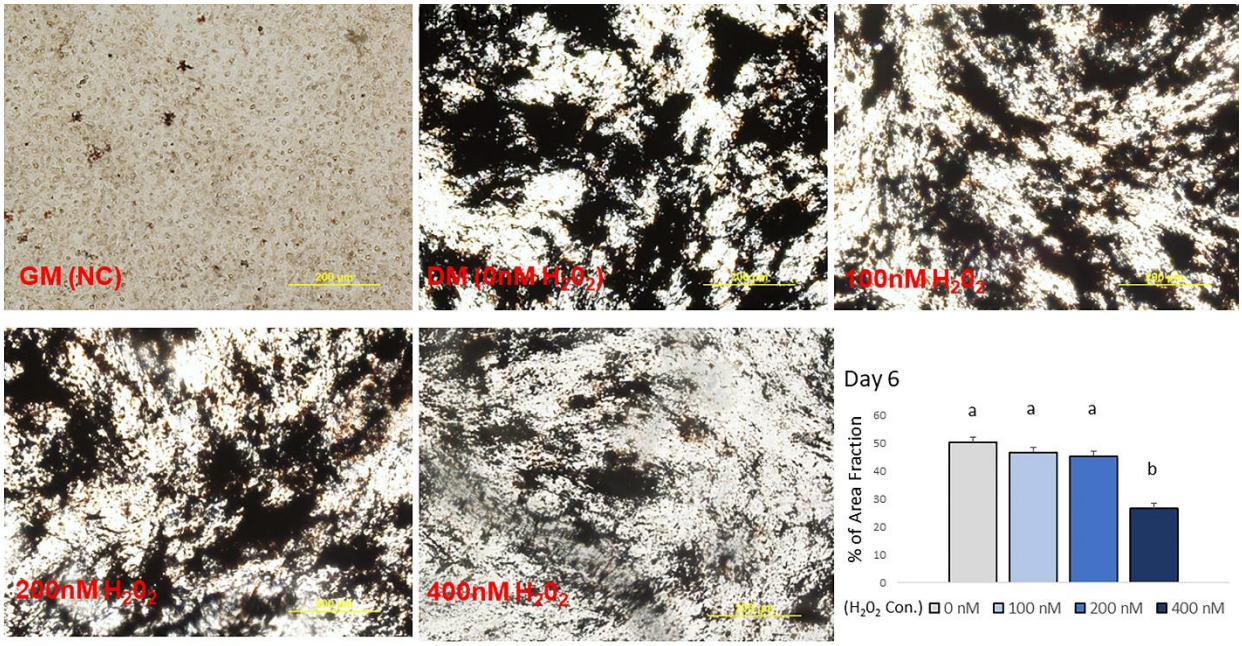
GM (NC)
DM (0nM H_2O_2)
100nM H_2O_2
200nM H_2O_2
400nM H_2O_2
Day 6
% of Area Fraction
a
a
a
b
(H_2O_2 Con.) 0 nM 100 nM 200 nM 400 nM

B

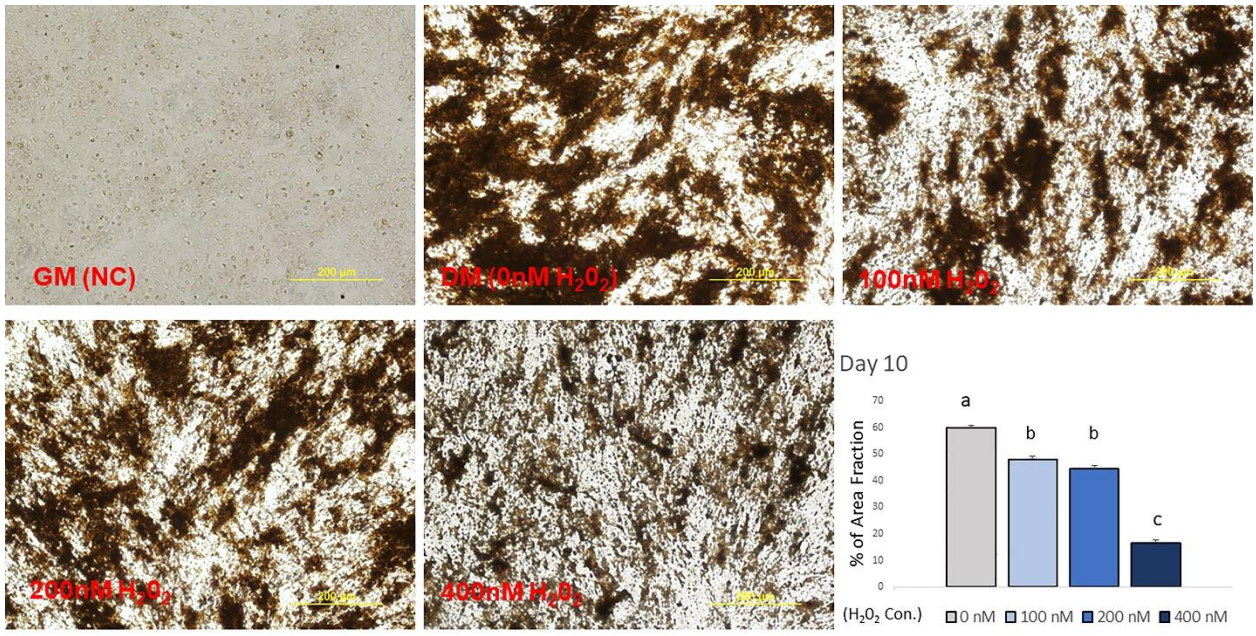
GM (NC)
DM (0nM H_2O_2)
100nM H_2O_2
200nM H_2O_2
400nM H_2O_2
Day 10
% of Area Fraction
a
b
b
c
(H_2O_2 Con.) 0 nM 100 nM 200 nM 400 nM

C

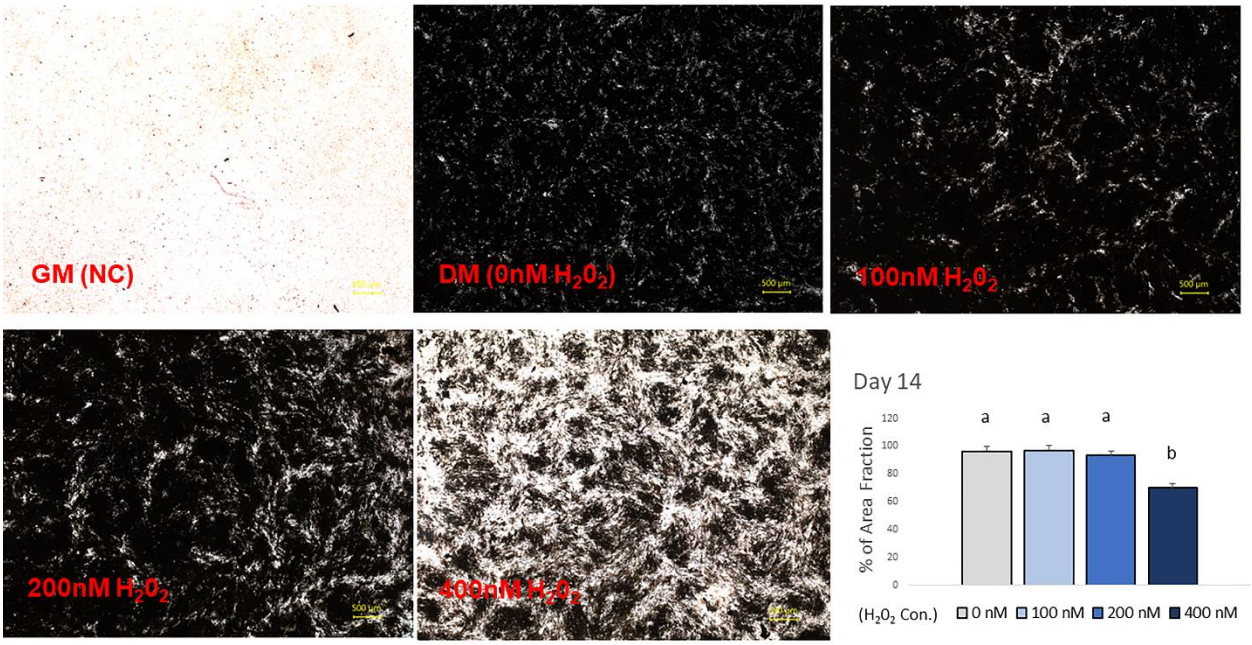

Figure 4.6: Von kossa staining for mineralization on day 6 (A), day 10 (B) and day 14 (C). Images were randomly acquired in 2× magnification and 4 images per well were analyzed. Black indicative of phosphate and calcium deposition. ImageJ analysis quantified percent area fraction for each treatment based on three independently sampled experiments of each species each value represents the mean ± SEM of three independent experiments (n = 3). [a, b] Treatments with different letters means a significantly difference between treatments by using Tukey's HSD test, $p < 0.05$.

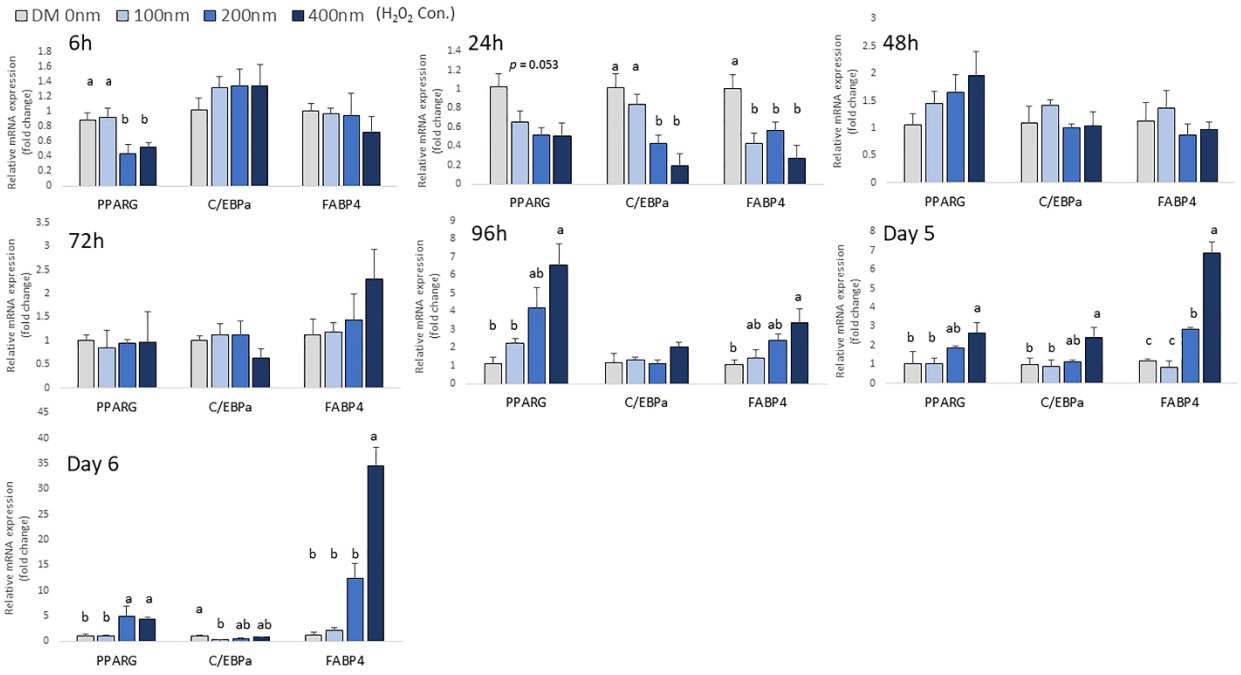

Figure 4.7: Effects of H_2O_2 on mRNA expression of adipogenic differentiation markers in chicken MSCs. Cells were treated with the indicated concentrations of H_2O_2 for 6 h, 24 h, 48 h, 72 h, 96 h, 5 days and 6 days. Each value represents the mean ± SEM of three independent experiments (n = 3). [a, ab, b] Treatments with different letters means a significantly difference between treatments by using Tukey's HSD test, $p < 0.05$.

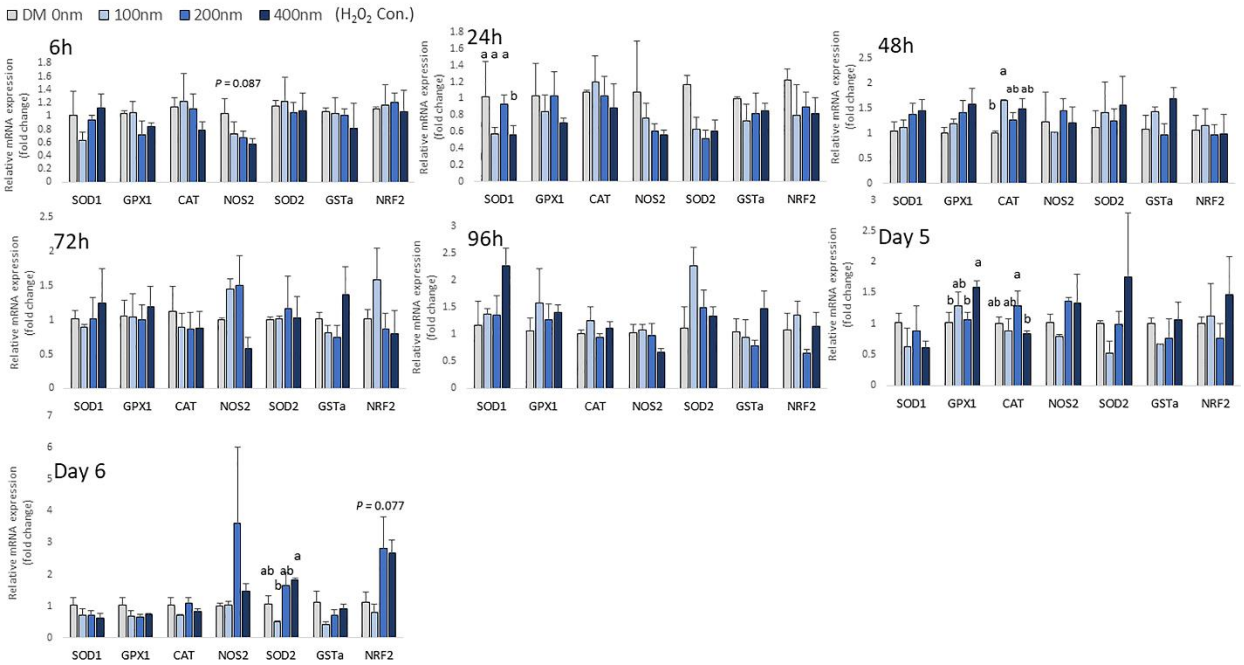

Figure 4.8: Effects of H_2O_2 on mRNA expression of antioxidant enzymes in chicken MSCs. Cells were treated with the indicated concentrations of H_2O_2 for 6 h, 24 h, 48 h, 72 h, 96 h, 5 days and 6 days. Each value represents the mean ± SEM of three independent experiments (n = 3). [a, ab, b] Treatments with different letters means a significantly difference between treatments by using Tukey's HSD test, $p < 0.05$.

CHAPTER 5

EFFECT OF HYDROGEN OXIDE-INDUCED OXIDATIVE STRESS ON BONE FORMATION AT THE EARLY EMBRYONIC DEVELOPMENT STAGE [4]

[4] Yuguo Tompkins, Guanchen Liu, Brett Marshall, Milan Kumar Sharma, Woo Kyun Kim. To be submitted to *Biomolecules*

Abstract

Modern poultry production systems expose chicken embryos to many stressors that may result in oxidative stress. The current study aimed to monitor the impact of H_2O_2-induced oxidative stress on avian bone formation at the early embryonic development stage. Fertilized Cobb broiler eggs were divided into 5 treatment groups micro-injected with different concentrations of H_2O_2 (PBS (0 nM) control, 10 nM, 30 nM, 100 nM and 300 nM) at embryonic day 3, followed by continued incubation. Embryos were collected at 6 h, 24h, 48 h, and 72h post-injection. The mRNA expression levels were determined for three groups of genes, including apoptotic markers, antioxidant enzymes, and early bone formation gene markers were measured. Results showed that the injection of H_2O_2 altered the mRNA expression pattern of the antioxidant enzyme during early embryogenesis; the increased expression of *iNOS* by 10 nM H_2O_2 treatment was observed at 6 h and 72 h. The changed expression of *SOD1* at 48 h, as well as a trend of changed expression of *GPX1* at 6h, 48 h and 72h was also observed with 10 nM H_2O_2 treatment. H_2O_2 injection suppressed the expression of bone formation gene markers with chronic effects. The short bone length was observed in high H_2O_2 treatment groups at 72 h post-injection. Decreased mRNA expression levels of *Col1A2* and *Col2A1* were observed at 6 h and 24 h post-injection.

Keyword: bone health, oxidative stress, chicken embryo, ROS, bone formation

Introduction

The intensive system of poultry production places the broiler under many stressors and results in exposure to oxidative stress, which is typically defined as an excess of reactive oxygen species (ROS) compared to the ability of a biological system to neutralize them (Mishra and Jha, 2019). A relatively low level of ROS is essential to maintain or initial biological and physiological function, but excess ROS or long-term ROS exposure is harmful, leading to DNA damage, protein denaturation, and lipid peroxidation (Covarrubias, et al., 2008; Dennery, 2010). The avian embryo develops in a closed system using the nutrients available within the egg before hatching. However, excessive ROS generated in tissues will deplete the antioxidant level and cause embryonic oxidative stress (PF, 2002). Oxidative stress has been associated with impaired early embryonic death, malformations, and post-hatch growth retardation in avian species and mammals (Dennery, 2007; Haussmann, et al., 2012). Conversely, maternal dietary supplementation antioxidants may partially alleviate the deleterious impact of oxidative stress in chicks (Ebeid, et al., 2017; Yang, et al., 2021). Egg quality and management are essential to limit the oxidative stress in the embryo because stress factors such as maternal exposure to environmental contamination (Moghaddam, et al., 2015), maternal diet quality (Gou, et al., 2021), and poor husbandry, including pro-long egg storage time or temperature stress can significantly reduce hatchability and chick quality by impairing antioxidant capacity (Tona, et al., 2003; Reijrink, et al., 2009; Haussmann, et al., 2012; Ebeid, et al., 2017; Saleh, et al., 2020). As such, there has been a growing interest in oxidative stress in chicken production in recent years. The role of

oxidative stress in fetal growth and fetal programming via epigenetic mechanisms are well studied and discussed in other species (Dennery, 2004; Dennery, 2010; Thompson and Al-Hasan, 2012). In mammals, fetal growth is sensitive to oxidative stress because of its low antioxidant capacity (Dennery, 2010); fetal oxidative stress compromises fetal growth and impaired fetal skeletal formation (Prater, et al., 2008). Oxidative stress has been widely accepted as a mediator of pathogenesis in human bone diseases, with the increased level of ROS in osteoblasts being a hallmark element in the pathophysiology of bone loss (Domazetovic, et al., 2017). Due to artificial selection, an exchange of rapid muscle accretion at the expense of skeletal health has appeared in broiler chickens over the past few decades (Hartcher and Lum, 2019; Rath and Durairaj, 2022). A number of studies have investigated the drivers of variation in oxidative stress and the oxidative machinery during a later stage of embryonic development (Heidinger, et al., 2012), and several methods were used to induce avian embryonic oxidative stress, such as maternal manipulation and amniotic sac injection (Korhonen, et al., 1984; Korn and Cramer, 2007; Jadhav* and Kengar, 2016; Paradowska, et al., 2022). Evidently, bone stems cells proliferation and differentiation of this stem niche is often pre-programmed at early stages and have significant impact on the future skeletal homeostasis (Newton, et al., 2019). However, the knowledge of oxidative stress on avian early embryonic bone development is limited. Thus, the current study aimed to present direct evidence between embryonic ROS and developmental retardation of the developing chicken embryo. The expression patterns of several sets of genes in osteogenesis, chondrogenesis, apoptosis,

and antioxidant enzyme expression from embryonic day 3 (ED3) to embryonic day 7 (ED7) were assessed.

Material and Method

Ethics Statement

All experiments followed the guidelines of the Institutional Animal Care and Use Committee and was conducted at research center of Department of Poultry Science, University of Georgia, Athens, GA.

H_2O_2 microinjection

The injection protocol was adapted from previous publications (Ben-Yair and Kalcheim, 2010; Chen, et al., 2021). Cobb500 fertilized eggs (Cleveland, GA, United States) were set on their long axis in the bench incubator (GQF 1502, Savannah, GA, United States) without egg turning at 38°C and 50% relative humidity. At 72h of incubation (E 3), eggs were sanitized with 70% ethanol and 1.5mL albumen was removed by piercing the prolate end with an 18g needle, followed by sealing with hot glue to avoid contamination and dehydration. An observation window was carefully drilled in the eggshell at apex of the long axis, and eggs were placed under a stereo microscope for microinjection (Olympus, PA, United States). The treatment H_2O_2 was diluted into the proper concentrations, and heat-pulled capillary micropipettes were loaded with H_2O_2 or PBS, and mounted onto an aspirator. The range of treatment concentration of H_2O_2 was selected based on our previous *in vitro* study, and the embryo mortality rate was evaluated at 24 h post-injection. Dorsal aorta was pierced using the tip of micropipettes (illustrate as Figure 5.1). The same volume of treatment solutions was injected into each

sample (10 pumps for each sample), the final concentration of treatment was set as 0 nM (PBS), 10 nM, 30 nM, 100 nM and 300 nM H_2O_2 (30% (w/w) solution, Sigma-Aldrich, St. Louis, MO, USA). Following injections, 100 uL 1× antibiotics (antibiotic antimycotic solution, 100× stock contains with 10,000 units penicillin, 10 mg streptomycin and 25 μg amphotericin B /mL; Sigma-Aldrich) was added. Glass coverslips (24 × 55 mm; ThermoFisher Scientific, Waltham, MA, USA) were used to seal the observation windows, the treated embryos are returned to incubator without turning. 16 eggs per treatment were injected at each time point, and heartbeat rate and embryo mortality after microinjection were monitored prior to collection to ensure viability (16 eggs × 5 treatments × 4 time points, 320 chicken embryos in total). Eight live embryos tissue with normal heartbeats rate were collected at each time point. Whole embryos were harvested at 6 h, 24 h, 48 h and 72 h post-injection. Samples for mRNA expression were stored at -80°C until analysis. Samples for embryo length measurement were fixing in 70% ethanol, and the length of the embryos was measured with a digital caliper (H-7352, ULINE, Pleasant Prairie, WI, USA).

Lipid Peroxidation and Antioxidant Status Assay

The level of embryo tissue lipid peroxidation was determined by using QuantiChrom TBARS Assay Kit (BioAssay Systems, Hayward, CA, USA). Embryo tissue samples were collected at 72 h post-injection, snap-frozen in liquid nitrogen, and then kept at -80°C. Samples were homogenized, 50 uL tissue were used and centrifuged in the assay buffer, and all assay procedures were performed according to the manufacturer's protocols. The protein concentration was measured by protein

quantification assay (Pierce BCA Protein Assay Kit, ThermoFisher Scientific) following manufacture instructions.

RNA Isolation, cDNA Synthesis, and Real-Time Polymerase Chain Reaction (qRT-PCR) Analysis

Embryo samples were homogenized, and 50 uL of samples were used for RNA isolation. Embryonic total RNA was extracted by using Qiazol reagents (Qiagen, Germantown, MD, USA) according to the manufacturer's instructions. Nano-Drop 1000 Spectrophotometer (ThermoFisher Scientific) was used to determine the quantity of extracted RNA. The cDNA was synthesized from total RNA (2000 ng) using high-capacity cDNA reverse transcription kits (Applied Biosystems, Foster City, CA, USA). Real-time quantitative polymerase chain reaction (RT-qPCR) was used to measure relative expression of specific transcripts. Primers were designed using the Primer-BLAST program (https://www.ncbi.nlm.nih.gov/tools/primer-blast/). Primer specificity was validated by PCR products were size-verified by gel electrophoresis and melting curve analysis. Details of primer sequences used for the experiment are presented in Table 5.1. RT-qPCR was performed on an Applied Biosystems StepOnePlus™ (ThermoFisher Scientific) with iTaq™ Universal SYBR Green Supermix (BioRad, Hercules, CA, USA) using the following conditions for all genes: 95°C for 10 minutes followed 40 cycles at 95°C for 15 seconds, annealing temperature (Table 5.1) for 20 seconds, and extending at 72°C for one minute. The geometric mean of housekeeping genes including hydroxymethylbilane synthase (*HMBS*), glyceraldehyde-3-phosphate dehydrogenase (*GAPDH*) and actin beta (*ACTB*) was used for normalization. The

stability of the housekeeping genes was confirmed by their consistent Ct values among the treatments ($p > 0.1$). Samples were run in duplicate, and relative gene expression data were analyzed using the $2^{-\Delta\Delta Ct}$. The mean ΔCt of each marker gene from the control group was used to calculate the ΔΔCt value, and $2^{-\Delta\Delta Ct}$ expression levels were normalized to 1 for the control group, and expression levels of the other treatment groups were presented as fold change relative to the control group.

Statistical analysis

All experimental data were expressed as mean with standard deviation (SD). Data were tested for homogeneity of variances. All gene expression data were analyzed by one-way ANOVA followed by Dunnett's test, and the embryonic survival rate means were submitted to two-way ANOVA by JMP Pro14 (SAS Institute, Cary, NC, USA), and the main effects and their interactions were considered. Statistical significance was set at $P \leq 0.05$, and $0.05 \leq P \leq 0.1$ were also presented to show the trend toward statistical significance (Thiese, et al., 2016; Serdar, et al., 2021). Pairwise correlations (JMP Pro14) were evaluated for expression of all antioxidant enzyme coding genes and bone formation genes.

Results

Embryonic survival rate after microinjection varies from 100% to 60% within 72 h post-injection (Figure 5.2) but was not a function of dosage. At 6 h post-injection, no embryonic mortality was observed in each group. At 24 h post-injection, the survival rate of injected embryos decreased by around 10% compared with PBS injected control. At 48 h post-injection, individuals injected with 300 nM showed 30% lower survival

rates than 10 nM. At 72 h post-injection, individuals injected with 100 nM showed lower survival rates than PBS-injected control. By comparing all the treatment groups at different time points, the results showed that the mortality rate was not in a dose-depend manner (P = 0.226), but incubation period has a significant impact on the survival rate (P = 0.003). There is no interaction between treatment dosage and incubation time (P = 0.878). Together, these data suggest that H_2O_2 was not a significant contributor of mortality. Supporting this, lipid peroxidation results shown the level of malonaldehyde (MDA) in the embryo did not change by H_2O_2 treatment (P = 0.711; Figure 5.3); H_2O_2 did not cause embryonic tissue lipid peroxidation after 72 h post-injections. This result showed the dose of H_2O_2 below levels where embryonic lipid peroxidation occurred at 72 h. Together, the concentrations of H_2O_2 used in the present study were safely below levels where any embryotoxicity occurs.

A decreased embryo length was observed in 100 nM and 300 nM H_2O_2 groups compared to the PBS-injected control (P < 0.05; Figure 5.4A and B). At 6 h post-injection, 10 nM H_2O_2 significantly increased the expression of *iNOS* compared with PBS-injected control (P < 0.05; Figure 5.5B), and H_2O_2 tended to alter the mRNA expression of *GPX1* among treatments (P = 0.080; Figure 5.5B). In addition,10 nM and 30 nM H_2O_2 significantly decreased the expression of *BCL2* compared with PBS-injected control (P < 0.05; Figure 5.5A). Meanwhile, a significantly decreased expression of *COL1A2* was observed in all H_2O_2 treatment groups compared with the control (P < 0.05; Figure 5.5C). For correlation analysis, *BMP2* was positively correlated with the

expression of *iNOS* ($P < 0.001$, $R^2 = 0.197$). *BAGLAP* was positively correlated with the expression of *iNOS* ($P < 0.001$, $R^2 = 0.366$).

At 24 h post-injection, the expression of *BCL2*, an anti-apoptosis regular, was significantly upregulated by 300 nM H_2O_2 injection compared to the control ($P < 0.01$, Figure 5.6A). Results for mRNA expression of bone/ chondrocyte formation markers indicated a general decrease in expression levels with a higher concentration of H_2O_2 injection. Moreover, the 30 nM and 300 nM H_2O_2 significantly decreased embryonic mRNA levels of *SPP1* ($P < 0.05$; Figure 5.6C). The 30 nM, 100 nM and 300 nM groups had lower level of *COL1A2* compared to control ($P < 0.05$; Figure 5.6C). The expression of chondrocyte collagen *COL2A1* was inhibited by 10 nM and 30 nM H_2O_2 compared to PBS injected control ($P < 0.05$; Figure 5.6C). In contrast, injection of 300 nM H_2O_2 produced a significantly higher mRNA level of *OPG* compared with control ($P < 0.05$; Figure 5.6C), and the expression of *SOX9* showed a trend of increasing with higher doses of H_2O_2 treatment ($P = 0.054$; Figure 5.6C). But H_2O_2 treatment did not change the mRNA expression of *ALP*, *BGLAP*, *BMP2* or *RUNX2* at 24 h post-injection. For correlation analysis, *RUNX2* was positively correlated with the expression of *SOD1* ($P < 0.001$, $R^2 = 0.253$), and *BMP2* was positively correlated with the expression of *SOD1* ($P = 0.002$, $R^2 = 0.218$) and *NOS2* ($P = 0.002$, $R^2 = 0.106$).

At 48 h post-injection, 300 nM H_2O_2 caused a significant increase in the expression of *CASP3*, an apoptotic marker gene, as compared to controls ($P < 0.05$; Figure 5.7A). The 30 nM H_2O_2 treatment significantly increased the expression of *SOD1* compared to the control ($P < 0.05$; Figure 5.7B); A trend of increasing in expression of

GPX1 was observed in low H_2O_2 treatments ($P = 0.065$; Figure 5.7B). H_2O_2 has an inhibitory effect on the embryonic bone formation. Expression of *RUNX2* was significantly decreased in the groups treated with H_2O_2 (10, 30, 100 and 300 nM) as compared to the PBS-injected control group ($P < 0.05$; Figure 5.7C), where expression of *BMP2* was significantly decreased in the groups treated with 10, 30 and 100nM H_2O_2 as compared to the control group ($p < 0.05$; Figure 5.7C). The mRNA expression of *OPG* was significantly increased by 300 nM H_2O_2 injection compared to the PBS injected control ($P < 0.05$; Figure 5.7C). The mRNA expression of *BGLAP* were significantly decreased by 30, 100, and 300 nM of H_2O_2 ($P < 0.05$; Figure 5.7C), whereas H_2O_2 treatment did not change mRNA expression of *SPP1*, *COL2A1*, *COL1A2* and *SOX9* ($P > 0.05$). For correlation analysis, *RUNX2* was positively correlated with the expression of *iNOS* ($P < 0.001$, $R^2 = 0.529$; Figure 5.7D), and *BMP2* was positively correlated with the expression of *iNOS* ($P = 0.013$, $R^2 = 0.200$; Figure 5.7D). *COL2A1* was positively correlated with the expression of *iNOS* ($P = 0.018$, $R^2 = 0.186$; Figure 5.7D), and *SOX9* was positively correlated with *iNOS* ($P = 0.003$, $R^2 = 0.272$; Figure 5.7D). However, *COL1A2* was negatively correlated with expression of *CAT* ($P = 0.020$, $R^2 = 0.202$; Figure 5.7D).

At 72 h of post-injection and the lethality rates were up to near 35%, but the mortality rate was not in a dose-depend manner. Besides, there were no significant changes in the expression of apoptosis-related marker genes among the treatments (*CASP3*, *CASP9* and *BCL2*; Figure 5.8A). Results showed a trend of increase in the expression of *CAT* ($P = 0.065$; Figure 5.8B) and *GPX1* ($P = 0.062$; Figure 5.8B) with

lower doses of H_2O_2 treatment. In addition, 10 nM and 100 nM of H_2O_2 significantly increased the expression of *COL1A2* compared with the control ($P < 0.05$; Figure 5.8C). The highest dose of H_2O_2 (300nM) suppressed the expression of *SPP1, ALP, RUNX2* and *BMP2* compared to the control ($P < 0.05$; Figure 5.8C). Moreover, *BGLAP* showed a trend of decreasing with higher H_2O_2 treatments ($P = 0.053$; Figure 5.8C). There was no difference in the expression of *OPG*, *COL2A1* and *SOX9* ($P > 0.05$). For correlation analysis, *RUNX2* was positively correlated with the expression of *iNOS* ($P = 0.008$, $R^2 = 0.233$) and *GPX* ($P = 0.023$, $R^2 = 0.189$). *COL2A1* was positively correlated with the expression of *SOD1* ($P = 0.046$, $R^2 = 0.140$), and *SOX9* was positively correlated with *GPX1* ($P = 0.003$, $R^2 = 0.292$).

Discussion

Based on the current data, we conclude that the injection of H_2O_2 altered the mRNA expression pattern of antioxidant enzyme during the early embryogenesis (ED 3 to ED 7). H_2O_2 induced oxidative stress suppressed bone formation gene marker expression with chronic effects. Oxidative stress negatively affects a number of performance parameters, such as feed consumption, egg production, and the meat quality of broilers (Mishra and Jha, 2019). In addition, the dwindling mineral content and changed physiologic characteristics of broilers bone during periods of oxidative stress have been reported in *in vivo* studies (Tompkins, et al., 2022). The chick embryo can serve as an excellent *in vivo* model for investigating the correlation between H_2O_2-induced oxidative stress and bone deformation because it allows measurable parameters in bone formation to be evaluated during early embryonic development. In order to

further understand the possible link between oxidative stress and bone homeostasis, the embryonic study was carried out in the current study. H_2O_2 is an active oxidizing reagent that can react with protein and lipids in embryos. While there are several potential delivery routes, such as air cell, amniotic sac, yolk sac or directly into the chicken embryos (Paradowska, et al., 2022), the direct injection to circulatory system via dorsal aorta ensures delivery to the embryo and provides immediate impact on the measurable gene expression (Jassim, et al., 1996; Surai, et al., 2016). Besides, dorsal aorta is a morphogenetic signaling center that initiates a molecular cascade of bone formation and secreted bone morphogenetic proteins (BMPs) during early embryonic development (Tzahor, et al., 2003; Sato, 2013). With the current injection method, H_2O_2-induced oxidative stress had a great chance of directly mediating key proteins for bone formation at the early embryonic development stage, and as the result presented, a suppressed collagen synthesis was observed under H_2O_2-induced oxidative stress. The pitfall of this injection method was associated with egg turn limitation after injection. ED 3 to ED 7 is a critical period for egg-turning in artificial chicken egg incubation (Deeming, 2009). Lack of egg-turning is detrimental to hatchability and embryo growth. But in the current study, in order to monitor the embryo viability through the shell window, the eggs had not been turning. It possibly caused the low embryo viability rate at 72 h of the incubation study period.

In the present study, the expression level of antioxidant enzymes genes was altered by low concentrations of H_2O_2 treatment. More specifically, the increased expression of *iNOS* by 10 nM H_2O_2 treatment was observed at 6 h and 72 h. The changed

expression of *SOD1* at 48 h as well as a trend of changed expression of *GPX1* at 6h, 48 h and 72h were also observed. The changed expression of the antioxidant enzyme genes showed the stimulation of the antioxidant defense system in the embryos. Antioxidant defense systems elaborately protect the embryo against lipid peroxidation derived from undesirable conditions (Yang, et al., 2021), and antioxidant content and antioxidant enzyme activity are positively correlated to the embryonic growth rate (Mousseau, 1998; Deeming and Pike, 2013; Parolini, et al., 2018). When the oxidative stress level is relatively low at a nontoxic level, the negative impact of H_2O_2 is reversible, and the alternation of oxidation reduction (redox) status can induce changes in mRNA expression of antioxidant enzymes, including superoxide dismutase, catalase, and peroxidases to regulate ROS level (Pomari, et al., 2014; Dell'Orco, et al., 2016). Although the changed expression of the antioxidant enzyme gene was not dose-dependent, we hypothesize that different treatment concentrations might have interacted with varying pathways of regulation and activated various defense metabolisms.

In current study, the expression of several osteogenesis marker genes was used to assess skeletal growth patterning under oxidative stress during the early embryonic development. Although chondrogenesis and osteogenesis are considered to be two separate processes during endochondral bone formation, chondrogenesis and osteogenesis processes closely share the signing pathway and co-regulator embryonic chondrogenesis and osteogenesis, thus two processes can be considered as a continuous developmental process (Jing, et al., 2017). In the early embryonic development stages, chondrogenesis is considered to be the earliest phase of bone formation and skeletal

development (Yoshino, et al., 2016). The avian embryonic skeletogenesis was modulated by signaling pathways including Shh, BMPs and FGF (Bruderer, et al., 2014; Pines and Reshef, 2015). Key regulators such as Runt-related transcription factor 2 (RUNX2) and BMPs are excellent transcriptional biomarkers to detect signaling changes in chondrification and osteogenesis during embryonic growth (Montero, et al., 2017; Chen, et al., 2021). RUNX2 and BMP are required for the expression of osteoblast and chondrocyte phenotype hallmarks, such as bone gamma-carboxyglutamate protein (*BGLAP*), secreted phosphoprotein 1 (*SPP1*, osteopontin), collagen type I alpha 2 chain (*COL1A2*), SRY-box transcription factor 9 (*SOX9*), and collagen type II alpha 1 chain (*COL2A1*). These markers are widely accepted biomarkers of new bone formation and growth (Javed, et al., 2010). We have observed a clear inhibitory function of H_2O_2 in osteogenesis after 72 h post-injection. At 6 h of post-injection, mRNA of *Col1A2* was suppressed by H_2O_2 injection; Decreased mRNA expression levels of *Col1A2* and *Col2A1* were observed at 24 h post-injection. It is well known that collagen fibers are crucial in primary mineralization process and bone strength (Garnero, 2012). The synthesis of collagen is regulated at the transcriptional and posttranslational levels (Karna, et al., 2020). Previous studies have detected a drastic increased level of *COL1A1* and *COL2A1* collagens RNA expression between ED 5 and ED 10 days of chick embryos (Merlino, et al., 1983). ROS suppresses collagen expression and stimulates collagen degradation (Laurent, 1987; Siwik, et al., 2001). Inhibited collagen production after oxidative stress exposure have been reported in various cell types, including muscle and cardiac fibroblasts (Merlino, et al., 1983; Siwik, et al., 2001). Therefore, we hypothesized

that the effects of oxidative stress at early development will initially inhibit collagen production, and the changes in collagen will interrupt bone formation and embryo development. Moreover, the expression profile of collagen types is essential to bone health, and changed expression patterns of collagen types have been associated with bone disorder in chickens. For example, chondrocytes derived from dyschondroplasic growth plates exhibited reduced type X collagen and increased type I collagen (Wardale and Duance, 1996). With the information above, it can be explained that increased expression of type I collagen at 72 h post-injection possibly signified chondrocyte dedifferentiation, and the altered expression profile of collagen types is closely associated with oxidative stress during embryonic development stages.

Several studies showed bone morphogenetic protein (BMP) is significant for skeletogenesis by mediating chondrogenic differentiation and osteogenic differentiation (Bandyopadhyay, et al., 2006; Yoshino, et al., 2016; Jing, et al., 2017). RUNX2 is a downstream target of BMPs, and both proteins are essential in inducing bone formation and osteoblast differentiation (Gaur, et al., 2005; Bruderer, et al., 2014). RUNX2 functions as the master regulatory factor that regulates osteoblast progenitors' proliferation, the commitment of stem cells to osteoblast lineage cells, and the expression of bone matrix protein genes (Komori, 2019). RUNX2 also mediates chondrocyte hypertrophy, contributing to longitudinal bone growth (Barreto and Wilsman, 1994; Li and Dong, 2016; Yoshino, et al., 2016). Notably, there was a relatively high correlation between the expression of *iNOS* with *RUNX2* and *BMP2* at 48 h post-injection (R^2 = 0.529) in the present study. iNOS activity and NO production have been implicated in

bone development and homeostasis (Amin and Abramson, 1998; An, et al., 2020). However, the function of NO on stem cell differentiation capacity stays controversial. For example, the studies with mice bone cell lines reported that cytokine-induced NO production inhibited osteoblast differentiation *in vitro* (Armour, et al., 2001; An, et al., 2020), whereas other studies demonstrated NO stimulated bone marrow-derived mesenchymal stem cells (MSCs) go through osteogenic differentiation (Ocarino, et al., 2008). NO also showed detrimental effects on chondrocyte function by inhibiting collagen synthesis and enhancing apoptosis (Amin and Abramson, 1998). Even though the possible role of iNOS activity in the current experiment remains unknown, but the result indicated that the decreased collagen mRNA level and decreased bone formation gene markers might involve a complex crosstalk between the presence of H_2O_2 and NO production. However, more evidences are needed.

Various factors in poultry production, including maternal nutrition and animal husbandry, are associated with oxidative stress in offspring. Oxidative stress can be an important factor that determines chick quality by the impact on bone growth during early development. Because animals metabolically produce different reactive oxygen species (ROS), effective antioxidant components, including vitamins A, C, and E, glutathione, and antioxidant enzymes, are essential in protecting the organism against damage caused by ROS. In avian species, the embryo develops within the confines of the closed egg. The egg contents, such as yolk lipid profile, albumin, hormone level, and antioxidant level, provide the nourishment required for healthy embryonic development and protection (Zhang, et al., 2013; Corino and Rossi, 2021). Avian embryos undergo rapid

development over a relatively short period of time and consequently experience high metabolic rates as well as high production rates of ROS (Watson, et al., 2018). Whether or not an increased oxidative challenge causes oxidative damage to the developing embryo is likely to depend on the capacity of yolk-derived antioxidants to buffer developing tissues (Surai, 2002). The antioxidant utilization during embryonic development or fertilized egg storage can result in antioxidant depletion, which causes oxidative stress. For example, a previous study showed a long egg storage time of eggs resulted in upregulated expression of pro-apoptotic gene and down-regulated expression of antioxidative gene in embryos compared with a short storage time group (Bakst, et al., 2016). Furthermore, it has been reported that antioxidants such as vitamin E in newly hatched chicks were dramatically depleted during the first few days (Surai, 2000; Surai, et al., 2016). Excessed ROS production results in oxidative damage to alter the cell fate decisions that can lead to structural and functional changes in developing animals during embryonic development (Mishra and Jha, 2019). Furthermore, oxidative stress during the chicken early development can deplete leftover nutrient in the egg and put the early post-hatch development in a disadvantage. Thus, maternal antioxidant supplementation could benefit offspring by improving oxidative stress defense and protecting the tissues of the progeny from oxidative injury (Li, et al., 2020). Embryo-skeletal growth is vital for chicks to break through the eggshell for successfully hatch. Poor embryonic bone quality will waste more energy in the process of hatching and is associated with lower hatchability (van der Pol, et al., 2014). The current study has provided direct evidence of the niche between oxidative stress and early embryonic bone development. We further

propose that maternal antioxidant supplementation has the potential to protect bone homeostasis from potential oxidative stress damage and eventually contribute to bone structural and metabolic integrity during embryonic development.

References

Amin, A. R., and S. B. Abramson. 1998. The role of nitric oxide in articular cartilage breakdown in osteoarthritis. Curr Opin Rheumatol 10:263-268.

An, S. Y., H. J. Lee, S. C. Lee, and J. S. Heo. 2020. Supplement of nitric oxide through calcium carbonate-based nanoparticles contributes osteogenic differentiation of mouse embryonic stem cells. Tissue Cell 66:101390.

Armour, K. J., K. E. Armour, R. J. Van 't Hof, D. M. Reid, X.-Q. Wei, F. Y. Liew, and S. H. Ralston. 2001. Activation of the inducible nitric oxide synthase pathway contributes to inflammation-induced osteoporosis by suppressing bone formation and causing osteoblast apoptosis. Arthritis & Rheumatism 44:2790-2796.

Bakst, M. R., G. R. Welch, R. Fetterer, and K. Miska. 2016. Impact of broiler egg storage on the relative expression of selected blastoderm genes associated with apoptosis, oxidative stress, and fatty acid metabolism. Poult Sci 95:1411-1417.

Bandyopadhyay, A., K. Tsuji, K. Cox, B. D. Harfe, V. Rosen, and C. J. Tabin. 2006. Genetic analysis of the roles of BMP2, BMP4, and BMP7 in limb patterning and skeletogenesis. PLoS Genet 2:e216.

Barreto, C., and N. J. Wilsman. 1994. Hypertrophic chondrocyte volume and growth rates in avian growth plates. Research in Veterinary Science 56:53-61.

Ben-Yair, R., and C. Kalcheim. 2010. Single cell transfection in chick embryos. J Vis Exp.

Bruderer, M., R. G. Richards, M. Alini, and M. J. Stoddart. 2014. Role and regulation of RUNX2 in osteogenesis. Eur Cell Mater 28:269-286.

Chen, C., D. L. White, B. Marshall, and W. K. Kim. 2021. Role of 25-Hydroxyvitamin D3 and 1,25-Dihydroxyvitamin D3 in Chicken Embryo Osteogenesis, Adipogenesis, Myogenesis, and Vitamin D3 Metabolism. Front Physiol 12:637629.

Corino, C., and R. Rossi. 2021. Antioxidants in Animal Nutrition. Antioxidants (Basel) 10.

Covarrubias, L., D. Hernandez-Garcia, D. Schnabel, E. Salas-Vidal, and S. Castro-Obregon. 2008. Function of reactive oxygen species during animal development: passive or active? Dev Biol 320:1-11.

Deeming, D. C. 2009. The Role of Egg Turning during Incubation. Avian Biology Research 2:67-71.

Deeming, D. C., and T. W. Pike. 2013. Embryonic growth and antioxidant provision in avian eggs. Biol Lett 9:20130757.

Dell'Orco, M., P. Milani, L. Arrigoni, O. Pansarasa, V. Sardone, E. Maffioli, F. Polveraccio, M. Bordoni, L. Diamanti, M. Ceroni, F. A. Peverali, G. Tedeschi, and C. Cereda. 2016. Hydrogen peroxide-mediated induction of SOD1 gene transcription is independent from Nrf2 in a cellular model of neurodegeneration. Biochim Biophys Acta 1859:315-323.

Dennery, P. A. 2004. Role of redox in fetal development and neonatal diseases. Antioxid Redox Signal 6:147-153.

Dennery, P. A. 2007. Effects of oxidative stress on embryonic development. Birth Defects Res C Embryo Today 81:155-162.

Dennery, P. A. 2010. Oxidative stress in development: nature or nurture? Free Radic Biol Med 49:1147-1151.

Domazetovic, V., G. Marcucci, T. Iantomasi, M. L. Brandi, and M. T. Vincenzini. 2017. Oxidative stress in bone remodeling: role of antioxidants. Clin Cases Miner Bone Metab 14:209-216.

Ebeid, T. A., F. A. Twfeek, M. H. Assar, A. M. Bealish, R. E. Abd El-Karim, and M. Ragab. 2017. Influence of pre-storage incubation on hatchability traits, thyroid hormones, antioxidative status and immunity of newly hatched chicks at two chicken breeder flock ages. Animal 11:1966-1974.

Garnero, P. 2012. The contribution of collagen crosslinks to bone strength. Bonekey Rep 1:182.

Gaur, T., C. J. Lengner, H. Hovhannisyan, R. A. Bhat, P. V. Bodine, B. S. Komm, A. Javed, A. J. van Wijnen, J. L. Stein, G. S. Stein, and J. B. Lian. 2005. Canonical WNT signaling promotes osteogenesis by directly stimulating Runx2 gene expression. J Biol Chem 280:33132-33140.

Gou, Z., Q. Fan, L. Li, Y. Wang, X. Lin, X. Cui, J. Ye, F. Ding, Z. Cheng, K. Abouelezz, and S. Jiang. 2021. High dietary copper induces oxidative stress and leads to decreased egg quality and reproductive performance of Chinese Yellow broiler breeder hens. Poult Sci 100:100779.

Hartcher, K. M., and H. K. Lum. 2019. Genetic selection of broilers and welfare consequences: a review. World's Poultry Science Journal 76:154-167.

Haussmann, M. F., A. S. Longenecker, N. M. Marchetto, S. A. Juliano, and R. M. Bowden. 2012. Embryonic exposure to corticosterone modifies the juvenile stress response, oxidative stress and telomere length. Proc Biol Sci 279:1447-1456.

Heidinger, B. J., J. D. Blount, W. Boner, K. Griffiths, N. B. Metcalfe, and P. Monaghan. 2012. Telomere length in early life predicts lifespan. Proc Natl Acad Sci U S A 109:1743-1748.

Jadhav*, J. T., and S. Kengar. 2016. Influence of hydrogen peroxide induced oxidative stress on survival rate of early chick embryo development. International Journal of Bioassays 5.

Jassim, E. W., M. Grossman, W. J. Koops, and R. A. Luykx. 1996. Multiphasic analysis of embryonic mortality in chickens. Poult Sci 75:464-471.

Javed, A., H. Chen, and F. Y. Ghori. 2010. Genetic and transcriptional control of bone formation. Oral Maxillofac Surg Clin North Am 22:283-293, v.

Jing, Y., J. Jing, L. Ye, X. Liu, S. E. Harris, R. J. Hinton, and J. Q. Feng. 2017. Chondrogenesis and osteogenesis are one continuous developmental and lineage defined biological process. Sci Rep 7:10020.

Karna, E., L. Szoka, T. Y. L. Huynh, and J. A. Palka. 2020. Proline-dependent regulation of collagen metabolism. Cell Mol Life Sci 77:1911-1918.

Komori, T. 2019. Regulation of Proliferation, Differentiation and Functions of Osteoblasts by Runx2. Int J Mol Sci 20.

Korhonen, A., K. Hemminki, and H. Vainio. 1984. Embryotoxic effects of eight organic peroxides and hydrogen peroxide on three-day chicken embryos. Environmental Research 33:54-61.

Korn, M. J., and K. S. Cramer. 2007. Windowing chicken eggs for developmental studies. J Vis Exp:306.

Laurent, G. J. 1987. Dynamic state of collagen: pathways of collagen degradation in vivo and their possible role in regulation of collagen mass. Am J Physiol 252:C1-9.

Li, J., and S. Dong. 2016. The Signaling Pathways Involved in Chondrocyte Differentiation and Hypertrophic Differentiation. Stem Cells Int 2016:2470351.

Li, K., L. Jiang, J. Wang, L. Xia, R. Zhao, C. Cai, P. Wang, X. Zhan, and Y. Wang. 2020. Maternal dietary supplementation with different sources of selenium on antioxidant status and mortality of chicken embryo in a model of diquat-induced acute oxidative stress. Animal Feed Science and Technology 261.

Merlino, G., C. McKeon, B. de Crombrugghe, and I. J. J. o. B. C. Pastan. 1983. Regulation of the expression of genes encoding types I, II, and III collagen during chick embryonic development. 258:10041-10048.

Mishra, B., and R. Jha. 2019. Oxidative Stress in the Poultry Gut: Potential Challenges and Interventions. Front Vet Sci 6:60.

Moghaddam, H. S., S. Samarghandian, and T. Farkhondeh. 2015. Effect of bisphenol A on blood glucose, lipid profile and oxidative stress indices in adult male mice. Toxicol Mech Methods 25:507-513.

Montero, J. A., C. I. Lorda-Diez, J. Francisco-Morcillo, J. Chimal-Monroy, J. A. Garcia-Porrero, and J. M. Hurle. 2017. Sox9 Expression in Amniotes: Species-Specific Differences in the Formation of Digits. Front Cell Dev Biol 5:23.

Mousseau, T. 1998. The adaptive significance of maternal effects. Trends in Ecology & Evolution 13:403-407.

Newton, P. T., L. Li, B. Zhou, C. Schweingruber, M. Hovorakova, M. Xie, X. Sun, L. Sandhow, A. V. Artemov, E. Ivashkin, S. Suter, V. Dyachuk, M. El Shahawy, A. Gritli-Linde, T. Bouderlique, J. Petersen, A. Mollbrink, J. Lundeberg, G. Enikolopov, H. Qian, K. Fried, M. Kasper, E. Hedlund, I. Adameyko, L. Savendahl, and A. S. Chagin. 2019. A radical switch in clonality reveals a stem cell niche in the epiphyseal growth plate. Nature 567:234-238.

Ocarino, N. M., J. N. Boeloni, A. M. Goes, J. F. Silva, U. Marubayashi, and R. Serakides. 2008. Osteogenic differentiation of mesenchymal stem cells from osteopenic rats subjected to physical activity with and without nitric oxide synthase inhibition. Nitric Oxide 19:320-325.

Paradowska, M., A. Dunislawska, M. Siwek, and A. Slawinska. 2022. Avian Cell Culture Models to Study Immunomodulatory Properties of Bioactive Products. Animals (Basel) 12.

Parolini, M., C. D. Possenti, F. Karadas, G. Colombo, M. Romano, M. Caprioli, I. Dalle-Donne, D. Rubolini, A. Milzani, and N. Saino. 2018. Yolk vitamin E positively affects prenatal growth but not oxidative status in yellow-legged gull embryos. Curr Zool 64:285-292.

PF, S. 2002. Natural antioxidants in avian nutrition and reproduction. Nottingham: Nottingham University Press.

Pines, M., and R. Reshef. 2015. Poultry bone development and bone disorders. Pages 367-377 in Sturkie's Avian PhysiologyElsevier.

Pomari, E., B. Stefanon, and M. Colitti. 2014. Effect of plant extracts on H2O2-induced inflammatory gene expression in macrophages. J Inflamm Res 7:103-112.

Prater, M. R., C. L. Laudermilch, C. Liang, and S. D. Holladay. 2008. Placental oxidative stress alters expression of murine osteogenic genes and impairs fetal skeletal formation. Placenta 29:802-808.

Rath, N. C., and V. Durairaj. 2022. Avian bone physiology and poultry bone disorders. Pages 529-543 in Sturkie's Avian PhysiologyElsevier.

Reijrink, I. A., R. Meijerhof, B. Kemp, E. A. Graat, and H. van den Brand. 2009. Influence of prestorage incubation on embryonic development, hatchability, and chick quality. Poult Sci 88:2649-2660.

Saleh, K. M. M., A. H. Tarkhan, and M. B. Al-Zghoul. 2020. Embryonic Thermal Manipulation Affects the Antioxidant Response to Post-Hatch Thermal Exposure in Broiler Chickens. Animals (Basel) 10.

Sato, Y. 2013. Dorsal aorta formation: separate origins, lateral-to-medial migration, and remodeling. Dev Growth Differ 55:113-129.

Serdar, C. C., M. Cihan, D. Yucel, and M. A. Serdar. 2021. Sample size, power and effect size revisited: simplified and practical approaches in pre-clinical, clinical and laboratory studies. Biochem Med (Zagreb) 31:010502.

Siwik, D. A., P. J. Pagano, and W. S. Colucci. 2001. Oxidative stress regulates collagen synthesis and matrix metalloproteinase activity in cardiac fibroblasts. Am J Physiol Cell Physiol 280:C53-60.

Surai, P. F. 2000. Effect of selenium and vitamin E content of the maternal diet on the antioxidant system of the yolk and the developing chick. Br Poult Sci 41:235-243.

Surai, P. F. 2002. Natural antioxidants in avian nutrition and reproduction. Nottingham University Press Nottingham.

Surai, P. F., V. I. Fisinin, and F. Karadas. 2016. Antioxidant systems in chick embryo development. Part 1. Vitamin E, carotenoids and selenium. Anim Nutr 2:1-11.

Thiese, M. S., B. Ronna, and U. Ott. 2016. P value interpretations and considerations. J Thorac Dis 8:E928-E931.

Thompson, L. P., and Y. Al-Hasan. 2012. Impact of oxidative stress in fetal programming. J Pregnancy 2012:582748.

Tompkins, Y. H., P. Teng, R. Pazdro, and W. K. Kim. 2022. Long Bone Mineral Loss, Bone Microstructural Changes and Oxidative Stress After Eimeria Challenge in Broilers. Front Physiol 13:945740.

Tona, K., F. Bamelis, B. De Ketelaere, V. Bruggeman, V. M. Moraes, J. Buyse, O. Onagbesan, and E. Decuypere. 2003. Effects of egg storage time on spread of hatch, chick quality, and chick juvenile growth. Poult Sci 82:736-741.

Tzahor, E., H. Kempf, R. C. Mootoosamy, A. C. Poon, A. Abzhanov, C. J. Tabin, S. Dietrich, and A. B. Lassar. 2003. Antagonists of Wnt and BMP signaling promote the formation of vertebrate head muscle. Genes Dev 17:3087-3099.

van der Pol, C. W., I. A. van Roovert-Reijrink, C. M. Maatjens, I. van den Anker, B. Kemp, and H. van den Brand. 2014. Effect of eggshell temperature throughout incubation on broiler hatchling leg bone development. Poult Sci 93:2878-2883.

Wardale, R. J., and V. C. Duance. 1996. Collagen expression in chicken tibial dyschondroplasia. J Cell Sci 109 (Pt 5):1119-1131.

Watson, H., P. Salmon, and C. Isaksson. 2018. Maternally derived yolk antioxidants buffer the developing avian embryo against oxidative stress induced by hyperoxia. J Exp Biol 221.

Yang, J., K. Y. Zhang, S. P. Bai, J. P. Wang, Q. F. Zeng, H. W. Peng, Y. Xuan, Z. W. Su, and X. M. Ding. 2021. The impacts of egg storage time and maternal dietary vitamin E on the growth performance and antioxidant capacity of progeny chicks. Poult Sci 100:101142.

Yoshino, T., H. Murai, and D. Saito. 2016. Hedgehog-BMP signalling establishes dorsoventral patterning in lateral plate mesoderm to trigger gonadogenesis in chicken embryos. Nat Commun 7:12561.

Zhang, J., O. P. Lazarenko, M. L. Blackburn, T. M. Badger, M. J. Ronis, and J. R. Chen. 2013. Blueberry consumption prevents loss of collagen in bone matrix and inhibits senescence pathways in osteoblastic cells. Age (Dordr) 35:807-820.

Tables

Table 5.1. Nucleotide sequences of the primers used for quantitative real-time RT-PCR.

Gene1	Primer sequence (5'-3')	Product length (bp)	Annealing temperature (°C)	Accession #
GAPDH	F-GCTAAGGCTGTGGGGAAAGT R-TCAGCAGCAGCCTTCACTAC	161	55	NM_204305.1
HMBS	F- GGCTGGGAGAATCGCATAGG R- TCCTGCAGGGCAGATACCAT	131	59	XM_004947916.3
ACTB	F-CAACACAGTGCTGTCTGGTGGTA R-ATCGTACTCCTGCTTGCTGATCC	205	61	NM_205518.1
ALPL	F-CGACCACTCACACGTCTTCA R-CGATCTTATAGCCAGGGCCG	140	60	NM_205360.1
RUNX2	F-ACTTTGACAATAACTGTCCT R-GACCCCTACTCTCATACTGG	192	60	XM_015285081.2
BGLAP	F-GGATGCTCGCAGTGCTAAAG R-CTCACACACCTCTCGTTGGG	142	57	NM_205387.3
SPP1	F-GCCCAACATCAGAGCGTAGA R-ACGGGTGACCTCGTTGTTTT	204	57	NM_204535.4
BMP2	F-TCAGCTCAGGCCGTTGTTAG R-GTCATTCCACCCCACGTCAT	163	57	XM_025148488.1
OPG	F-ACGCTTGTGCTCTTGGACAT R-CAGCGTAGTACTGGTCTGGG	193	60	NM_001033641.1

COL1A2	F- CTGGTGAAAGCGGTGCTGTT R-CACCAGTGTCACCTCTCAGAC	222	60	NM_001079714.2
COL2A1	F- GGACCAGCAAGACGAAAGAC R-TGTAGGCGATGCTGTTCTTG	189	59	NM_204426.2
SOX9	F-AGGAAGCTGGCTGACCAGTA R-CGTTCTTCACCGACTTCCTC	193	61	XM_046929245.1
SOD1	F-ATTACCGGCTTGTCTGATGG R-CCTCCCTTTGCAGTCACATT	173	58	NM_205064.1
CAT	F-ACTGCAAGGCGAAAGTGTTT R-GGCTATGGATGAAGGATGGA	222	60	NM_001031215.1
NOS2	F-CCTGTACTGAAGGTGGCTATTGG R-AGGCCTGTGAGAGTGTGCAA	66	58	NM_204961.2
GPX1	F-AACCAATTCGGGCACCAG R-CCGTTCACCTCGCACTTCTC	122	60	NM_001277853.2
CASP3	F-TGGTATTGAAGCAGACAGTGGA R-GGAGTAGTAGCCTGGAGCAGTAGA	103	60	XM_015276122.2
CASP9	F-ATTCCTTTCCAGGCTCCATC R- CACTCACCTTGTCCCTCCAG	130	60	XM_046931415.1
BCL2	F-GAGTTCGGCGGCGTGATGTG R-TTCAGGTACTCGGTCATCCAGGTG	92	63	XM_046910476.1

[1] GAPDH: glyceraldehyde-3-phosphate dehydrogenase; HMBS: hydroxymethylbilane synthase; ACTB: actin beta; OPG: TNFRSF11B, TNF receptor superfamily member 11b; IL1B: interleukin 1 beta; SPP1: secreted phosphoprotein, osteopontin; BMP2:

bone morphogenetic protein 2; BGLAP: bone gamma-carboxyglutamic acid-containing protein (osteocalcin). RUNX2: runt-related transcription factor 2; ALPL: alkaline phosphatase, biomineralization associated; COL1A2: collagen type I alpha 2 chain; COL2A1: collagen type II alpha 1 chain; SOX9: SRY-box transcription factor 9; CAT: catalase; SOD: superoxide dismutase; GPX1: glutathione peroxidase 1; NOS2: nitric oxide synthase 2; CASP3: caspase 3, apoptosis-related cysteine protease; CASP9: caspase 9, apoptosis-related cysteine protease; BCL2: anti-apoptotic gene B-cell lymphoma 2

Figures

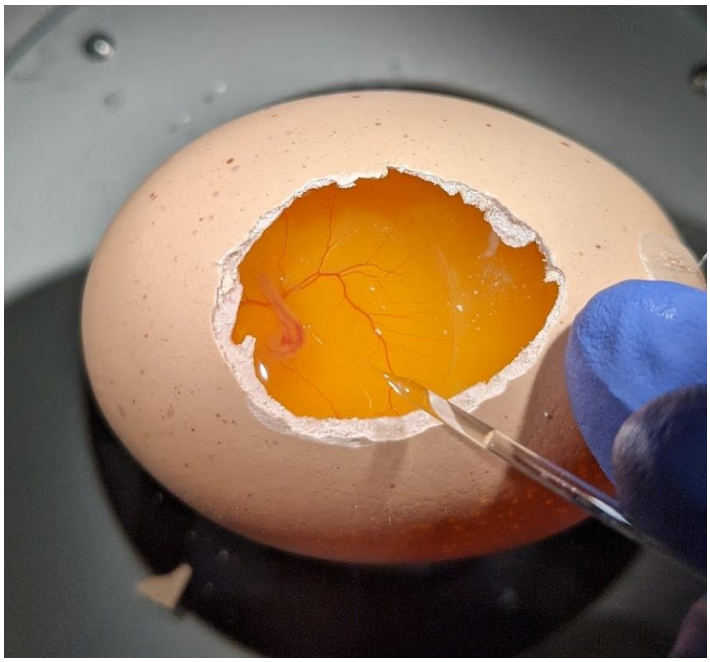

Figure 5.1: Illustration of microinjection method on chicken embryos at embryo day 3 (ED3). The dorsal aorta was pierced using the tip of micropipettes, and sample volume of hydrogen peroxide (H_2O_2) treatment solutions were injected into Cobb500 embryos. Glass coverslips (24 X 55 mm) were used to seal the observation windows, the treated embryos are returned to incubator without turning.

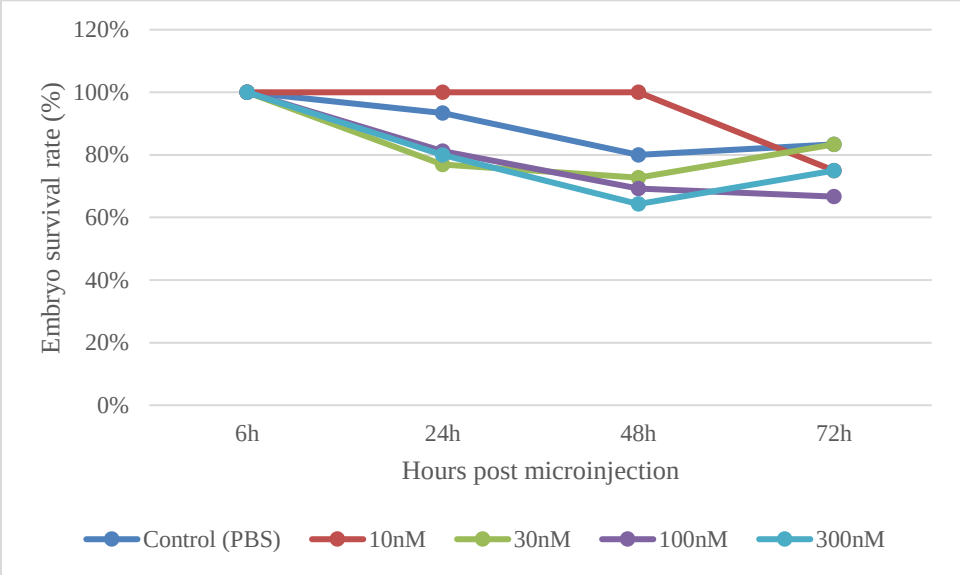

Figure 5.2. Embryo viability rate in the presence of different H_2O_2 concentrations at 6h, 24h, 48h and 72h post-injection. H_2O_2 treatment has no effect on mortality rate ($P > 0.05$; N = 16). Viability data from all the time points were pooled together for statistical analysis. Treatments were compared with the control using Dunnett's test.

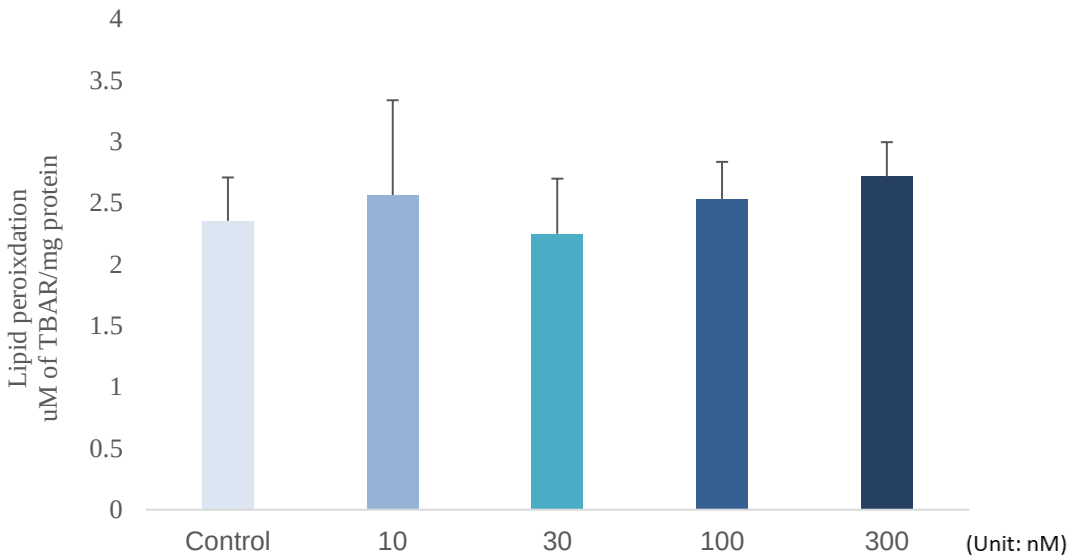

Figure 5.3. The effects of H_2O_2 on the lipid peroxidation (MDA ELISA method) in chick embryos at 72 h post-injection. whole embryo tissues were collected and homogenized, 50 uL tissues were used for TBAR analysis. H_2O_2 did not alter the embryonic lipid peroxidation at 72 h post-injection. The result indicated that the chicken embryo has fully covert active H2O2 residual into nonactive form at 72 h post-injection. Treatment groups were compared with the control using Dunnett's test ($P > 0.05$; N = 8).

Figure 5.4: A decreased embryo length was observed in 100 nM and 300 nM H_2O_2 groups compared to the PBS-injected control. (A) Illustration of embryo length measurement at E7 (72 h post-injection). (B) The length of the embryos was measured with a digital caliper. Each value represents the mean ± SEM (N = 6). Treatments with * showed a significant difference compared with the control using Dunnett's test, $p < 0.05$.

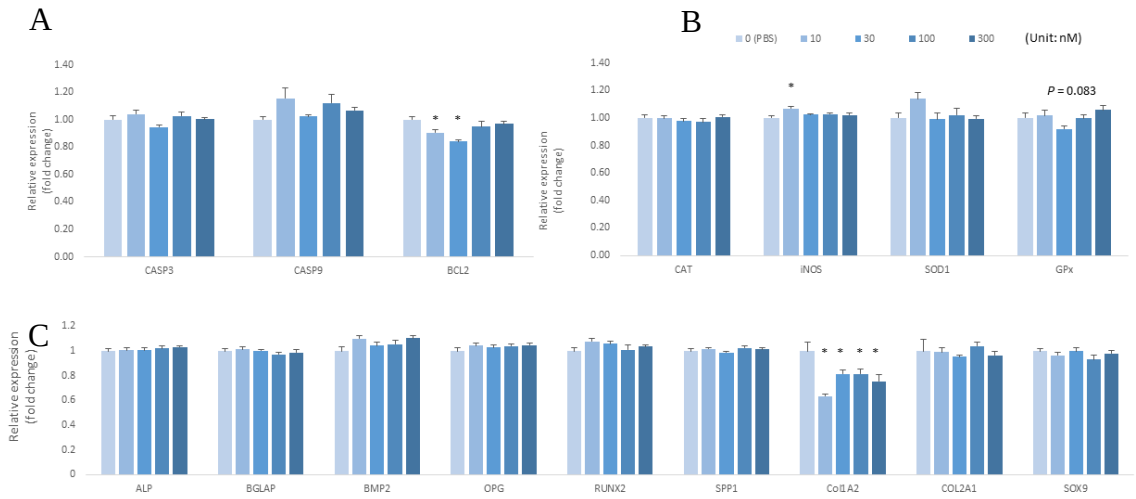

Figure 5.5: Effects of H_2O_2 on mRNA expression of several sets of genes in chicken embryos at 6 h post-injection. (A) apoptotic gene expression (B) Antioxidant enzyme gene expression (C) expression of bone formation biomarkers. Embryos were injected with different concentrations of H_2O_2 and continuously incubation for 6 h. Each value represents the mean ± SEM (N = 8). Treatments with * showed a significant difference compared with the control using Dunnett's test, $p < 0.05$.

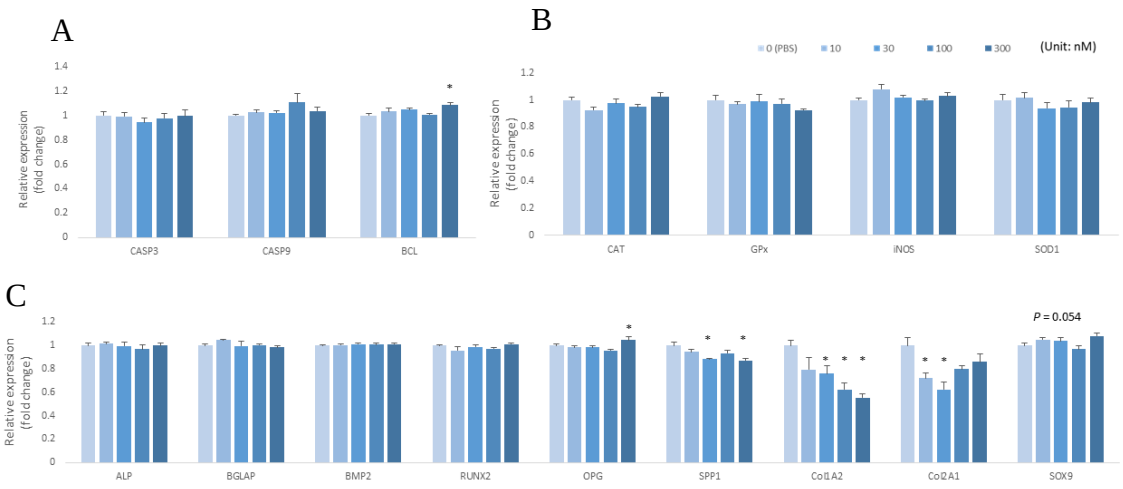

Figure 5.6: Effects of H_2O_2 on mRNA expression of several sets of genes in chicken embryos at 24 h post-injection. (A) apoptotic gene expression (B) antioxidant enzyme gene expression (C) expression of bone formation biomarkers. Embryos were injected with the different concentrations of H_2O_2 and continuously incubation for 24 h. Each value represents the mean ± SEM (N = 8). Treatments with * showed a significant difference compared with the control using Dunnett's test, $p < 0.05$.

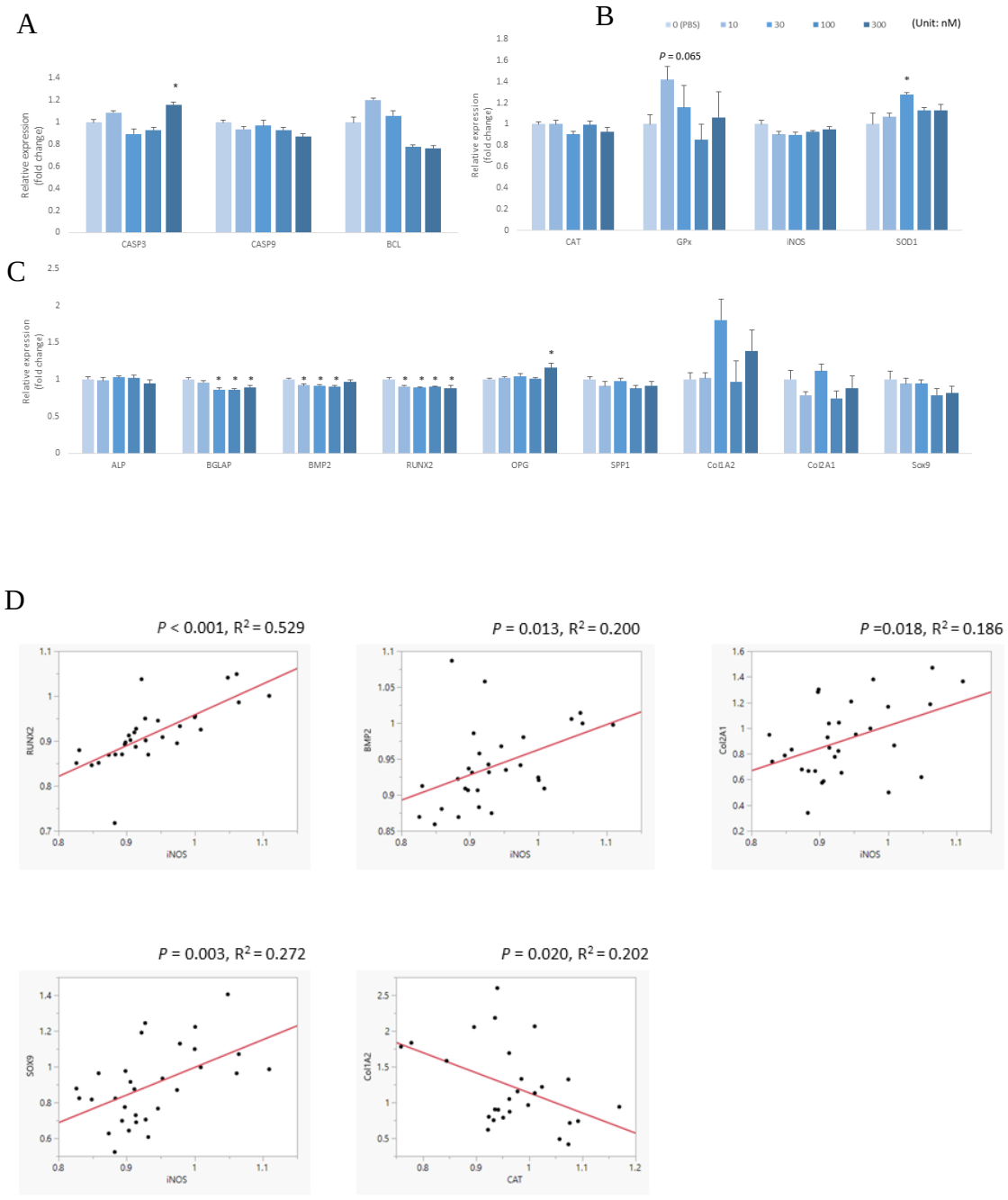

Figure 5.7: Effects of H_2O_2 on mRNA expression of three sets of genes in chicken embryos at 48 h post-injection. (A) apoptotic gene expression (B) antioxidant enzyme

gene expression (C) expression of bone formation biomarkers (D) correlation between mRNA expression of bone formation markers and antioxidant enzyme coding genes. Embryos were injected with different concentrations of H_2O_2 and continuously incubation for 48 h. Each value represents the mean ± SEM (N = 8). Treatments with * showed a significant difference compared with the control using Dunnett's test, $p < 0.05$.

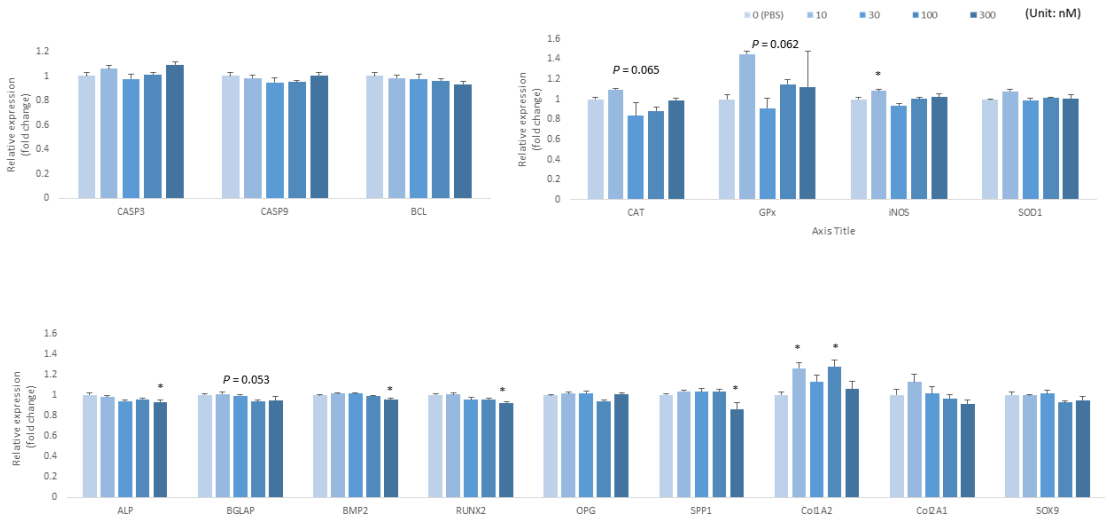

Figure 5.8: Effects of H_2O_2 on mRNA expression of three sets of genes in chicken embryos at 72 h post-injection. (A) apoptotic gene expression (B) antioxidant enzyme gene expression (C) expression of bone formation biomarkers. Embryos were injected with different concentrations of H_2O_2 and continuously incubation for 72 h. Each value represents the mean ± SEM (N = 8). Treatments with * showed a significant difference compared with the control using Dunnett's test, $p < 0.05$.

CHAPTER 6

N-3 ENRICHED FISH OIL DIET ENHANCES INTESTINAL BARRIER INTEGRITY AND REDUCES GROWTH PERFORMANCE LOSS IN BROILERS AFTER *EIMERIA* INFECTION [5]

[5]Yuguo Hou Tompkins, Venkata Sesha Reddy Choppa, Hanyi Shi, Woo Kyun Kim

To be submitted to *Biomolecules*

Abstract

Coccidiosis caused by *Eimeria spp.* has caused a substantial economic loss in the poultry industry. The objective of the present study was to test the effects of dietary supplementation of n-3 PUFA-enriched fish oil diet on growth performance, intestinal immune response, and bone characteristics in broilers challenged with *Eimeria spp*. A total of 576 14-days old broilers were randomly distributed according to a completely randomized design in a 3x2 factorial arrangement, including two different diets supplemented with either 5% fish oil or 5% soybean oil; Three *Eimeria* spp. infection levels, including non-challenge control, the low *Eimeria* challenge dose, and the high challenge dose. Results showed that *Eimeria* infection significantly decreased growth performance, increased gut lesion, altered intestinal morphology, and caused intestinal lesions. For diet variables, the fish oil supplement did not alter the total antioxidant level in the serum compared with the soybean oil diet but increased feed intake during the early infection stage (0-6 days post infection: DPI). Fish oil diet groups showed a trend of increase in body weight gain compared to the soybean oil groups under the *Eimeria* infection condition. Fish oil supplements significantly reduced gut permeability and reduced the intestinal lesion over the jejunum/ ileum junction compared to soybean oil. In conclusion, the dietary supplements of fish oil benefit gut health and growth performance under *the Eimeria* infection during the early infection stage, and short-term use of fish oil during the early infection stage can be a nutritional strategy to minimize growth performance loss during coccidiosis.

Keyword: fish oil; n-3 PUFA; coccidiosis; *Eimeria*; gut permeability; bone health

Introduction

With the market preference for drug-free poultry production, the gastrointestinal immune system is continuously challenged by intestinal pathogens infection (Smith, 2011; Gaucher, et al., 2015). Coccidiosis, one of the costliest parasitic diseases in the broiler industry, is caused by infection of *Eimeria spp*., which leads to intestinal damage (Dalloul and Lillehoj, 2006; Blake, et al., 2020). *Eimeria* infection interferes the poultry health and triggers the immune response, chicken can experience lower digestibility, poor nutrient absorption, low feed intake, and malnutrition that significantly suppresses growth and production under coccidia infection (Teng, et al., 2020a). In our previous studies, coccidiosis decreased bone mineral content and density in young broiler chickens infected with *Eimeria* (Tompkins, et al., 2022b). Several mechanical factors, including gut leakage and immunology cost, can lead to a low bone formation rate with the parasite infection model (Akbari Moghaddam Kakhki, et al., 2019).

Fish oil, which contains a high level of n-3 polyunsaturated fatty acids (n-3 PUFA), is widely accepted as a nutritional supplement in human studies. The two main bioactive n-3 PUFAs in fish oil are eicosatetraenoic acid (EPA; 20:5 n-3) and docosahexaenoic acid (DHA; 22:6 n-3) (Alagawany, et al., 2019). It is becoming increasingly clear that dietary n-3 PUFA can act as immune modulators, affecting both humoral and cellular responses in monogastric species (Fritsche and Cassity, 1992; Swiatkiewicz, et al., 2015; Al-Khalaifah, 2020). Long-chain n-3 PUFAs exhibit a natural anti-inflammatory property (Calder, 2006; Kalinski, 2012; Xiang, et al., 2016) because they can be incorporated into intestinal epithelial cell membranes, reduce the production

of pro-inflammatory cytokines, and induce the production of anti-inflammatory factors (Calder, 2006; Durkin, et al., 2021). Controlling intestinal inflammation with fish oil supplements can benefit intestinal health and protect intestinal mucosal barrier integrity under hostile environments, which is critical in maintaining efficient growth performance when defending against pathogenic condition (Lauridsen, 2020; Tarradas, et al., 2020; Durkin, et al., 2021). In the transgenic mice study, mice that endogenously biosynthesize n-3 PUFA and had high concentrations of EPA and DHA in intestinal epithelial cells were endowed with improved colon morphology traits and reduced epithelial lesion after dextran sodium sulfate exposure (Hudert, et al., 2006). DHA supplementation can ease the severity of necrosis in rat challenge model (Lu, et al., 2007). In pigs, EPA and DHA have been shown to reduce stress in wean piglets (Lee, et al., 2019; Lauridsen, 2020), and also improve barrier function in weaned pig after lipopolysaccharide challenges (Zhu, et al., 2016).

In poultry studies, several investigations have shown that a dietary n-3 PUFA-enriched diet significantly reduced broiler cecal lesions caused by *Eimeria tenella* (Allen, et al., 1996; Barua, et al., 2016). The reduction in cecal lesion was associated with decreased colonization and suppressed the development of coccidia (Allen, et al., 1996; Danforth, et al., 1997; Allen and Danforth, 1998; Barua, et al., 2016). Previous studies indicated that pro-oxidation nature of n-3 PUFA played a significant role in controlling coccidia development, where the incorporation of n-3 PUFA into both host and parasite membranes increased the volubility of the parasite and infected host, which altered the stability of the environment for the parasite to further develop (Danforth, et al., 1997).

With a more profound understanding of the benefit of fish oil as dietary supplement, studies also showed the protective role of fish oil in improving growth performance in broilers by presenting a high immune response to defend against coccidiosis (Barua, et al., 2016). Although there were some inconsistencies in the role of fish oil on broiler gut health with *Eimeria spp.* infection (Yang, et al., 2006), most conclusions agreed that the dietary supplementation of the n-3 PUFAs can be a potential dietary anticoccidial strategy confronting coccidiosis in poultry production (Allen, et al., 1996; Danforth, et al., 1997; Korver, et al., 1997; Allen and Danforth, 1998; Barua, et al., 2016). Moreover, several studies have reported the positive impact of n-3 PUFA on poultry bone health (Ebeid, et al., 2011; Tompkins, et al., 2022a). The broilers' bone mineral loss was closely associated with the inflammation with *Eimeria* infection (Akbari Moghaddam Kakhki, et al., 2019). With the anti-inflammatory property in gut health and the beneficial role in bone health, this study was focused on the impact of n-3 PUFA supplementation on broiler growth and gut integrity during *Eimeria* infection with an emphasis on bone homeostasis.

Materials and Methods

Ethics Statement

The protocol was approved by the Institutional Animal Care and Use Committee (IACUC) at the University of Georgia. The experiment followed the guideline of IACUC and was conducted at the Poultry Research Center, University of Georgia, Athens, GA.

Experimental Design

The experiment followed a 2 × 3 factorial design with diets and infection status as the main effects. Before birds were allocation into different treatment groups, broiler chicks were fed with same standard starter diet during 0-14 d of age. A total of 576 14-day-old male Cobb 500 (Cleveland, GA, USA) broiler chickens were randomly distributed into six treatment groups with eight replicates and twelve birds per cage. There are two diet variables, including 5% fish oil diet (Virginia Prime Gold, Omega Protein; Houston, TX, USA) and 5% soybean oil diet (Harvest value, US Foods; Austin, TX, USA), and three levels of *Eimeria* challenge doses, including non-challenge control: gavaged with water; Low *Eimeria spp*. challenge dose: gavaged with 12,500 oocysts of *E. maxima*; 12,500 oocysts of *E. tenella*; 62,500 oocysts of *E. acervulina*; and High challenge dose: gavaged with 50,000 oocysts of *E. maxima*, 50,000 oocysts of *E. tenella*, and 250,000 oocysts of *E. acervuline*. The fatty acid profiles of fish oil and soybean oil are shown in Table 6.1. Experimental groups included T1: uninfected broilers fed soybean oil diet *ad libitum*; T2: uninfected broilers fed fish oil diet *ad libitum*; T3: a low *Eimeria*-infected group fed soybean oil diet *ad libitum*; T4: a low *Eimeria*-infected group (Low) fed fish oil diet *ad libitum*; T5: a severely *Eimeria*-infected group (High) fed soybean oil diet *ad libitum* diet; and T6: a severely *Eimeria*-infected group (High) fed fish oil diet *ad libitum* diet. All chicks were raised under the same house, feeding and environmental management conditions based on the Cobb500 broiler management guide (Cobb, 2019). Both starter and grower (15-26 d of age) diets were formulated following the Cobb500 broiler management guide. Diet information is shown in Table

6.2. Chicks were allowed to consume water on an *ad libitum* basis, and daily feed intake was measured during the study.

Growth performance and body composition

The body weight (BW) of birds was recorded on the first day of the experiment (0 day post-infection; 0 DPI), 6 DPI, and 12 DPI. The body weight gain (BWG), feed intake (FI), and feed conversion ratio (FCR) were calculated through 0-6 DPI and 7-12 DPI. Any mortalities were removed and recorded to adjust FCR.

Dual energy x-ray absorptiometry (DEXA; GE Healthcare, Chicago, IL, USA) was used to determine the body composition on 6 and 12 DPI. Three birds per pen were randomly selected for body composition measurement at each time point. After euthanasia, the birds were placed face-up on the DEXA scanner and scanned using the small animal software module (Lunar Prodigy from GE, encore software version 12.20.023, GE Medical Systems, Madison, WI, USA). After defining the whole bird as a region of interest (ROI), the DEXA provided measurements in bone mineral content (BMC), bone mineral density (BMD), fat mass, lean mass, fat percentage, lean percentage, and total tissue mass for each bird.

Gut Permeability and intestine lesion score

The gut permeability was measured on 5 DPI by the method used in our previous study (Teng, et al., 2020a; Teng, et al., 2020b). Briefly, fluorescein isothiocyanate dextran (FITC-d; MW 4000; Sigma-Aldrich, Ontario, Canada) was dissolved in distilled water and made into 2.2 mg/mL solution. One bird per cage was randomly selected and gavaged with 1 mL of FITC-d solution. Two hours after inoculation, the blood was

collected from birds and kept in the dark at room temperature for clotting. The clotted blood was centrifuged at 1,500 *g* for 15 min for serum collection. The standard curve solution was made from a serial dilution FITC-d stock (2.2 mg/mL). Dilution buffer was made from the pooled serum of non-infection birds with a basal diet. Sample and standard solutions were loaded into black 96-well plates, and FITC-d concentrations were measured by a spectrophotometer (SpectraMax M5; Molecular Devices, San Jose, CA, USA). The excitation wavelength was set at 485 nm, and the emission wavelength was set at 528 nm.

The intestine lesion score was measured on 6 DPI according to a four-score scale (Johnson and Reid, 1970), where the 0 is no appearance of gross lesions and 4 indicates the most severe lesions. Three birds per pen were randomly selected and sacrificed by cervical dislocation. Duodenum, middle intestinal tract (jejunum and ileum connected section), and ceca were collected for scoring (Conway and McKenzie, 2007). Data were analyzed in a nonparametric way to determine the average score, and the average values of each section were calculated for data analysis.

Calcein Labeling

For dynamic histomorphometry measures of bone formation, calcein (Sigma Aldrich, St. Louis, MO, USA) was dissolved in a 1 M sodium hydroxide solution and then mixed with sterilized distilled water to make the 2.0% working solution. The birds were injected with the calcein solution intraperitoneally at 20 mg/kg of body weight. On day 4 after the first injection of calcein, the birds were injected again as previously described. Bone samples were collected on 4 days after the second injection. The muscle

was removed immediately, and bones were preserved in 70% ethanol. Upon analysis, a thin slice of bone was taken from mid-diaphysis by a circular saw and then mounted on a glass slide. Calcein has a high calcium affinity and translates into a relatively broad fluorescent band. A fluorescence microscope (Keyence bz-x8000, Keyence Corp., Osaka, Japan) was used to visualize new bone formation and determine the distance between the two calcein labels on the bones. Eight measurements at different angles were performed using ImageJ software (National Institutes of Health, Bethesda, MD, USA). The average values were calculated for data analysis.

Intestine morphology and bone marrow fat cell measurement

On 6 and 12 DPI, one bird per replicate was randomly selected to collect intestine tissue samples (8 per treatment/ per time point). Around 3 cm long of tissues from the midpoint of the duodenum, jejunum, and ileum were dissected from 1 bird per pen, then tissues were rinsed with phosphate buffer saline, and immediately fixed in 10% neutral buffered formalin solution. The fixed tissue samples were transported to the Poultry Diagnostic and Research Center (University of Georgia, Athens, GA), where they were further processed. Briefly, the intestinal tissues were dehydrated with increasing concentrations of ethyl alcohol, and cleared with xylene and embedded in paraffin and cut into a 4 mm slide by using a microtone. The slide pictures were stained with hematoxylin and eosin (H&E) and examined under a light microscope at 4×objective (Keyence bz-x8000), while representative fields were photographed and digital images were captured for morphometric analysis. Intestinal histomorphology traits, including mucosa villi height, crypts depth and villi width were measured. The villi height was

measured from each of the villus tip to the bottom, excluding the intestinal crypts. Measurements of the villi apical width were done from the middle part of the villi. Five measurements of the villi height, crypt depth and villi apical width of mucosa were conducted in favorably oriented per sample using the ImageJ software (National Institutes of Health, Bethesda, MD, USA), and the mean value was calculated for statistical analysis. The ratio of villi height to crypts depth of each field was calculated, and the mean ratio of each sample was used for statistical analysis.

Tibia was collected on 6 DPI and stored in 70% ethanol before transporting to the Poultry Diagnostic and Research Center (University of Georgia, Athens, GA) for further processing. Briefly, bones were cut through the sagittal plane to obtain half of tibia metaphysis section, then tissues were embedded in paraffin and cut into 4 mm slide by using a microtone. Slides were stained with hematoxylin and eosin (H&E). By using growth plate as land mark to fix the location, three pictures per samples were obtained at 40X objective magnification. The proximal metaphyseal adipocyte number and size per filed were measured using the ImageJ software (National Institutes of Health, Bethesda, MD, USA). To avoid any bias in the final analysis, all measurements were conducted in a blinded way without knowledge of the treatment. The mean of each field was calculated for statistical analysis.

Total Antioxidant Status Assay

Chicken total antioxidant capacity in serum was analyzed using a QuantiChrom antioxidant assay kit (BioAssay Systems, Hayward, CA, USA). On 6 DPI, one bird per pen was randomly selected for blood collection. Blood samples were clotted and

centrifuged, and then kept at -80°C. All assay procedures were performed within one month of sample collection and followed the manufacturer's protocols. The protein concentration was measured by protein quantification assay (Pierce BCA Protein Assay Kit, Thermo Scientific, Rockford, IL, USA) following the procedure indicated in our previous publication (Tompkins, et al., 2022b).

Real-time Quantitative PCR Analysis of Gene Expression in Bone Marrow

On 6 DPI, one bird per replicate was randomly selected for tissue sample collecting. Bone marrow from tibias was collected. Cecal tonsils, spleen, and bone marrow were snap-frozen in liquid nitrogen and stored immediately at -80°C until RNA isolation. Tissue total RNA was extracted using Qiazol reagent (Qiagen, Valencia, CA, USA) according to the manufacturer's instructions. A Nano-Drop 1000 Spectrophotometer (ThermoFisher Scientific, Pittsburgh, PA, USA) was used to determine the quantity of RNA. The cDNA was synthesized from total RNA (2000 ng) using high-capacity cDNA reverse transcription kits (Thermo Fisher Scientific, Waltham, MA, USA).

A real-time reverse transcription polymerase chain reaction (RT-qPCR) was performed to measure mRNA expression. Primers (Table 6.3) were designed using the Primer-BLAST program (https://www.ncbi.nlm.nih.gov/tools/primer-blast/). The specificity of primers was validated by melting curve analysis and gel electrophoresis. RT-qPCR was performed on an Applied Biosystems StepOnePlus™ (Thermo Fisher Scientific, Waltham, MA, USA) with iTaq™ Universal SYBR Green Supermix (BioRad, Hercules, CA, USA) using the following conditions for all genes: 95°C for 10 minutes

followed by 40 cycles at 95°C for 15 seconds, annealing temperature for 20 seconds, and extending at 72°C for 1 minute.

The geometric mean of 18S ribosomal 1(*18S*) and glyceraldehyde-3-phosphate dehydrogenase (*GAPDH*) was used for mRNA expression normalization (Vandesompele, et al., 2002). The stability of housekeeping genes were confirmed by the consistent Ct values among the treatments (Stephens, et al., 2011). Bone gamma-carboxyglutamate protein (*BGLAP*), runt-related transcription factor (*RUNX2*) and bone morphogenetic protein 2 (*BMP2*) were used as genetic markers of bone formation in the bone marrow, nuclear factor kappa B subunit 1(*NFKB1*), receptor activator of nuclear factor kappa-B ligand (*RANKL*), sclerostin *(SOST)*, osteoprotegerin (*OPG*), and the ratio of *RANKL/OPG* were used as the genetic markers for osteoclastic activity and bone remodeling in the bone marrow (Atkins, et al., 2003; Paludo, et al., 2017). Peroxisome proliferator-activated receptor gamma (*PPARG*), CCAAT/enhancer-binding protein beta (*CEBPB*), and fatty acid binding protein 4 (*FABP4*) were used as the early adipogenic-differentiation markers (Tompkins, et al., 2022a). In the cecal tonsils and the spleen, the expression of interleukin 10 (*IL10*), interleukin 1 beta (*IL1B*), nuclear factor kappa B subunit 1 (*NFKB1*), chicken tumor necrosis factor-like (*TNF*) and interferon gamma (*IFNG*) were measured to evaluate the immune responses, and the ratio of *RANKL/OPG* was calculated for bone remodeling analysis. Details of primer sequences used for the experiment are presented in Table 6.3. Samples were run in duplicate, and relative gene expression data were analyzed using the $2^{-\Delta\Delta Ct}$. The mean ΔCt of each gene marker from the non-infected soybean oil diet (T1) was used to calculate the ΔΔCt value, and 2^{-}

$^{\Delta\Delta Ct}$ expression levels were normalized to 1 for T1, and the treatment groups expression level was presented as fold changes.

Statistical Analysis

All experimental data were tested for homogeneity of variances and normality of studentized residual at first, and data were presented as mean with standard error of the means (SEM). The means were subjected to two-way ANOVA, and the main effects (diets and challenge doses) and their interactions were considered. In the case of significant differences, Tukey's test was further conducted to test differences among sample means. All statistical procedures were performed using JMP Pro14 (SAS Institute, Inc., Cary, NC, USA). Statistical significance was set at $P \leq 0.050$, and $0.050 < p < 0.100$ were also presented to show the trend toward statistical significance (Thiese, et al., 2016). Pair-wise correlations (JMP Pro14) were used to evaluate the correlation between bone formation markers and remodeling markers in the bone marrow.

Results

Growth performance

The mortality was less than 1% in each treatment group, which indicates lower mortality in the study (data not shown) The average daily feed intake was significantly affected by infection ($P < 0.001$; Table 6.4). The average daily feed intake started to drop significantly from 4 DPI with the low and high *Eimeria* infectious doses ($P < 0.001$), whereas the reduction of feed intake was *Eimeria spp.*-challenge dose-dependent; the high infectious dose led to an additional reduction in average daily feed intake between 4 DPI to 6 DPI ($P < 0.001$). From 7 to 12 DPI, both low and high *Eimeria* infectious doses

showed a significant effect of reducing the average daily feed intake compared with non-infected control ($P < 0.050$), but changes were not significantly different between the infection levels ($P > 0.05$). For diet effect, the average daily FI was significantly affected by dietary treatments ($P < 0.001$) on 5, 6 and 7 DPI, whereas the fish oil diet significantly increased average daily feed intake on 5 DPI and 6 DPI compared with soybean oil groups under *Eimeria*-challenged condition. Besides, there was a significant interaction between challenge doses and diet variables ($P < 0.050$) on 5 and 6 DPI.

The main effects of *Eimeria spp.* challenge doses and diet treatments on performance variables over the periods post-infection are presented in Table 6.5. All challenged groups had lower body weight (BW) compared to non-challenged control on 6 DPI ($P < 0.001$) and 12 DPI ($P < 0.001$). During the acute infection phase (0–6 DPI) and the recovery phase (7-12 DPI), the *Eimeria*-infection significantly repressed growth performance by reducing FI ($P < 0.050$), BWG ($P < 0.001$) and FCR ($P < 0.001$) in broiler chickens. The fish oil diet also showed a positive impact on growth during the acute infection phase, where the fish oil diet increased BWG by 10 % and showed a trend toward higher BWG when compared to soybean oil groups ($P = 0.071$). However, fish oil did not affect growth performance during the recovery phase ($P > 0.050$). Over the entire study (0-12 DPI), birds that received the challenge had low BWG ($P < 0.001$), FI ($P < 0.050$), and worse FCR ($P < 0.001$) when compared with the non-challenged birds through the experiment ($P < 0.050$). FI showed a nonsignificant trend of increase with the fish oil diet ($P = 0.064$), but there was no significant interaction between challenge doses and diet variables ($P > 0.050$).

Body composition

The body composition results are presented in Table 6.6. On 6 DPI, the *Eimeria* infection significantly reduced BMC ($P < 0.050$), bone area ($P < 0.001$), fat percent ($P < 0.001$), total tissue ($P < 0.001$), fat mass ($P < 0.001$) and lean mass ($P < 0.050$), but not BMD ($P > 0.050$). The high challenge groups (T5 and T6) had the worse fat and lean mass compared to the non-challenge control. The fish oil diet significantly increased total tissue weight ($P < 0.050$) and lean mass ($P < 0.050$), and showed a trend of increase in BMD ($P = 0.092$), BMC ($P = 0.054$) and fat mass ($P = 0.083$) compared with the soybean oil diet groups. There was a trend of interaction between diets and infectious doses on fat percent ($P = 0.068$) and fat mass ($P = 0.077$). Likewise, on 12 DPI, BMC, BMD, bone area, fat percent, tissue weight, fat mass and lean mass were all significantly reduced by different levels of *Eimeria* infection ($P < 0.001$) but not diet ($P > 0.05$). No significant interaction between diet and infectious doses was found on 12 DPI.

Lesion score, gastrointestinal permeability and intestinal morphology

On 5 DPI, the results of intestinal permeability (Figure 6.1) showed that the serum concentrations of FITC-d were significantly affected by infection ($P < 0.001$) and diet ($P = 0.001$), and there was a significant interaction between infection and diet variables ($P = 0.050$). The concentration of FITC-d (μg/mL) in the serum was significantly increased by different doses of *Eimeria* infection ($P < 0.001$). The fish oil diet significantly decreased the serum level of FITC-d compared with soybean oil diet groups ($P < 0.050$) under each challenge level.

Lesion score reading on 6 DPI (Figure 6.2) indicated that the severity of intestinal lesions of duodenum, jejunum and ileum, and ceca were significantly affected by *Eimeria* infection ($P < 0.001$). No lesion was found in the intestine or ceca of birds from unchallenged groups. The diet factor has a positive affected that fish oil reduced the lesion score at the jejunum and ileum junction ($P = 0.029$). There was no interaction between infectious doses and diet variables ($P > 0.050$) over the different regions of the intestine.

Histopathological examination of the affected intestine demonstrated characteristic microscopic signs of coccidiosis in the affected-broilers on 6 DPI (Figure 6.3; Table 6.6). The villi height, crypt depth, and villus /crypt ratios of the duodenum and jejunum were significantly affected by *Eimeria* infection ($P < 0.001$). But the *Eimeria* infection had no significant impact on ileum villi height ($P > 0.05$). *Eimeria* infection did not alter the villi width at the duodenum, jejunum, or ileum ($P > 0.05$). The diet variable did no effect on intestinal morphology traits ($P > 0.05$). There was a significant interaction between infectious doses and diets on jejunum crypt depth ($P < 0.05$), but no significant interaction between infectious doses and diets on the other morphology traits ($P > 0.05$).

Bone growth variables

The bone growth rate, which was measured by the calcein labeling method, showed a significant reduction in the *Eimeria*-infected groups (Figure 6.4A and B; $P < 0.001$). The higher *Eimeria* challenge doses (T5 and T6) showed a more significant suppression in bone formation. However, the diet variable did not affect the bone

formation rate ($P > 0.050$), or there was no interaction between infection and diet treatments on bone formation rate with the calcein labeling method ($P > 0.050$).

By measuring the expression of bone formation biomarkers in the bone marrow, results showed *Eimeria* infection significantly decreased the mRNA expression of *BGLAP* ($P < 0.001$; Figure 6.4C), *RUNX2* ($P < 0.001$), and showed a trend of decreasing in *BMP2* ($P = 0.072$; Figure 6.4C). The fish oil diet had no significant impact on bone formation ($P > 0.05$), and there was no interaction between infection and diet treatments on bone formation biomarkers in the bone marrow ($P > 0.05$). Besides, a higher expression level of *FABP4* was detected in the bone marrow of *Eimeria*-challenged chickens than non-infected control groups ($P < 0.05$; Figure 6.5A). The adipocyte cell walls were observed in the bone marrow (Figure 6.5B). However, neither *Eimeria* infection nor diets changed the size ($P > 0.05$; Figure 6.5C) or the number of fat cells in the bone marrow ($P > 0.05$; Figure 6.5D).

Bone remodeling status

Eimeria-challenge significantly decreased the expression of *OPG* compared to non-challenged control in the bone marrow ($P < 0.001$; Figure 6.6A), in the cecal tonsils ($P < 0.001$; Figure 6.6C) and in the spleen ($P < 0.001$; Figure 6.6D). The infectious doses and diet had a significant interaction on the mRNA expression of *RANKL* in bone marrow (Figure 6.6A; $P = 0.032$). The effect of the diet treatment showed an infectious dose-depend manner, where fish oil decreased bone marrow *RANKL* expression compared with soybean oil in the low challenge dose groups (T3 vs. T4; $P < 0.050$), and fish oil diet increased the bone marrow expression of *RANKL* in the high challenge groups compared

with soybean oil groups (T5 vs. T6; $P < 0.050$). In contrast to the expression pattern in bone marrow, *Eimeria* infection significantly decreased the mRNA expression of *RANKL* in the spleen ($P < 0.050$). Moreover, the mRNA ratio of *RANKL/ OPG*, a standard index biomarker of osteoclastogenic stimulation and bone remodeling, was significantly increased by *Eimeria* infection in the spleen ($P < 0.050$), indicating an increased bone remodeling state in infected birds. Moreover, there was a positive correlation between mRNA expression of *TNF* and *SOST* in bone marrow (Figure 6.6B; $P < 0.001$; $R^2=0.523$).

Total antioxidant capacity and immune response

Total antioxidant capacity affected by infection (Figure 6.7A; $P < 0.050$) but not diet factor on 6 DPI. However, neither infection or diet significantly affected the serum total antioxidant capacity on 12 DPI (Figure 6.7B; $P > 0.050$).

In cecal tonsils, the mRNA expression of *NFKB1*, *IL10* and *IL1B* was reduced by *Eimeria* infection on 6 DPI compared to uninfected control groups ($P < 0.05$; Figure 6.8A). The mRNA expression of *TNF* and *IFNG* reminds unchanged with infection ($P > 0.05$). For the diet variable, the fish oil diet significantly increased *IL10* expression compared with the soybean oil diet ($P < 0.05$). There was no interaction between diet and infection variables on immune response-related marker genes expression in cecal tonsils. In the spleen, in contrast to the effect of *Eimeria* infection in cecal tonsils, a trend of increased expression of *IL10* was observed in *Eimeria*-infected birds compared to uninfected control ($P = 0.072$; Figure 6.8B). There was a lower level of mRNA expression of *TNF* in high-challenge doses than low-infection groups and uninfected

control groups ($P < 0.050$; Figure 6.8B). There was no interaction between diet and infection variables on the expression of immune response gene in the spleen.

Discussion

Fatty acids, especially essential fatty acids, are gaining more attention in poultry nutrition research in recent years because of their benefits on the health of birds. The results of this study, as well as those previously reported (Allen, et al., 1996; Danforth, et al., 1997; Allen and Danforth, 1998; Yang, et al., 2006), clearly showed that fish oil diet reduced intestinal lesions caused by *Eimeria* infection, especially in the jejunum. Studies have shown that the n-3 PUFA exhibited a dual role as a prooxidant and antioxidant depending on the cell types under treatment (Di Nunzio, et al., 2011; Radzikowska, et al., 2019). Mitochondrial membranes have a high DHA content, that PUFAs can be inserted into the cell membranes and affects the antioxidant signaling to control oxidative stress level (Garrel, et al., 2012). Supplying fish oil diet to rats resulted in a higher expression and activity of the antioxidant enzyme superoxide dismutase (SOD) and a lower membrane peroxidation in plasma (Erdogan, et al., 2004; Garrel, et al., 2012). And many studies concluded that dietary supplementation of n-3 PUFA may enhance resistance to free radical attacks and reduce lipid peroxidation (Oppedisano, et al., 2020). On the other hand, the n-3 PUFA-enriched fish oil diet is also highly susceptible to oxidation due to multiple double bonds (Awada, et al., 2012). Oxidized lipid is a pro-apoptotic factor that can induce cell damage and causes extensive tissue damage that causes losses in productive performance (Awada, et al., 2012). Antioxidants in the diet play a protective role in reducing fat oxidation in the n-3 PUFA-enriched diet, as well as protecting the

tissue from oxidative damage caused by lipid oxidation (Lesson and Summers, 2001). The additional antioxidant content is required with increased polyunsaturated oil content in chicken diets (Surai, 2007). More specifically, when soybean oil content increased by 1% in the diet, it was advised to increase vitamin E level by 20 IU. And as for increased fish oil by 1%, the requirement for additional vitamin E is 8 IU (Lesson and Summers, 2001). Based on the current experiment setting, the soybean oil group might display more significant antioxidant depletion, and that oxidative stress might be a factor that suppressed growth in soybean oil diet groups compared with the fish oil diet. However, we did not observe any significant differences in serum total antioxidant capacity. It is unclear whether the n-3 PUFA-enriched fish oil is antioxidative or prooxidative under *Eimeria* infection in the current study.

It is well known that eicosapentaenoic acid (EPA; 20:5n-3), docosahexaenoic acid (DHA; 22:6n-3), and arachidonic acid (AA, n-6 PUFA) are common constituents of the cell membrane, where AA commonly act as a pro-inflammatory factor (Alhusseiny and El-Beshbishi, 2020). The amounts and ratio of those long-chain fatty acids on different types of cell membranes can be modulated by dietary supplementation of n-3 PUFA (Calder, 2013). Dietary fats can modulate the immune response and affect both humoral and cellular responses in human clinical research and mice models (Erickson, 1986; Radzikowska, et al., 2019). Increased consumption of long-chain n-3 PUFAs could reduce the amount of AA in cells membrane and change the inflammatory state of cells, or change the response of immune cells, repressing the production of proinflammatory mediators, including proinflammatory cytokines and inflammatory eicosanoids (Calder,

2006; Eilati, et al., 2013). A large number of studies have shown the anti-inflammatory effects of the n-3 PUFAs in mammal endothelial cells (Radzikowska, et al., 2019; Lauridsen, 2020). In chickens, several unique avian lymphoid organs, including cecal tonsils and bursa of Fabricius, have evolved in the defendant system to defend against intestinal pathogens such as coccidia (Yun, et al., 2000). In the current study, *Eimeria* infected groups showed a numerically higher level of *IL10* in the spleen compared with non-infected control. As for the diet variable, the expression of *IL10* was increased by the fish oil diet in cecal tonsils. Chicken *IL10* mRNA expression was identified mainly in the bursa of Fabricius and the cecal tonsils (Rothwell, et al., 2004). *IL10* is an anti-inflammatory cytokine that plays a crucial role in preventing overproduced inflammatory factors. However, previous studies hypothesized that protozoan parasites take advantage of host IL10 to trick the chicken immune response in surrounding microenvironments (Arendt, et al., 2019). Several studies reported that the serum level or intestine level of *IL10* increased by *Eimeria* infected (Cornelissen, et al., 2009; Morris, et al., 2015), and using an antibody to suppress the *Eimeria*-induced *IL10* might reduce the performance loss (Sand, et al., 2016; Arendt, et al., 2019). We hypothesized that the different pattern of immune response might depend on the dose administered, genetic components of host species and *Eimeria* species, sampling tissue, and different time points of sampling. Besides, the lipid content, dietary fat peroxidation level, and diet antioxidant content could all possibly affect the immune response (Fries-Craft, et al., 2021). Based on the current study, we conclude that fish oil positively impacts gut integrity during *Eimeria* infection compared with the soybean oil diet. The production of *IL10* can possibly be a

key factor in regulating the immune response and mediating gut permeability after *Eimeria* infection with a fish oil diet. More detailed research is in need to better understand the function of n-3 PUFA under pathogen challenge conditions.

Moreover, as for the current results, the growth performance of broilers showed a trend of improvement with the fish oil supplement compared with soybean oil. The supplementation of fish oils positively impacted FI on 5, 6 and 7 DPI after *Eimeria* infection. And the jejunum is where the significant interaction between diet treatments and infectious doses occurred. Previous studies reported a severe gut leakage on 5, 6 and 7 DPI with *Eimeria* challenge (Teng, et al., 2020a), and explained that the severe tissue damage might be due to the *Eimeria* reproduction and expanding stage of its life cycle. The jejunum is the main intestinal compartment responsible for lipid absorption, and a small portion of the digestion of fat continues in the upper ileum (Tancharoenrat, et al., 2014; Rodriguez-Sanchez, et al., 2019). The less severe damage over the jejunum can result in a higher absorption rate of lipid content. With a fish oil diet, abnormal shedding of the asexual and sexual parasite was observed in the cecal lumen in the previous study, indicating the suppression of coccidia development with fish oil supplement (Danforth, et al., 1997). Moreover, several investigations have indicated that cecal tonsils lymphocytes involved in the intestinal immune response to *Eimeria*, the number of $CD4^+$ cecal tonsil lymphocytes in chickens increased at 4 and 6 DPI (Lillehoj and Trout, 1996; Yun, et al., 2000). The innate immune response plays a significant role in controlling coccidia development. Therefore, the modulation of the immune response by fish oil supplements can positively impact on the immune state in intestine which led to higher FI.

Furthermore, studies reported that *Eimeria* can repress host cells from apoptosis at early stages of development, and the inhibition of host cell apoptosis can be beneficial to the intracellular growth and development of *E. tenella* (Zhang, et al., 2015; Wang, et al., 2021). The pro-apoptotic nature of n-3 PUFA-enriched fish oil can also contribute to the suppression of *Eimeria* development. High dietary n-3 PUFA can possibly alter the host cell membrane component and change the host cell environment to limit the development of the parasite. Although the underlying mechanism or exact roles of fish oil in controlling avian coccidiosis remain unclear, we could conclude that fish oil supplement has a beneficial role in chicken intestinal integrity under *Eimeria* infection at the early infection stage. This statement is agreed with the suggestion from a previous study that suggested a short-term use of fish oil during the acute infection stage can be a nutritional strategy for minimizing the production loss caused by coccidiosis (Allen, et al., 1996). Future studies focusing on the interaction between n-3 PUFA and the life cycle of *Eimeria* are important to understand the character of this parasite. Effective doses for n-3 PUFA are difficult to determine due to inconsistencies in dose and time of exposure between different *in vivo* and *in vitro* models. Further research is needed to determine the anti-inflammatory potential of less-studied ω-3 PUFAs as a feed alternative to control coccidia infection in chickens.

In the current study, an increased ratio in *RANKL/OPG* within infection groups indicated a higher remodeling status in *Eimeria*-infection groups compared to non-infected control, showing pathogen infection might be a factor that regulated bone homeostasis under infected conditions. In the bone marrow, a positive correlation

between *SOST and TNF* in bone marrow was observed in this study. This result was consistent with previous reports that TNF plays a positive role in sclerostin expression in bone marrow (Thakker, et al., 2017). The pro-inflammatory cytokines can up-regulate the expression and activity of sclerostin, which inhibits the bone formation related pathways and down-regulated expression of bone formation genes. Sclerostin is primarily secreted by osteocytes that play an important negative role in bone formation and mineralization (Thakker, et al., 2017). Studies with *in vitro* cells showed, TNF increased sclerostin expression in osteocytes, and the level of *SOST* mRNA was increased by *TNF* (Osta, et al., 2014; Ohori, et al., 2019). For diet variables, N-3 PUFA on osteoimmunology has been largely researched in human and mice models. Studies reported a lower expression of osteoclastogenic cytokines (RANKL, TNF-α, and IL-6) was detected in rodents that was supplied fish oil diet (Fong, et al., 2012). Studies indicated that the change in immune states has a direct impact on the activation of bone resorption (Ambrozova, et al., 2010). Some studies in human indicated that n-3 PUFA can reduce bone loss under stress or during aging (Salari Sharif, et al., 2010; Dou, et al., 2022). Our previous report also showed the immune response is a major factor that led to decreased bone mineral density by increasing osteoclast number and activity (site my paper). In the current study, bone mineral density data showed a trend of increasing in fish oil diet groups compared to soybean oil groups by using DEXA body composition analysis. However, the diet variable showed no effect on the expression of any bone remodeling markers. We hypothesize that the mechanisms of action of the n-3PUFA on bone health are complex. The energy level (feed intake amount), nutrition absorption ability and gut integrity could

all affect bone homeostasis, and nutritional factors greatly impact on bone homeostasis. Thus, it is hard to illustrate the direct evidence based on our current *in vivo* experimental setting, and more studies are necessary to prove whether n-3 PUFA supplementation plays a significant role in bone health.

References

Akbari Moghaddam Kakhki, R., Z. Lu, A. Thanabalan, H. Leung, M. Mohammadigheisar, and E. Kiarie. 2019. Eimeria challenge adversely affected long bone attributes linked to increased resorption in 14-day-old broiler chickens. Poult Sci 98:1615-1621.

Al-Khalaifah, H. 2020. Modulatory Effect of Dietary Polyunsaturated Fatty Acids on Immunity, Represented by Phagocytic Activity. Front Vet Sci 7:569939.

Alhusseiny, S. M., and S. N. El-Beshbishi. 2020. Omega polyunsaturated fatty acids and parasitic infections: An overview. Acta Trop 207:105466.

Allen, P. C., and H. D. Danforth. 1998. Effects of dietary supplementation with n-3 fatty acid ethyl esters on coccidiosis in chickens. Poult Sci 77:1631-1635.

Allen, P. C., H. D. Danforth, and O. A. Levander. 1996. Diets high in n-3 fatty acids reduce cecal lesion scores in chickens infected with Eimeria tenella. Poult Sci 75:179-185.

Ambrozova, G., M. Pekarova, and A. Lojek. 2010. Effect of polyunsaturated fatty acids on the reactive oxygen and nitrogen species production by raw 264.7 macrophages. Eur J Nutr 49:133-139.

Arendt, M., J. Elissa, N. Schmidt, E. Michael, N. Potter, M. Cook, and L. J. Knoll. 2019. Investigating the role of interleukin 10 on Eimeria intestinal pathogenesis in broiler chickens. Vet Immunol Immunopathol 218:109934.

Atkins, G. J., P. Kostakis, B. Pan, A. Farrugia, S. Gronthos, A. Evdokiou, K. Harrison, D. M. Findlay, and A. C. Zannettino. 2003. RANKL expression is related to the differentiation state of human osteoblasts. J Bone Miner Res 18:1088-1098.

Awada, M., C. O. Soulage, A. Meynier, C. Debard, P. Plaisancie, B. Benoit, G. Picard, E. Loizon, M. A. Chauvin, M. Estienne, N. Peretti, M. Guichardant, M. Lagarde, C. Genot, and M. C. Michalski. 2012. Dietary oxidized n-3 PUFA induce oxidative stress and inflammation: role of intestinal absorption of 4-HHE and reactivity in intestinal cells. J Lipid Res 53:2069-2080.

Barua, M., G. Buddha Das, K. Islam, S. Chowdhury, M. Emran Hoss, B. Kanti Nath, and M. Shafiqul I. 2016. Effect of Fish Oil on Performance, Coccidiosis Prevention and Serum Lipid Profile in Broiler. Asian Journal of Poultry Science 11:20-30.

Blake, D. P., J. Knox, B. Dehaeck, B. Huntington, T. Rathinam, V. Ravipati, S. Ayoade, W. Gilbert, A. O. Adebambo, I. D. Jatau, M. Raman, D. Parker, J. Rushton, and F. M. Tomley. 2020. Re-calculating the cost of coccidiosis in chickens. Vet Res 51:115.

Calder, P. C. 2006. n-3 polyunsaturated fatty acids, inflammation, and inflammatory diseases. Am J Clin Nutr 83:1505S-1519S.

Calder, P. C. 2013. Omega-3 polyunsaturated fatty acids and inflammatory processes: nutrition or pharmacology? Br J Clin Pharmacol 75:645-662.

Clemente, T. E., and E. B. Cahoon. 2009. Soybean oil: genetic approaches for modification of functionality and total content. Plant Physiol 151:1030-1040.

Cobb. 2019. Cobb 500 broiler performance and nutrient supplement guide. . Siloam Springs (AR): Cobb-Vantress.

Conway, D. P., and M. E. McKenzie. 2007. Poultry coccidiosis: diagnostic and testing procedures. John Wiley & Sons.

Cornelissen, J. B., W. J. Swinkels, W. A. Boersma, and J. M. Rebel. 2009. Host response to simultaneous infections with Eimeria acervulina, maxima and tenella: a cumulation of single responses. Vet Parasitol 162:58-66.

Dalloul, R. A., and H. S. Lillehoj. 2006. Poultry coccidiosis: recent advancements in control measures and vaccine development. Expert Rev Vaccines 5:143-163.

Danforth, H. D., P. C. Allen, and O. A. Levander. 1997. The effect of high n-3 fatty acids diets on the ultrastructural development of Eimeria tenella. Parasitol Res 83:440-444.

Di Nunzio, M., V. Valli, and A. Bordoni. 2011. Pro- and anti-oxidant effects of polyunsaturated fatty acid supplementation in HepG2 cells. Prostaglandins Leukot Essent Fatty Acids 85:121-127.

Dou, Y., Y. Wang, Z. Chen, X. Yu, and D. Ma. 2022. Effect of n-3 polyunsaturated fatty acid on bone health: A systematic review and meta-analysis of randomized controlled trials. Food Sci Nutr 10:145-154.

Durkin, L. A., C. E. Childs, and P. C. Calder. 2021. Omega-3 Polyunsaturated Fatty Acids and the Intestinal Epithelium-A Review. Foods 10.

Ebeid, T., A. Fayoud, S. Abou El-Soud, Y. Eid, and M. El-Habbak. 2011. The effect of omega-3 enriched meat production on lipid peroxidation, antioxidative status, immune response and tibia bone characteristics in Japanese quail . Czech Journal of Animal Science 56:314-324.

Eilati, E., C. C. Small, S. R. McGee, N. K. Kurrey, and D. B. Hales. 2013. Anti-inflammatory effects of fish oil in ovaries of laying hens target prostaglandin pathways. Lipids Health Dis 12:152.

Erdogan, H., E. Fadillioglu, S. Ozgocmen, S. Sogut, B. Ozyurt, O. Akyol, and O. Ardicoglu. 2004. Effect of fish oil supplementation on plasma oxidant/antioxidant status in rats. Prostaglandins Leukot Essent Fatty Acids 71:149-152.

Erickson, K. L. 1986. Dietary fat modulation of immune response. International Journal of Immunopharmacology 8:529-543.

Fong, L., B. S. Muhlhausler, R. A. Gibson, and C. J. Xian. 2012. Perinatal maternal dietary supplementation of omega3-fatty acids transiently affects bone marrow microenvironment, osteoblast and osteoclast formation, and bone mass in male offspring. Endocrinology 153:2455-2465.

Fries-Craft, K. A., M. M. Meyer, S. C. Lindblom, B. J. Kerr, and E. A. Bobeck. 2021. Lipid Source and Peroxidation Status Alter Immune Cell Recruitment in Broiler Chicken Ileum. J Nutr 151:223-234.

Fritsche, K. L., and N. A. Cassity. 1992. Dietary n-3 fatty acids reduce antibody-dependent cell cytotoxicity and alter eicosanoid release by chicken immune cells. Poult Sci 71:1646-1657.

Garrel, C., J. M. Alessandri, P. Guesnet, and K. H. Al-Gubory. 2012. Omega-3 fatty acids enhance mitochondrial superoxide dismutase activity in rat organs during post-natal development. Int J Biochem Cell Biol 44:123-131.

Gaucher, M. L., S. Quessy, A. Letellier, J. Arsenault, and M. Boulianne. 2015. Impact of a drug-free program on broiler chicken growth performances, gut health, Clostridium perfringens and Campylobacter jejuni occurrences at the farm level. Poult Sci 94:1791-1801.

Hudert, C. A., K. H. Weylandt, Y. Lu, J. Wang, S. Hong, A. Dignass, C. N. Serhan, and J. X. Kang. 2006. Transgenic mice rich in endogenous omega-3 fatty acids are protected from colitis. Proc Natl Acad Sci U S A 103:11276-11281.

Johnson, J., and W. M. Reid. 1970. Anticoccidial drugs: Lesion scoring techniques in battery and floor-pen experiments with chickens. Experimental Parasitology 28:30-36.

Kalinski, P. 2012. Regulation of immune responses by prostaglandin E2. J Immunol 188:21-28.

Korver, D. R., P. Wakenell, and K. C. Klasing. 1997. Dietary fish oil or lofrin, a 5-lipoxygenase inhibitor, decrease the growth-suppressing effects of coccidiosis in broiler chicks. Poult Sci 76:1355-1363.

Lauridsen, C. 2020. Effects of dietary fatty acids on gut health and function of pigs pre- and post-weaning. J Anim Sci 98.

Lee, A. V., L. You, S. Y. Oh, Z. Li, A. Code, C. Zhu, R. E. Fisher-Heffernan, T. R. H. Regnault, C. F. M. De Lange, L. A. Huber, and N. A. Karrow. 2019. Health Benefits of Supplementing Nursery Pig Diets with Microalgae or Fish Oil. Animals (Basel) 9.

Lesson, S., and J. J. U. b. G. Summers, Canada. 2001. Scott's nutrition of the chicken.

Lillehoj, H. S., and J. M. Trout. 1996. Avian gut-associated lymphoid tissues and intestinal immune responses to Eimeria parasites. Clin Microbiol Rev 9:349-360.

Lu, J., T. Jilling, D. Li, and M. S. Caplan. 2007. Polyunsaturated fatty acid supplementation alters proinflammatory gene expression and reduces the incidence of necrotizing enterocolitis in a neonatal rat model. Pediatr Res 61:427-432.

Morris, A., R. Shanmugasundaram, J. McDonald, and R. K. Selvaraj. 2015. Effect of in vitro and in vivo 25-hydroxyvitamin D treatment on macrophages, T cells, and layer chickens during a coccidia challenge. J Anim Sci 93:2894-2903.

Ohori, F., H. Kitaura, A. Marahleh, A. Kishikawa, S. Ogawa, J. Qi, W. R. Shen, T. Noguchi, Y. Nara, and I. Mizoguchi. 2019. Effect of TNF-alpha-Induced Sclerostin on Osteocytes during Orthodontic Tooth Movement. J Immunol Res 2019:9716758.

Oladiji, A. T., K. L. Shoremekun, and M. T. Yakubu. 2009. Physicochemical properties of the oil from the fruit of Blighia sapida and toxicological evaluation of the oil-based diet in Wistar rats. J Med Food 12:1127-1135.

Oppedisano, F., R. Macri, M. Gliozzi, V. Musolino, C. Carresi, J. Maiuolo, F. Bosco, S. Nucera, M. Caterina Zito, L. Guarnieri, F. Scarano, C. Nicita, A. R. Coppoletta, S. Ruga, M. Scicchitano, R. Mollace, E. Palma, and V. Mollace. 2020. The Anti-Inflammatory and Antioxidant Properties of n-3 PUFAs: Their Role in Cardiovascular Protection. Biomedicines 8.

Osta, B., G. Benedetti, and P. Miossec. 2014. Classical and Paradoxical Effects of TNF-alpha on Bone Homeostasis. Front Immunol 5:48.

Paludo, E., A. M. G. Ibelli, J. O. Peixoto, F. C. Tavernari, C. A. V. Lima-Rosa, J. R. C. Pandolfi, and M. C. Ledur. 2017. The involvement of RUNX2 and SPARC genes in the bacterial chondronecrosis with osteomyelitis in broilers. Animal 11:1063-1070.

Radzikowska, U., A. O. Rinaldi, Z. Celebi Sozener, D. Karaguzel, M. Wojcik, K. Cypryk, M. Akdis, C. A. Akdis, and M. Sokolowska. 2019. The Influence of Dietary Fatty Acids on Immune Responses. Nutrients 11.

Rodriguez-Sanchez, R., A. Tres, R. Sala, F. Guardiola, and A. C. Barroeta. 2019. Evolution of lipid classes and fatty acid digestibility along the gastrointestinal tract of broiler chickens fed different fat sources at different ages. Poult Sci 98:1341-1353.

Rothwell, L., J. R. Young, R. Zoorob, C. A. Whittaker, P. Hesketh, A. Archer, A. L. Smith, and P. Kaiser. 2004. Cloning and characterization of chicken IL-10 and its role in the immune response to Eimeria maxima. J Immunol 173:2675-2682.

Salari Sharif, P., M. Asalforoush, F. Ameri, B. Larijani, and M. Abdollahi. 2010. The effect of n-3 fatty acids on bone biomarkers in Iranian postmenopausal osteoporotic women: a randomized clinical trial. Age (Dordr) 32:179-186.

Sand, J. M., M. K. Arendt, A. Repasy, G. Deniz, and M. E. Cook. 2016. Oral antibody to interleukin-10 reduces growth rate depression due to Eimeria spp. infection in broiler chickens. Poult Sci 95:439-446.

Smith, J. A. 2011. Experiences with drug-free broiler production. Poult Sci 90:2670-2678.

Stephens, A. S., S. R. Stephens, and N. A. Morrison. 2011. Internal control genes for quantitative RT-PCR expression analysis in mouse osteoblasts, osteoclasts and macrophages. BMC Res Notes 4:410.

Surai, P. F. Year. Natural antioxidants in poultry nutrition: new developments. Proc. Proceedings of the 16th European symposium on poultry nutrition.

Swiatkiewicz, S., A. Arczewska-Wlosek, and D. Jozefiak. 2015. The relationship between dietary fat sources and immune response in poultry and pigs: An updated review. Livestock Science 180:237-246.

Tancharoenrat, P., V. Ravindran, F. Zaefarian, and G. Ravindran. 2014. Digestion of fat and fatty acids along the gastrointestinal tract of broiler chickens. Poult Sci 93:371-379.

Tarradas, J., N. Tous, E. Esteve-Garcia, and A. J. Brufau. 2020. The Control of Intestinal Inflammation: A Major Objective in the Research of Probiotic Strains as Alternatives to Antibiotic Growth Promoters in Poultry. Microorganisms 8.

Teng, P. Y., S. Yadav, F. L. S. Castro, Y. H. Tompkins, A. L. Fuller, and W. K. Kim. 2020a. Graded Eimeria challenge linearly regulated growth performance, dynamic change of gastrointestinal permeability, apparent ileal digestibility, intestinal morphology, and tight junctions of broiler chickens. Poult Sci 99:4203-4216.

Teng, P. Y., S. Yadav, T. S. Dos Santos, A. L. Fuller, and W. K. Kim. 2020b. 2-Nitro-1-propanol improved nutrient digestibility and oocyst shedding but not growth performance of Eimeria-challenged broilers. Poult Sci 99:4314-4322.

Thakker, R. V., M. P. Whyte, J. Eisman, and T. Igarashi. 2017. Genetics of bone biology and skeletal disease. Academic Press.

Thiese, M. S., B. Ronna, and U. Ott. 2016. P value interpretations and considerations. J Thorac Dis 8:E928-E931.

Tompkins, Y. H., C. Chen, K. M. Sweeney, M. Kim, B. H. Voy, J. L. Wilson, and W. K. Kim. 2022a. The effects of maternal fish oil supplementation rich in n-3 PUFA on

offspring-broiler growth performance, body composition and bone microstructure. PLoS One 17:e0273025.

Tompkins, Y. H., P. Teng, R. Pazdro, and W. K. Kim. 2022b. Long Bone Mineral Loss, Bone Microstructural Changes and Oxidative Stress After Eimeria Challenge in Broilers. Front Physiol 13:945740.

Vandesompele, J., K. De Preter, F. Pattyn, B. Poppe, N. Van Roy, A. De Paepe, and F. Speleman. 2002. Accurate normalization of real-time quantitative RT-PCR data by geometric averaging of multiple internal control genes. Genome Biol 3:RESEARCH0034.

Wang, P., Y. Jia, Y. Han, W. Wang, Y. Zhu, J. Xu, C. Guan, J. Ying, S. Deng, J. Wang, X. Zhang, M. Chen, C. Cheng, and H. Song. 2021. Eimeria acervulina Microneme Protein 3 Inhibits Apoptosis of the Chicken Duodenal Epithelial Cell by Targeting the Casitas B-Lineage Lymphoma Protein. Front Vet Sci 8:636809.

Xiang, J., C. Wan, R. Guo, and D. Guo. 2016. Is Hydrogen Peroxide a Suitable Apoptosis Inducer for All Cell Types? Biomed Res Int 2016:7343965.

Yang, X., Y. Guo, Z. Wang, and W. Nie. 2006. Fatty acids and coccidiosis: effects of dietary supplementation with different oils on coccidiosis in chickens. Avian Pathol 35:373-378.

Yun, C. H., H. S. Lillehoj, and K. D. Choi. 2000. Eimeria tenella infection induces local gamma interferon production and intestinal lymphocyte subpopulation changes. Infect Immun 68:1282-1288.

Zhang, Y., M. X. Zheng, Z. Y. Xu, H. C. Xu, X. Z. Cui, S. S. Yang, W. L. Zhao, S. Li, Q. H. Lv, and R. Bai. 2015. Relationship between Eimeria tenella development and host cell apoptosis in chickens. Poult Sci 94:2970-2979.

Zhu, H., Y. Liu, S. Chen, X. Wang, D. Pi, W. Leng, F. Chen, J. Zhang, and P. Kang. 2016. Fish oil enhances intestinal barrier function and inhibits corticotropin-releasing hormone/corticotropin-releasing hormone receptor 1 signalling pathway in weaned pigs after lipopolysaccharide challenge. Br J Nutr 115:1947-1957.

Tables

Table 6.1: Fatty acids profiles of fish oil and soybean oil used in current study.

Fatty acids	Area of Total Faty Acids (%)	
	Fish oil [1]	Soybean oil [2]
Myristic, C14:0	08.90	0.1
Palmitic, C16:0	18.28	10.30
Palmitoleic, C16:1	12.51	5.20
Stearic, C18:0	03.08	3.80
Oleic, C18:1	09.07	22.80
Linoleic, C18:2 (omega-6)	01.41	51.00
Alpha Linolenic, C18:3 (omega-3)	01.36	6.80
Stearidonic, C18:4 (omega-3)	02.81	-
Arachidonic, C20:4 (omega-6)	01.07	0.3
Eicosapentaenoic, C20:5 (omega-3)	14.67	-
Docosapentaenoic, C22:5 (omega-3)	02.50	-
Docosahexaenoic, C22:6 (omega-3)	11.51	0.2
Other	12.81	-

[1] Fish oil: Virginia Prime Gold, Omega Protein. It is a refined long-chain omega-3 fish oil specifically formulated as a palatable feed ingredient. Fish oil contains approximately 35% total omega-3 fatty acids with a balanced concentration of EPA and DHA.[2] Soybean oil: Harvest value, USA. The nutrition facts shown a total saturated fat content is 11%. The soybean oil profile is referred to previous publications (Clemente and Cahoon, 2009; Oladiji, et al., 2009).

Table 6.2. Composition and calculated contents of the experimental diets.

Ingredient (%)	Starter (0-13 d)	Grower (14-26 d)	
		Soybean oil diet	Fish oil diet
Corn	58.17	55.41	55.41
Soybean meal -48%	34.08	30.44	30.44
Soybean oil	2.00	5.00	0
Fish oil	0	0	5.00
Limestone	0.50	0.47	0.47
Dical. Phos.	1.80	1.70	1.70
Common salt	0.23	0.22	0.22
Vitamin premix[1]	0.25	0.25	0.25
Mineral premix[2]	0.08	0.08	0.08
DL-methionine	0.28	0.25	0.25
L-lysine-HCL	0.16	0.13	0.13
Threonine	0.05	0.04	0.04
Sand	1.00	6.01	6.01
Energy and nutrient composition			
ME, kcal/kg	3008	3086	3086
Crude protein %	21.00	19.00	19.00
Lysine %	1.18	1.05	1.05
Methionine %	0.59	0.54	0.54
Arginine %	1.36	1.23	1.23
Threonine %	0.77	0.69	0.69
Tryptophan %	0.25	0.22	0.22
Valine %	1.03	0.94	0.94

Total sulfur amino acid %	0.88	0.80	0.80
Ca %	0.90	0.84	0.84
Available P %	0.45	0.42	0.42

[1]Vitamin premix include provides the following per kg of diet: Vitamin A 2,204,586 IU, Vitamin D3 200,000 ICU, Vitamin E 2,000 IU, Vitamin B12 2 mg, Biotin 20 mg, Menadione 200 mg, Thiamine 400 mg, Riboflavin 800 mg, d-Pantothenic Acid 2,000 mg, Vitamine B6 400 mg, Niacin 8,000 mg, Folic Acid 100 mg, Choline 34,720 mg.

[2]Mineral premix provides the following per kg of diet: Ca 0.72 g, Mn 3.04 g, Zn 2.43 g, Mg 0.61 g, Fe 0.59 g, Cu 22.68 g, I 22.68 g, Se 9.07 g.

Table 6.3: Nucleotide sequences of the primers used for real-time RT-PCR.

	Primer sequence (5'-3')	Product length (bp)	Annealing temperature (°C)	Accession #
GAPDH	F-GCTAAGGCTGTGGGGAAAGT R-TCAGCAGCAGCCTTCACTAC	161	55	NM_204305.1
RNA18S1	F-AGCCTGCGGCTTAATTTGAC R-CAACTAAGAACGGCCATGCA	121	56.5	AF_173612.1
BMP2	F-TCAGCTCAGGCCGTTGTTAG R-GTCATTCCACCCCACGTCAT	163	57	XM_025148488.1
RUNX2	F-ACTTTGACAATAACTGTCCT R-GACCCCTACTCTCATACTGG	192	60	XM_015285081.2
BGLAP	F-GGATGCTCGCAGTGCTAAAG R-CTCACACACCTCTCGTTGGG	142	57	NM_205387.3
NFKB1	F-GAAGGAATCGTACCGGGAAC A	131	59	XM_015285418.2

	R- CTCAGAGGGCCTTGTGACAG TAA			
SOST	F- GACAGAAATCATCCCCGAGA R- CCTGGTTCATCGTGTTGTTG	83	58	XM_040653287 .2
OPG	F- ACGCTTGTGCTCTTGGACAT R- CAGCGTAGTACTGGTCTGGG	193	60	NM_001033641 .1
RANKL	F- ACACGCCCTTTGAAAATCAG R- GCAAAAGGTTGCTTCTCTGG	196	60	XM_015275777 .2
FABP4	F- GCAGAAGTGGGATGGCAAA G R- GTTCGCCTTCGGATCAGTCC	153	60	NM_204290.1
PPARG	F- GAGCCCAAGTTTGAGTTTGC R- TCTTCAATGGGCTTCACATTT	131	58	XM_025154400 .1
CEBPB	F- CCGCTCCATGACCGAACTTA R- GCCGCTGCCTTTATAGTCCT	205	60	NM_205253.2

IL10	F-CATGCTGCTGGGCCTGAA R- CGTCTCCTTGATCTGCTTGAT G	94	61	NM_001004414 .4
IL1B	F- AGATGAAGCGGGTCAGCTC R- GCATCAAGGGCTACAAGCTC	120	59	XM_015297469 .2
TNF	F- CGTGGTTCGAGTCGCTGTAT R-CCGTGCAGGTCGAGGTAC	100	60	XM_040694846 .2
IFNG	F- AACCTTCCTGATGGCGTGAA R- GCTTTGCGCTGGATTCTCAA	86	60	NM_205149.2

[1] GAPDH: glyceraldehyde-3-phosphate dehydrogenase; RNA18S1: RNA, 18S ribosomal 1; BGLAP: bone gamma-carboxyglutamate protein; RUNX2: runt-related transcription factor 2; BMP2: bone morphogenetic protein 2; NFKB1: nuclear factor kappa B subunit 1; RANKL: TNFSF11, TNF superfamily member 11, also known as receptor activator of nuclear factor kappa-B ligand; SOST: sclerostin; OPG: osteoprotegerin also known as osteoclastogenesis inhibitory factor or tumour necrosis factor receptor superfamily member 11B; FABP4: fatty acid binding protein 4; PPARG: peroxisome proliferator activated receptor gamma; CEBPB: CCAAT

enhancer binding protein beta; IL10: interleukin 10; IL1B: interleukin 1 beta; TNF: chTNF-α, chicken tumor necrosis factor-like; INFG: interferon gamma.

Table 6.4: Daily feed intake (g) from 0 DPI to 12 DPI.

Daily feed intake (g)	Diet	Challenge Doses	Dpi 1	Dpi 2	Dpi 3	Dpi 4	Dpi 5	Dpi 6
T1	SO	-	77.9	68.4	82.4	77.9 [a]	71.4 [a]	101.2 [a]
T2	FO	-	82.2	71.5	84.4	80.7 [a]	69.5 [a]	101.3 [a]
T3	SO	Low	78.4	68.1	83.8	68.8 [b]	49.7 [bc]	60.0 [cd]
T4	FO	Low	82.1	68.0	81.4	67.7 [b]	53.9 [b]	78.1 [b]
T5	SO	High	81.4	67.2	81.5	58.5 [c]	36.4 [d]	52.6 [d]
T6	FO	High	84.0	68.6	80.6	59.2 [c]	47.1 [c]	70.3 [bc]
SEM			0.692	0.568	0.557	1.344	1.898	2.937
p-value	ANOVA		0.059	0.370	0.316	<0.001	<0.001	<0.001
	Diets		0.010	0.207	0.712	0.486	0.001	<0.001
	Challenge Doses		0.136	0.282	0.215	<.0001	<0.001	<0.001
	Challenge*Diets		0.970	0.531	0.261	0.431	0.001	0.002
Daily feed intake (g)	Diet	Challenge Doses	Dpi 7	Dpi 8	Dpi 9	Dpi 10	Dpi 11	Dpi12
T1	SO	-	103.8 [a]	107.0 [a]	115.9 [a]	120.1 [a b]	128.7 [a]	99.8 [a]
T2	FO	-	104.4 [a]	105.1 [a]	116.3 [a]	129.8 [a]	133.5 [a]	100.5 [a]
T3	SO	Low	80.7 [b]	95.0 [b]	104.1 [b]	115.9 [ab]	115.5 [b]	87.4 [b]
T4	FO	Low	83.6 [b]	97.2 [b]	97.1 [b]	116.7 [ab]	114.4 [b]	83.3 [b]
T5	SO	High	72.6 [b]	89.2 [b]	94.7 [b]	109.6 [b]	112.9 [b]	85.2 [b]

T6	FO	High	85.6 [b]	101.5 [b]	97.9 [b]	114.3 [b]	110.3 [b]	86.2 [b]
p-value	ANOVA		2.111	1.573	1.664	1.606	1.719	1.427
	Diets		<0.001	0.005	<0.001	0.049	<0.001	<0.001
	Challenge Doses		0.040	0.134	0.600	0.077	0.880	0.906
	Challenge*Diets		<0.001	0.004	<0.001	0.002	<0.001	<0.001

[1]T1, control group with soybean oil diet; T2, control group with fish oil diet; T3, soybean oil diet group that challenge with low dose of *Eimeria* solution; T4, fish oil diet group that challenge with low dose of *Eimeria* solution; T5, soybean oil diet group that challenge with high dose of *Eimeria* solution; T6, fish oil diet group that challenge with high dose of *Eimeria* solution.

[a, b, c, d] Treatments with different letters means a significantly difference between treatments by using Tukey' s HSD test, $p < 0.05$, N = 8.

Table 6.5: Cumulative feed intake (FI), body weight gain (BWG, g) and feed conversion ratio (FCR) from 0 DPI to 12 DPI.

Treatmemts[1]	Diet	Challenge	BW (g)			Dpi 0-6		
			DPI0	DPI6	DPI12	FI (g)	BWG (g)	FCR
T1	SO	-	331.0	623.6 [a]	1067.8 [a]	479.3 [a]	292.5 [a]	0.615[a]
T2	FO	-	331.8	639.2 [a]	1103.7 [a]	489.6 [a]	307.3 [a]	0.610 [a]
T3	SO	Low	331.7	545.8 [b]	920.5 [b]	408.8 [b]	214.1 [bc]	0.467 [b]
T4	FO	Low	331.0	568.5 [b]	908.0 [b]	431.3 [b]	237.5 [b]	0.536 [ab]
T5	SO	High	330.4	512.7 [c]	838.6 [b]	379.2 [b]	194.3 [c]	0.481 [b]
T6	FO	High	328.6	537.6 [b]	884.6 [b]	411.3 [b]	209.0 [bc]	0.535 [ab]
SEM			0.505	7.867	16.570	6.338	8.197	0.013
P-value	ANOVA		0.501	<0.001	<0.001	<0.001	<0.001	<0.001
	Diets		0.595	0.088	0.162	0.111	0.071	0.530
	Challenge doses		0.227	<0.001	<0.001	0.029	<0.001	<0.001
	Challenge*Diets		0.594	0.858	0.309	0.387	0.865	0.719
			Dpi 7-12			Dpi 0-12		
Treatmemts[1]	Diet	Challenge	FI (g)	BWG (g)	FCR	FI (g)	BWG (g)	FCR
T1	SO	-	575.4 [a]	444.2 [ab]	0.654	1054.7 [a]	736.7 [a]	0.638 [a]

T2	FO	-	589.1 a	464.5 a	0.657	1078.8 a	771.9 a	0.638 a
T3	SO	Low	511.2 b	374.7 abc	0.615	920.0 b	588.8 b	0.555 b
T4	FO	Low	508.9 b	339.4 c	0.605	940.2 b	577.0 b	0.577 ab
T5	SO	High	479.1 b	304.1 c	0.600	858.3 b	498.4 b	0.554 b
T6	FO	High	509.6 b	347.0 bc	0.557	920.9 b	556.0 b	0.549 b
SEM			8.352	11.077	0.013	13.777	16.487	0.009
P-value	ANOVA		0.091	<0.001	0.255	<0.001	<0.001	<0.001
	Diets		0.133	0.642	0.975	0.064	0.153	0.746
	Challenge doses		0.147	<0.001	0.033	0.026	<0.001	<0.001
	Challenge*Diets		0.156	0.238	0.311	0.156	0.304	0.386

[1]T1, control group with soybean oil diet ; T2, control group with fish oil diet ; T3, soybean oil diet group that challenge with low dose of *Eimeria* solution; T4, fish oil diet group that challenge with low dose of *Eimeria* solution; T5, soybean oil diet group that challenge with high dose of *Eimeria* solution; T6, fish oil diet group that challenge with high dose of *Eimeria* solution.

[a, b, c] Treatments with different letters means a significantly difference between treatments by using Tukey's HSD test, $p < 0.05$, N = 8.

Table 6.6: Body composition of broiler chick on 6 DPI and 12 DPI.

	Treatment[1]	Diet	Challenge	BMD[2]	BMC	Area	Fat percent	Total tissue	Fat mass	Lean mass
6 DPI				(g/cm^2)	(g)	(cm^2)	(%)	(g)	(g)	(g)
	T1	SO	-	0.122	7.188 ^{a}	58.563	13.906 ^{a}	599.989 ^{a}	84.538 ^{a}	518.115 ^{ab}
	T2	FO	-	0.122	7.425 ^{a}	60.375	13.163 ^{a}	622.924 ^{a}	81.987 ^{a}	540.908 ^{a}
	T3	SO	Low	0.124	6.369 ^{ab}	50.750	7.638 ^{bc}	546.919 ^{abc}	41.759 ^{bc}	505.188 ^{ab}
	T4	FO	Low	0.132	7.488 ^{a}	56.312	9.5944 ^{b}	591.512 ^{ab}	56.897 ^{b}	534.672 ^{a}
	T5	SO	High	0.125	5.619 ^{b}	44.688	7.106 ^{c}	485.910 ^{c}	34.813 ^{c}	451.069 ^{b}
	T6	FO	High	0.132	6.488 ^{ab}	49.000	7.388 ^{ab}	521.631 ^{bc}	38.924 ^{c}	482.565 ^{ab}
SEM				0.001	0.197	1.347	0.365	8.913	2.581	7.3633
p-value	ANOVA			0.1139	0.0376	0.0028	<0.001	<0.001	<0.001	<0.001
	Challenge dose			0.102	0.026	<0.001	<0.001	<0.001	<0.001	0.019
	Diets			0.092	0.054	0.214	0.293	0.027	0.083	0.044
	Challenge*Diets			0.209	0.623	0.564	0.068	0.845	0.077	0.964
12 DPI	T1	SO	No	0.146^{a}	16.341 ^{a}	110.455 ^{a}	15.409 ^{a}	1039.86 ^{a}	162.922 ^{a}	876.876 ^{a}
	T2	FO	No	0.145^{ab}	15.791 ^{a}	107.000 ^{a}	15.691 ^{a}	1021.22 ^{a}	161.066 ^{a}	860.237 ^{ab}
	T3	SO	Low	0.136 ^{bc}	11.039 ^{b}	79.130 ^{b}	11.574 ^{b}	847.82 ^{ab}	102.216 ^{b}	745.587 ^{abc}

	T4	FO	Low	0.134[c]	10.761[b]	78.304[b]	11.365[b]	796.19[b]	93.815[b]	702.338[bc]
	T5	SO	High	0.134[c]	10.473[b]	77.318[b]	9.765[b]	757.33[b]	77.028[b]	672.904[c]
	T6	FO	High	0.134[c]	10.522[b]	78	9.5	763.57[b]	74.803[b]	688.671[bc]
SEM				0.001	0.425	2.361	0.296	22.604	4.981	18.264
p-value	ANOVA			0.015	<0.001	<0.001	<0.001	<0.001	<0.001	<0.001
	Challenge dose			0.001	<0.001	<0.001	<0.001	<0.001	<0.001	<0.001
	Diets			0.898	0.752	0.756	0.683	0.606	0.532	0.681
	Challenge*Diets			0.866	0.935	0.925	0.701	0.848	0.943	0.770

[1]T1, control group with soybean oil diet; T2, control group with fish oil diet; T3, soybean oil diet group that challenge with low dose of *Eimeria* solution; T4, fish oil diet group that challenge with low dose of *Eimeria* solution; T5, soybean oil diet group that challenge with high dose of *Eimeria* solution; T6, fish oil diet group that challenge with high dose of *Eimeria* solution.

[2]BMD, bone mineral density; BMC, bone mineral content; Area, bone area; Fat percent (%), fat percentage; Lean percent (%), lean percentage; Total tissue (g), lean mass plus and fat mass; Fat (g), fat mass; Lean (g), muscle mass; BM(g), total body mass. SO, soybean oil group; FO, fish oil group.

Table 6.7: the villi height, villi width, crypts depth, and villus/crypt ratio in the duodenum, jejunum and ileum of broilers on 6 DPI.

Treatment[1]	Challenge Doses	Diets	Duodenum (μm)			
			V[2]	Vw[3]	C[4]	V:C[5]
T1	-	SO	710.26 [ab]	66.28	55.56 [b]	14.42 [a]
T2	-	FO	730.98 [a]	91.00	56.17 [b]	14.11[a]
T3	Low	SO	541.69 [c]	58.83	118.44[a]	4.89 [b]
T4	Low	FO	567.65 [bc]	67.00	108.27 [a]	5.52 [b]
T5	High	SO	455.98 [c]	78.28	121.50 [a]	4.30 [b]
T6	High	FO	422.940[c]	74.37	135.92 [a]	3.56 [b]
SEM			21.99	3.54	6.06	0.83
P-value	ANOVA		<0.001	0.118	<0.001	<0.001
	Challenge dose		<0.001	0.071	<0.001	<0.001
	Diets		0.749	0.315	0.919	0.888
	Challenge*Diets		0.78	0.432	0.973	0.879
Jejunum						
Treatment[1]	Challenge Doses	Diets	V	Vw	C	V:C
T1	-	SO	449.930[a]	64.83	63.77 [b]	7.65 [a]
T2	-	FO	408.54 [ab]	45.69	55.38 [b]	7.69 [a]
T3	Low	SO	302.18 [bc]	73.54	97.36 [ab]	3.25 [b]
T4	Low	FO	253.89 [c]	56.16	121.702[a]	2.11 [b]
T5	High	SO	308.79[bc]	82.02	125.31[a]	2.62 [b]
T6	High	FO	276.22[bc]	60.59	83.58 [ab]	3.85 [b]
SEM			21.99	3.54	16.84	3.88
P-value	ANOVA		<0.001	<0.001	0.104	0.001
	Challenge dose		<0.001	<0.001	0.102	0.006

	Diets		0.749	0.977	0.107	0.419
	Challenge*Diets		0.78	0.171	0.994	0.047
Ileum						
Treatment[1]	Challenge Doses	Diets	V	Vw	C	V:C
T1	-	SO	209.95	55.26	48.903[b]	4.85 [a]
T2	-	FO	193.48	55.94	38.90 [b]	5.17 [a]
T3	Low	SO	219.26	58.76	81.52 [a]	2.78 [b]
T4	Low	FO	199.69	69.59	75.75 [a]	2.72 [b]
T5	High	SO	172.44	67.77	84.19 [a]	2.19 [b]
T6	High	FO	192.46	68.37	81.65 [a]	2.49 [b]
SEM			5.79	2.32	3.54	0.25
P-value	ANOVA		0.26	0.24	<0.001	<0.001
	Challenge dose		0.70	0.09	<0.001	<0.001
	Diets		0.483	0.486	0.161	0.572
	Challenge*Diets		0.550	0.578	0.550	0.767

[1]T1, control group with soybean oil diet; T2, control group with fish oil diet; T3, soybean oil diet group that challenge with low dose of *Eimeria* solution; T4, fish oil diet group that challenge with low dose of *Eimeria* solution; T5, soybean oil diet group

that challenge with high dose of *Eimeria* solution; T6, fish oil diet group that challenge with high dose of *Eimeria* solution.

[2] V: villi height; [3] Vw: villi width; [4] C: crypts depth [5]: V:C, villus height / crypt depth ratio.

[ab] Means followed by superscript letters are different by Tukey's test ($P<0.05$); N=8.

Figures

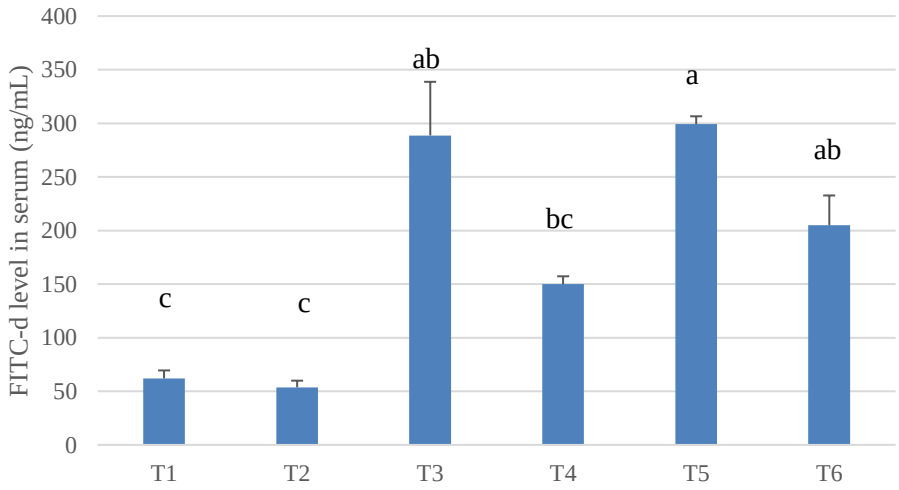

Figure 6.1: Gut permeability on 5 DPI. *Eimeria* infection had a significant effect on gut permeability at 5 DPI ($P < 0.001$), and the diet treatment also significantly affected the gut permeability ($P = 0.001$). There was a significant interaction between infection and diets ($P = 0.050$). Higher concentration of FITC-d (ng/mL) in the serum revealed more severe damage to the gut epithelium owing to the *Eimeria* challenge.

T1, control group with soybean oil diet; T2, control group with fish oil diet; T3, soybean oil diet group that challenge with low dose of *Eimeria* solution; T4, fish oil diet group that challenge with low dose of *Eimeria* solution; T5, soybean oil diet group that challenge with high dose of *Eimeria* solution; T6, fish oil diet group that challenge with high dose of *Eimeria* solution.[a, ab, b] Treatments with different letters means a significantly difference between treatments by using Tukey's HSD test, $P < 0.05$, N = 8.

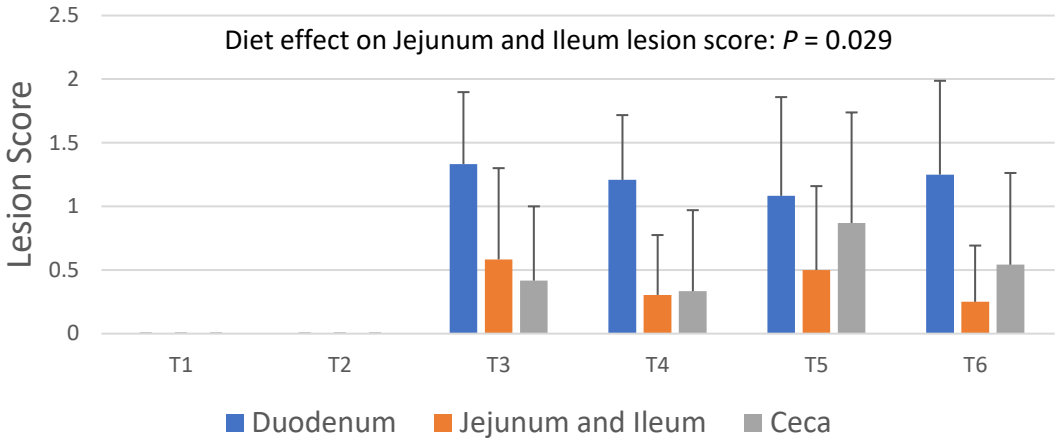

Figure 6.2: Lesion score on 6 DPI. No lesion was found in the intestine or ceca of birds from unchallenged groups. The severity of intestinal lesions of duodenum ($P < 0.001$), jejunum and ileum ($P < 0.001$), and ceca ($P < 0.001$) were significantly affected by *Eimeria* infection. The diet factor has a positive affected that fish oil reduced the lesion score at the jejunum and ileum junction ($P = 0.029$), but had no effect on intestinal lesion at duodenum or ceca ($P > 0.050$). There was no interaction between infectious doses and diet variables ($P > 0.050$).

T1, control group with soybean oil diet; T2, control group with fish oil diet; T3, soybean oil diet group that challenge with low dose of *Eimeria* solution; T4, fish oil diet group that challenge with low dose of *Eimeria* solution; T5, soybean oil diet group that challenge with high dose of *Eimeria* solution; T6, fish oil diet group that challenge with high dose of *Eimeria* solution.

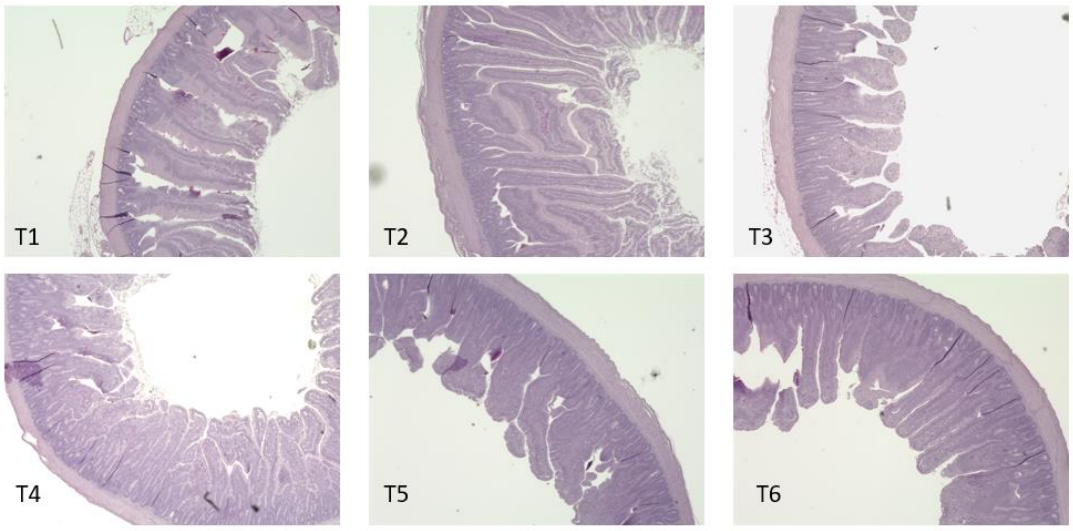

Figure 6.3: Histopathological examination of the affected intestinal demonstrated characteristic microscopic signs of coccidiosis in the affected broilers on 6 DPI. The villi height, crypt depth, and villus /crypt ratios of the jejunum were significantly affected by *Eimeria* infection ($P < 0.001$). The diet variable has no effect on intestinal morphology traits ($P > 0.05$). There was a significant interaction between infectious doses and diets on jejunum crypt depth ($P < 0.05$), but no significant interaction between infectious doses and diets on the other morphology traits ($P > 0.05$).

T1, control group with soybean oil diet; T2, control group with fish oil diet; T3, soybean oil diet group that challenge with low dose of *Eimeria* solution; T4, fish oil diet group that challenge with low dose of *Eimeria* solution; T5, soybean oil diet group that challenge with high dose of *Eimeria* solution; T6, fish oil diet group that challenge with high dose of *Eimeria* solution.

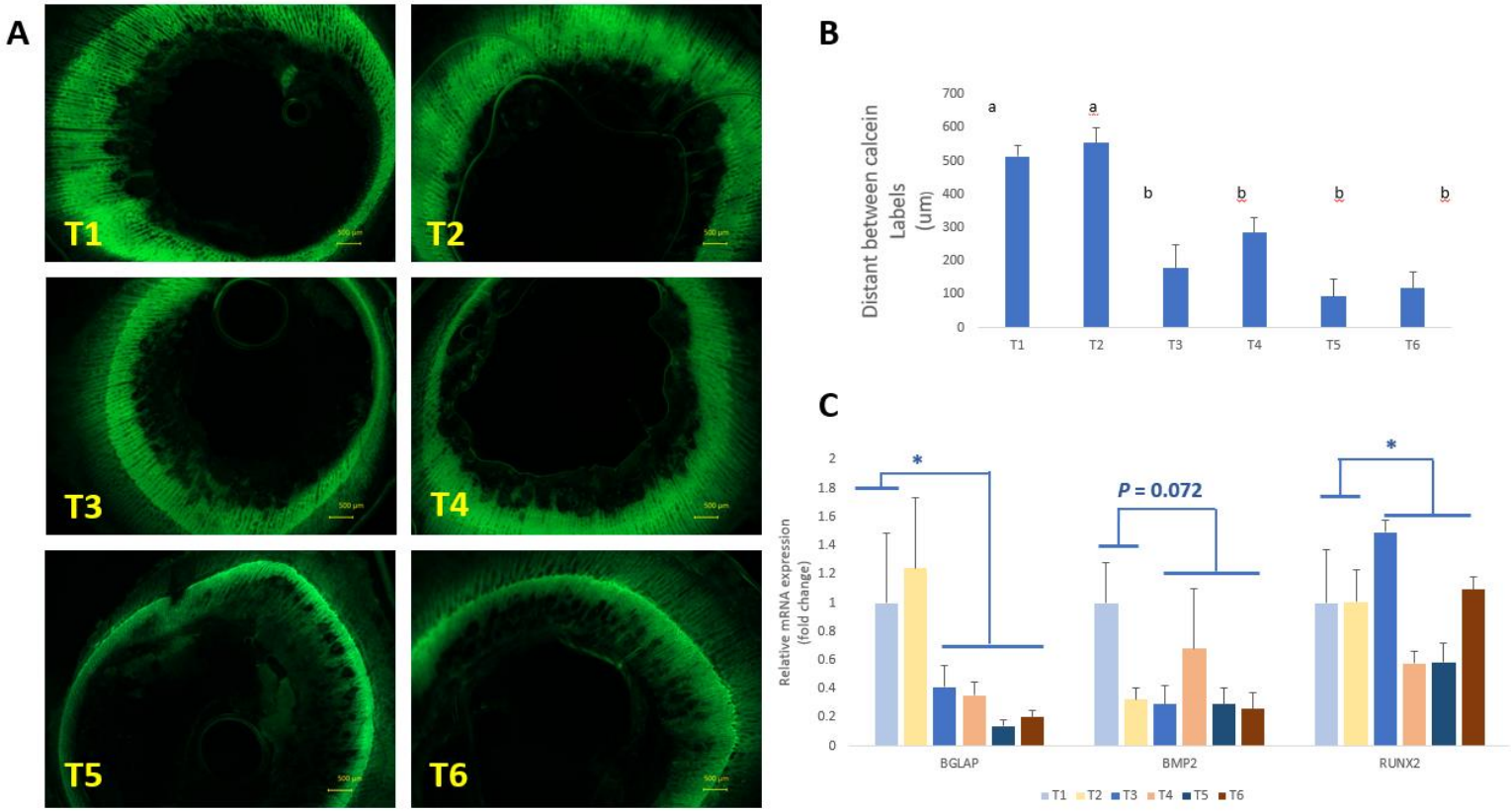
A
T1
T2
T3
T4
T5
T6
B
Distant between calcein Labels (um)
700
600
500
400
300
200
100
0
a
a
b
b
b
b
T1
T2
T3
T4
T5
T6
C
Relative mRNA expression (fold change)
2
1.8
1.6
1.4
1.2
1
0.8
0.6
0.4
0.2
0
*
P = 0.072
*
BGLAP
BMP2
RUNX2
T1 T2 T3 T4 T5 T6

Figure 6.4: Bone formation measurement. (A) Fluorescence image of the tibia cross-section of broilers. Bone formation rate was visualized by double calcein labels. (B) The measurement results of the distance between calcein labels. (C) By measuring the expression of bone formation biomarkers in bone marrow, results shown *Eimeria* infection significantly decreased the mRNA expression of *BGLAP* ($P < 0.001$), *RUNX2* ($P < 0.001$), *OPG* ($P < 0.001$), and showed a trend of decreasing in *BMP2* ($P = 0.072$). The fish oil diet had no significant impact on bone formation ($P > 0.05$), and there was no interaction between infection and diet treatments on bone formation biomarker in bone marrow ($P > 0.05$).

[a, ab, b] Treatments with different letters means a significantly difference between treatments by using Tukey's HSD test, $P < 0.05$, N = 8. * Indicated there was a significant difference between challenged and non-challenged groups. T1, control group with soybean oil diet; T2, control group with fish oil diet; T3, soybean oil diet group that challenge with low dose of *Eimeria* solution; T4, fish oil diet group that challenge with low dose of *Eimeria* solution; T5, soybean oil diet group that challenge with high dose of *Eimeria* solution; T6, fish oil diet group that challenge with high dose of *Eimeria* solution.

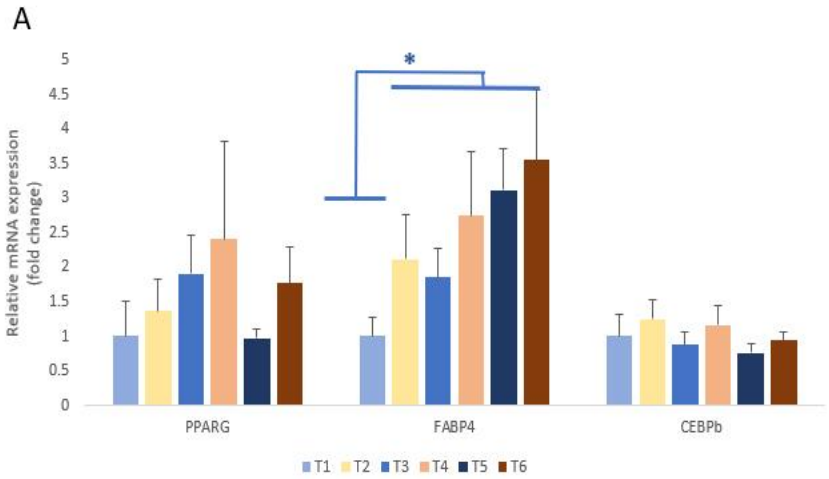
A
Relative mRNA expression (fold change)
5
4.5
4
3.5
3
2.5
2
1.5
1
0.5
0
*
PPARG
FABP4
CEBPb
T1 T2 T3 T4 T5 T6

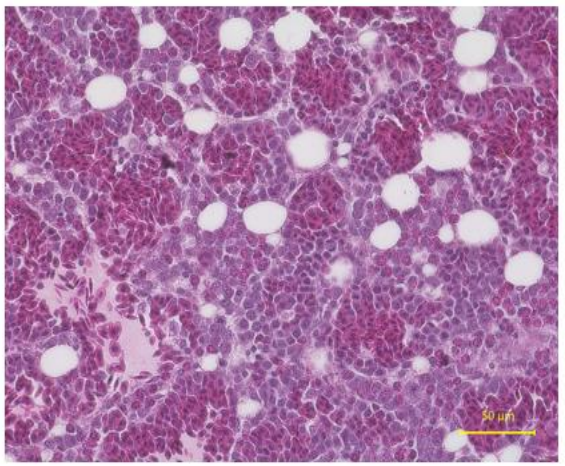
B
50 µm

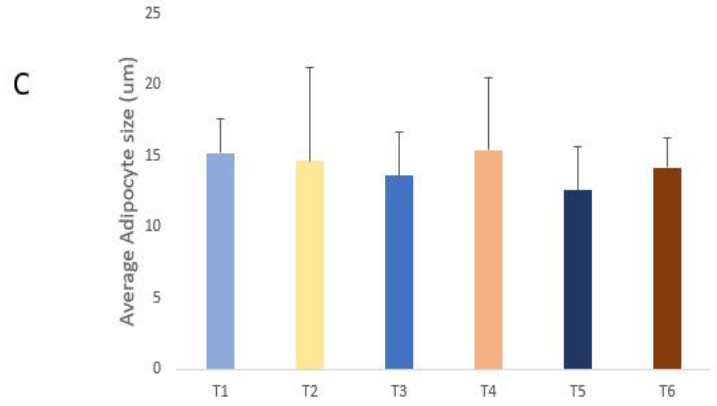
C
Average Adipocyte size (um)
25
20
15
10
5
0
T1
T2
T3
T4
T5
T6

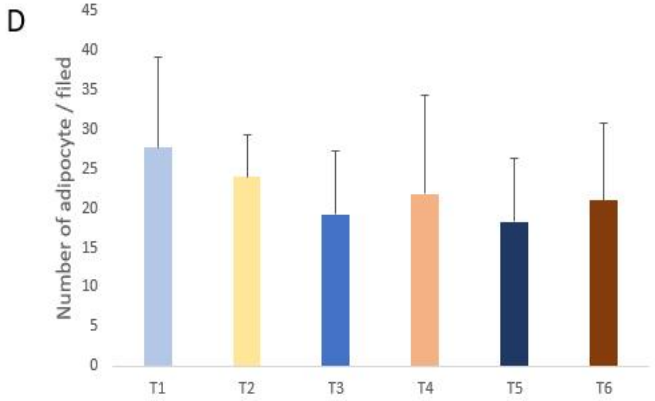
D
Number of adipocyte / filed
45
40
35
30
25
20
15
10
5
0
T1
T2
T3
T4
T5
T6

Figure 6.5: The measurement of adipogenesis in bone marrow. (A) an increased level of *FABP4* was detected in bone marrow of *Eimeria*-challenged groups than non-infected control ($P < 0.05$; Figure 5A). (B) Histology image of bone marrow adipocyte wall with H&E stanning. (C) Infection or diet variables did not change the size of adipocytes in bone marrow ($P > 0.05$). (D) Infection or diet variables did not change the number of adipocytes in bone marrow ($P > 0.05$).

* Indicated there was a significant difference between challenged and non-challenged groups. T1, control group with soybean oil diet; T2, control group with fish oil diet; T3, soybean oil diet group that challenge with low dose of Eimeria solution; T4, fish oil diet group that challenge with low dose of Eimeria solution; T5, soybean oil diet group that challenge with high dose of Eimeria solution; T6, fish oil diet group that challenge with high dose of *Eimeria* solution.

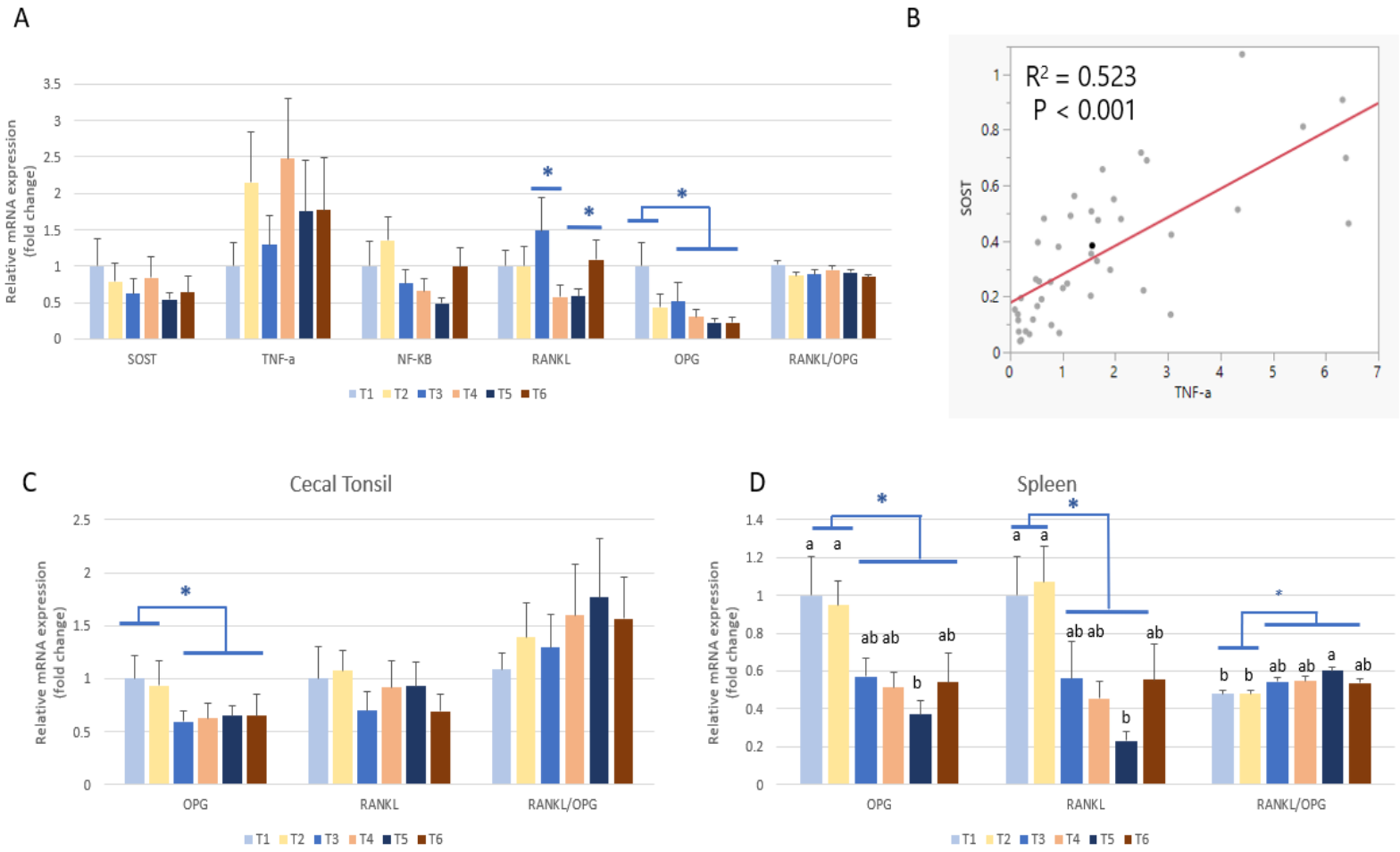
A
Relative mRNA expression (fold change)
SOST
TNF-a
NF-KB
RANKL
OPG
RANKL/OPG
T1 T2 T3 T4 T5 T6
B
R² = 0.523
P < 0.001
SOST
TNF-a
C
Cecal Tonsil
Relative mRNA expression (fold change)
OPG
RANKL
RANKL/OPG
T1 T2 T3 T4 T5 T6
D
Spleen
Relative mRNA expression (fold change)
OPG
RANKL
RANKL/OPG
T1 T2 T3 T4 T5 T6

Figure 6.6: The effect of diet and *Eimeria*-infection on bone remodeling gene marker expression. (A) *Eimeria*-challenge significant decreased the expression of *OPG* in the bone marrow ($P < 0.001$). The infectious doses and diet had a significant interaction on mRNA expression of *RANKL* in bone marrow ($P = 0.032$), compared to non-challenged control. The effect of the diet treatment showed an infectious dose-depend manner, where fish oil decreased bone marrow *RANKL* expression compared with soybean oil in the low challenge dose groups (T3 VS. T4; $P < 0.050$), and fish oil diet increased the bone marrow expression of *RANKL* in the high challenge groups compared with soybean oil groups (T5 VS T6; $P < 0.050$). (B) There was a positive correlation between mRNA expression of *TNF* and *SOST* in bone marrow ($P < 0.001$; $R^2 = 0.523$). (C) *Eimeria*-challenge significant decreased the expression of *OPG* in cecal tonsils ($P < 0.001$). (D) *Eimeria*-challenge significant decreased the expression of *OPG* ($P < 0.001$) and *RANKL* ($P < 0.001$) in the spleen. Moreover, the mRNA ratio of RANKL/ OPG, a common index biomarker of bone remodeling, were significant increased by *Eimeria* infection in the spleen ($P < 0.050$).

[a, ab, b] Treatments with different letters means a significantly difference between treatments by using Tukey's HSD test, $P < 0.05$, N = 8. * Indicated there was a significant difference between challenged and non-challenged groups. T1, control group with soybean oil diet; T2, control group with fish oil diet; T3, soybean oil diet group that challenge with low dose of *Eimeria* solution; T4, fish oil diet group that challenge with low dose of *Eimeria* solution; T5, soybean oil diet group that challenge with high dose of

Eimeria solution; T6, fish oil diet group that challenge with high dose of *Eimeria* solution.

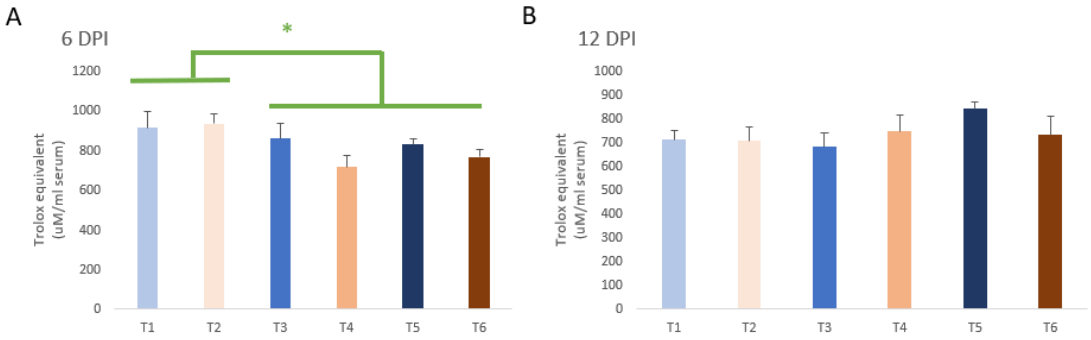

Figure 6.7: Total antioxidant capacity in serum. (A) Total antioxidant capacity affected by infection ($P < 0.050$) but not by diet on 6 DPI. (B) Neither infection or diet significantly affected the serum total antioxidant capacity on 12 DPI ($P > 0.050$).

* Indicated there was a significant difference between challenged and non-challenged groups. T1, control group with soybean oil diet; T2, control group with fish oil diet; T3, soybean oil diet group that challenge with low dose of *Eimeria* solution; T4, fish oil diet group that challenge with low dose of *Eimeria* solution; T5, soybean oil diet group that challenge with high dose of *Eimeria* solution; T6, fish oil diet group that challenge with high dose of *Eimeria* solution.

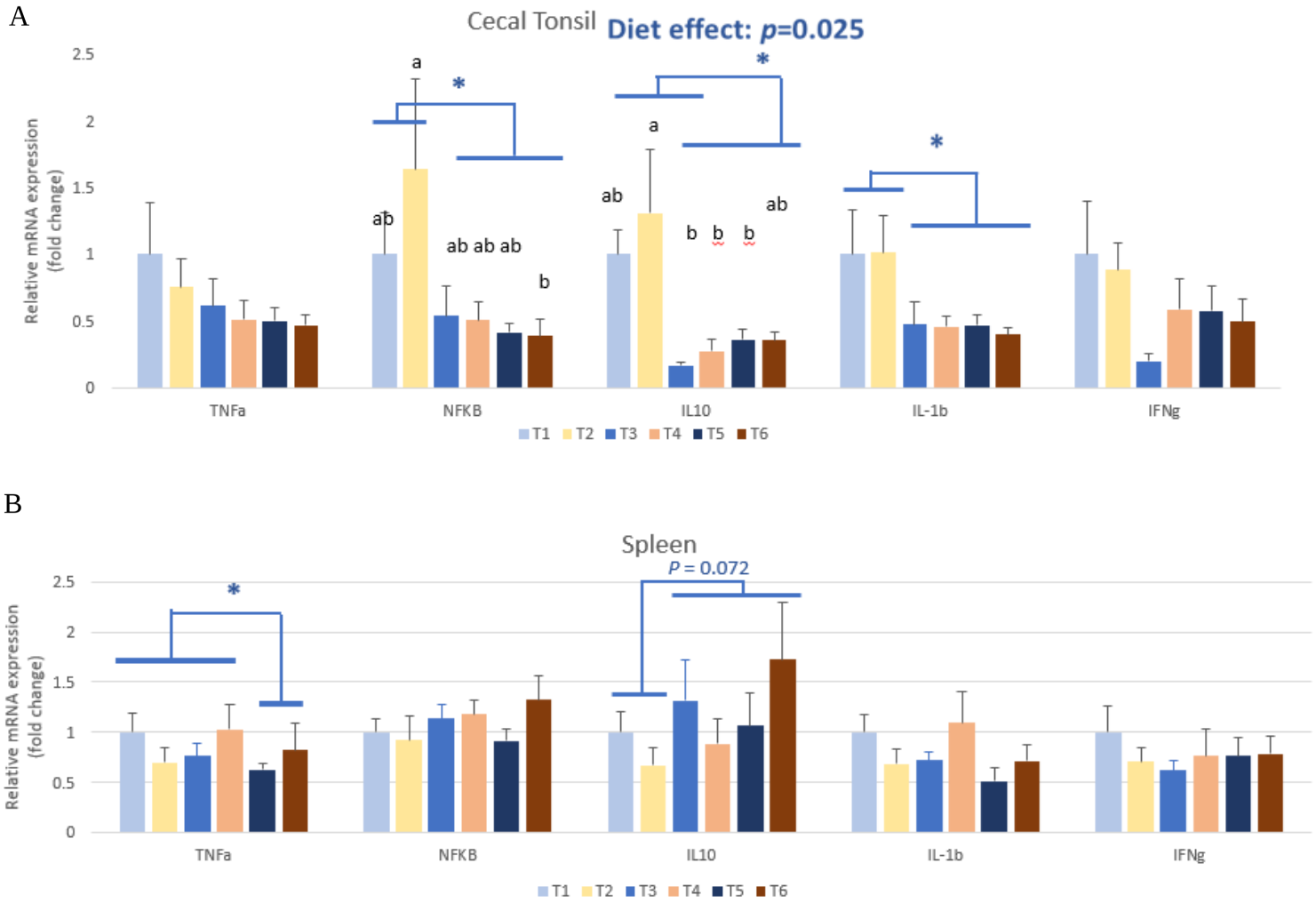
A
Cecal Tonsil
Diet effect: p=0.025
Relative mRNA expression (fold change)
2.5
2
1.5
1
0.5
0
a
ab
ab ab ab
b
ab
a
b b b
ab
TNFa
NFKB
IL10
IL-1b
IFNg
T1 T2 T3 T4 T5 T6
B
Spleen
P = 0.072
Relative mRNA expression (fold change)
TNFa
NFKB
IL10
IL-1b
IFNg
T1 T2 T3 T4 T5 T6

Figure 6.8: The immune response in the cecal tonsils and the spleen. (A) In cecal tonsils, the mRNA expression of *NFKB1*, *IL10* and *IL1B* was reduced by *Eimeria* infection on 6 DPI compared to uninfected control groups ($P < 0.05$). The mRNA expression of *TNF* and *IFNG* reminds unchanged with infection ($P > 0.05$). For the diet variable, the fish oil diet significantly increased *IL10* expression compared with the soybean oil diet ($P < 0.05$). There was no interaction between diet and infection variables on immune response-related marker genes expression in cecal tonsils. (B) In the spleen, in contrast to the effect of *Eimeria* infection in cecal tonsils, a trend of increased expression of *IL10* was observed in *Eimeria*-infected birds compared to uninfected control ($P = 0.072$). There was a lower level of mRNA expression of *TNF* in the high challenge doses than the low-infection groups and uninfected control groups ($P < 0.050$). There was no interaction between diet and infection variables on the mRNA expression of immune response makers in the spleen.

T1, control group with soybean oil diet; T2, control group with fish oil diet; T3, soybean oil diet group that challenge with low dose of *Eimeria* solution; T4, fish oil diet group that challenge with low dose of *Eimeria* solution; T5, soybean oil diet group that challenge with high dose of *Eimeria* solution; T6, fish oil diet group that challenge with high dose of *Eimeria* solution. [a, ab, b] Treatments with different letters means a significantly difference between treatments by using Tukey's HSD test, $P < 0.05$, N = 8. * Indicated there was a significant difference between challenged and non-challenged groups.

CHAPTER 7

SUMMARY AND CONCLUSIONS

With increasing concerns around farm animal welfare, poultry bone abnormalities have become one of the significant challenges for the poultry industry. For a long time, bone health in broiler production yet gained enough attention. Bone marrow contains different cell types that perform bone formation and resorption and serves as the cradle of hematopoiesis and a reservoir of bone-related stem cells and cytokines, providing an ideal environment for communicating between bone metabolism and the immune system. The *Eimeria*-challenge model was chosen as a disease in *vivo* study model to understand the possible link between intestinal parasite infection and bone health in the current study. Results showed that the factors that affect bone metabolism and homeostasis during pathogen infection include but are not limited to malabsorption of nutrients, the data emphasized the delayed bone development in the parasite-challenged groups was attributable to an uncoupling of osteoblast and osteoclast activity, whereby increased bone resorption and decreased bone formation were closely associated with immune response/oxidative stress during *Eimeria* infection. In order to further understand the direct interaction between bone homeostasis and antioxidant status, in *vitro* and in *ovo* investigation was used to confirm the functional significance of antioxidants in bone homeostasis. Treatment with H_2O_2 altered cellular antioxidant enzyme gene expression,

and long-term treatment of H_2O_2 impaired osteogenic differentiation potential but was also associated with a greater potential for adipogenesis in chicken MSCs with oxidative stress, highlighting that cellular oxidative stress caused by exogenous H_2O_2 accumulation modulate stem cell differentiation capacity. The embryonic study showed that H_2O_2-induced oxidative stress suppressed bone formation gene marker expression with chronic effects. In the last part of the study, fish oil was used as a nutritional supplementation that improved gut integrity after *Eimeria spp.* infection. Although the fish oil supplement didn't alter the bone mineral density, an increased bone remodeling status was observed in *Eimeria*-infection groups in this study, indicated pathogen infection caused immune response regulated bone homeostasis.

Taken together, with the long-held notion that the central pathophysiology of bone disorder was nutrition deficiency and physical stress, we demonstrated that bone disorder is also closely connected with bone modeling and remodeling which are associated with immune response/oxidative stress. In fact, the long bone should be considered as an essential multifunctional organ that dynamically responds to immune status, gut health and oxidative stress in broiler chicken. Further studies on osteoimmunology and oxidative stress are needed to address bone disorder issues and will further lead to a more precise understanding of the mechanism underlying the pathogenesis of bone mineral loss and bone disease in broilers. More studies on antioxidation supplementation in chicken bone health are needed for improving animal production and welfare in the future.